Techno-Economic Performance Evaluation of Photovoltaic based Micro-Grid with Energy Management Strategies

Arvind Sharma

UiA University of Agder

Doctoral Dissertations at the University of Agder 313

Arvind Sharma

Techno-Economic Performance Evaluation of Photovoltaic based Micro-Grid with Energy Management Strategies

Doctoral Dissertation for the Degree Philosophiae Doctor (PhD) at
the Faculty of Engineering and Science, Specialisation in Renewable Energy

University of Agder
Faculty of Engineering & Science
2021

Doctoral dissertations at the University of Agder: 313
ISSN: 1504-9272
ISBN: 978-82-8427-018-0

Printed by Media 07
Kristiansand

Abstract

The operational performance of grid connected micro-grid system can be affected by many factors e.g. techno-economic sizing, appropriate energy management strategy, geographical locations, grid constrains and electricity energy pricing dynamics. To make renewable energy based micro-grid system more reliable as well as efficient and economically viable, it is imperative to consider a holistic approach and investigate all these factors for design and operation of the micro-grid system. In this work, techno-economic sizing of distributed generator(s) with energy storage are analyzed for operating grid connected PV based system as a micro-grid, even during the possible grid outage period. Energy management strategies have been proposed and evaluated for improving techno-economic performance of the PV based micro-grid system. Performance of the micro-grid system can be significantly improved using appropriate energy management strategies for maximizing the use of local energy resources and battery energy throughput. Impact of electricity energy pricing dynamics has been analyzed for techno-economic operation of the grid connected PV based micro-grids at the selected geographical locations (i.e. Tropical and Nordic climates). The local grid limits on the operation of the micro-grid system has been evaluated for maximizing the local energy resources utilization with consideration of peak demand and energy pricing. The regional energy pricing dynamics and local grid limits have considerable impact on performance of the PV based micro-grid. The maximum penetration of PV based micro-grid (i.e. hosting capacity study) within the distribution power network has been assessed considering the network constraints (e.g. voltage or/and loading of the power lines, etc.) and they have significant impact on PV capacity installations at different buses. The increasing penetration of PV based micro-grid system affects the voltage quality within the distribution network. The reactive power versus voltage (Q-V) droop control technique has been evaluated for managing the voltage profile within the prescribed limits. The Q-V droop function has been implemented in the PV inverter and tested its operation using the real time digital simulator and power hardware- in- loop method for improving the voltage profile within the distributed network. The presented results in this work are going to be useful for promoting the PV based micro-grid within the distribution network.

Acknowledgements

First and foremost, I am deeply grateful to the almighty God for providing me strength and good health. Without His grace and blessing this study would have not been possible.

I am very grateful to the Royal Norwegian Embassy, New Delhi and Ministry of Foreign Affairs, Norway for providing me golden opportunity of doing PhD as a part of project work (2017-2020) under the theme of 'Sustainability and Clean Energy'. It was under the framework agreement between The Energy and Resources Institute (TERI), India and the University of Agder (UiA), Norway through the Royal Norwegian Embassy, New Delhi. This PhD work would have not been possible without financial support from the Ministry of Foreign Affairs, Norway.

I whole-heartedly appreciate my gratitude to my parent organization The Energy and Resources Institute (TERI) India for permitting me to pursue the doctoral study at the UiA. I am extremely grateful to Dr. Ajay Mathur, Director General TERI; Dr. Ashvini Kumar, Senior Director of Renewable Energy Technologies Division TERI; Mr. Shirish Garud, Senior Fellow, TERI; and TERI team for their continuous guidance, encouragement, and valuable support. I am very grateful to Dr. Vivek Kumar from the Royal Norwegian Embassy New Delhi for providing me support throughout the PhD period.

I express my sincere and deepest gratitude to my supervisor, Dr. Mohan Lal Kolhe, Professor at UiA. His expertise, invaluable guidance, deep understanding of the subject and continual inspiration has great contribution in completing my work timely. His encouragement and high degree of freedom to me during this study is highly appreciated.

I would also like to express my sincere and deepest gratitude to my co-supervisor, Dr. Nils Ulltveit-Moe, Associate Professor at UiA. Despite of his health problem, he is always available for reviewing my work and provided me timely feed-back.

I am thankful to the Rector of the UiA, Prof. Sunniva Whittaker; Dean of the Faculty of Engineering and Science, Prof. Michael Rygaard Hansen; Head of the Department Prof. Geir Grasmo; Section leader Prof. Henrik Kofoed Nielsen; PhD Coordinator Emma E. Horneman and Senior Consultant Sissel Stenersen for providing me the necessary facilities and pleasant working environment for academic work.

I would like to express my great thanks to the Skagerak Energi for providing data of the micro-grid facility of Soccer Club of Skagerak Arena, Norway. I am greatly obliged to Henrik Landsverk, Signe Marie Oland, Stig Simonsen and team for their continuous support and constructive feed-back on research work.

I am very much thankful to the 'ERIGrid H2020 Research Infrastructure Project consortium for the transnational lab access for providing me an opportunity to one of its testing and simulation facilities at SmartRUE Electric Energy Systems laboratory at the National Technical University of Athens, Greece. My great thanks to the researchers; Prof. Nikos Hatziargyriou, Dr. Panos Kotsampopoulos, Alkistis Kontou, Dimitrios Lagosat and team for their assistance during real-time power hardware in-the-loop simulation experiments.

I would like to express my thanks to the Aalborg University, Denmark for giving opportunity to participate in the PhD courses.

I am very much thankful to anonymous reviewers for providing me constructive feedback for improving quality of research publications from this work. I would like to express my sincere gratitude to the authors of the articles, referred in the thesis.

Special thanks for my PhD colleagues Konara, Nils, Milad, Ahmed, Basant, Madhwa, Sissel, Lorenzo, Antoine, Saba, Bernard for their support and motivation during my PhD studies.

Last but not least, I would like to express my ultimate gratitude to my father Mr. Vachaspati Sharma and my mother Mrs. Kamla Sharma for their endless prays and their outstanding support. I would also like to express my gratitude to my in-laws for their pray and their outstanding support. Heartfelt thanks for my wife Mrs. Ranjana Sharma and our daughter Abhishri Sharma. Thanks to my wife for her encouragement in the decision, always gives me motivation and her continuous support in the most difficult times during the period of the study.

List of Publications

The following peer-reviewed published articles are based on research activities conducted by the author.

Peer Reviewed Journal Publications

1. A. Sharma, M. Kolhe, "Techno-Economic Evaluation of PV based Institutional Smart Micro-grid under Energy Pricing Dynamics," *Journal of Cleaner Production (Elsevier)*, vol. 264, pp. 1-14, 2020. doi: 10.1016/j.jclepro.2020.121486.

2. A. Sharma, M. Kolhe, K.M.S.Y. Konara, N. Ulltveit-Moe, K. Muddineni, A. Mudgal, S. Garud, "Performance Assessment of Institutional Photovoltaic based Energy System for Operating as a Micro-grid," *Sustainable Energy Technologies and Assessments (Elsevier)*, vol. 37, pp. 1-13, 2020. doi: 10.1016/j.seta.2019.100563

3. P. Sharma, M. Kolhe, A. Sharma, "Economic Performance Assessment of Building Integrated Photovoltaic System with Battery Energy Storage under Grid Constraints," *Renewable Energy (Elsevier)*, vol. 145, pp. 1901-1909, 2020. doi: 10.1016/j.renene.2019.07.099.

4. K.M.S.Y. Konara, M. Kolhe, A. Sharma, "Power Flow Management Controller within a Grid Connected Photovoltaic based Active Generator as a Finite State Machine using Hierarchical Approach with Droop Characteristics," *Renewable Energy (Elsevier)*, vol. 155, pp. 1021-1031, 2020. doi: 10.1016/j.renene.2020.03.138.

5. K.M.S.Y. Konara, M. Kolhe, A. Sharma, "Power Dispatching Techniques as a Finite State Machine for a Standalone Photovoltaic System with a Hybrid Energy Storage," *AIMS Energy*, vol. 8, no. 2, pp. 214-230, 2020. doi: 10.3934/energy.2020.2.214.

6. A. Sharma, S. Pandey, M. Kolhe, "Global Review of Policies & Guidelines for Recycling of Solar PV modules," *International Journal of Smart Grid and Clean Energy*, vol. 8, no. 5, pp. 597-610, 2019. doi: 10.12720/sgce.8.5.597-610.

Peer Reviewed Conference Proceeding Publications

1. A. Sharma, M. Kolhe, S. Oluf Kristiansen, S. Simonsen, H. Landsverk, S. Marie Oland, "Techno-Economic Case Study of Micro-Grid System at Soccer Club of Skagerak Arena Norway," 5th International Conference on Smart and Sustainable Technologies (SpliTech), *IEEE*, pp. 1-5, 2020. doi: 10.23919/SpliTech49282.2020.9243789.

2. A. Sharma, M. Kolhe, N. Ulltveit-Moe, A. Mudgal, K. Muddineni and S. Garud, "Performance Analysis of Institutional Hybrid Energy System for Electrical Energy Tariffs," *DES Transactions*, 3rd International Conference on Energy, Ecology and Environment (ICEEE), pp. 1-4, 2019. doi:10.12783/dteees/iceee2019/31812.

3. A. Sharma, M. Kolhe, K.M.S.Y. Konara, K. Muddineni, A. Mudgal, S. Garud and U. Nils, "Operational Analysis of Institutional Energy System for Developing a Micro-grid," IOP Conference Series- Materials Science and Engineering, vol. 605, pp. 1-8, 2019. doi:10.1088/1757-899X/605/1/012008.

4. A. Sharma, M. Kolhe, K.M.S.Y. Konara, K. Muddineni, A. Mudgal, S. Garud and U. Nils, "Performance Assessment of Building Integrated Photovoltaic and Battery Energy System: A Case Study of TERI-Retreat Faculty in India," 4th International Conference on Smart and Sustainable Technologies (SpliTech), *IEEE*, pp. 1-5, 2019. doi: 10.23919/SpliTech.2019.8783046.

5. P. Sharma, M. Kolhe, A. Sharma, "Role of Subsidies for PV solar Installations in India: A Cost-benefit Analysis," International conference on Smart Technologies for Energy, Environment & Sustainable Development (ICSTEESD), *Springer Proceedings in Energy*, (accepted, in press), 2020.

6. A. Sharma, M. Kolhe, N. Ulltveit-Moe, A. Mudgal, K. Muddineni and S. Garud, "Comparative Analysis of Different Types of Micro-grid Architectures and Controls," International Conference on Advances in Computing, Communication Control and Networking (ICACCCN), *IEEE*, pp. 1200-1208, 2018. doi: 10.1109/ICACCCN.2018.8748491.

7. K.M.S.Y. Konara, M. Kolhe, A. Sharma, ‘Load Compensator with an Energy Storage for a Grid Connected PV Based Active Generator’, IOP Conference series- Materials Science and Engineering, vol. 605, no. 012009, pp. 1-8, 2019. doi:10.1088/1757-899X/605/1/012009.

8. P. Sharma, M. Kolhe, A. Sharma, “Economic Analysis of a Building Integrated Photovoltaic System Without and With Energy Storage,” IOP Conference series- Materials Science and Engineering, vol. 605, no. 012013, pp 1-7, 2019.
doi:10.1088/1757-899X/605/1/012013.

9. A. Sharma, M. Kolhe, N. Ulltveit-Moe, K. Muddineni, A. Mudgal and S. Garud, "Voltage Rise Issues and Mitigation Techniques Due to High PV Penetration into the Distribution Network," International Conference on Automation and Computational Engineering (ICACE), *IEEE*, pp. 72-78, 2018. doi: 10.1109/ICACE.2018.8687041.

10. M. A. M. Yassin, M. Kolhe, A. Sharma, S. Garud, “Battery Capacity Estimation for Building Integrated Photovoltaic System: Design Study for Different Geographical Location(s)”, *Energy Procedia (Elsevier)*, vol. 142, 2017, pp. 3433-3439, 2017. doi: 10.1016/j.egypro.2017.12.226.

11. D. Dharshana, M. Kolhe, A. Sharma, S. Garud, V. Dehalwar and V. K. Singh, "Review of information and communication technologies for smart micro-grid automation," International Conference on Power Systems, *IEEE*, pp. 842-848, 2018. doi: 10.1109/ICPES.2017.8387406.

Contents

Abstract v
Acknowledgements vii
List of Publications ix
List of Figures xvii
List of Tables xxi
List of Abbreviations xxii
Chapter 1 1
1. Introduction 1
1.1. State-of-Art Literature Review 2
1.2. Research Objectives 8
1.3. Thesis Organization 8
Chapter 2 11
2. Energy Management Strategies for Techno-Economic Assessment of PV Based Institutional Micro-Grid 11
2.1 Summary 11
2.2 Introduction 11
2.3 Description of Energy System with Grid and DG (i.e. Case 2.a) 14
2.3.1 Results & Analysis of Case 2.a 16
2.4 Energy Management Strategy for PV & Battery based Grid-Connected System 19
2.5 Results & Analysis of Case 2.b 23
2.5.1 Annual Energy Contributions 24
2.5.2 Month Wise Energy Contributions 25
2.5.3 Energy Contribution from DERs for the Best Month 26
2.5.4 Energy Contribution from DERs for the Worst Month 27
2.5.5 Energy Contribution for a Typical Day 29
2.5.6 Battery Performance Analysis 30
2.6 Economic Performance Analysis and Comparison of Cases 2.a & 2.b 31
2.7 Conclusions 34
Chapter 3 37
3. Techno-Economic Performance Evaluation of PV based Institutional Micro-Grid under Energy Pricing Dynamics 37
3.1 Summary 37
3.2 Introduction 37

3.3 Energy Management Strategy for Micro-Grid Operation with ToU Tariffs 39
3.4 Results & Analysis of Micro-Grid with Different ToU Tariffs 43
3.5 Results & Analysis of Micro-Grid with Different Selling Prices to Grid 46
3.6 Sensitivity Analysis 48
3.6.1 Impact of PV, Battery, and Fuel's Cost on the CoE 48
3.6.2 Impact of Battery Capacity on the CoE, NPC, Battery Energy Throughput and Fuel Consumption 50
3.7 Conclusions 51
Chapter 4 53
4. Techno-Economic Analysis of PV based Micro-Grid System at Skagerak Arena Norway 53
4.1 Summary 53
4.2 Introduction 53
4.3 Energy System Description of Skagerak Arena (i.e. Case 4.a) 55
4.3.1 Results & Analysis of the Energy System at Skagerak Arena (i.e. Case 4.a) 56
4.4 Energy Management Strategy for Operation of Micro-Grid System 58
4.5 Performance Analysis of Micro-Grid System of Skagerak Arena (i.e. Case 4.b) 62
4.5.1 Annual Energy Contributions 62
4.5.2 Month Wise Energy Contributions 64
4.5.3 Energy Contribution from DERs for the Best Month 65
4.5.4 Energy Contribution from DERs for the Worst Month 66
4.5.5 Energy Contribution for a Typical Day 67
4.5.6 Battery Performance Analysis 68
4.6 Economic Analysis and Comparison of Cases 4.a & 4.b 69
4.7 Comparative Analysis of Performance of the Micro-Grid System in India and Norway Geographical Locations 72
4.7.1 Specific PV Output 72
4.7.2 Energy Contribution without and with Micro-grid System in India and Norway 73
4.7.3 Comparative Battery Performance Analysis for India and Norway 75
4.8 Conclusions 76

Chapter 5 ..... **77**
5. Impact of Energy Pricing Dynamics with Geographical Locations on Techno-Economic Performance of PV based Micro-Grid System **77**
5.1 Summary 77
5.2 Introduction 77
5.3 Energy Management Strategy for Micro-grid Operation 82
5.3.1 Results & Analysis of Micro-Grid with Increasing Tariffs 85
5.3.2 Results & Analysis of Micro-grid with Different Selling Prices to Grid 89
5.4 Impact of PV, Battery, and Energy Tariff on the CoE 93
5.5 Economic Performance Analysis for Micro-grid System in India and Norway at Selected Geographic Locations 94
5.6 Impacts on CoE of the Micro-grid System with Different Grid Buying and Selling Prices in India and Norway Geographical Locations 95
5.7 Conclusions 97
Chapter 6 ..... **99**
6. PV based Micro-Grid Hosting Capacity and Voltage Quality Analysis within a Distributed Network **99**
6.1 Summary 99
6.2 Introduction 99
6.3 Distributed Network Without PV Integration (i.e. Case 6.a) 102
6.3.1 System Description 102
6.3.2 Results & Analysis for Case 6.a 104
6.4 Hosting Capacity Analysis within a Distributed Network 108
6.4.1 Methodology for Estimating PV Hosting Capacity 108
6.4.2 PV Hosting Capacity Estimation 110
6.5 Impact of PV Penetration into the Distribution Network (i.e. Case 6.b) 112
6.5.1 Testing Setup 113
6.5.2 Results and Analysis of Case 6.b 114
6.6 Impact of Q-V Droop Control Strategy using DRTS and PHIL Methods (i.e. Case 6.c) 118
6.6.1 Results and Analysis of Case 6.c 119
6.7 Impact of PV Penetration within Mesh Network (Cases 6.d & 6.e) 123
6.7.1 Comparison of Cases 6.d and 6.e with 6.b 123
6.8 Conclusions 129

Chapter 7 131
7. Conclusions 131
7.1 Future Scope of Work 134
Appendix I 135
References of Chapter 1 141
References of Chapter 2 147
References of Chapter 3 150
References of Chapter 4 152
References of Chapter 5 154
References of Chapter 6 156

List of Figures

Fig. 2.1 Schematic of Energy System with DG and Grid (i.e. Case 2.a) 15
Fig. 2.2 Yearly Load Variation..... 15
Fig. 2.3 Hourly Variation of the Total Load of a Typical Week..... 16
Fig. 2.4 Energy Contribution from Grid Throughout Year (Case 2.a)..... 16
Fig. 2.5 Energy Contribution from DG Throughout Year (Case 2.a) 17
Fig. 2.6 Block Diagram of the Institutional Micro-grid System (Case 2.b)..... 18
Fig. 2.7 Flow Chart of Energy Management Strategy for Micro-Grid (Case 2.b) 23
Fig. 2.8 Annual Grid Energy Supply (Case 2.b)..... 24
Fig. 2.9 Annual PV Energy Production (Case 2.b)..... 24
Fig. 2.10 Annual DG Energy Contribution (Case 2.b) 25
Fig. 2.11 Annual Battery's SoC (Case 2.b) 25
Fig. 2.12 Energy from Grid, PV & DG, and Battery Energy Throughput..... 26
Fig. 2.13 Energy Contribution from 1-15 Days of March (Case 2.b) 27
Fig. 2.14 Energy Contribution from 16-31 Days of March (Case 2.b) 27
Fig. 2.15 Energy Contribution from 1-15 Days of August (Case 2.b)..... 28
Fig. 2.16 Energy Contribution from 16-31 Days of August (Case 2.b)..... 29
Fig. 2.17 Energy Contributions of a Typical Day in August (Case 2.b)..... 30
Fig. 2.18 Hourly Variation of Battery SoC (Case 2.b)..... 31
Fig. 2.19 Cashflow Summary of Different Components in the Case 2.b..... 34
Fig. 3.1 Variation of the Time-of-Use Tariff of a Day..... 40
Fig. 3.2 Variation of Different Time-of-Use Tariff of a Year..... 40
Fig. 3.3 Variation of Different ToU Tariffs for a Day 41
Fig. 3.4 Energy Management Strategy for Micro-grid under ToU Tariffs 43
Fig. 3.5 DG and SoC without Energy Management Strategy (Case 3.a)..... 44
Fig. 3.6 DG and SoC with Energy Management Strategy (Case 3.b)..... 44
Fig. 3.7 Battery & Grid's Energy, and Grid's Tariff Variation in a Year (Case 3.b) 44
Fig. 3.8 Variation of CoE and Battery Energy Throughput with ToU..... 46
Fig. 3.9 Daily Variation of Electricity Selling Price to Grid..... 47
Fig. 3.10 Energy Bill Saving with Electricity Selling Prices to Grid..... 47
Fig. 3.11 CoE and Battery Energy Throughput at Selling Prices to Grid 48
Fig. 3.12 Variation of CoE with PV, Battery and Fuel Cost..... 50
Fig. 3.13 Impact of Battery Capacity on CoE, NPC, Battery Throughput and Fuel

.....50

Fig. 4.1 Schematic of Skagerak Arena Load Configuration with Grid (Case 4.a) 55
Fig. 4.2 Avg. Daily Load Profile for Year 2015 to 2018 56
Fig. 4.3 Load Variation in Year 2018.....56
Fig. 4.4 Energy Contribution from the Grid Throughout the Year 57
Fig. 4.5 Block Diagram of Micro-grid at Skagerak Arena, Norway (Case 4.b) 58
Fig. 4.6 Energy Management Strategy for Micro-grid Operation (Case 4.b) 61
Fig. 4.7 PV Generation Profile Throughout the Year 62
Fig. 4.8 Energy Demand, Grid Limit and Energy, Demand Rate (Case 4.b).....63
Fig. 4.9 Annual Variation of Battery's SoC (Case 4.b) 63
Fig. 4.10 Peak Energy Demand from Grid for Cases 4.a and 4.b 64
Fig. 4.11 Energy from Grid & PV, and Battery Energy Throughput (Case 4.b) .65
Fig. 4.12 Energy Contribution from 1-15 Days of July (Case 4.b).....65
Fig. 4.13 Energy Contribution from 16-31 Days of July (Case 4.b).....66
Fig. 4.14 Energy Contribution from 1-15 Days of December (Case 4.b) 67
Fig. 4.15 Energy Contribution from 16-31 Days of December (Case 4.b) 67
Fig. 4.16 A Typical Day Profile of the July (Case 4.b).....68
Fig. 4.17 Battery Energy Throughput and Saving (Case 4.b) 69
Fig. 4.18 Cost Comparison of Micro-grid's Components.....70
Fig. 4.19 Net Cashflow Summary of Different Components.....71
Fig. 4.20 Specific Energy of PV at Selected Locations of India & Norway.....72
Fig. 4.21 Specific Energy Per Day of PV in India 73
Fig. 4.22 Specific Energy Per Day of PV in Norway.....73
Fig. 4.23 Energy Contribution without and with Micro-grid System in India....74
Fig. 4.24 Energy Contribution without and with Micro-grid System in Norway74
Fig. 4.25 Monthly Battery Energy Throughput in India and Norway.....75
Fig. 4.26 Variation of Battery' SoC 75
Fig. 5.1 Hourly Variation of the Electricity Energy Prices for Years 2015 and 2018.....80
Fig. 5.2 Variation of Different Energy Tariff.....81
Fig. 5.3 Energy Management Strategy for Micro-grid Operation.....85
Fig. 5.4 Energy from PV, Grid and Battery @100% Tariff (Case 5.a).....86
Fig. 5.5 Energy from PV, Grid and Battery @200% Tariff (Case 5.e).....86
Fig. 5.6 Variation of CoE and Battery Energy Throughput with Different Tariffs

.....88
Fig. 5.7 Monthly Electricity Bill with Different Energy Tariffs 88
Fig. 5.8 Variation of Energy Sold to the Grid with Diferent Energy Tariffs 89
Fig. 5.9 Energy from PV, Grid & Battery, Grid Selling Price @100% (Case 5.f) 90
Fig. 5.10 Energy from PV, Grid & Battery, Grid Selling Price @200% (Case 5.j) 90
Fig. 5.11 CoE and Battery Energy Throughput with Different Grid Selling Prices 91
Fig. 5.12 Monthly Electricity Bill with Different Grid Selling Prices 92
Fig. 5. 13 Energy Sold to the Grid with Diferent Grid Selling Prices 92
Fig. 5.14 Variation of CoE with PV, Battery and Grid Traiffs 94
Fig. 5.15 Changes on CoE with Different Grid Buying Prices 96
Fig. 5.16 Changes on CoE with Different Selling Price to Grid 96
Fig. 5.17 Micro-grid Component's Cost for India (left) and Norway (right) 97
Fig. 6.1 Line Diagram of MV CIGRE Electrical Network 103
Fig. 6.2 A Typical Load Profile.....104
Fig. 6.3 Variation of Bus Voltages in Group A of Case 6.a.....105
Fig. 6.4 Variation of Line Loading of Group A of Case 6.a 105
Fig. 6.5 Variation of Bus Voltages of Group B of Case 6.a.....106
Fig. 6.6 Variation of Line Loadings of Group B of Case 6.a 106
Fig. 6.7 Variation of Bus Voltages of Group C of Case 6.a.....107
Fig. 6.8 Variation of Line loadings of Group C of Case 6.a 107
Fig. 6.9 Variation of Transformers Loading of the Typical Day of Case 6.a 108
Fig. 6.10 Flow Diagram for Estimating HC of the Network.....110
Fig. 6.11 Hosting Capacity without and with Loading 111
Fig. 6.12 Laboratory Testing Setup of and PHIL.....113
Fig. 6.13 PV, Battery and PV+ Battery Profiles 114
Fig. 6.14 Variation of Bus Voltages of Group A of Case 6.b 115
Fig. 6.15 Variation of Line Loading of Group A of Case 6.b 115
Fig. 6.16 Variation of Bus Voltages of Group B of Case 6.b 116
Fig. 6.17 Variation of Line Loadings of Group B of Case 6.b.....116
Fig. 6.18 Variation of Transformers Loading of Case 6.b 117
Fig. 6.19 The Q-V Droop Characteristics 118
Fig. 6.20 Reactive Power from PV Connected at B_7, B_8, B_9 and B_{10}.....119
Fig. 6.21 Variation of Bus Voltages of Group A of Case 6.c 120

Fig. 6.22 Variation of Line Loading of Case A of Case 6.c 120
Fig. 6.23 Variation of Bus Voltages of Group B of Case 6.c 121
Fig. 6.24 Variation of Line Loadings of Group B of Case 6.c 121
Fig. 6.25 Variation of Transformers Loading of Case 6.c 122
Fig. 6.26 Bus Voltages of Group A in Case 6.d 124
Fig. 6.27 Bus Voltages of Group A in Case 6.e 124
Fig. 6.28 Line Loading of L_{2-3} for Cases 6.b, 6.d and 6.e 125
Fig. 6.29 Bus Voltages of Group B in Case 6.d 125
Fig. 6.30 Bus Voltages of Group B in Case 6.e 126
Fig. 6.31 Line Loading of Line L_{3-8} for Cases 6.b, 6.d and 6.e 126
Fig. 6.32 Bus Voltages of Group C for Case 6.d 127
Fig. 6.33 Bus Voltages of Group C for Case 6.e 127
Fig. 6.34 Line Loading of L_{13-14} for Cases 6.b, 6.d and 6.e 128
Fig. 6.35 Loading of Transformer T_1 for Cases 6.b, 6.d and 6.e 128
Fig. 6.36 Loading of Transformer T2 for Cases 6.b, 6.d and 6.e 129
Fig. A.1 Rated Power vs. Fuel Consumption Curve of a Diesel Generator 137

List of Tables

Table 2.1 Energy Supply and Electricity Bill Summary of Case 2.a 17
Table 2.2 Comparative Results of Cases 2.a & 2.b 32
Table 2.3 Economic Performance of the Case 2.b 33
Table 2.4 Net Present Cost of the Different Components in the Case 2.b 34
Table 3.1 Economic Results without & with Energy Management Strategy..... 45
Table 4.1 Energy Supply and Electricity Bill Summary of Case 4.a 57
Table 4.2 Economic Results Comparison of Case 4.b with Case 4.a 71
Table 5.1 Performance Results of Micro-grid with Different Grid Tariffs..... 87
Table 5.2 Economic Performance of Micro-grid with Different Selling Prices . 91
Table 5.3 Economic Performance of the Case 2.b and Case 4.b..... 95
Table 6.1 Hosting Capacity of Each Bus in a Distribution Network 111

List of Abbreviations

BES	Battery Energy Storage
BIPV	Building Integrated Photovoltaic
CoE	Cost of Energy Generation
DERs	Distributed Energy Resources
DG	Distributed Generator
HC	Hosting Capacity
INR	Indian Rupee
kV	kilovolt
kVA	kilovolt-Ampere
kW	kilowatt
kWh	kilowatt hours
kWp	kilowatt-peak
LHV	Lower Heating Value
LV	Low Voltage
m_{fuel}	Mass Flow Rate of Fuel
MV	Medium Voltage
MVA	Mega Volt Ampere
MVAr	Mega Volt Ampere Reactive Power
MWh	Megawatt Hour
NOK	Norwegian Krone
NPC	Net Present Cost
PHIL	Power Hardware in Loop
PV	Photovoltaic
Q-V	Reactive Power vs. Voltage
RTDS	Real Time Digital Simulator
SoC	State-of-Charge
ToU	Time-of-Use
ZEB	Zero Energy Building

Chapter 1

1. Introduction

The grid connected institutional photovoltaic (PV) based energy systems are increasing, and they are creating an opportunity to operate them as micro-grid [1.1]. The PV based institutional energy system integrated with battery energy storage and distributed generators have large potential to function as microgrid in the grid-connected mode as well in the islanding mode. However, the integration of large number of solar PV system within the distribution network are creating many technical challenges (e.g. voltage quality, power quality, techno-economic operations, etc.). It is imperative for such micro-grid systems to maintain the power quality, reliability and optimize the energy supply according to the load characteristics. The specific characteristics of a micro-grid system are described in the literatures [1.2] along with their key functionalities e.g. operational modes, control architectures, protection mechanism etc. A micro-grid system has to be integrated within the low voltage (LV) or medium voltage (MV) distribution network with appropriate operational architecture. Within the micro-grid, distributed energy sources need to have appropriate energy storage for providing the controllable and dispatchable power, and to contribute to the demand-side-management. A micro-grid system design should consider autonomy during the grid outage conditions for ensuring uninterrupted and reliable electricity supply to the load [1.3]. The micro-grid systems should be inter-operatable with the existing electrical grid network infrastructure, and it should contribute in making the overall system more stable, reliable and sustainable. There are variety of micro-grid's applications from small off-grid system for rural electrification to the large industry applications, and these systems can be easily scalable according to the demand and availability of local distributed energy resources (DERs) [1.4]. The sizing and selection of DERs are important for operating as a micro-grid system with integration of intermittent renewable energy resources, and it is necessary to operate micro-grid with appropriate energy management strategies for effective utilization of DERs [1.5]. The energy management strategies can effectively contribute in developing micro-grid architecture as well as controlling the energy flow through intelligent power conditioning devices. Such type of micro-grids can be operated using AC micro-grid architecture, and it can contribute in regulating the operational frequency and voltage within the micro-grid during grid connected

as well as in the islanded modes [1.6]. While design and developing a micro-grid system, it is very essential to consider different aspects (e.g. techno-economic sizing, appropriate energy management strategy, geographical locations, grid constrains and electricity energy pricing dynamics) and analyze their impacts for improving the operational performance of the micro-grid system.

1.1. State-of-Art Literature Review

The optimum selection of DERs is important for operating it as a micro-grid system for reliable, secure, and stable operation. The selection of appropriate DERs should be done based on the geographical locations and the load demand. Sizing of DERs along with the battery, based on maximum utilization of local distributed energy resources, have been presented in ref [1.7], but grid outages scenarios have not considered. A techno-economic sizing of off-grid renewable energy system has been presented for supplying the electricity to a rural community in the Sri Lanka [1.8]. Although the ref. [1.8] has found the economic viability of the RE based system for off-grid applications, but seasonal techno-economic performance analysis has not been reported. It has been reported in ref. [1.8] that the battery capacity based on the seasonal load profile may not contribute efficiently throughout the year, and similarly battery capacity estimated by using annual load profile may not perform well for remaining period of the year. A techno-economic study of a residential community in Beijing (China) has investigated a micro-grid for fulfilling local energy demand, with maximizing contribution from local sources [1.9], but battery energy throughput and grid outages scenarios are not considered. In several previous studies [1.7-1.10], optimal size of a renewable energy systems has examined based on average hourly daily load profile, or monthly average daily load. Also, in ref [1.11] the monthly average daily demand profile has considered, however the temporal position of peak demand in the profile remain has kept fixed. In another study [1.12], only the average energy consumption of an application is considered, when sizing a wind-PV-battery hybrid system. In most of the reviewed literatures [1.7-1.12], the presented approaches do not consider the grid outage scenario with maximum utilization of local distributed energy sources and battery energy contribution. Techno-economic sizing of distributed generator(s) with energy storage are required for operating grid connected renewable energy-based system as a micro-grid, even during the possible grid outage period.

Energy management strategies are required for operation of renewable energy based micro-grid to improve the techno-economic performance even during the non-expected grid outage conditions. The International Electrotechnical Commission (IEC) has published a standard IEC 61970, which defines the effective operation of electrical power system and to assure the adequate safety and reliability of energy supply at the minimum cost [1.13]. The IEC standards can be useful for developing energy management strategies for effective functioning of the DERs, and for managing them within the environment of micro-grid. Some of the energy management strategies have been presented for achieving the optimal energy generation cost and efficient operation of the micro-grid [1.14]. The impacts of electricity energy pricing dynamics on the operational performance of aggregated home energy management system with renewables is not sufficiently addressed in the ref [1.15]. A control strategy, based on demand side management, for micro-grid has been proposed in ref [1.16], for reducing the grid dependency through shifting of the operation of non-essential loads. The voltage / power ratios of different DERs have been considered to control the operation of the non-essential loads, and it has been reported that significant saving can be achieved [1.16] and operation of the micro-grid with grid constraint is not covered significantly, while integration of renewable energy system. To ensure the energy management and control in a micro-grid system, a control scheme has been proposed in ref [1.17] and demonstrated the micro-grid operation in grid connected and islanding modes, but maximum utilization of local energy resources has not addressed sufficiently. The energy management strategy using 'equivalent loss factor' has been presented [1.18], to minimize the system's cost and as well as to reduce the greenhouse gas emission but maximization of local energy sources with battery storage participation are not covered. Another, techniques have been implemented to achieve the minimum generation and environmental cost, considering operation and maintenance costs of the entire system [1.19], but market price variation of different technologies has not been addressed and its impact on the system cost has not been presented. In ref [1.20], technical characteristics of the system (e.g. phase angle, power balance data, etc.), are used to achieve the best economic solution, and electricity energy pricing dynamics are not sufficiently addressed. It has been observed that minimum cost of energy is calculated without maximizing the local energy production, which can increase dependency on the grid supply and compromise the system reliability, if grid outage occurs [1.21-1.22].

There are some other techniques e.g. scalarization, weighted average energy resources, which are also used to optimize the output of the local energy sources for micro-grid. Most of these techniques described in the literatures [1.15-1.22], are focused on cost minimization, environmental benefits with limited technical functionalities. The issues related to maximum penetration of local renewable sources (e. g. to maximize PV production) and DERs, optimum usage of energy storage along with minimum cost of electricity generation are not reported in the most of literature [1.15-1.22]. Appropriate energy management strategies should be researched with grid constraints and considering the maximum utilization of the DERs through battery energy throughput within the micro-grid environment.

During the last few years, electricity demand and energy pricings are increasing significantly, and especially for the commercial / institutional consumers [1.23]. The electricity distribution companies are introducing dynamic energy pricing (e.g. Time-of-Use (ToU) energy tariffs, real time tariffs, power tariffs, seasonal energy pricing, etc.) for reducing the peak demand [1.23]. The ToU electricity tariffs can provide consumers some reward-risk profile; however, the real-time energy pricing can offer more incentive, but may be at some risk (e.g. rebound effect, etc.) [1.24]. It has reported by the American Council for an Energy-Efficient Economy (ACEEE) that the demand response programs along with a reduction in the peak demand has saved around 200 billion kWh unit of electricity in the US during 2015 [1.25]. In ref. [1.26], economic performance of building integrated photovoltaic system (BIPV) with and without energy storage has evaluated under energy pricing and grid constraints for a typical residential household located at southern Norway, but it has not sufficiently included the energy management strategies for operation of BIPV with energy storage. A Time-of-Use (ToU), pricing tool is recommended for the electricity utility companies to encourage the customers for reducing their loads during the peak hours and achieve the potential of saving in the electricity bill [1.27]. The significant annual electricity bill saving, and emission can be achieved for a typical BIPV house [1.28], however, the techno-economical operational energy performance should be significantly elaborated under market energy pricing dynamics. The market-energy pricing dynamics is going to impact the micro-grid operation and energy management within the distributed network.

The industries' / institutions' energy system can be operated in coordination with local renewable energy sources as a micro-grid, considering market energy pricing as well as grid constraints [1.29]. The demand side management strategies

are used for controlling the operation of non-essential power intensive loads (e.g. thermal load), and it has been demonstrated in the EU FP7 project 'Scalable Energy Management Strategies for Households' [1.15], but the energy tariffs and renewable energy integration with energy storage have not appropriately considered. In Anhui province in China, the impact of increase in the ToU energy tariffs as well as block tariffs for demand side management on residential customers have been reported for finding an opportunity of BIPV system [1.30].

It has been reported in ref. [1.31-1.33] that the market energy pricing dynamics are going to affect the operation and performance of distributed network with renewable energy systems, and energy management strategies can play very important role during the market energy pricing dynamics. In most of the available literatures [1.21-1.33], the techno-economic evaluation of institutional PV based micro-grid, considering implementation of market energy pricing dynamics in the operational energy management strategies have not significantly analyzed for maximum utilization of local DERs even during the grid outage as well as contribution for peak demand reduction.

The operational performance of PV based micro-grid system is significantly affected by the local meteorological conditions (e.g. solar irradiance conditions, temperature, wind speed, etc.). In the last few years, many studies [1.7-1.33,] have evaluated PV system performance for different geographical regions, but they have not sufficiently addressed the techno-economic performance of the grid integrated PV based micro-grid. However, some studies [1.1, 1.15, 1.26, 1.34] have reported operation of PV based micro-grid in the Nordic climatic conditions, but they have not adequately considered electrical energy market dynamics and maximizing the use of local energy resources with battery energy throughput. Within the Nordic countries, Norway is using mainly hydroelectricity (i.e. 96%), but in the recent years PV market is growing rapidly [1.34]. The installed cumulative PV capacity in Norway has reached 119.8 MWp at the end of 2019, and it was only 15.3 MWp at the end of 2015[1.35]. It indicates that the PV market has increased eightfold in the last five years. It is mainly due to National policy such as Plusskundeordningen, subsidy payouts for small solar PV installations, etc. The BIPV system for a typical South Norwegian household has been studied for economic sizing of energy storage [1.36], but local energy management through battery energy throughput has not been considered. Thermal load management can be used for demand side management [1.37], but the battery energy system can contribute more effectively for electrical energy supply and demand management.

The increasing PV penetration as well as energy market dynamics of the Norwegian system can contribute for local energy management for institutional systems to operate as micro-grid [1.34-1.37].

The most of PV based micro-grid system systems are integrated in low voltage (LV) or medium voltage (MV) distribution network. Due to the limitation of the distribution power system, a certain capacity of PV can be incorporated within the network. It is important to analyze the PV hosting capacity (HC) without violating the network limits and without making any further modifications within the existing distribution network infrastructure [1.38]. HC of an electrical network can be determined using power flow methods with consideration of network parameters. The voltage, reverse current flow, short circuit current, line loadings etc. are some of the network parameters can be considered, while examining the HC of PV system to be integrated within the distribution network. Few studies [1.39-1.40] have attempted the estimation of HC in the distribution network and they have categorized in two groups: (i) study presented in ref [1.39] proposed a methodology based on grid performance and load characteristics, and (ii) study [1.40] is used to predict the impacts on operation and future planning of electrical network. Both types of studies have considered performance parameters of distribution network measures (e.g. bus overvoltage, line overloading, or power quality etc.), and estimated the HC of distributed generation that could be connected to the individual bus. Impacts of harmonic distortion due to HC have been explained in the ref [1.41]. The HC calculations depend on the network parameters, however very few studies [1.42] have considered only daily generation profiles of the DERs and not evaluated impact on network performance considering key technical parameters. Therefore, it is very essential to analyze the HC within the distributed network considering daily load profiles, DERs generation with impact on key operational parameters of the distributed network performance.

There are many challenges for increasing the penetration of PV into distributed network, as it has raised operational and control difficulties within the micro-grid [1.43-1.45]. In ref [1.46], PV penetration study has conducted by the Department of Energy's SunShot Program, and it is reported that the voltage at the PV plant, close to a capacitor bank, surpasses the 1.05 p.u. during daytime, when the PV generation is maximum. But the study [1.46] didn't examine the potential mitigation techniques. A PV impact analysis study for urban LV network in Sri Lanka has reported in ref [1.47], and mentioned the feeder voltage rise during

daytime and when the energy demand is lower. But it [1.47] has not provided any mitigation techniques. In ref [1.48], the major impacts of PV integration have been presented for power quality issues, protection relays etc., but daily load and generation profiles are not effectively considered. Some countries have implemented few technical solutions at the power conditioning device level (e.g. PV inverter) to address problems related to high PV penetration. In Germany, to overcome over-voltage events, from January 2012, a fixed limitation of the active power (i.e. 70% of the nominal peak-output power of the PV system) feed-in by each PV system has become mandatory [1.49]. Some other alternative solutions to curtailment of active power by domestic load shifting, to increase local consumption, and energy storage are discussed in ref. [1.50]. Impact of increasing penetration of PV based micro-grid on distribution network are not sufficiently evaluated considering the daily load and PV generation profiles. Also, the mitigation techniques to keep the network performance parameters within the limits have not been presented sufficiently with some testing results using real time digital simulator. Integration of distributed energy sources via intelligent power conditioning devices within the micro-grid can help in controlling the power dispatching from the DERs for effective power management within the micro-grid, as well as in improving the power quality, stability and control within the distributed network. It is significantly important to investigate and analyze the potential issues with high PV system penetration in the distribution networks and implement some of the mitigation techniques (e.g. reactive power versus voltage droop functionality, etc.) which can contribute in addressing some of the challenges (e.g. voltage deviation, line loading limits, etc.).

To develop a reliable, cost effective, efficient, and sustainable PV based micro-grid system, some of the key aspects (e.g. techno-economic sizing, appropriate energy management strategy, geographical locations, grid constrains and electricity energy pricing dynamics, distributed network performance, etc.) need to be considered. Appropriate techno-economic sizing of the grid connected micro-grid system is very important for reducing the local energy generation cost of DERs as well as increase utilization of local energy sources even during the grid outages conditions. The role of energy management strategy becomes very essential for effective operation of PV based micro-grid system under energy pricing dynamics and grid constraints. To increase penetration of PV based micro-grid within the distributed network, hosting capacity analysis and appropriate mitigation technique(s) are to be implemented and tested using proper platform.

1.2. Research Objectives

Based on identified research gaps through state-of-art literature review, following are the key objectives of the thesis:

- Techno-economic sizing of renewable energy sources for grid connected system to operate as a micro-grid with anticipation of frequent grid outage conditions to supply the reliable power within micro-grid.
- Development of micro-grid operational energy management strategies with minimization of energy generation cost of local resources.
- To maximize the local resources energy utilization through appropriate energy management strategies by enhancing the local energy storage participation with consideration of grid power shortage.
- To improve the operational performance of institutional energy system through micro-grid by reducing the grid dependency (e.g. islanding, peak reduction, etc.) and enhancing the distributed generator(s) participations
- Impact of electrical energy pricing dynamics on techno-economic operation of micro-grid and participation of local energy resources with micro-grid energy generation cost.
- Influence of geographical locations and local grid conditions on techno-economic performance of the renewable energy (e.g. PV based) micro-grid with regional electrical energy market pricing mechanism.
- Hosting capacity analysis within the distributed power network for maximizing the penetration of PV based micro-grid.
- Evaluation of operational performance (e.g. voltage quality) within the distribution network due to increasing penetration of PV based micro-grid.
- Mitigation technique (e.g. reactive power versus voltage droop functionality) for improving operational performance (e.g. voltage quality) of the distribution network with increasing penetration of PV based micro-grid.

1.3. Thesis Organization

The presented work has been organized in seven chapters. The **Chapter 1** has covered the state-of-art literature review for identifying key research objectives of the work.

Chapter 2: In this chapter, techno-economic sizing of renewable energy based distributed generators for operating as a micro-grid has presented,

considering a typical case. The energy management techniques have been presented for minimizing the grid contribution and energy cost of locally generated electricity with maximization of PV contribution and battery energy throughput to meet the institutional load demand.

Chapter 3: In this chapter, the impact of the electricity energy pricing dynamics on techno-economic performance of a typical institutional micro-grid system from India is studied. Operational energy management strategies for grid connected PV based micro-grid functioning has been presented and evaluated for maximizing the local energy resources utilization with contemplation of peak demand even under grid outage conditions and market energy pricing dynamics.

Chapter 4: In this chapter, a functioning PV based micro-grid from the Norwegian climatic conditions is considered for techno-economic performance analysis. Also, techno-economic comparative performance analysis of PV based micro-grid with and without energy management strategies for Indian and Norwegian climatic conditions are presented.

Chapter 5: Impacts of geographical locations (i.e. India and Norway) and local grid constrains on the operation of the micro-grid system has been presented in this chapter. The focus has been to compare the local energy resources maximum use with contemplation of peak demand under energy pricing dynamics.

Chapter 6: In this chapter, the hosting capacity of a selected distribution network is presented considering voltage or/and voltage and loading as constraints. This chapter has further presented voltage quality problems due to increasing penetration of PV based micro-grid, while operating the selected buses at maximum hosting capacity. Appropriate mitigation techniques have been presented with testing results using platform to keep the network performance parameters within the limits.

Chapter 7: This chapter concludes the key findings of this work. Suggestions for future work have also presented.

Chapter 2

2. Energy Management Strategies for Techno-Economic Assessment of PV Based Institutional Micro-Grid[1]

2.1 Summary

Building integrated photovoltaic (PV) system with energy storage within an institution may need appropriate coordination among distributed energy resources (DERs). It is required to have an appropriate energy management strategy to improve the system performance as well as to operate it as a micro-grid even during the grid outage condition. In this chapter, an institutional energy system has been used, and its performance with distributed generator(s) has been assessed with operational strategies for fulfilling the institutional load demand in coordination with the PV, grid and battery storage; and with possibility of operating it as a micro-grid even during the grid outage period too. The energy management techniques have been proposed for minimizing the grid contribution and energy cost of locally generated electricity with maximization of PV contribution, and battery energy throughput to meet the institutional load demand. Techno-economic benefits have been investigated using proposed energy management strategy for operating an institutional energy system as a micro-grid.

2.2 Introduction

Deployment of Building Integrated Photovoltaic (BIPV) systems for institutional campus's building have been raised significantly around the world over the past few years. The BIPV system, integrated with battery energy storage, can be used as a dispatchable power source for operating the energy system as a micro-grid. Such type of systems requires to maintain the power quality, reliability and to optimize the energy supply according to the load characteristics within the micro-grid [2.1]. Micro-grid should have specific characteristics and they have been described in the literatures along with their key functionalities [2.2]. A micro-grid system can be integrated to the low voltage (LV) or medium voltage (MV) distribution network with appropriate control architecture. Within the micro-grid,

[1] This chapter is based on the peer reviewed journal paper, A. Sharma, *et.al.*, 'Performance Assessment of Institutional Photovoltaic based Energy System for Operating as a Micro-grid, *Sustainable Energy Technologies and Assessments* (Elsevier), vol.37, pp. 1-13, 2020. Doi: 10.1016/j.seta.2019.100563.

distributed energy sources need to have appropriate energy storage for providing the controllable power within the micro-grid and to participate in the demand side management. A micro-grid system design should consider enough days of autonomy during the grid outage conditions for ensuring uninterrupted electricity supply [2.3]. The micro-grid systems should be compatible with the existing electrical grid network infrastructure, and it should make the overall system more stable, reliable, and sustainable. There are variety of micro-grid's applications from small off-grid system for rural electrification to the large industry applications, and these systems can be easily scalable according to the demand and availability of local distributed energy resources (DERs). The selection of appropriate DERs is done based on the geographical location and the load demand. The optimum selection of DERs is important for operating it as a micro-grid system for reliable, secure and stable operation [2.4]. To operate the micro-grid, it is necessary to develop appropriate energy management strategies for effective utilization of DERs. The energy management strategies can effectively contribute for developing micro-grid architecture and accordingly going to contribute in the intelligent operation of the power conditioning devices of the DERs in coordination with the load. Such type of systems can also be operated using AC micro-grid architecture, and it can regulate the frequency and voltage within the micro-grid during grid connected as well as in the islanded modes [2.5-2.6].

The techno-economic sizing of DERs for an institutional load is important to operate it as a micro-grid and sizing of DERs along with the battery, based on energy maximization of local distributed energy resources. A techno-economic sizing of off-grid renewable energy system has been presented for supplying the electricity to a rural community in the Sri Lanka [2.7]. Although the paper [2.7] has found the economic viability of the RE based system for off-grid applications, but seasonal performance analysis has not been reported. It has been reported in ref. [2.8] that the battery capacity based on the seasonal load profile may not contribute efficiently throughout the year, and similarly battery capacity estimated by using annual load profile may not perform well for other seasons of the year. It is mainly due to the improper sizing and the lack of energy management strategy, and coordination among the different DERs and the battery energy storage.

The use of appropriate energy management strategy is very useful for effective utilization of battery and other DERs. The International Electrotechnical Commission (IEC) has published a standard IEC 61970, which defines the effective operation of electrical power system and to assure the adequate safety of

energy supply at the minimum cost [2.9]. The IEC standards can be useful for developing energy management strategies for effective functioning of the DERs, and for controlling them within the environment of micro-grid. Some of the energy management strategies have been presented for achieving the optimal energy generation cost and efficient operation of the micro-grid [2.10].

A control strategy, based on demand-side-management, for micro-grid has been proposed in ref [2.11], for reducing the grid dependency through shifting of the operation of non-essential loads. The voltage / power ratios of different DERs have been considered to control the operation of the non-essential loads, and it has been reported that significant saving can be achieved [2.11]. Appropriate energy management strategies should be developed for effective demand side management with grid constraints and considering the maximum utilization of the DERs as well, within the micro-grid environment [2.12]. The demand side management strategies can be used for controlling the operation of non-essential power intensive loads (e.g. thermal load) and it has been demonstrated in the EU FP7 project Scalable Energy Management Strategies for Households [2.12].

To ensure the power management and control in a micro-grid system, a supervisory control scheme has been proposed in ref [2.13] and has demonstrated in the operation of grid connected and islanding modes. The energy management strategy using 'equivalent loss factor' has been presented [2.14], to minimize the system's cost and as well as to reduce the greenhouse gas emission. Another, techniques have been implemented to achieve the minimum generation and environmental cost, considering operation and maintenance costs of the entire system [2.15]. In this study, market price variation of different technologies has been considered and its impact on the system cost has been analyzed. In ref [2.16], technical characteristics of the system e.g. phase angle and power balance data, are used to achieve the best economic solution. There are other techniques e.g. scalarization, weighted average energy resources, which are also used to optimize the output of the local energy sources for micro-grid. Most of the techniques described above, are focused on cost minimization, environmental benefits with limited technical functionalities of the system [2.13-2.18]. The issues related to maximum penetration of local renewable sources (e. g. maximize PV production) and DERs, optimum usage of energy storage along with minimum cost of electricity generation are not reported in the above-described literatures. It has been observed that minimum cost of energy is calculated without maximizing the local energy production, which can increase dependency on the grid supply and

compromise the system reliability, if grid outage occurs [2.19-2.20]. The main aim of this paper is to propose energy management strategy(s) while considering the minimum cost of generation with more use of local PV production and to enhance the battery energy participation (i.e. battery energy throughput) within the micro-grid.

In this work, a typical energy system integrated with distributed generator (DG) and grid, is described and techno-economic sizing for PV and battery energy storage is presented in the Section 2.3. In the Section 2.4, the energy management techniques are proposed with integration PV and battery energy storage for improving the energy system performance by minimizing the grid and DG energy contribution well as levelized cost of locally generated electricity with maximization of the PV contribution to meet the institutional load demand. The performance assessment of the considered energy system with PV & battery energy storage, have been analyzed in the Section 2.5. Economic performance of the considered energy system (i.e. without and with PV and battery) have been compared and analyzed in the Section 2.6. Conclusion and further improvement for operation of described energy system especially during grid outage time has been presented in the Section 2.7.

2.3 Description of Energy System with Grid and DG (i.e. Case 2.a)

In this work, a typical Indian institutional energy system is considered as a base case scenario (i.e. Case 2.a) from the region of Haryana, India. A typical institutional load profile (i.e. non-domestic type) of 50 kW at LV distribution network is taken for the analysis purpose. In order to meet the institutional demand, grid supply is primarily available however, to address the grid outages conditions a 50-kVA diesel generator (DG) is considered. A typical power capacity vs. fuel consumption curve of a DG set at different load factors is used [2.21-2.24]. The block diagram of considered PV and battery-based grid connected system is shown in the Fig. 2.1.

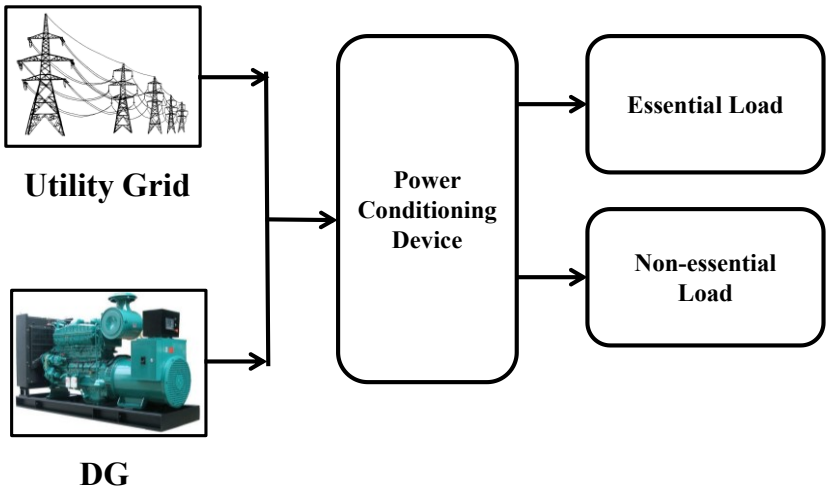

Fig. 2.1 Schematic of Energy System with DG and Grid (i.e. Case 2.a)

The typical institutional load profile of maximum 50 kW (taken as 1 p.u.) is classified into the essential and non-essential loads. The illustration of total load with essential part is shown in the Fig. 2.2. The essential loads are operated for all the time, and non-essential loads are turned off during the grid outage conditions. The value of 'average annual daily essential load' and 'average annual daily non-essential load' are 266 kWh/day and 114 kWh/day respectively. The annual total energy demand is 135,173 kWh. As per the classification of the regional electricity distribution company (i.e. Dakshin Haryana Bijli Vitran Nigam (DHBVN)), the months 'April-September' are representing as the summer season, however the months 'October-March' represent the winter season [2.25]. The average load for the summer season is 24% higher than the average load of winter season.

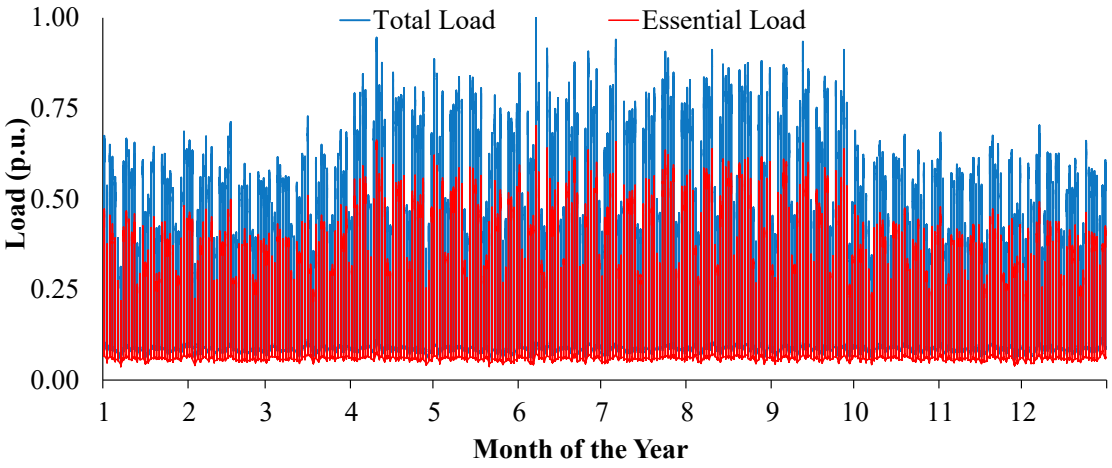

Fig. 2.2 Yearly Load Variation

The typical institutional load has more energy consumption during working days (i.e. Monday to Friday) as compare to the weekend (i.e. Saturday and Sunday) [2.26]. A typical weekly load profiles (first week of January) has shown in the Fig. 2.3.

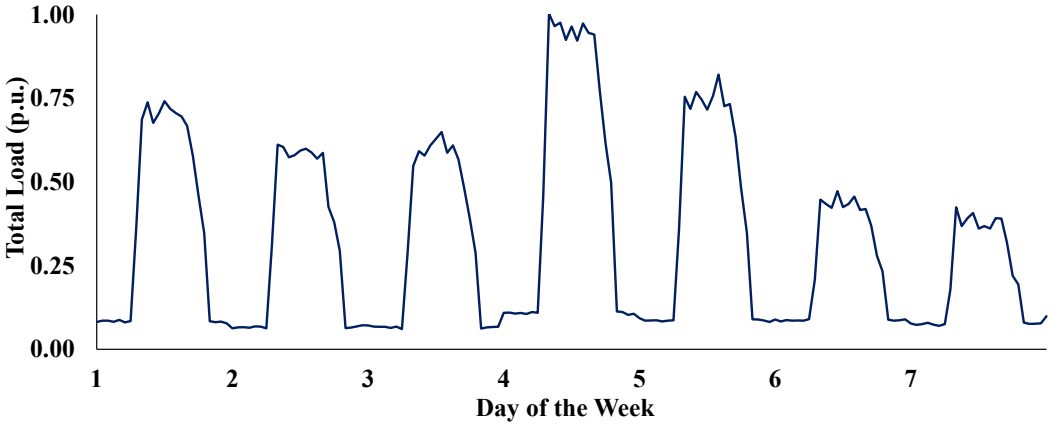

Fig. 2.3 Hourly Variation of the Total Load of a Typical Week

2.3.1 Results & Analysis of Case 2.a

It has been assumed that total load demand has met by the Grid, and during the grid outage from the DG. Two hours of grid outage per day has taken into consideration and it has random time distribution throughout the year. It has discussed with DHBVN to represent realistic scenario. It has been analyzed from the results that the annual energy contributions from the Grid and DG to meet the demand of the institutional load are 87.3% and 12.7% respectively. The annual energy contribution from the Grid and DG are shown the Figs. 2.4 and 2.5 respectively.

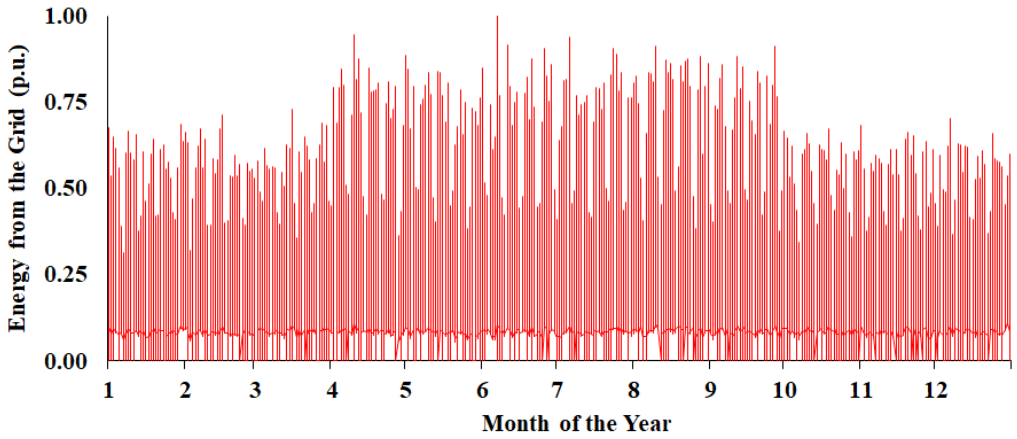

Fig. 2.4 Energy Contribution from Grid Throughout Year (Case 2.a)

Fig. 2.5 Energy Contribution from DG Throughout Year (Case 2.a)

Since the load demand is more during the summer season, it has been observed that during the summer season, the grid contribution is 12% more than to the winter season. However, DG contribution is 11% more in the winter season compare to the summer season.

For the economic analysis, the project lifetime of 25 years, discount rate 6.25%, inflation 4.25%, grid buying price 12.15 INR, and fuel cost of 70 INR/ lit are considered. The INR refers to the Indian currency in Rupees. The monthly electrical energy supply with peak demand as well as the electricity charges have summarized in the Table 2.1 for Case 2.a.

Table 2.1 Energy Supply and Electricity Bill Summary of Case 2.a

Month of the year	Energy Purchased (kWh)	Peak Load demand (kW)	Energy Charge (INR)	Demand Charge (INR)	Total Electricity Charge (INR)
Jan	9998	34	82986	5487	88473
Feb	8584	36	71244	5702	76946
Mar	9800	36	81343	5824	87167
Apr	11920	47	98938	7564	106501
May	11657	44	96752	7091	103843
Jun	11871	50	98529	8023	106552
July	11636	47	96579	7518	104097
Aug	12643	46	104940	7293	112233
Sep	11081	46	91973	7293	99266
Oct	9498	34	78835	5374	84208
Nov	9139	34	75853	5468	81320
Dec	9115	35	75651	5625	81276
Annual	126942	50	1053622	78261	1131883

Results, obtained from the Case 2.a, show that the DG's contribution is 12.7% of the total energy contribution and it has major contribution in increasing the CoE. The Case 2.a also indicates that there is lot of potential to reduce the grid, and DG contribution by integrating the local distributed energy sources e.g. PV system as the annual average solar radiation in Haryana region (India) is 5.2 kWh/m^2/day [2.27]. Therefore, integration of PV system along with appropriate battery storage can be one of the best options to use locally produce solar energy and to reduce the grid and DG dependency. The idea of integrating PV and battery energy storage within the institutional energy system is to operate it as a micro-grid and maximize the local energy resources utilization. However, appropriate sizing of PV and battery is very important to get best techno-economic value.

In this work, techno-economic sizing of the energy system at a typical institutional load has been estimated based on the 'lowest economic cost indicators' (i.e. Net Present Cost (NPC) and Energy Generation Cost (CoE)) to achieve the maximum PV energy contribution with appropriate sizing of the battery and DG. In this study, PV capacity has fixed to 50 kWp at latitude tilt. It has estimated that 120 kWh of lead acid battery bank has needed to meet the essential load demand during the grid outrage conditions, and the 30 kVA DG has considered for sufficient to meet the total load demand during the grid outage. In the analysis, the total energy throughput of 1 kWh battery is taken 840 kWh and battery overall efficiency to be 80% [2.26]. Two hours of grid outage per day has taken into consideration and it is randomly time distributed throughout the year [2.28].

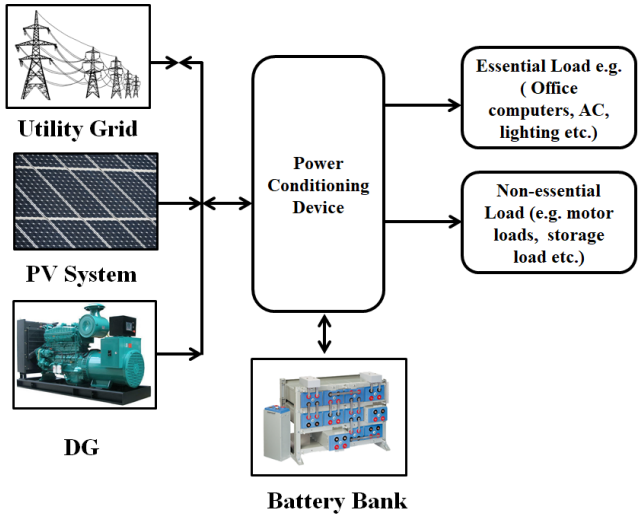

Fig. 2.6 Block Diagram of the Institutional Micro-grid System (Case 2.b)

After integrating the PV, battery energy storage and DG with the existing energy system (i.e. Case 2.a), the modified system (i.e. Case 2.b) has shown in the Fig. 2.6. In the next section (i.e. Section 2.4), the energy management strategy proposed, and its operation has been described in detail.

2.4 Energy Management Strategy for PV & Battery based Grid-Connected System

It is required to have appropriate energy management strategy for operating the system with techno-economic consideration after introducing a PV and battery for reducing grid and DG's dependency of the institutional load supply. Such type of system can have possibility to operate as a micro-grid. The main aim of this paper is to formulate the energy management strategy and to minimize the 'Annual Generation Cost' of DERs, and to minimize the grid and DG contribution for fulfilling the energy demand as well as to increase the energy reliability of the system, especially during the grid outage time. In this work, overall annual energy cost (i.e. $f_{(cost)}$) minimization approach has been used, and it has been explained through the Eq. (2.1).

$$\min f_{(cost)} = \sum_{t=1}^{T} \begin{bmatrix} [(P_{Grid}(t) * d(\Delta t)) * (E_{Grid}(t)] \\ +[(P_{PV}(t) * d(\Delta t)) * (E_{PV})] \\ +[(P_{Bat}(t) * d(\Delta t)) * (E_{Bat})] \\ +[(P_{Sell}(t) * d(\Delta t)) * (E_{Sell}(t)] \\ +[(P_{DG}(t) * d(\Delta t)) * (E_{DG})] \end{bmatrix} \quad \text{Eq. (2.1)}$$

where:

$P_{Grid}(t)$: Power bought from the grid at time t

$E_{Grid}(t)$: Grid electricity buying price at time t

$d(\Delta t)$: Time duration

$P_{PV}(t)$: PV power at time t

E_{PV}: PV energy generation cost

$P_{Bat}(t)$: Power from the battery at time t

E_{Bat}: Battery energy cost

$P_{Sell}(t)$: Power sold to the grid at time t

E_{Sell}: Grid electricity selling price at time t

$P_{DG}(t)$: Power from the DG at time t

E_{DG}: DG energy generation cost

T: Total cumulative time interval in a year

In this work, the upgraded system (i.e. Case 2.b.) is considered to operate in the grid-connected mode as well as in the islanding mode and therefore, all DERs along with the grid have been operated with the constraints using the operational limits. The details of considered constraints are explained in the following sub-sections.

Power Balance Through DERs

The power from all DERs along with the grid at time (t) is expressed in the Eq. (2.2).

$$P_{Grid}(t) + P_{PV}(t) + P_{Dis}(t) + P_{DG}(t) = P_{Load}(t) + P_{Chg}(t) + P_{Sell}(t) + P_{Loss}(t) \quad \text{Eq. (2.2)}$$

It should be noted that battery discharging has been taken as positive, whereas battery charging as negative. P_{Load} (t) and P_{Loss} (t) represent the total system's load and power loss at time t.

Grid Outage

In this work, the 'Grid-outage' has considered as a random distribution through pseudo-random time step for doing analysis. The selected inputs parameters are the "Main Failure Frequency", "Mean repair time (h)" and "Repair Time Variability (%)" [2.22]. In this work, two hours of grid outages (or load shedding) in a day, has considered [2.23]. The 2 hours grid outage per day is randomly distributed within the 24 hours period throughout the year. The limitation on the imported power from the grid has been described through Eq. 2.3.

$$0 \leq P_{Grid}(t) \leq Max.\, P_{Grid}(t) \quad \text{Eq. (2.3)}$$

Power from PV Array

The PV power output (P_{out}) has been calculated using solar radiation data from the US National Renewable Energy Laboratory (NREL) [2.28]. The PV power output ($P_{PV}(t)$) limits are given in Eq. 2.4.

$$0 \leq P_{PV}(t) \leq Max.\, P_{PV}(t) \qquad \text{Eq. (2.4)}$$

The detail description of the annualized energy cost calculation of the PV array has presented in Appendix I.

Battery Energy Storage

The minimum SoC of the battery is taken as 40% and initial SoC to be 100%. The battery energy content has been calculated using Eq. (2.2) and is expressed as battery energy throughput considering after charging and before discharging losses. The battery energy content limits are given in Eq. (2.5), and it has been described through Eqs. (2.6) and (2.7) for charging and discharging respectfully. The charging and discharging efficiency of the battery are η_{Chg} & η_{Dis} .

$$SoC_{min} \leq SoC(t) \leq SoC_{max} \qquad \text{Eq. (2.5)}$$

$$SoC(t + \Delta t) = SoC(t) + \eta_{Chg}.\, P_{Chg}(t).\, \Delta t \qquad \text{Eq. (2.6)}$$

$$SoC(t + \Delta t) = SoC(t) - \frac{P_{Dis}(t).\, \Delta t}{\eta_{Dis}} \qquad \text{Eq. (2.7)}$$

The key input battery parameters are 'battery capacity', 'battery voltage', 'depth of discharge', and 'lifetime throughput' have been explained in the previous sections. The detail description of the annualized energy cost calculation of the battery has been described in the Appendix I.

Power from the DG

In this work, the energy efficiency of a DG is taken as the ratio of electrical energy delivered by the DG to the chemical energy of the fuel going in (Eq. (2.8)) [2.21-2.24], where m_{fuel} and LHV_{fuel} are representing the mass flow rate of the fuel (kg/hr) and lower heating value of the fuel respectively. The detail description of the annualized energy cost calculation of the DG and rated power capacity vs. fuel consumption curve of a DG set at different load factors have given in Appendix I.

$$\eta_{DG} = \frac{3.6 * P_{DG}}{m_{fuel}.LHV_{fuel}} \qquad \text{Eq. (2.8)}$$

Working Principle of Energy Management Strategy

The proposed energy management strategy (as shown in the Fig. 2.7) is used and implemented for evaluating performance of the energy system of Case 2.b. The cost of electricity energy generation from the PV, battery and DG have been estimated and used for the selection of appropriate energy sources to meet the institutional load demand with grid energy supply and selling energy prices. As explained in the previous sections, the main aim of the energy management strategy is to minimize the annual generation cost and reduce grid contribution with maximizing the local PV production through battery energy throughput.

As illustrated in Fig. 2.7, the program starts at t=0 and it checked whether Grid is available or not. Even though grid is available, PV has given the main priority to fulfil the load demand. In case, the PV production is more than the load demand, the extra energy will be used to charge the battery (if $SoC(t) < SoC_{max}(t)$) or feed into the grid (if $SoC(t) = SoC_{max}(t)$). However, if the PV production is less comparing the load demand, then extra energy to meet the institutional load demand will be delivered by the battery (if, $E_{Bat}(t) < E_{Grid}(t)$) or by the grid supply (if, $E_{Grid}(t) < E_{Bat}$). Here, E_{Bat} and $E_{Grid}(t)$ are the cost of energy generation from the battery and grid respectively.

In case grid supply is not available, then the PV along with battery are used to fulfill the total load demand. In the proposed energy management strategy, lowest priority has been given to the DG, and it operates only when the PV along with battery could not provide enough power to meet the institutional load demand. In case, battery's SoC is reached below than 50% level and, no other sources are available to charge the battery then DG is initiated the battery charging, in addition to meet the load demand. In this work, selection of DERs is based on lowest energy generation cost and therefore it minimizes the overall energy generation cost of the system. The energy management techniques, proposed in this work, will also be useful to increase the annual battery energy throughput. The energy management strategy is considered in the upgraded system (i.e. Case 2.b.) at the institutional building to operate the entire system as a micro-grid and results are discussed in the subsequent Sections.

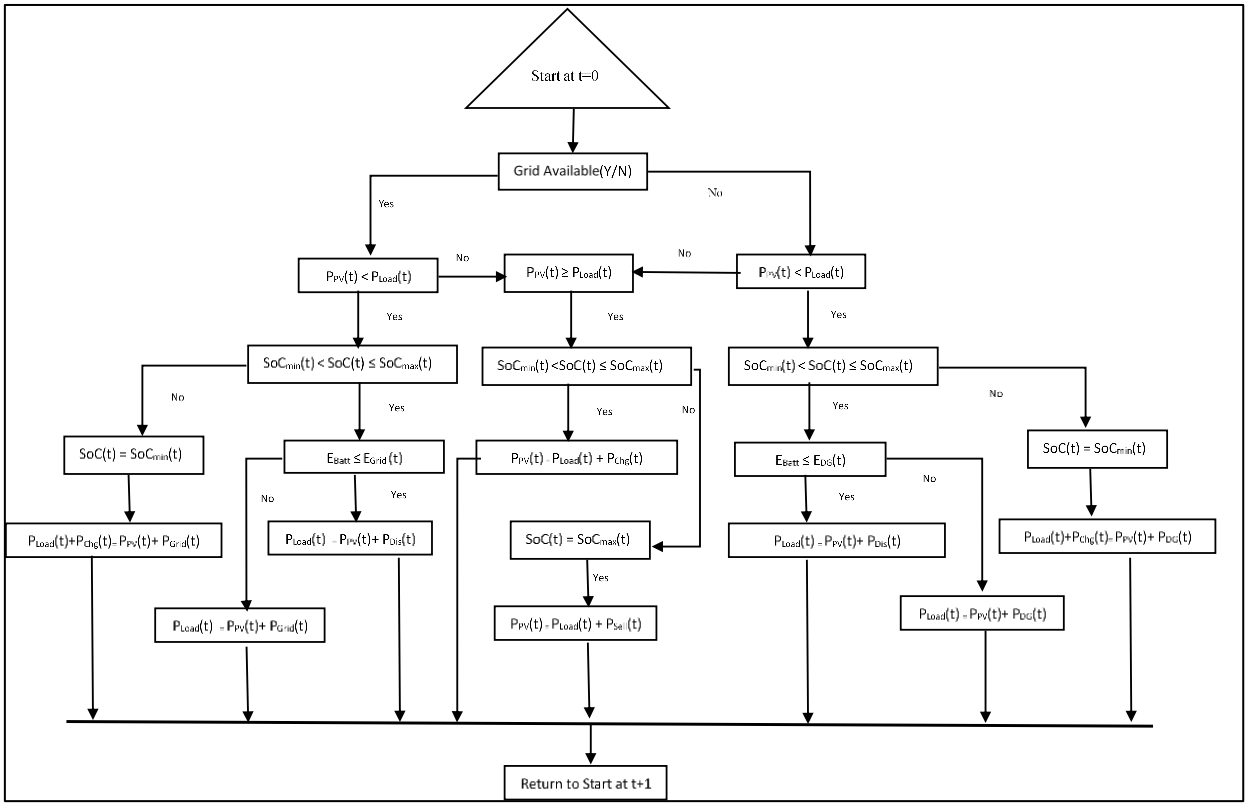

Fig. 2.7 Flow Chart of Energy Management Strategy for Micro-Grid (Case 2.b)

2.5 Results & Analysis of Case 2.b

The configuration of upgraded system consists of 50 kWp Solar PV, 120 kWh lead acid battery bank, grid supply and 30 kVA DG to meet the institutional load. A schematic of the Case 2.b system configuration has shown in the Fig. 2.6 (with PV and battery energy storage). Further analysis of the Case 2.b. is carried out for annual, selected months (i.e. best and worst month of the year), and for a typical day, and the results are discussed in the subsequent sub-sections. The ratio of 'average daily PV output' to 'average daily load' are used for defining the best and worst months for analysis purpose and represented by 'k'. It has been observed that the March month represented the best month of the year with ratio (k) 0.63; however, August month represented the worst month as the ratio (k) is 0.43. The initial SoC of the battery is considered at 100% and minimum SoC is taken 40%. The lifetime energy throughput of a 1 kWh battery is considered 840 kWh and battery roundtrip efficiency to be 80% [2.26]. The grid outage conditions and operating parameters for DG are same as for the described for Case 2.a and details are in the Section 2.3.1.

2.5.1 Annual Energy Contributions

The annual energy contribution from the Grid, PV, DG and battery's SoC for Case 2.b. are shown in the Figs. 2.8, 2.9, 2.10 and 2.11, respectively. It has been observed that annual energy contribution from the grid is 48%, PV 51% and DG 1%. It has been noticed that out of total local energy contribution, 96% is used to meet the load demand and remaining 4% is sold to the grid. It has been observed that the grid and DG's contributions are reduced by 39.3% and 11.7% respectively (Figs. 2.8 and 2.10) compare to the Case 2.a. The DG operates only 54 hours in a year and battery participates throughout the year. Only few instances battery's SoC has reached to the lowest level (i.e. SoC 40%) (Fig. 2.11).

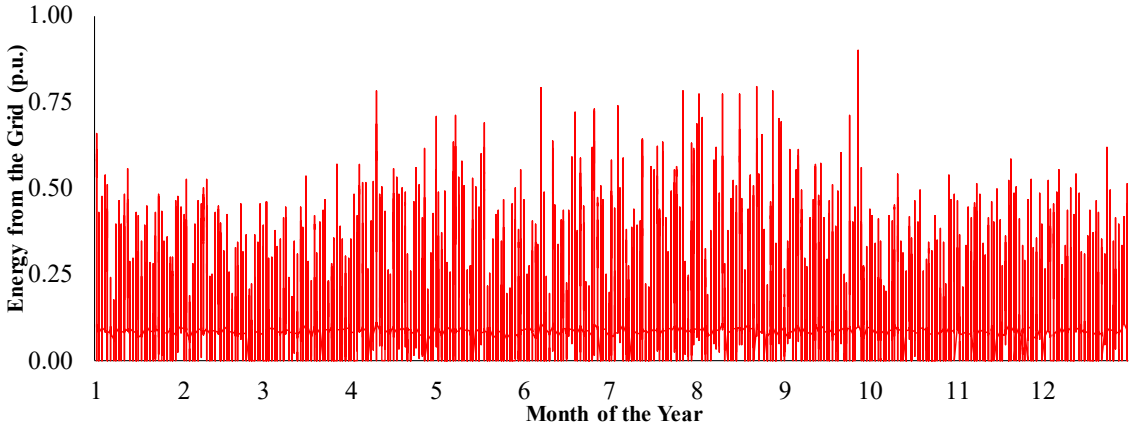

Fig. 2.8 Annual Grid Energy Supply (Case 2.b)

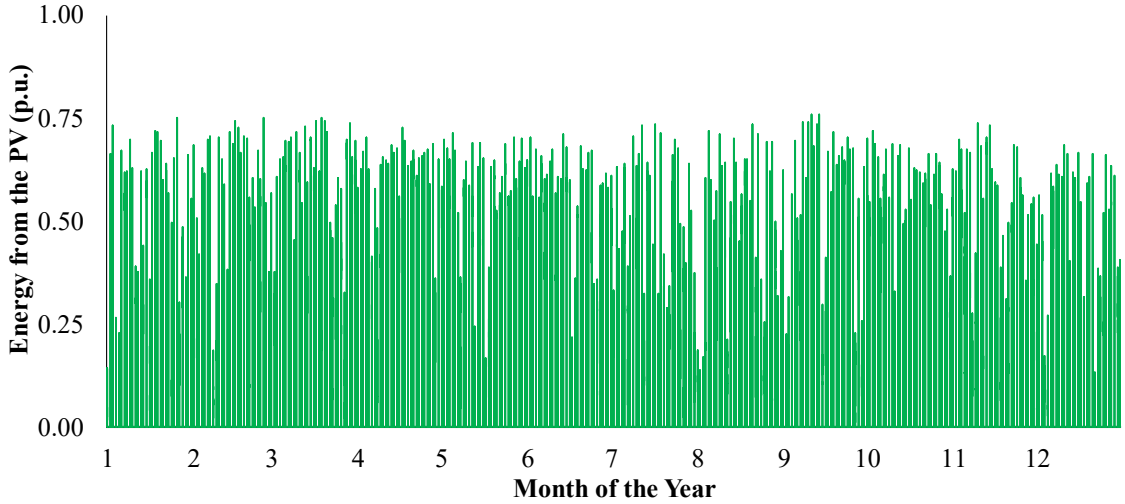

Fig. 2.9 Annual PV Energy Production (Case 2.b)

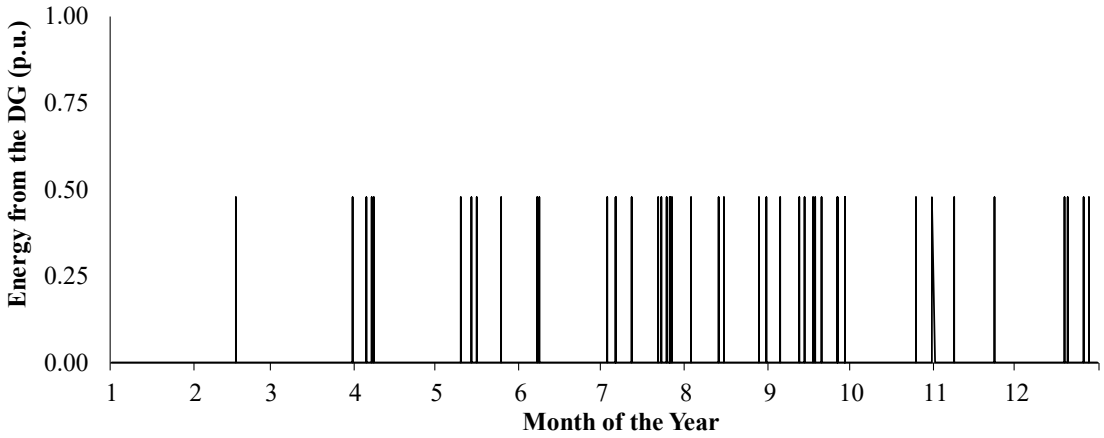

Fig. 2.10 Annual DG Energy Contribution (Case 2.b)

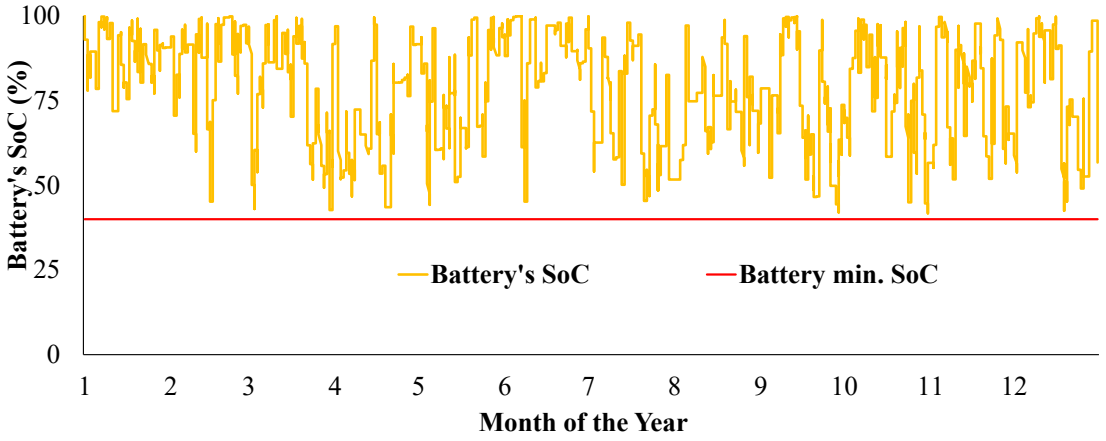

Fig. 2.11 Annual Battery's SoC (Case 2.b)

2.5.2 Month Wise Energy Contributions

The month wise energy contributions from the Grid, PV and DG, and battery energy throughput are shown in the Fig. 2.12. Selection of best month and worth months has already described in the Section 2.5 and it has observed that the March month represented the best month of the year however, August month represented the worst month. Although, the average load of the summer season has 12% more compare to the winter season, but it has observed that the PV contributions for the summer and winter seasons, have 52% and 48% respectively (Fig. 2.12). It has observed that 4 % more PV contribution has taken place in the summer season compare to the winter season. DG has operated only eight months (i.e. excluding Jan, Feb, Mar and Oct) of the year and its energy contribution varies from 1-3%. During the remaining months, the battery has contributed for essential loads at the time of grid outage. Battery has participated in the charging-discharging cycle

throughout the year and it has observed that 'battery energy throughput varies in between 21 to 43 %.

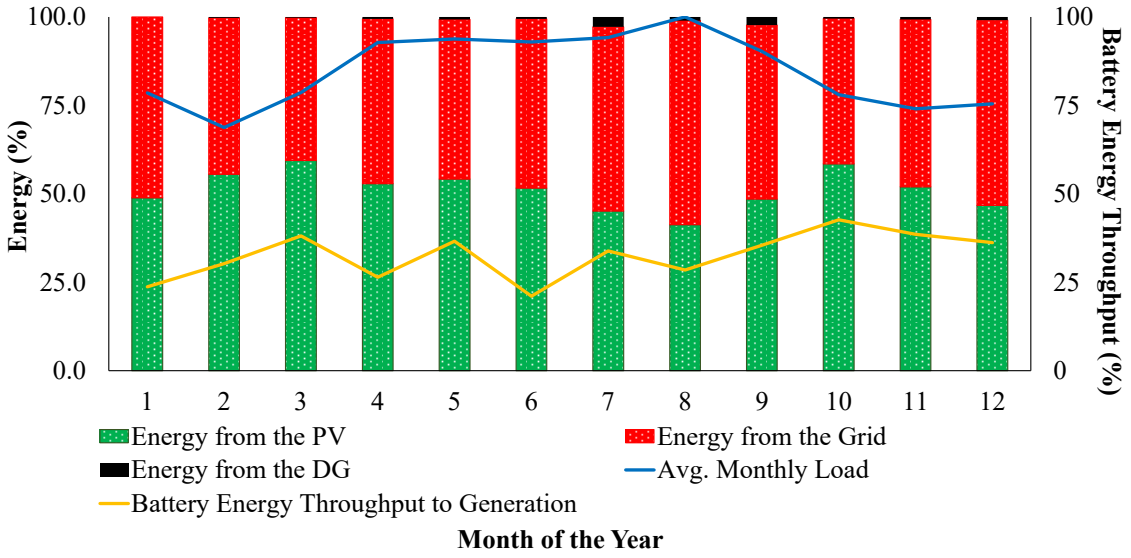

Fig. 2.12 Energy from Grid, PV & DG, and Battery Energy Throughput

2.5.3 Energy Contribution from DERs for the Best Month

Energy contribution with time from the different energy sources e.g. energy from the Grid, energy from the PV, energy from the battery (i.e. battery energy throughput), energy from the DG and battery energy contents, are shown for March month in the Figs. 2.13 & 2.14. In the March month, 31 days are represented in two graphs, days 1 to 15 in Fig. 2.13, and days 16 to 31 in Fig. 2.14. It has been analyzed for March month that the PV, Grid and DG have contributed 59.4%, 44.4% and 0.2% respectively to meet the institutional building load and the battery energy throughput has reached to 38%. Battery has primarily charged through the PV and only get discharged when 'Grid Outrage' occurred, and the PV does not have enough power to meet the load demand. The DG has primary responsibility to meet instantaneous load demand during grid outages condition and gives the second priority for battery charging if the energy content in the battery goes below to 50%.

It has been observed from the Fig. 2.13, that from day 1 to day 15, DG is not needed to operate during grid outages condition as the PV along with battery have enough power to provide back up to the load. The moment grid outage occurred at nighttime when PV is not available battery starts discharging and meet the load demand. In the beginning of the third day, when battery's SoC reached 43% level and then PV charged the battery in addition to meet to meet the load demand.

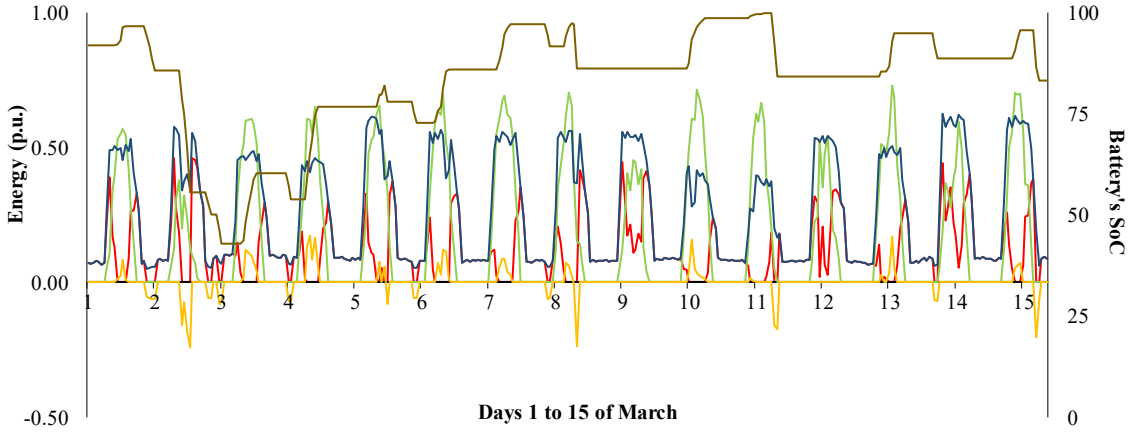

Fig. 2.13 Energy Contribution from 1-15 Days of March (Case 2.b)

It has been observed from the Fig 2.14 that the DG is operated only for 1 hour on the 30th day when battery's SoC reached to 43% and this time PV and grid supply were not available therefore DG not only met the institutional load demand but also charged the battery. It has been very clear that the DG has given lower priority among all distributed energy sourced and therefore DG's energy contribution in the March month is only 0.20% to the load demand.

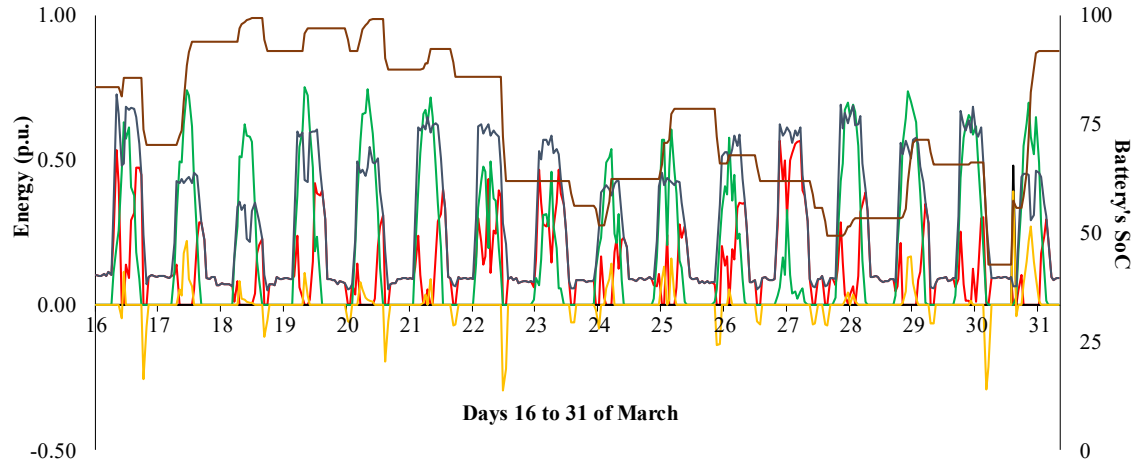

Fig. 2.14 Energy Contribution from 16-31 Days of March (Case 2.b)

2.5.4 Energy Contribution from DERs for the Worst Month

As discussed in the Section 2.5 that August month is considered as the worst-case scenario due to the lowest percentage of PV contribution (i.e. 41.3%) to meet institutional load demand and the relatively highest average load. Therefore, role of DG has become important during grid outages and as it can

provide the backup power along with the PV and battery. Like the March month, energy contributions from different energy sources to meet the institutional building load demand are shown in Figs. 2.15 and 2.16. It has been analyzed for the August month that the PV, Grid and DG have contributed 41.3%, 57.7% and 1% respectively to meet the institutional load demand and battery energy throughput is 28%. It has been observed that DG has operated almost 6 hrs. in the August month, and it has contributed 1% of the load demand. However, battery followed the similar operational characteristics as for the Mach month and it has primarily charged by PV and discharge when PV doesn't generate enough power to meet the load demand.

It has been observed from the Fig. 2.15 that battery's SoC is 52% on the day 1 to 2 but battery is not getting charge as PV does not have enough power to charge the battery however grid and PV are meeting the load demand. On the day 3, when PV as well as grid are not available to meet the load demand then DG is operated, and it not only supply power to the load but also charge the battery during the operation. The moment grid power comes back DG supply has reduced to zero and grid take cares of entire load. During the DG operation on the day 3, battery's SoC rises from 52% to 57% but after that on the days 4 and 5, battery is charged by PV and its SoC has reached to 97% in the beginning of day 6. This has been repeated on the 13 and DG is operated to meet the instantaneous load demand as well as change the battery.

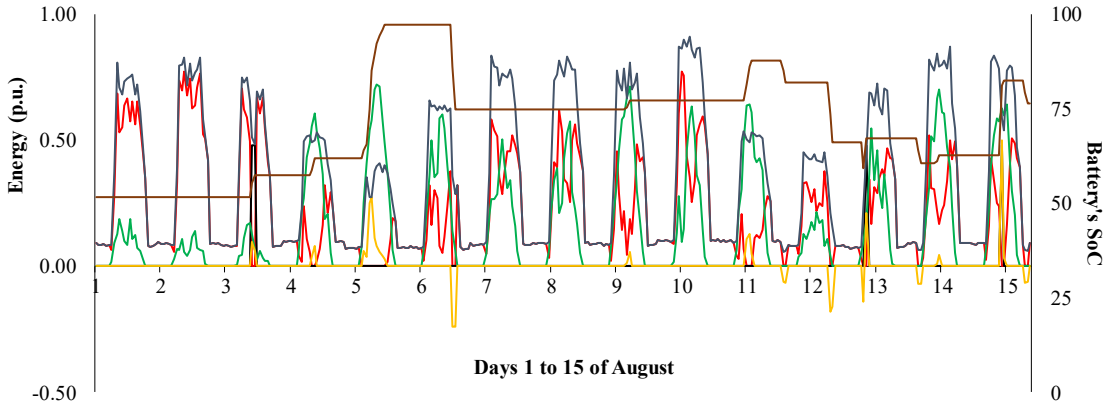

Fig. 2.15 Energy Contribution from 1-15 Days of August (Case 2.b)

It has been observed from the Fig. 2.16, DG has not operated from day 16-30 and during this period PV and grid have met the load demand however battery has charged by the PV during the daytime. On the day 31, DG has operated as PV

and grid are not available and during this time DG has met the load demand as well as charged the battery and therefore battery's SoC has reached from 60% to 68%.

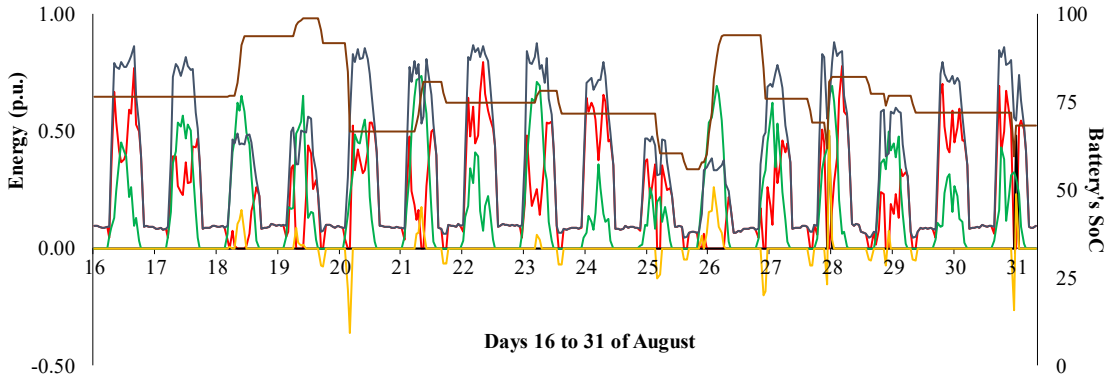

Fig. 2.16 Energy Contribution from 16-31 Days of August (Case 2.b)

It has been analyzed that integration of PV and battery energy storage in the existing institutional building and use of energy management strategy has improved the overall system performance and especially useful for reducing the DG contribution to the load from 12.7% to only 0.9%. DG is operated only 54 hours throughout the years in which 43 hours is operated in the summer (i.e. April-September) and only 11 hours in the winter season (i.e. October-March). The DG contribution in the summer season has noted higher as compare to the winter season because load demand in the summer season has also 23% higher as compare to the winter season and PV, grid and battery could not meet the load demand on many instances in the summer season.

2.5.5 Energy Contribution for a Typical Day

Energy contribution from different sources for a typical day of the August month has shown in the Fig. 2.17. It has been observed that during the daytime (e.g. 08:00 hours to 19:00 hours) the total load demand is met through solar PV and the grid; however, grid demand has reduced with increasing in the PV output. In addition to meet the load demand, PV generation has also used to charge the battery energy storage during the daytime (e.g. 11:00 hours to 15:00 hours). In the Fig. 2.17, battery charging, and discharging have shown with (+) positive and (-) negative signs respectively. The moment grid outage occurred at 20:00 hours, grid contribution is reduced to zero and then battery provided backup to the essential load from 20:00 hours to 21:00 hours. Here, the DG is given the lowest priority and it operates only when PV and battery didn't have enough energy to meet the load demand. It has observed that PV has given the main priority to meet the load

demand as well as to charge the battery. During the grid outage period (i.e. 20:00 hours to 21:00 hours), the battery's SoC has reached to the 60% and other time of the day battery' SoC remained above the 60% level. It has noticed that DG has not operated throughout the day as PV and battery have taken care of the entire load. Since there is no additional PV generation during the day, which can feed into the grid, therefore energy sold to the grid has shown zero in the Fig. 2.17.

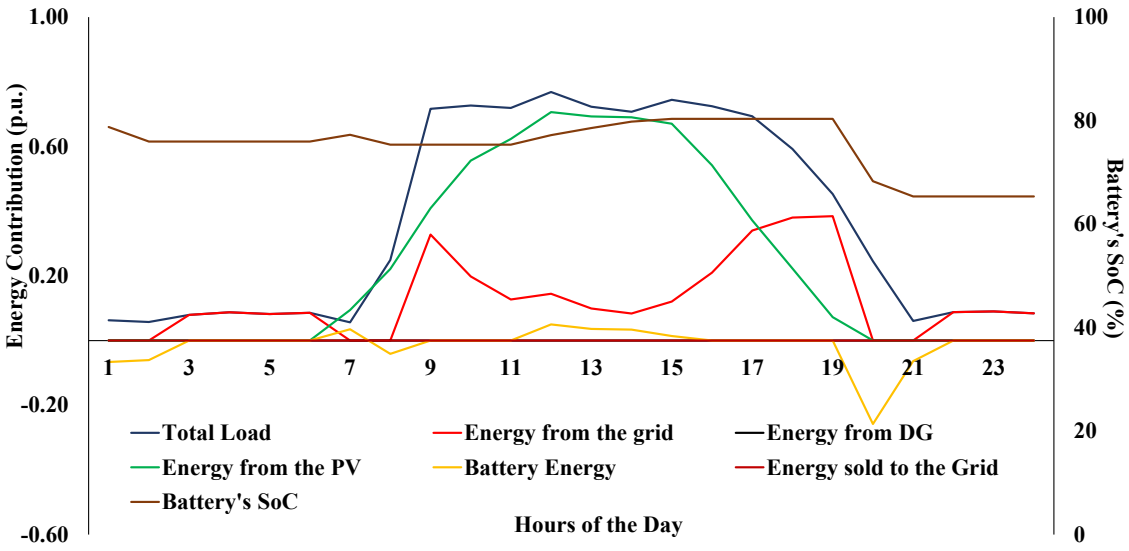

Fig. 2.17 Energy Contributions of a Typical Day in August (Case 2.b)

2.5.6 Battery Performance Analysis

The performance evaluation of the battery energy storage is very important in a micro-grid system for analyzing the battery's usage pattern and impact on the cycle life. Battery also plays critical role to provide the instantaneous power backup to the essential load and ensure the system's reliability. However, it has been observed that battery's usage pattern or participation within the system depends on various parameters e.g. coordination among the different energy sources, demand and supply pattern, energy management strategy, etc. A better coordination of the different energy sources allows battery to use its maximum potential by enhancing the annual energy throughput of the battery. Positive and negative signs of battery energy represent that a battery is charging or discharging. The input parameters for battery are the same as for the case 2.b and details have been given in the Section 2.5. The performance of the battery is evaluated based on the hourly variation of energy content in the battery, and it is monthly & annual energy throughput. The variation in the battery' SoC for each month of the year has illustrated in the Fig. 2.18. Although, few instances are observed in the months

of March, April, May, September, October and November when battery's SoC reached to below 45% but due to availability of DG, the blackout situation has never been happened.

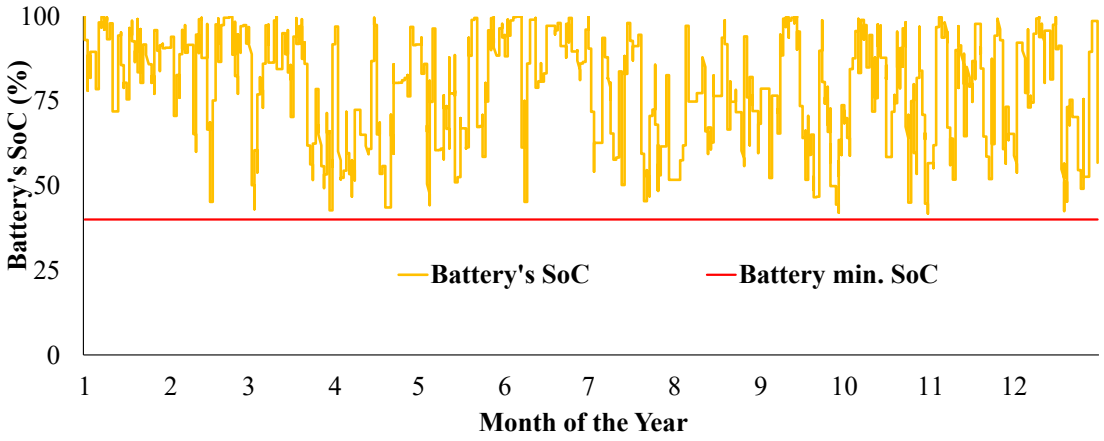

Fig. 2.18 Hourly Variation of Battery SoC (Case 2.b)

A monthly variation of the battery energy throughput is illustrated in Figure 2.12. In this analysis, the six months from 'April to September' have been considered to represent as 'summer' and the remaining six months 'October to March' as winter. It has been observed that average battery energy throughput of the winter season (i.e. October-March) is 5% more as compare to the summer season (i.e. April-September). This indicates that battery is used more during the winter season compare to the summer season. The battery energy throughput is always more than 25% throughout the year except for January and June months. However, average annual throughout of the battery is 33% and there are four months (i.e. March, May, Oct, Nov and Dec) represent more than 35% of energy throughput.

2.6 Economic Performance Analysis and Comparison of Cases 2.a & 2.b

In this section, economic performance of the Case 2.b has analyzed and compared with the Case 2.a results. By integrating the PV and battery energy storage with the institutional energy system, the annual average grid energy demand has been reduced from 50 kW to 45 kW, and the annual electricity bill saving of INR 5,06,885 has been achieved. A comparison of month-wise peak demand, DG contribution and electricity bill saving for Cases 2.a & 2.b have shown in the Table 2.2.

Table 2.2 Comparative Results of Cases 2.a & 2.b

Month of the Year	Peak Load Demand from Grid (kW)		DG Contribution (kWh)		Monthly Saving through electricity bill (INR)	PV Energy Contribution (%)
	Case 2.a	Case 2.b	Case 2.a	Case 2.b	Case 2.b	Case 2.b
Jan	34	33	1350	0	37538	49
Feb	36	26	1300	24	37686	56
Mar	36	28	1800	24	46156	59
Apr	47	39	1209	72	51106	53
May	44	35	1579	96	49967	54
Jun	50	39	1026	72	49641	52
Jul	47	39	1596	360	42208	45
Aug	46	40	1228	144	40545	41
Sep	46	45	1639	288	41197	49
Oct	34	27	2000	48	43269	58
Nov	34	29	1800	72	36541	52
Dec	35	31	1900	96	31030	47
Annual Average	50	45	1900	96	506885	51

A comparison of economic performance results of Case 2.b. with Case 2.a, have given in the Table 2.3. The sign downward (↓) indicates percentage reduction in the parameter's value of Case 2.b as compare to Case 2.a. It has been observed that using local distributed energy sources, it not only makes the entire system economically viable, but also contributing in reducing the grid and DG dependency. The CoE (in the Case 2.b) has reduced by 47 % compare to the Case 2.a. In addition, the DG capacity in the Case 2.b has reduced from 50 kVA to 30 kVA, and the DG has operated only for 54 hours and consumed 407 L of fuel. Out of total energy generation, 96% has used for fulfilling the institutional load demand; however, 4% has sold to the grid. The average annual PV energy contribution has 51%.

Table 2.3 Economic Performance of the Case 2.b

S. No.	Parameters	Value of Case 2.b	Changes as compare to the Case 2.a (%)
1.	CoE (INR/kWh)	6.36	48 (↓)
2.	Net present cost (10^6 INR)	18.1	47 (↓)
3.	Annual grid contribution to the total generation ratio (%)	48	45 (↓)
4.	Annual DG contribution to the total generation ratio (%)	1	92 (↓)
5.	Annual PV contribution to the total generation ratio (%)	51	No PV in Case I
6.	Annual battery energy throughput to the total generation (%)	33	No battery in Case I
7.	Annual energy sold to the total generation ratio (%)	4	No grid sells in Case I
8.	Annual electricity bill (INR)	624998	45 (↓)
9.	Annual DG fuel consumption (Litre)	407	93 (↓)

The signs downward (↓) and upward (↑) indicate, percentage reduction and increment in the parameter's value.

The cash flow summary of different components during the project lifetime of 25 years for Case 2.b, has shown in the Fig. 2.19 and their values have given the in the Table 2.4. It has been observed that total capital cost of 2.98 million INR has needed in the first year of the project and 50% of the capital cost has come from solar PV however, battery, DG and system converter cost shares are 24%, 15% and 10% respectively. In this work, the operational and maintenance cost of PV, battery and DG have taken '1% per kWp cost', '2% per kWh cost' and 'INR 65 per hour of DG operation' respectively. Over the period of 25 years, the grid operational cost (i.e. net present cost of the grid supply) has 95% of the total operational cost of the micro-grid system, whereas remaining components (i.e. battery, PV, DG and system converter) all together present only 5% contribution in the operational cost. The lifetime of the battery, system converter, DG have taken 10 years, 15 years and 20,000 operation hours respectively. During the project lifetime of 25 years, DG has operated only 1825 hours, therefore it has not replaced. However, the battery and system converter have replaced two times and one time respectively, and their cost shares are 82% and 18% respectively of the total net present replacement cost of the micro-grid system. It also indicates that grid has major contribution (72%) of the total net present value of the micro-grid system followed by the battery (11%), solar PV (10%), DG (4%) and system converter (3%). The performance evaluation all cases (e.g. Cases 2.a and 2.b) have been tested with the 'Homer Pro' tool. Although, 50% of the initial capital cost has

come from solar PV; but over the project lifetime of 25 years, the solar PV cost has only 10% share of the net present value of the micro-grid system.

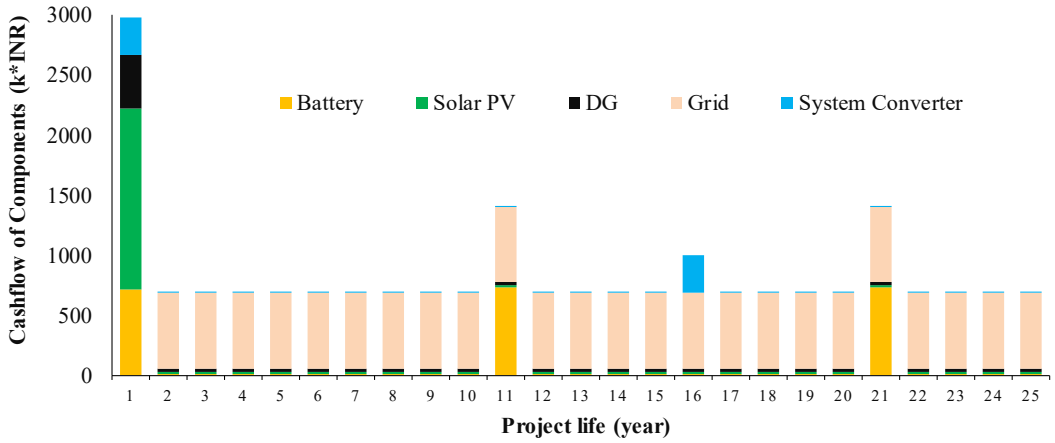

Fig. 2.19 Cashflow Summary of Different Components in the Case 2.b

Table 2.4 Net Present Cost of the Different Components in the Case 2.b

Name of the component	Capital (10^3*INR)	Operational (10^3*INR)	Replacement (10^3*INR)	Salvage (10^3*INR)	DG Fuel (10^3*INR)	Total (10^3*INR)
Battery Storage	720 (24%)	300 (2%)	1170 (82%)	-252.31	0.00	1930 (11%)
Solar PV	1500 (50%)	313 (2%)	0.00	0.00	0.00	1810 (10%)
DG	450 (15%)	99.12 (0.95%)	0.00	-286.60	545.15	807 (4%)
Grid	0.00	13100 (95%)	0.00	0.00	0.00	13100 (72%)
System Converter	311(11%)	6.52 (0.05%)	252 (18%)	-72.87	0.00	497 (3%)
Total cost	2980 (100%)	13800 (100%)	1420 (100%)	-611.78	545.15	18100 (100%)

The economics performance results obtained in the Case 2.b indicate, that the integration of solar PV system and battery energy storage in the existing system (i.e. Case 2.a) with appropriate energy management strategy can be viable to operate as a micro-grid and makes it more economically viable for reducing the grid and DG dependency.

2.7 Conclusions

In this work, the potential techno-economic benefits have been investigated using appropriate energy management strategy for operating an institutional energy system with integration of PV, battery and DG as a micro-grid. In the Case 2.a scenario (Section 2.3) (i.e. without PV and battery), the peak load demand, grid contribution and DG contribution have the values of 50 kW, 87.3% and 12.7% of

total generation respectively. However, with the techno-economic sizing of local energy resources (i.e. Case 2.b - with PV, battery energy storage and DG), the obtained results have indicated that the peak load demand on the grid is reduced by 10%, DG contribution reduced by 92% and electricity bill by 45% compare to the Case 2.a. It has been observed that the grid and DG's contributions are reduced by 39.3% and 11.7% respectively (Figs 2.8 and 2.10) compare to the Case 2.a (Figs. 2.4 and 2.5).

In this Chapter, it has been observed that for economically viable operation of PV based institutional energy system as micro-grid, an appropriate sizing of battery and DG, are required, and it depends on the electricity energy tariffs. However, the economic performance of an energy system or institutional micro-grid also depends on the time-of-use-tariff (ToU) energy tariffs. During the ToU tariffs period, appropriate operational energy management strategy and use of battery energy storage are very important, so that the maximum load demand could be fulfilled by the local energy sources. This work has been further investigated in the Chapter 3 for evaluating the impacts of electrical energy ToU tariffs with techno-economics of the institutional energy system for operating as a micro-grid.

Chapter 3

3. Techno-Economic Performance Evaluation of PV based Institutional Micro-Grid under Energy Pricing Dynamics[2]

3.1 Summary

The PV system with battery energy storage have a lot of potential to provide reliable and cost-effective electricity and as well as contributing to micro-grid operation. However, the operational performance of PV based micro-grid system depends on many factors (e.g. techno-economic sizing, energy management among the sources, market energy prices dynamics, energy management strategies, etc.). In this chapter, a typical Indian institutional energy system has considered for techno-economic performance evaluation for operating as a smart micro-grid under market energy pricing dynamics. An operational energy management strategy for micro-grid has proposed and evaluated for maximizing the local energy resources utilization with contemplation of peak demand considering grid outage conditions under market energy pricing dynamics. The impacts of different cost components on the const of energy generation (CoE), net present cost (NPC) and battery energy throughput are analyzed through sensitivity analysis.

3.2 Introduction

The grid connected institutional photovoltaic (PV) based energy systems are increasing, and they are creating an opportunity to operate them as micro-grid and to affect the electricity market [3.1-3.2]. The PV based institutional energy system integrated with battery energy storage and distributed generators have large potential to function as micro-grid in the grid-connected mode as well the islanding mode. In India, the PV systems connected within the low voltage distributed network are increasing exponentially with cumulative average growth rate of 88% over the last 5 years [3.3]. The commercial / institutional buildings have a lot of possibility for developing PV based micro-grid for reducing their peak demand from the grid [3.4]. During the last few years, electricity demand and energy

[2] This chapter is based on the peer reviewed journal paper, A. Sharma, *et.al.*,'Techno-economic evaluation of PV based institutional smart micro-grid under energy pricing dynamics, *Journal of Cleaner Production* (Elsevier), vol. 264, pages 1-14, 2020. doi: 10.1016/j.jclepro.2020.121486

pricings are increasing significantly, and especially for the commercial / institutional consumers [3.5]. Therefore, the electricity distribution companies are introducing dynamic energy pricing (e.g. Time-of-Use (ToU) energy tariffs, real time tariffs, demand response programs, etc.) for reducing the peak demand [3.5].

The ToU electricity tariffs can provide consumers to the lowest reward-risk profile; however, real-time energy pricing can offer the maximum incentive but may be at the highest risk [3.6]. It has reported by the American Council for an Energy-Efficient Economy that the demand response programs along with a reduction in the peak demand has saved about 200 billion kWh unit of electricity in the US during 2015 [3.7]. The economics performance of building integrated photovoltaic system (BIPV) with and without energy storage has evaluated with energy pricing and grid constraints for a typical residential southern Norway BIPV system [3.8]. A Time-of-Use (ToU), pricing tool is recommended for the electricity utility companies to encourage their customers for reducing their loads during the peak hours and to achieve the potential saving in the electricity bill [3.9]. The introduction of market-energy tariff dynamics as an economic monitor is going to promote the micro-grid within the distribution network. The significant annual electricity bill saving, and emission can be achieved for a typical BIPV house [3.10], however, the techno-economical operational performance should be significantly elaborated under market energy pricing dynamics.

The manufacturing industries can participate in demand side management considering ToU tariffs and can also recommend appropriate operational strategies for enabling such industries to be more eco-friendly with implementation of micro-grid [3.11]. At Anhui province in China, the impact of increase in the ToU tariffs as well as block tariffs for demand side management on residential customers have been reported for finding opportunity of BIPV system [3.12]. The market energy pricing dynamics are going to affect the operation and performance of distributed network with renewable energy systems [3.13-3.15]. The institutional PV based micro-grid's operation and performance can have significant impact with implementation of energy management strategies in coordination with market energy pricings. It has observed that a way forward for effective micro-grid operation is to increase the utilization of local energy sources, and to have more techno-economics benefits. In most of the available literatures, the techno-economic evaluation of institutional PV based micro-grid considering implementation of market energy pricing dynamics in the operational energy

management strategies have not significantly analyzed for grid outage as well as peak demand reduction.

In this work, an institutional PV based energy system (i.e. Case 2.b) integrated PV, battery, DG and grid has considered, and it is described in the Chapter 2. The institutional energy system with appropriate distributed generators has used for evaluating the techno-economic benefits under market energy pricing dynamics, and energy management strategies have implemented for a typical realistic Indian scenario. An Indian electricity distribution company (i.e. Dakshin Haryana Bijili Vitran Nigan i.e. DHBVN) has already implemented ToU tariff schemes for different categories of commercial / institutional electricity consumers [3.16] and it's ToU tariff schemes are used in this study. The key objective of this work is to maximize the usage of local energy resources through battery energy throughput considering peak demand as well as the grid outage time, and to evaluate the techno-economic performance under ToU electricity tariffs.

The chapter has divided into the mainly seven sections; the first section (i.e. Section 3.2) begins with introduction and state-of-art literature review, follows with the Section 3.3 that presents energy management strategy for micro-grid operation. The operational performance of PV based micro-grid has analyzed with ToU tariffs results, have reported in Section 3.4. In the Section 3.5 the impact of different electricity selling prices on techno-economic operational performance of micro-grid has been presented. The impacts of different cost components on the CoE, NPC and battery energy throughput with sensitivity analysis, are presented in Section 3.6. The key economic benefits with future opportunities for operating an institutional energy system as a micro-grid have concluded in the Section 3.7.

3.3 Energy Management Strategy for Micro-Grid Operation with ToU Tariffs

In this work, the ToU tariffs from DHBVN India [3.16], has used for performance evaluation. The ToU tariff has classified into three categories i.e. peak demand hours, off-peak demand hours and normal demand hours and they have illustrated in the Fig. 3.1. The DHBVN has applied the ToU tariffs only for the 6 months (i.e. 'Jan to Mar' and 'Oct to Dec') of a year, whereas normal tariffs rates have applied for the remaining months (i.e. 'Apr to Sept'). Based on ToU tariff variation (shown in Fig 3.1), it has observed that the ToU tariff is high during evening time (i.e. 18:00 hours to 22:00 hours) and low at night-time (i.e. 22:00

hours to 06:00 hours), whereas the normal tariff rate is applicable during the day-time (i.e. 06:00 hours to 18:00 hours) [3.16].

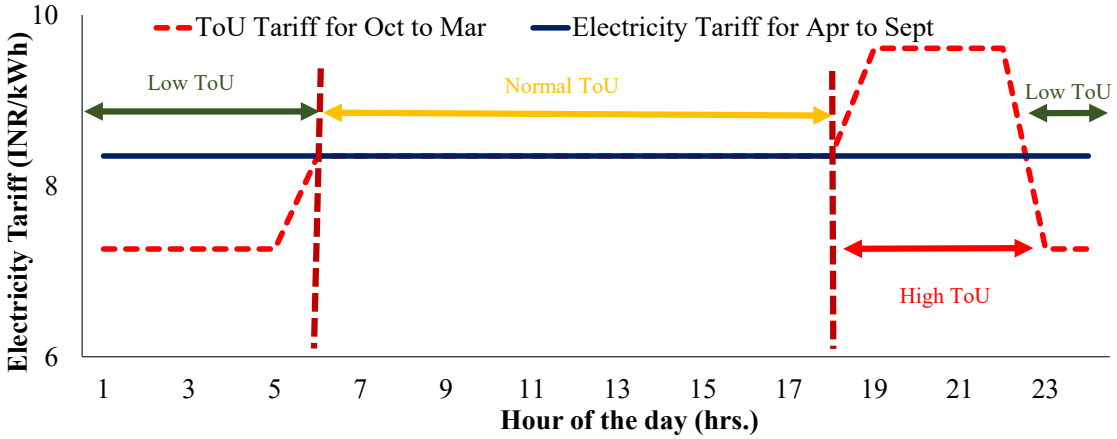

Fig. 3.1 Variation of the Time-of-Use Tariff of a Day

In order to analyze the impact of ToU tariffs on the operation of the institutional micro-grid system, different ToU tariffs are selected. It has reported in [3.17], that the average cost of electricity supply during the period 2004-05 to 2015-16 had increased from 2.54 INR/kWh to 5.43 INR/kWh (i.e. 113% high compare to the 2004-06). Therefore, it has assumed that the ToU tariffs may vary from 100% to 200% and these variations are considered in the analysis with 25% intervals (i.e. 'ToU Normal or ToU 100%', 'ToU 125%', 'ToU 150%', 'ToU 175%' and 'ToU 200%' as shown in the Fig. 3.2). The variation of the selected ToU tariffs, for a typical day, is shown in the Fig. 3.3.

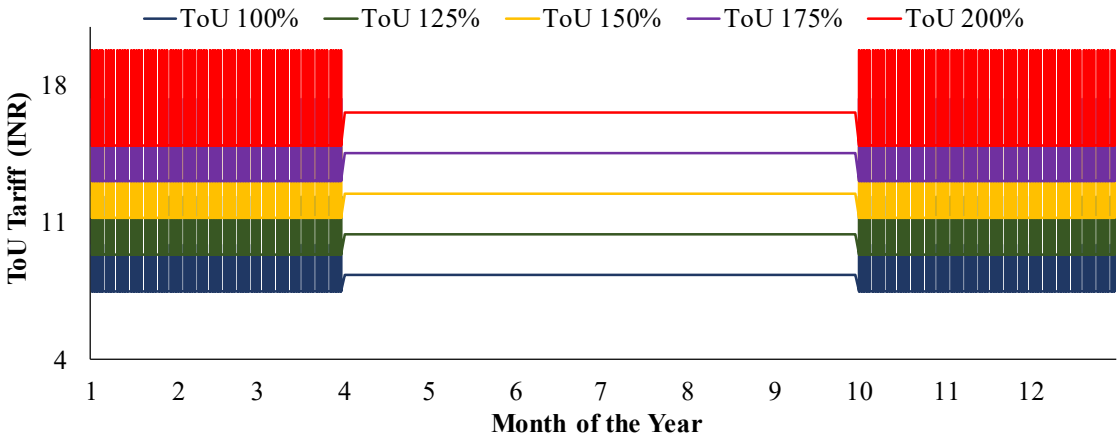

Fig. 3.2 Variation of Different Time-of-Use Tariff of a Year

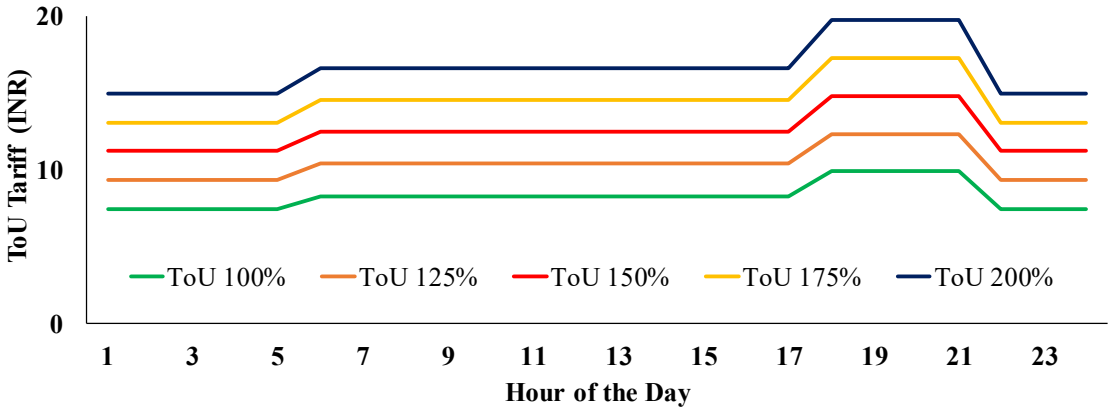

Fig. 3.3 Variation of Different ToU Tariffs for a Day

The proposed energy management strategy of DERs is illustrated in the Fig. 3.4. In the considered energy management strategy, the operation of institutional micro-grid has classified into the two categories; the off-peak demand hours and normal demand hours come under the category (i), and the peak demand hours follow the category (ii). In this analysis, battery's capacity has used for reducing the peak demand, and therefore the battery has charged during the off-peak demand hours and / or normal demand hours and allowed to discharge during the peak demand hours.

In this work, minimization of overall annual electricity generation cost (i.e. $E_{(cost)}$) approach has used and elaborated through the Eq. (3.1).

$$\min E_{(cost)} = \sum_{t=1}^{N} \begin{bmatrix} [(S_{Grid}(t) * d(\Delta t)) * (G_{Grid}(t)] \\ +[(S_{PV}(t) * d(\Delta t)) * (G_{PV})] \\ +[(S_{Chg}(t) * d(\Delta t)) * (G_{Chg})] \\ +[(S_{Dis}(t) * d(\Delta t)) * (G_{Dis})] \\ +[(S_{Sell}(t) * d(\Delta t)) * (G_{Sell}(t)] \\ +[(S_{DG}(t) * d(\Delta t)) * (G_{DG})] \end{bmatrix} \quad \text{Eq. (3.1)}$$

where:

$S_{Grid}(t)$: Power purchased from the grid at time t

$G_{Grid}(t)$: Time-of-Use tariffs at time t

$d(\Delta t)$: Time interval

$S_{PV}(t)$: PV output power at time t

G_{PV}: Energy generation cost of PV system

$S_{Chg}(t)$: Battery charging power from the battery at time t

G_{Chg}: Energy generation cost of battery

$S_{Dis}(t)$: Battery discharging power at time t

$G_{Dis:}$ Energy generation cost of battery

$S_{Sell}(t)$: Power sold to the grid at time t

$G_{Sell}(t)$: Selling price of grid electricity at time t

$S_{DG}(t)$: DG power at time t

$G_{DG:}$ Energy generation cost of DG

N: Total cumulative time in a year

The main priority has given to the PV for fulfilling the load demand; even the grid electricity has availability to use. In the energy management strategy (Fig. 3.4), the energy generation from different energy sources is examined and compared with the load demand. For example, if the PV generation is higher than the load, then the extra energy is used to charge the battery (if $SoC(t) < SoC_{max}(t)$) or feed into the grid (if $SoC(t) = SoC_{max}(t)$). And, in the situation, if the PV generation is lower output than the load demand, then the extra energy (delivered by the battery energy storage) is used to fulfill the institutional load. In the circumstances, when the PV and battery are not able to fulfill the total load, then grid supply meets the remaining load. However, least priority is assigned to the DG to operate mainly during the grid outage conditions. It has assumed that the energy management is started at time (t) and check the ToU tariffs period. The energy management strategy with ToU tariffs is elaborated in the Fig. 3.4.

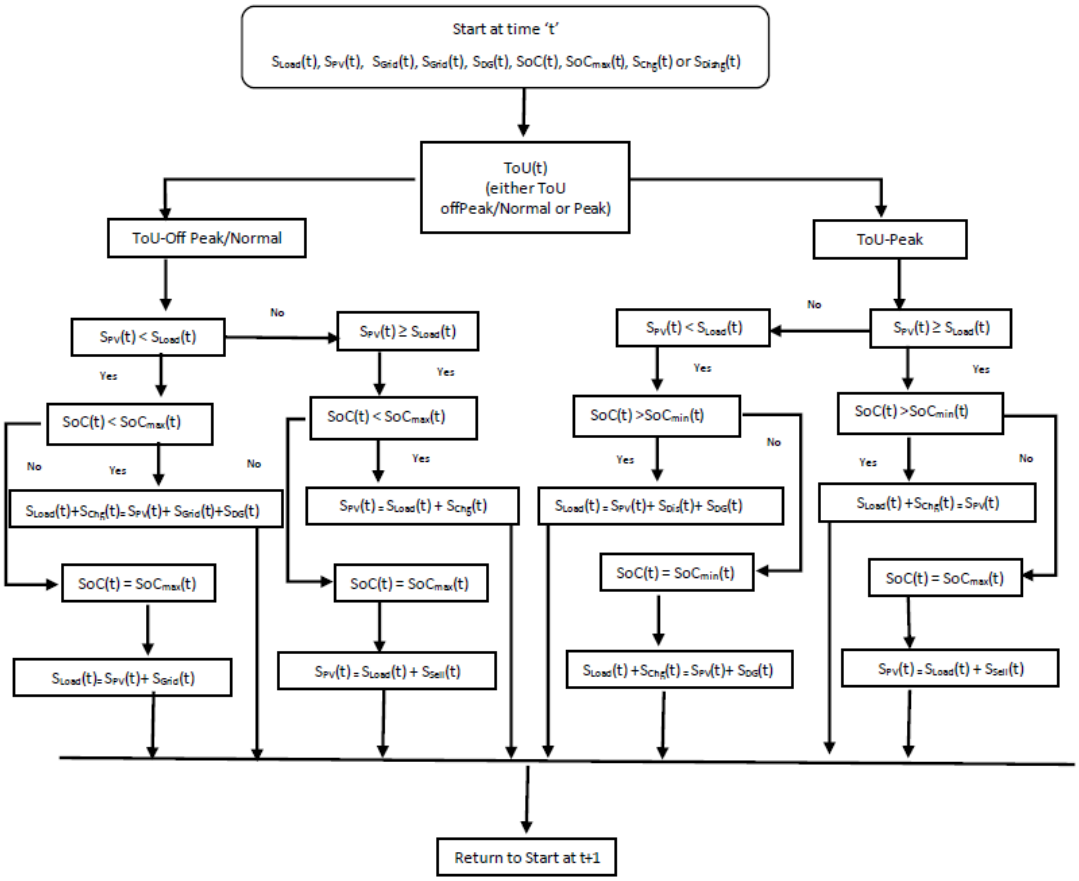

Fig. 3.4 Energy Management Strategy for Micro-grid under ToU Tariffs

In this work, energy supply selection from the DERs is based on the ToU tariffs for maximizing the local PV utilization and battery energy throughput, as well as reducing the grid electricity demand with minimizing the total energy generation cost of the system. The considered DERs have their operational limits / constraints, and they are described in ref. [3.4].

3.4 Results & Analysis of Micro-Grid with Different ToU Tariffs

In this work, the impact of different ToU tariffs on the operation and performance of the micro-grid system, is evaluated. During the period of high ToU tariff, the role of battery energy storage and role of energy management strategies become very critical. In order to get the maximum economic benefits from the institutional micro-grid system, battery is considered to charge by the local DERs (e.g. PV). Therefore, it is necessary to use the battery power in the best manner, when the grid is not available, or grid electricity prices are high (i.e. ToU tariff high).

To analyze the role of battery energy storage during the ToU energy tariff, two scenarios are considered. In the first scenario, battery's performance is

analyzed without using energy management strategy (i.e. Case 3.a). However, in the second scenario, operational energy management strategy (as illustrated in the Fig. 3.4) is used especially for the peak load saving (i.e. Case 3.b). The operational performance of the battery energy storage and DG (for both Cases 3.a and 3.b) are shown in the Figs. 3.5 and 3.6 respectively.

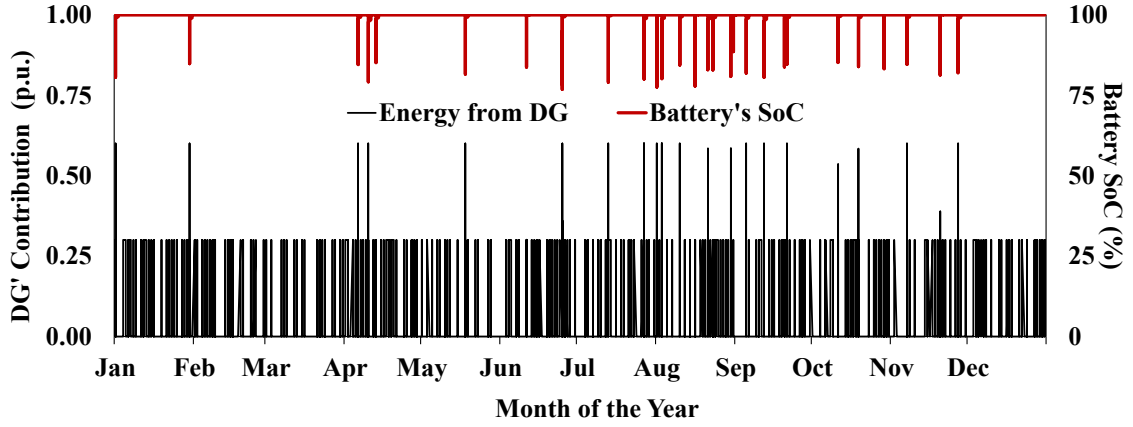

Fig. 3.5 DG and SoC without Energy Management Strategy (Case 3.a)

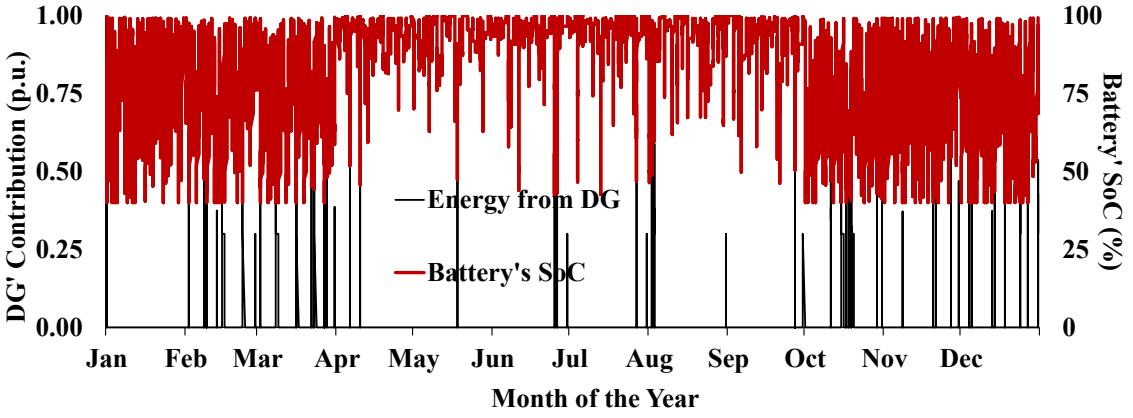

Fig. 3.6 DG and SoC with Energy Management Strategy (Case 3.b)

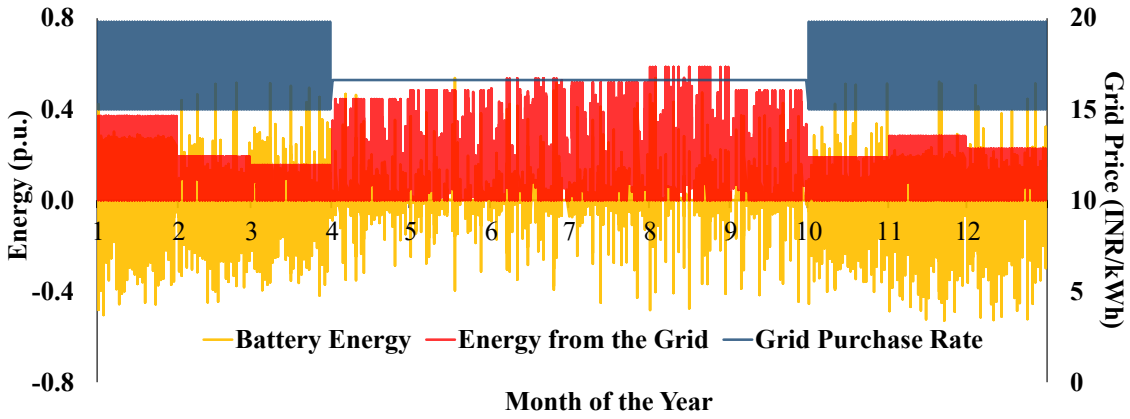

Fig. 3.7 Battery & Grid's Energy, and Grid's Tariff Variation in a Year (Case 3.b)

It has been observed from the Fig. 3.5 that the annual battery contribution is very low (i.e. battery energy throughput to generation ratio only 0.40 %) and the

DG contribution is 7%. It indicates that in the Case 3.a, battery is not optimally used throughout the year, as its SoC level has never gone below than 75%. However, in the Case 3.b, when energy management strategy is used for peak load saving, the battery energy contribution (i.e. battery energy throughput to generation ratio) is increased to 10% and the DG contribution has decreased to 2%.

The energy contribution from grid and battery as well as grid's price variation for Case 3.b, are shown in the Fig. 3.7. During ToU tariff season (i.e. winter), the maximum grid supply limit varies from 0.15 to 0.40 p.u. and battery is used to meet the peak load demand whereas in the summer season grid limit varies 0.5 to 0.6 p.u. but battery is not used for peak load demand. It has been observed from the Figs. 3.6 & 3.7 that battery is more used during the winter season and average battery energy throughput for winter and summer seasons has 63% and 37% respectively. It has been observed that the annual DG contribution for institutional load has decreased by 5%, when operational energy management strategy has used for the peak load saving. In addition, the annual electricity bill has reduced approximately to INR 26,000. A relative comparison of the economic performance results, at 200% increase in ToU (Fig. 3.2), without and with operational energy management strategy (i.e. Cases 3.a and 3.b) are shown in the Table 3.1. It has been observed that the CoE is approximately 10% less, when battery is optimally utilized for peak load saving.

Table 3.1 Economic Results without & with Energy Management Strategy

Performance parameters	Operation without Energy Management Strategy (Case 3.a)	Operation with Energy Management Strategy (Case 3.b)
CoE (INR)	11.27	10.30
Net present cost (10^6 INR)	33.70	30.30
Annual grid energy contribution (%)	40	45
Annual DG energy contribution (%)	7	2
Annual PV energy contribution (%)	53	53
Annual battery energy throughput (%)	0.40	10
Annual load to energy generation (%)	87	90
Annual energy sold to energy generation (%)	13	10
Renewable energy fraction (%)	49.4	51.30
Annual bill (10^6 INR)	1.13	1.11

It has been observed that energy management strategy plays very crucial role to optimize battery operation during the ToU tariff. The optimal use of battery not only enhance the technical performance of the institutional micro-grid, but also improve the economic benefits. In future, the grid power supply may become more expensive as ToU energy tariffs and demand charges are increasing specially for non-domestic consumers [3.16]. Therfore, impacts of different ToU tariffs on the CoE has evaluated, and its comparison has shown in the Fig. 3.8 with change in battery energy throughput.

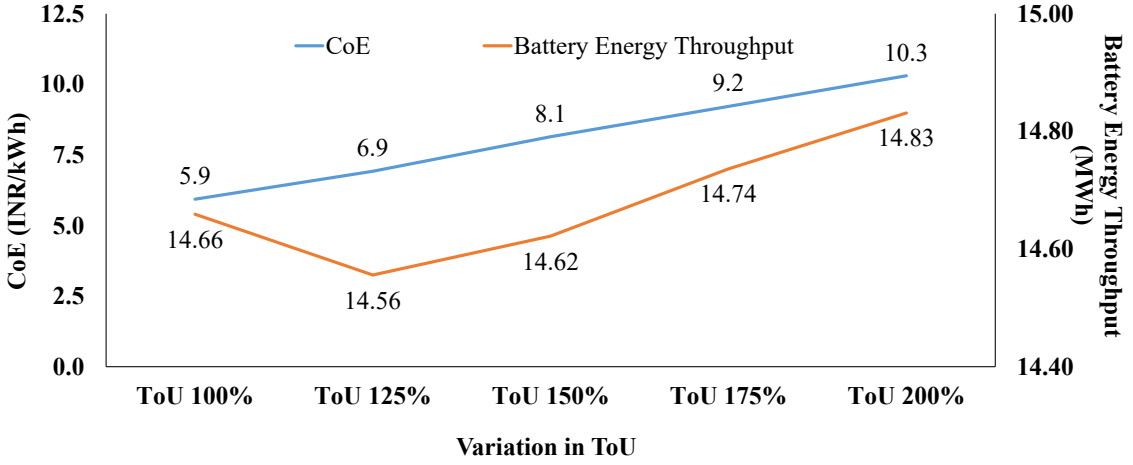

Fig. 3.8 Variation of CoE and Battery Energy Throughput with ToU

It has been observed from the Fig. 3.8 that CoE has increased from INR 6 to INR 10.30 with ToU changes from ToU 100% to ToU 200%. Here, battery's operational energy management strategy is used to reduce the peak load demand and therefore battery energy contribution (i.e. battery energy throughput) is increased with the ToU tariff increase and it is illustrated in the Fig. 3.8.

3.5 Results & Analysis of Micro-Grid with Different Selling Prices to Grid

In order to analyze the impact of electricity selling prices for the operation of the institutional micro-grid system, different selling tariffs to the grid, are considered (i.e. Case 3.c). In this analysis, the five electricity selling prices are considered (i.e. from 100% to 200% with 25% intervals: 'Grid Sell Normal or Grid Sell 100%', 'Grid Sell 125%' 'Grid Sell 150%', 'Grid Sell 175%', and 'Grid Sell 200%'). The normal energy tariff is at ToU 100%. The variation of selected electricity selling prices for a typical day is shown in the Fig. 3.9. Since ToU tariffs are applicable to the winter months only; therefore, higher grid selling prices are considered for winter season and it is not applied for remaining month of the year.

Similar, to the Case 3.b (i.e. with different ToU tariffs), in the Case 3.c energy management strategy is used in the battery opeation for peak load saving. It has been observed that the battery energy contribution (i.e. battery energy throughput) has increased to 10% and the DG contribution has decreased to 1%. However, in the Case 3.c it is important to analyze the energy saving through the electricity selling to the grid, as it has major contributions to decrease the CoE.

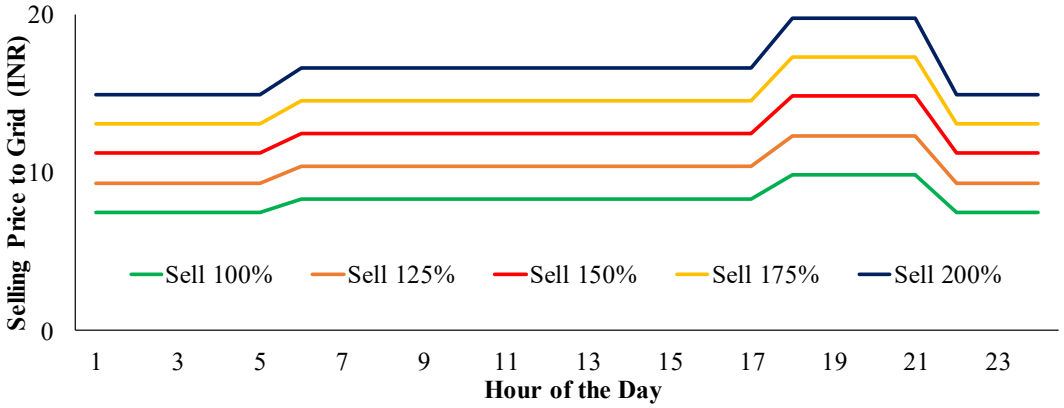

Fig. 3.9 Daily Variation of Electricity Selling Price to Grid

It has been observed that the electricity bill saving in the winter season is 70% of the total saving of a year. It is due to the high selling price during the peak demand hours (i.e. 18:00 hours to 22:00 hours) in the winter season. The energy bill saving through electricity selling to the grid at different prices are shown in the Fig. 3.10.

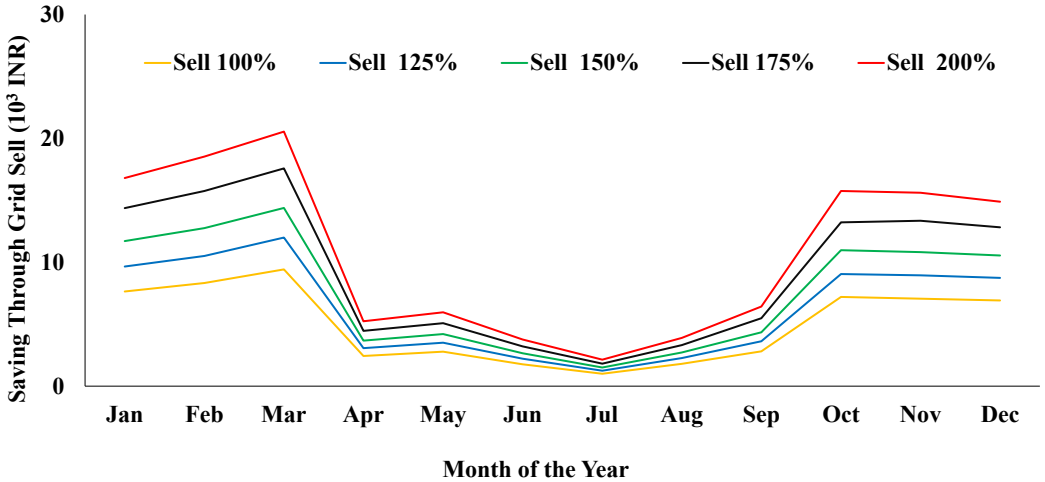

Fig. 3.10 Energy Bill Saving with Electricity Selling Prices to Grid

The variation of CoE and battery energy throughput at different selling prices are shown in the Fig. 3.11. There is almost 8% reduction in the CoE when

selling price to grid increased from 100% to 200%. The battery energy throughput has also increased with increase in the selling price, and it indicates the active participation of the battery energy storage within the institutional micro-grid with dynamics of energy pricing.

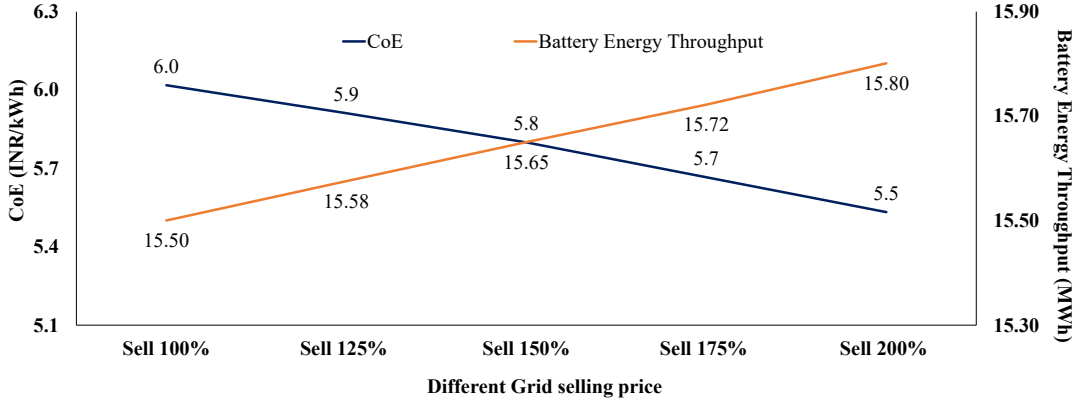

Fig. 3.11 CoE and Battery Energy Throughput at Selling Prices to Grid

It has been noticed that the energy contributions from DERs are not changed but the annual electricity bill saving of 70 k INR is achieved at selling price of 200% compare to the selling price of 100%. It has been observed that the renewable energy fraction for all cases of the selling prices to the grid is 50.20%, and battery energy throughput 10%. The techno-economic performance evaluations in all considered cases are tested through the Homer Pro ®. It indicates that appropriate operation energy management strategy can play significant role to enhance the system performance under the dynamics of market energy tariffs.

3.6 Sensitivity Analysis

The economic performance of the micro-grid very much depends on the different cost components e.g. PV, battery, power conditioning devices, DG genset, fuel etc. However, the cost of PV, battery and DG genset's fuel represent significant share of the net present cost therefore impacts of these three variables on CoE are very important to analyze. In the subsequent section the impacts of different cost components on the CoE, NPC and battery energy throughput are analyzed.

3.6.1 Impact of PV, Battery, and Fuel's Cost on the CoE

As cost of PV, battery and DG genset's fuel represent significant share of the net present cost therefore impacts of these three variables on CoE are analyzed with multiplier factors of 0.5, 1, 1.5 and 2. Here, the multiplier factor '1' represents the base case scenario having component cost as described in Case 3.b, therefore

change in the CoE with multiplier factor ‘1’ is zero. In the Fig 3.12, ‘BBx0.5’, ‘BBx1’, ‘BBx1.5’ and ‘BBx2’ are representing battery cost with multiplier factors of ‘0.5’, ‘1’, ‘1.5’ and ‘2’ respectively. In this analysis 50% of battery capacity is used for peak load saving and remaining 50% for grid outage.

It has been analyzed from the Fig. 3.12 that multiplier factors 0.5 for PV (PVx0.5), battery (BBx0.5) and fuel cost (FCx0.5) reduce the CoE by 9% whereas with multiplier factor ‘2’ increased CoE by 19%. To analyze the impact of fuel cost on the CoE, multiplier factor is kept ‘1’ for PV (PVx1) and battery (BBx1) whereas the multiplier factor of fuel cost is changed from 1 (FCx1) to 2 (FCx2) and 0.5 (FCx0.5). It has been observed that changing fuel multiplier factor from 1 (FCx1) to 2 (FCx2) and 0.5 (FCx0.5), CoE is increased by 7% and decreased by 4% respectively. Similarly, to analyze the impact of battery cost on the CoE, multiplier factor is kept ‘1’ for PV (PVx1) and fuel cost (FCx1) whereas the multiplier factor of battery cost is changed from 1(BBx1) to 2 (BBx2) and 0.5 (BBx0.5). It has been observed that changing multiplier factor of battery cost from 1 (BBx1) to 2 (BBx2) and 0.5 (BBx0.5), CoE is increased by 4% and decreased by 2% respectively. In the same way, the impact of PV cost on the CoE has been analyzed and therefore multiplier factor is kept ‘1’ for battery (BBx1) and fuel cost (FCx1) whereas the multiplier factor of PV cost is changed from 1 (PVx1) to 2 (PVx2) and 0.5 (PVx0.5). It has been observed that changing multiplier factor of PV cost from 1(PVx1) to 2 (PVx2) and 0.5 (PVx0.5), CoE is increased by 8% and decreased by 4% respectively. It indicates that PV cost has more impact on the CoE as compare to the battery and fuel cost as the CoE varies -4% to 7% with multiplier factor from 0.5 to 2.

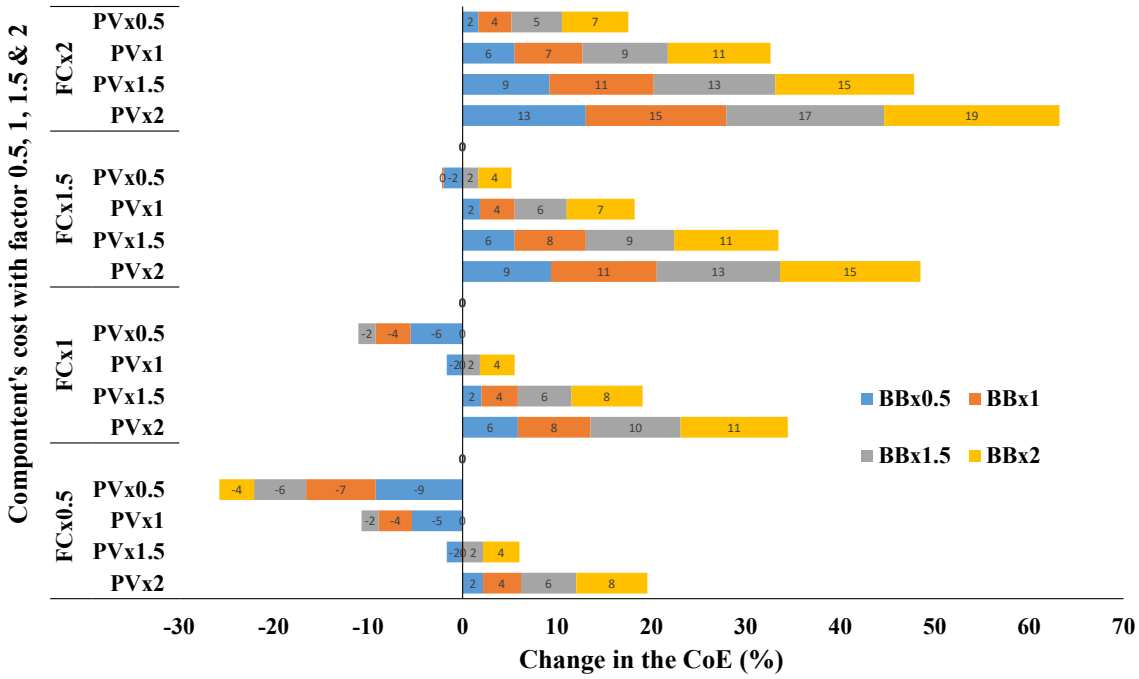

Fig. 3.12 Variation of CoE with PV, Battery and Fuel Cost

3.6.2 Impact of Battery Capacity on the CoE, NPC, Battery Energy Throughput and Fuel Consumption

As discussed in the previous section that role of battery becomes important as it is used during the grid outage situation as well as for the peak load saving. In this analysis, battery capacity has been increased with multiplier factors 1.25, 1.5, 1.75 and 2 and its impacts on the CoE, NPC, battery energy throughput and fuel consumption are analyzed and shown in the Fig. 3.13.

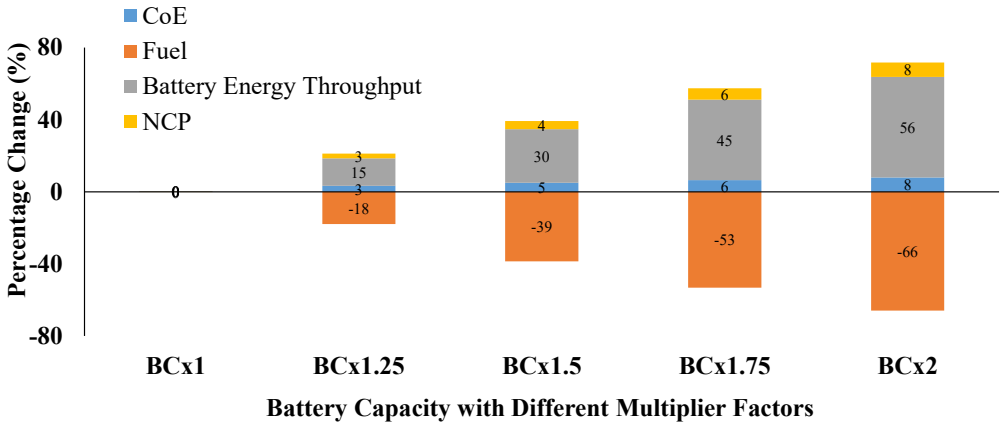

Fig. 3.13 Impact of Battery Capacity on CoE, NPC, Battery Throughput and Fuel

It has been analyzed that the impacts of battery capacity on the CoE and NCP are almost same and their value increased proportionally in the all cases. However, fuel consumption is decreased by 18%, 39%, 53% and 66% with

multiplier factors of 1.25, 1.5, 1.75 and 2 respectively as compare to the Case 3.b. Morever, battery energy throughput is increased by 15%, 30%, 45% and 56% with multilier factors of 1.25, 1.5, 1.75 and 2 respectively as compare to the Case 3.b.

3.7 Conclusions

In this work, an operational energy management strategy for micro-grid has presented and evaluated for maximizing the local energy resources utilization with contemplation of peak demand and grid outage conditions considering energy pricing dynamics. With proposed energy management strategy, the annual battery energy throughput has increased from 0.4% to 10%, and the DG's contribution has decreased from 7% to 2%, and 10% reduction in CoE is achieved. The recommended energy management strategy has used for evaluating the techno-economic performance of the institutional energy system considering different ToU energy tariffs (i.e. Case 3.b) and the electricity selling prices to the grid (i.e. Case 3.c). In the Case 3.b, it has observed that the CoE has increased by 71.6% when the ToU changes from 100% to 200% with selling price to the grid at 100%. However, 8% reduction in the CoE has observed for the Case 3.c, when the selling price to grid has increased from 100% to 200% at ToU of 100%.

It has observed that the appropriate operational energy management strategy plays significant role to achieve maximum utilization from the DERs, and battery energy storage, under dynamics of market energy pricings. However, the operation and performance of PV based micro-grid system is also affected by the meteorological conditions (e.g. solar irradiance conditions, temperature, etc.). The weather conditions vary in magnitude at different locations, therefore performance of a PV based micro-grid mainly depends on its geographical location. In this work, it has been further investigated the impacts on the operation and performance of PV based micro-grid system in the Norwegian climatic conditions and results are presented in the Chapter 4.

Chapter 4

4. Techno-Economic Analysis of PV based Micro-Grid System at Skagerak Arena Norway[3]

4.1 Summary

Integration of PV with battery system at institutional energy system can be operated as a micro-grid for reducing peak demand from the grid and enhance the techno-economic performance. In this chapter, a functioning micro-grid of 800 kW_p PV system and 1 MWh lithium-ion battery integrated at energy system of Soccer Club of Skagerak Arena (Norway), is used for analyzing peak demand reduction with techno-economic evaluation. The system performance has been evaluated for identifying the techno-economic performance, and contributions from the PV and battery energy storage for reducing peak demand from the grid. The results have been studied for annual, monthly, and a typical day of the year along with the battery system performance.

4.2 Introduction

Solar Photovoltaic system and battery energy storage have a potential to operate energy system as a micro-grid, however appropriate operational energy management strategy and demand-side management schemes are very much required [4.1]. A micro-grid system can be designed for different applications e.g. residential, institutional, industrial, community based etc. The energy management strategies (s) have significant impact on the performance of the PV and battery energy storage [4.2-4.3]. The micro-grid system can contribute to the demand side management through battery energy throughput using appropriate energy management strategies [4.4]. The operational performance of a micro-grid system can be improved significantly with integration of distributed generator considering grid outage conditions [4.5]. The impacts of electricity energy tariffs into the micro-grid performance have been further investigated in [4.6], and it has been observed that appropriate energy management strategy is useful for effective energy management among the energy sources and battery energy throughput

[3]This chapter is based on paper, A. Sharma, *et.al.* "Techno-Economic Case Study of Micro-Grid System at Soccer Club of Skagerak Arena Norway", 5th International Conference on Smart and Sustainable Technologies, IEEE, pp. 1-5, 2020. doi: 10.23919/SpliTech49282.2020.9243789.

[4.6]. For developing a micro-grid project, selection of appropriate technologies, effective coordination among the distributed energy sources and loads, are needed [4.7-4.10].

The operational performance of PV based micro-grid system is significantly affected by the local meteorological conditions (e.g. solar irradiance conditions, temperature, wind speed, etc.). In the last few years, many studies [4.1.-4.10] have evaluated PV system performance for different geographical regions, but they have not sufficiently addressed the techno-economic performance of the grid integrated PV based micro-grid. However, some studies [4.11-4.14], have reported operation of PV based micro-grid in the Nordic climatic conditions, but they have not adequately considered electrical energy market dynamics and maximizing the use of local energy resources with battery energy throughput. Within the Nordic countries, Norway is using mainly hydroelectricity (i.e. 96%), but in the recent years PV market is growing rapidly [4.11]. The installed cumulative PV capacity in Norway has reached 119.8 MWp at the end of 2019, and it was only 15.3 MWp at the end of 2015 [4.11]. It indicates that the PV market has increased eightfold in the last five years. It is mainly due to National policy such as Plusskundeordningen, subsidy payouts for small solar PV installations, etc. The increasing PV penetration as well as energy market dynamics of the Norwegian system can contribute for local energy management for institutional systems to operate as micro-grid. The BIPV system for a typical South Norwegian household has been studied for economic sizing of energy storage [4.12], but local energy management through battery energy throughput has not been considered. Thermal load management can be used for demand side management [4.13], but the battery energy contribution has not effectively covered for electrical energy demand management. In the ref. [4.14], the economic performance of building integrated photovoltaic system (BIPV) with and without energy storage has evaluated under energy pricing and grid constraints for a typical residential southern Norway BIPV system, but it has not sufficiently included the energy management strategies for operation of BIPV with energy storage. The institutional and industry electricity consumers have a lot of potential for peak demand saving through PV based micro-gird integration, as electricity distribution companies are applying high electricity tariffs during peak demand hours [4.14-4.15].

In this work, operational load from years 2015 to 2018 at the of Skagerak Arena (Norway), is analysed for techno-economic analysis and understanding the possible operational strategies of energy storage system with grid constraints and PV output for operating as micro-grid and it is described in the Section 4.3. In the Section 4.4, energy management techniques are presented for improving the operational performance of the energy system at Skagerak Arena by minimizing the grid contribution as well as levelized cost of locally generated electricity with maximization of the PV contribution. The performance assessment of the system at Soccer Club Skagerak Arena without and with PV& battery (i.e. Case 4.a and 4.b respectively), have been compared and analysed in the Section 4.5. In the Section 4.6, economic performance analysis of Case 4.a and Case 4.b, have been analysed and presented. A comparative operational performance of PV based micro-grid system for India and Norway climatic zones has been presented in the Section 4.7. Conclusion and further improvement for operation of the micro-grid system has been presented in the Section 4.8.

4.3 Energy System Description of Skagerak Arena (i.e. Case 4.a)

In this work, load profile driven by grid of the Skagerak Arena, located at the Porsgrunn Norway (latitude 59.1386° N, longitude 9.6555 E), is used as a base case scenario (i.e. Case 4.a). The hourly load profile of the Skagerak Arena from years 2015 to 2018 has analyzed and system configuration has shown in the Fig. 4.1.

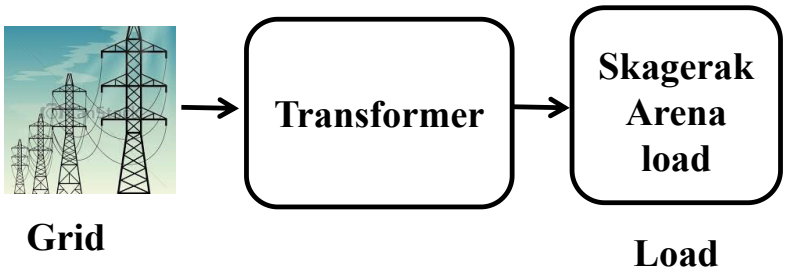

Fig. 4.1 Schematic of Skagerak Arena Load Configuration with Grid (Case 4.a)

In this study, the months April-Sept and Oct-March are considered as summer and winter months, respectively. The Skagerak Arena's load has analyzed through retrieved data and annual average daily load profiles in kWh per hour from years 2015 to 2018, has shown in Fig 4.2. It has observed through the operational load, the average summer and winter load demands from 2015 to 2018 were increased by 8.47% and 6.41% respectively, and the average annual growth rate was 7.55%. In this study, the hourly peak demand of 1052 kWh has been taken as

1 p.u. The hourly variation of the annual load profile of Skagerak Arena has shown in the Fig. 4.3. It has been observed that the average winter's demand of year 2018 is 7.14% more than the summer demand. However, winter's peak demand of the year 2018 (i.e. 09:00 hours to 15:00 hours) is 3.54% more compare to summer.

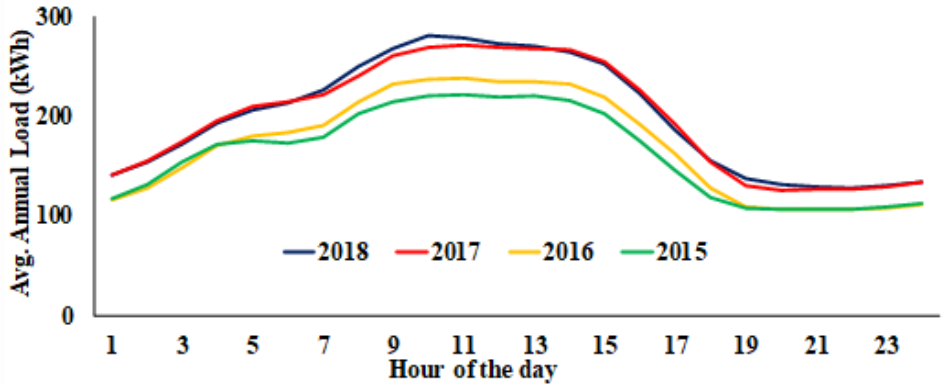

Fig. 4.2 Avg. Daily Load Profile for Year 2015 to 2018

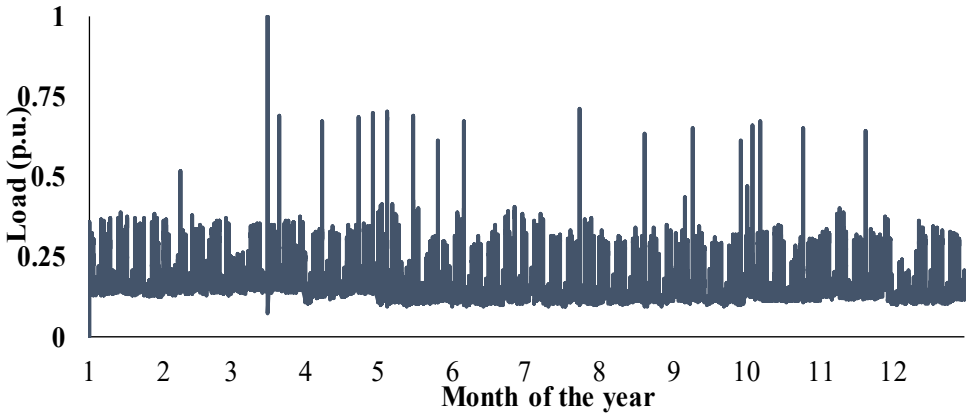

Fig. 4.3 Load Variation in Year 2018

4.3.1 Results & Analysis of the Energy System at Skagerak Arena (i.e. Case 4.a)

Since the grid supply is quite reliable in the Norway therefore no grid outages scenarios are considered in the existing system (i.e. Case 4.a) and the total load demand of Skagerak Arena has met by grid supply and no other distributed energy sources are connected. The annual energy contribution from the Grid to meet the Skagerak Arena load demand has shown the Fig. 4.4.

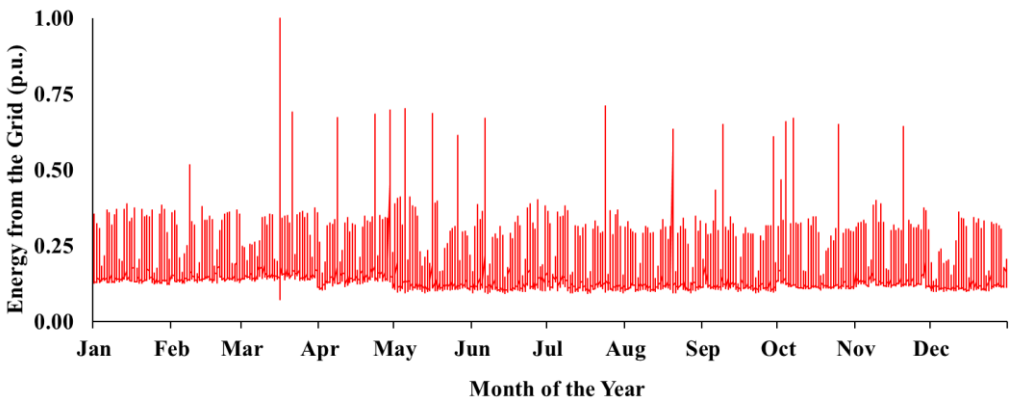

Fig. 4.4 Energy Contribution from the Grid Throughout the Year

The monthly electrical energy supply with peak demand as well as the electricity bills are summarized in the Table 4.1 for Case 4.a. Electricity tariffs for this study have been taken from ref [4.15].

Table 4.1 Energy Supply and Electricity Bill Summary of Case 4.a

Month of the year	Energy Purchased (kWh)	Peak Load demand (kW)	Energy Charge (NOK)	Demand Charge (NOK)	Total Electricity Charge (NOK)
Jan	161485	409	50818	61350	112168
Feb	145281	544	54432	81600	136032
Mar	163752	1,51	65856	157685	223541
Apr	154201	734	57091	110040	167131
May	147457	737	47786	110610	158396
Jun	135982	706	57819	105960	163779
July	137449	748	67492	112155	179647
Aug	135261	668	66007	100185	166192
Sep	135462	684	62200	102600	164800
Oct	148709	705	59984	105765	165749
Nov	153430	676	71453	101340	172793
Dec	133484	381	69440	57180	126620
Annual	1751953	1,51	730378	1206470	1936848

Results, obtained from the Case 4.a, show that total 1751 MWh energy purchased from grid supply in a year. The Case 4.a also indicates that there is lot of potential to reduce the grid supply dependency and it could be possible by integrating the local distributed energy sources (e.g. solar PV) and battery storage along with appropriate energy management strategies.

In this work, techno-economic sizing of the solar photovoltaic system and battery energy storage is done based technical feasibility and available rooftop area for solar installation. A total of 800 kWp PV along with 1MWh lithium-ion battery

bank along with power conditioning and energy management unit have been integrated with the existing system (i.e. Case 4.a), and the configuration of upgraded system represented as Case 4.b. The schematic diagram of the Case 4.b has shown in the Fig. 4.5.

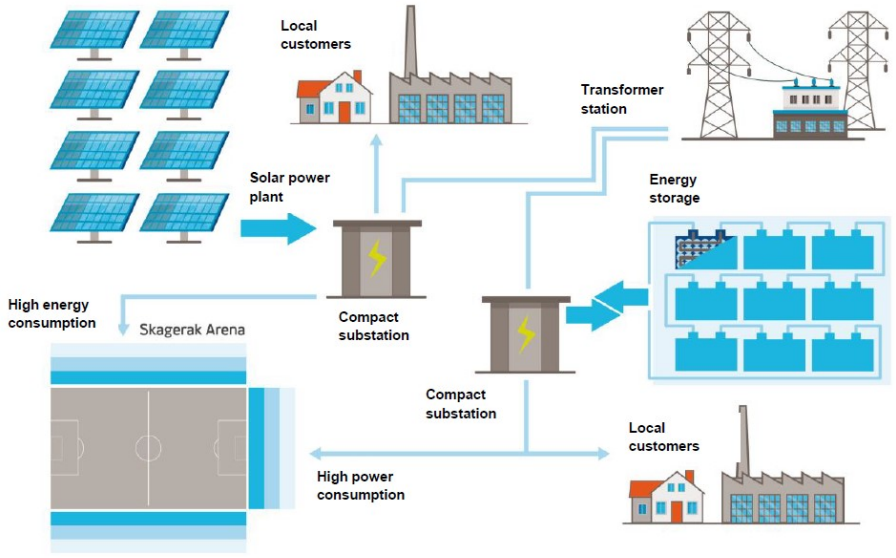

Fig. 4.5 Block Diagram of Micro-grid at Skagerak Arena, Norway (Case 4.b)

In the next Section 4.4, energy management strategy has been discussed for peak demand saving and maximizing PV energy contribution within the micro-grid system.

4.4 Energy Management Strategy for Operation of Micro-Grid System

The energy management strategy is very important for improving techno-economic performance of micro-grid system. In this work, the main aim is to formulate energy management strategy for reducing peak load demand from the grid and increase PV energy contribution via battery energy throughput. In this work, the overall grid energy cost (i.e. $f_{(cost)}$) minimization approach has been used, and it has been described in the Eq. (4.1). The cost function includes energy cost from the grid, reduction in peak demand cost and battery energy cost. In the Eq. (4.1), if $P_{Grid}(t)$-$P_{PV}(t)$ is positive (+ve), then $E_{Grid}(t)$ price is considered and $E_{Sell}(t)$ price is zero; whereas in case $P_{Grid}(t)$-$P_{PV}(t)$ is negative (-ve) then $E_{Sell}(t)$ price is considered and $E_{Grid}(t)$ price is zero.

$$\min f_{(cost)} = \sum_{t=1}^{T} \begin{bmatrix} [((P_{Grid}(t) - (P_{PV}(t)) * d(\Delta t)) * (E_{Grid}(t)] \\ + [((P_{PV}(t) - P_{Grid}(t)) * d(\Delta t)) * E_{Sell}(t)] \\ [D_n(t) * (D_{Grid}(t)] \\ + [(P_{Bat}(t) * d(\Delta t)) * (E_{Bat})] \end{bmatrix} \quad \text{Eq. (4.1)}$$

where:

$P_{Grid}(t)$: Power bought from the grid at time t

$D_n(t)$: Grid electricity demand at time t

$D_{Grid}(t)$: Grid electricity demand price at time t

$E_{Grid}(t)$: Grid electricity buying price at time t

$E_{Sell}(t)$: Grid electricity selling price at time t

$d(\Delta t)$: Time duration

$P_{Bat}(t)$: Power from the battery at time t

E_{Bat}: Battery energy cost

T: Total cumulative time interval in a year

The upgraded system at Soccer Club's Skagerak Arena is considered to operate in the grid-connected mode as well as in the islanding mode and therefore, PV, battery and the grid are operated with the constraints using the operational limits. The details of considered constraints are explained in the following sub-sections.

Power Balance Through DERs

The power from all DERs along with the grid at time (t) is expressed in the Eq. (4.2).

$$P_{Grid}(t) + P_{PV}(t) + P_{Dis}(t) = P_{Load}(t) + P_{Chg}(t) + P_{Sell}(t) + P_{Loss}(t) \quad \text{Eq. (4.2)}$$

In this work, due to configuration of the micro-grid, energy generated from PV is directly fed into the grid without battery interface. Skagerak Arena's load is supplied through the grid with battery interface. For economic calculation, the Skagerak Arena energy system is considered as a unit and the net energy provided to the grid is taken as $P_{PV}(t)$-$P_{Load}(t)$. It should be noted that battery discharging has

been taken as positive, whereas battery charging as negative. $P_{Load}(t)$ and $P_{Loss}(t)$ represent the total system's load and power loss at time t.

Power from PV Array

The PV power output (P_{out}) has been calculated using solar radiation data from the US National Renewable Energy Laboratory (NREL) [4.17-4.18]. The PV power output ($P_{PV}(t)$) limits are given in Eq. (4.3).

$$0 \leq P_{PV}(t) \leq Max.P_{PV}(t) \qquad \text{Eq. (4.3)}$$

The detail description of the annualized energy cost calculation of the PV array has presented in Appendix I.

Battery Energy Storage

The minimum SoC of the battery is taken as 20% and initial SoC to be 100%. The battery energy content has been calculated using Eq. (4.2) and it is expressed as battery energy throughput considering after charging and before discharging losses [4.16]. The battery energy content limits are given in Eq. (4.4), and it has been described through Eqs. (4.5) and (4.6) for charging and discharging respectfully. The charging and discharging efficiency of the battery are η_{Chg} & η_{Dis} respectively.

$$SoC_{min} \leq SoC(t) \leq SoC_{max} \qquad \text{Eq. (4.4)}$$

$$SoC(t + \Delta t) = SoC(t) + \eta_{Chg}.P_{Chg}(t).\Delta t \qquad \text{Eq. (4.5)}$$

$$SoC(t + \Delta t) = SoC(t) - \frac{P_{Dis}(t).\Delta t}{\eta_{Dis}} \qquad \text{Eq. (4.6)}$$

The key input battery parameters are 'battery capacity', 'battery voltage', 'depth of discharge', and 'lifetime throughput' are explained in the Section 4.5. The detail description of the annualized energy cost calculation of the battery has been described in the Appendix I.

Energy Management Strategy

The energy management strategy (as shown in the Fig. 4.6) is used and implemented for evaluating performance of the energy system at Skagerak Arena. The main aim of the energy management strategy is to minimize the annual generation cost and maximize the battery energy throughput as well as to reduce the peak load demand from the grid considering demand charges.

As illustrated in the Fig. 4.6, the program starts at t=0 and it checked if grid maximum power limit is more than the load demand, the extra energy will be used to charge the battery (if $SoC(t) < SoC_{max}(t)$). However, if the maximum grid power limit is less comparing the load demand, then extra energy to meet the institutional load demand will be delivered by the battery (if, $SoC_{min}(t) < SoC(t)$).

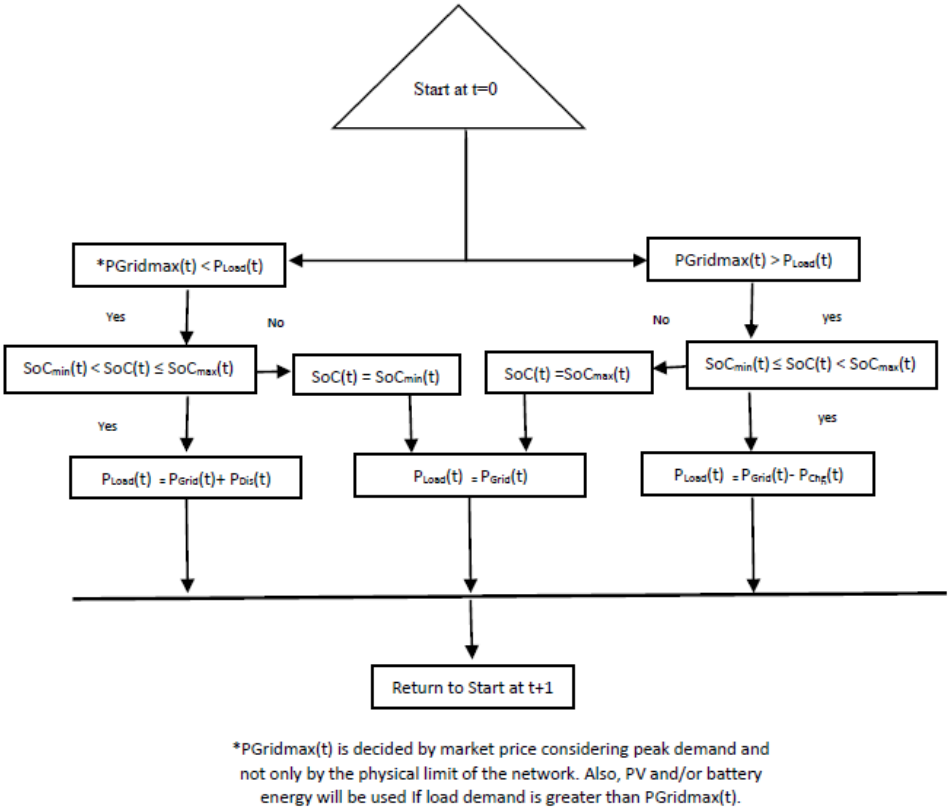

Fig. 4.6 Energy Management Strategy for Micro-grid Operation (Case 4.b)

In this work, energy management strategy is used for optimal battery operation to minimize the overall energy generation cost of the system and to reduce grid dependency. In the next Section 4.5, annual, monthly, and daily operational performance of the Case 4.b are analyzed.

4.5 Performance Analysis of Micro-Grid System of Skagerak Arena (i.e. Case 4.b)

The configuration of upgraded system at Skagerak Arean has shown in the Fig. 4.5 and it consists of 800 kWp Solar PV, 1 MWh lithium-ion battery bank and grid supply to meet the institutional load. Further analysis of the Case 4.b. is carried out for annual, selected months (i.e. best and worst month of the year), and for a typical day, and the results are discussed in the subsequent sub-sections. The ratio ('m') of 'average daily PV output' to 'average daily load' are used for defining the best and worst months for analysis purpose and represented by 'm'. It has been observed that the July month represented the best month of the year with ratio (m) 0.69; however, December month represented the worst month as the ratio (m) is 0.09. The initial SoC of the battery is considered at 100% and minimum SoC is taken 20%. The lifetime energy throughput of a 1 MWh battery is considered 2,000 MWh and battery roundtrip efficiency to be 80% [4.19]. In this study, the PV system power output (Pout) has been calculated using hourly solar radiation data available from the US National Renewable Energy Laboratory (NREL) [4.17-4.18].

4.5.1 Annual Energy Contributions

In the Case 4.b analysis, annual variations of the energy contribution from the PV, Grid and battery's SoC are shown in the Figs. 4.7, 4.8 and 4.9 respectively. The maximum peaks of PV production are recorded 0.73 p.u in the of February and September months. The solar PV output for summer and winter seasons are observed 65% and 35% respectively of the total annual PV generation. The hourly variation of the PV output is shown in Fig. 4.7.

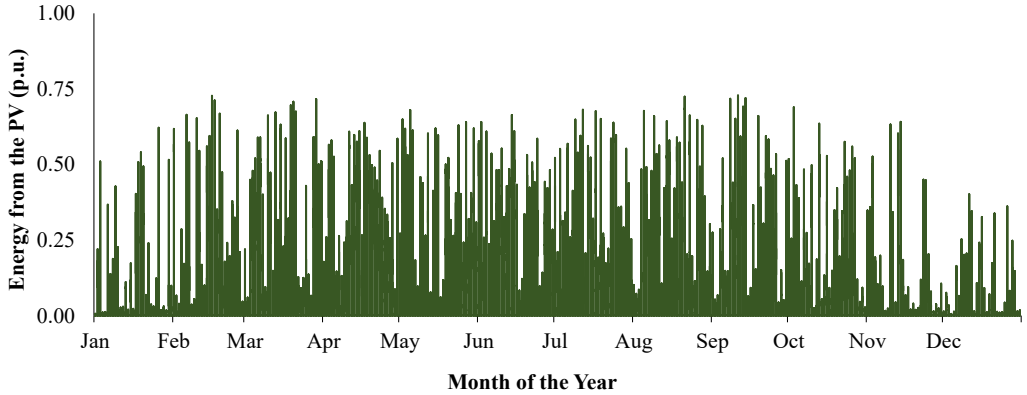

Fig. 4.7 PV Generation Profile Throughout the Year

It has been observed that the annual grid contribution has reduced by 38% (Figs. 4.4 and 4.8) compare to the Case 4.a. The grid energy contribution for summer and winter seasons for Case 4.b, are observed 41% and 59% respectively

of the total annual grid contribution. The hourly variation of the energy demand, grid energy contribution, grid limit and grid demand rate for Case 4.b, are shown in the Fig. 4.8. The grid demand rate is considered constant throughout the year. The monthly grid limits have been introduced for reducing the grid contribution in peak load demand.

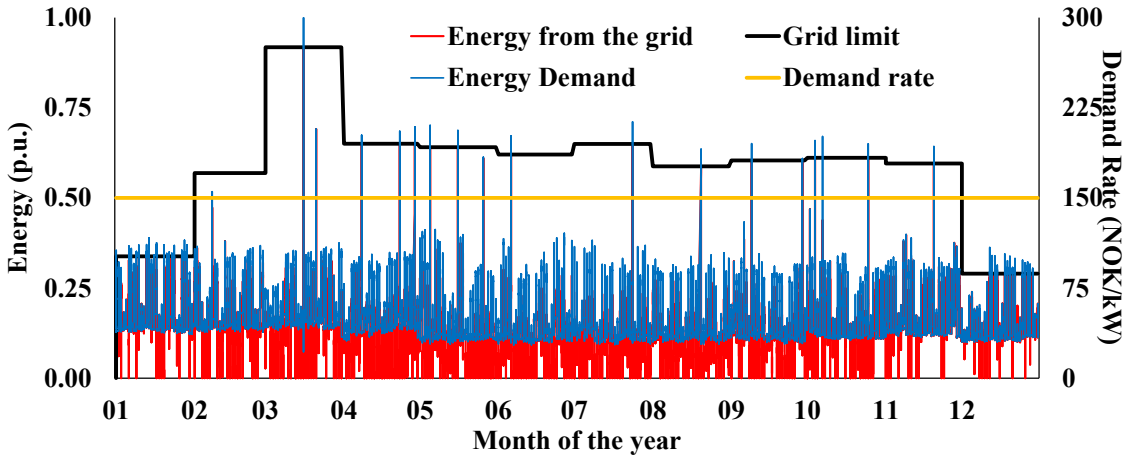

Fig. 4.8 Energy Demand, Grid Limit and Energy, Demand Rate (Case 4.b)

The variation on the battery's SoC has shown in the Fig. 4.9. It has been observed that throughout the year battery's SoC never reached to lowest level (i.e. 20%) and battery's SoC varied in between 40% to 100%. Battery is representing more charging and discharging cycles in the summer season as compare to the winter season and therefore average battery energy throughput of the summer season is double compare to the winter season.

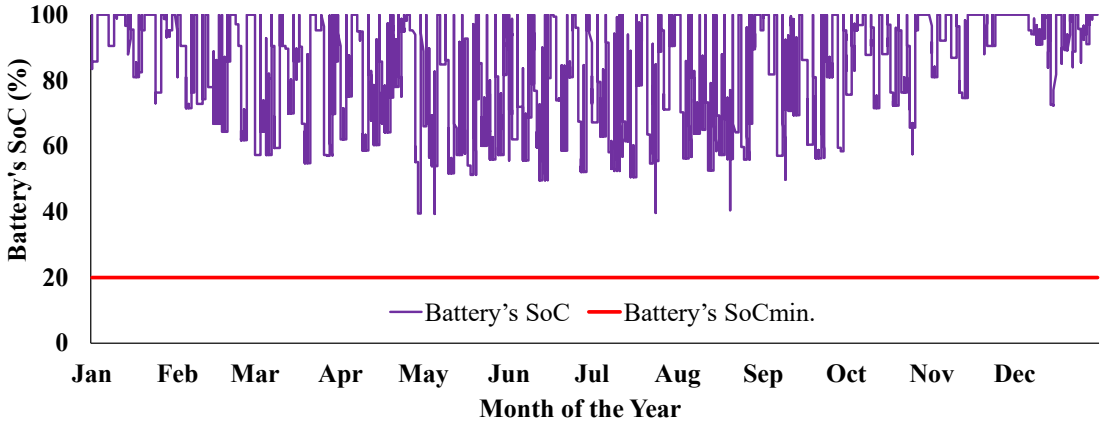

Fig. 4.9 Annual Variation of Battery's SoC (Case 4.b)

A change in the peak load demand for Cases 4.a and 4.b are shown in the Fig. 4.10. It has been observed that the average annual peak demand is reduced by 32% in the Case 4.b. The reduction in the average peak load demand for winter and summer seasons are observed 20% and 46% respectively. It indicates that there is high PV generation in the summer season as compare to the winter season and it makes significant contribution in reducing of peak energy demand from the grid.

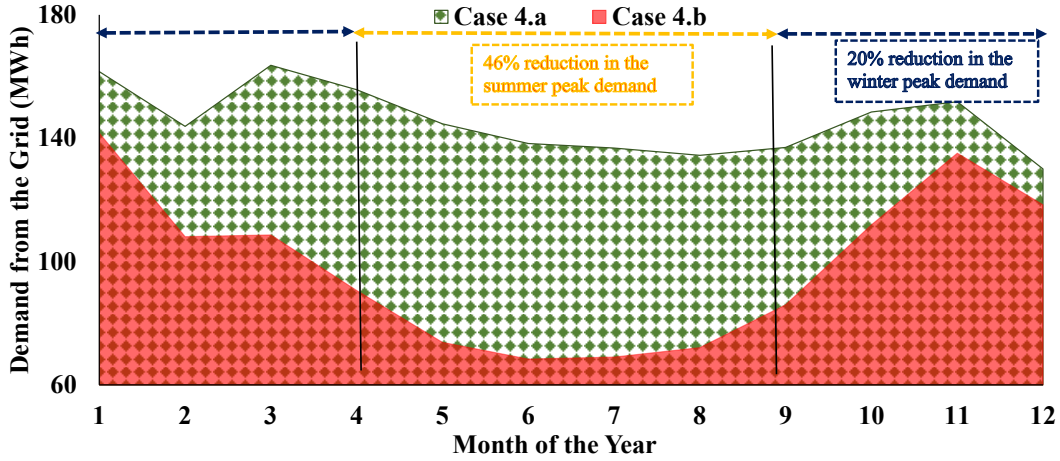

Fig. 4.10 Peak Energy Demand from Grid for Cases 4.a and 4.b

4.5.2 Month Wise Energy Contributions

The month wise energy contributions from the Grid, PV, and battery energy throughput are shown in the Fig. 4.11. The ratio of 'average daily PV output' to 'average daily load' has been used for defining the best and worst months for analysis purpose and represented by 'm'. It has already been discussed in the beginning of Section 4.5, that July represents the best month and December the worst month. It has been observed that the average load of the winter season is 7.14% more compare to the summer season however PV generation is 83% more in the summer season as compare to the winter season. The battery energy throughput in the summer season in 153% more as compare to the winter season. The PV energy generation for months of November, December and January are below 5% of the annual PV generation and battery energy throughput for these three months (i.e. November, December, and January) is recorded under 15%. Battery performs each month of the year and its energy throughput varies from 11% to 61%.

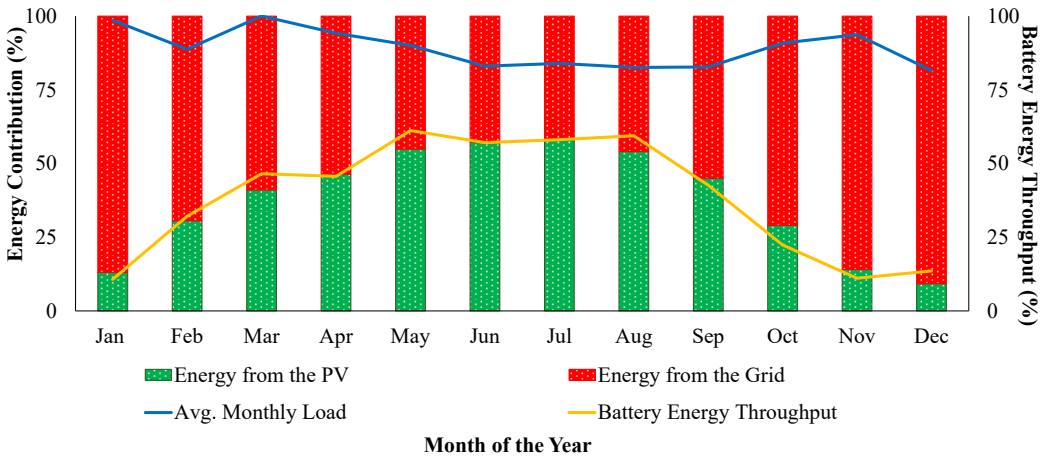

Fig. 4.11 Energy from Grid & PV, and Battery Energy Throughput (Case 4.b)

4.5.3 Energy Contribution from DERs for the Best Month

Energy contribution from the Grid, PV, battery (i.e. battery energy throughput), and battery energy contents, are shown for July month in the Figs. 4.12 & 4.13. In the July month, 31 days are represented in two graphs, day 1 to 15 in Fig. 4.12 and day 16 to 31 in Fig. 4.13. It has been analyzed for July month that the Grid supply contribution has been reduced to 42% and battery energy throughput is recorded 57%. It has been observed that almost 15 days of July month energy is fed into the grid. Battery has been discharged each day of the July month (except Day 2, 28 and 31) and effectively contributing for reducing peak load demand.

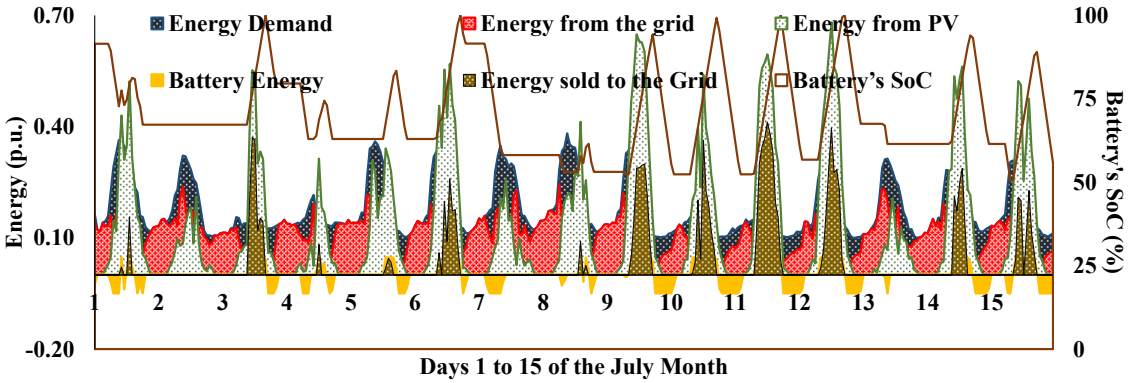

Fig. 4.12 Energy Contribution from 1-15 Days of July (Case 4.b)

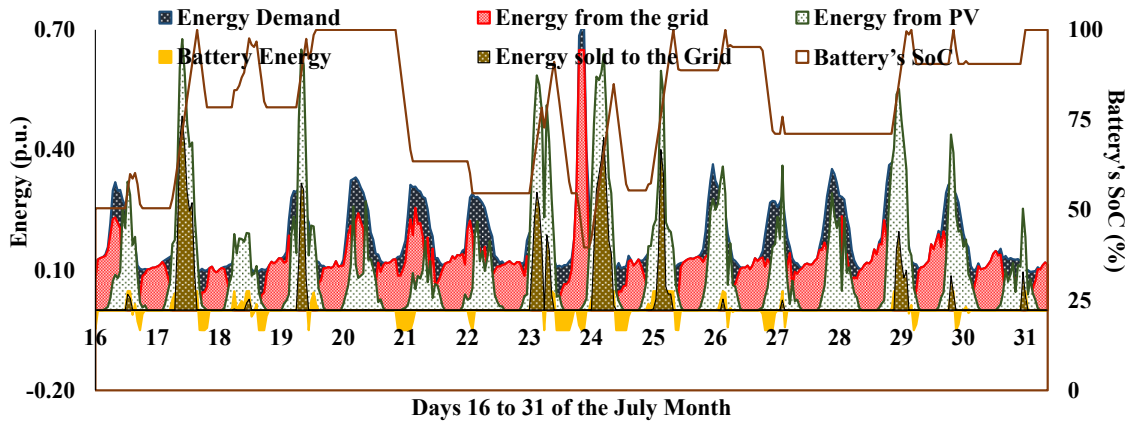

Fig. 4.13 Energy Contribution from 16-31 Days of July (Case 4.b)

It has been observed from the Figs. 4.12 & 4.13 that contribution of the grid majorly appeared during night-time in the July month whereas PV has contributed to meet the load demand during daytime. There are few days (i.e. days 20, 21 and 22) in which grid contribution has been observed during daytime as PV generation is low. In the July month, battery's SoC is varied from 37% to 100%. It indicates that battery'SoC is always above the lowest SoC of 20%.

4.5.4 Energy Contribution from DERs for the Worst Month

As discussed in the Section 4.5 that December month is considered as the worst-case scenario as PV output is only 9% of the total energy generation. Like the July month, energy contributions from different energy sources to meet the institutional building load demand are shown in Figs. 4.14 and 4.15. It has been analyzed for the December month that the grid demand is reduced by 9% and battery energy throughput is recorded 11%. However, battery followed the similar operational characteristics as for the July month and it is charged during daytime and discharged during peak demand hours.

It has been observed from the Fig. 4.14 that battery's SoC is 100% on the day 1 to 5 and load demand is majorly fulfilled by grid. On the day 6, when PV generation is enough then battery is being charged and discharged. It has also been observed that there are few days 8, 9, 11 and 16 when extra PV energy is fed into the grid. It has been observed from the Figs. 4.14 & 4.15 that battery's SoC varies from 75% to 100% and battery gets charge-discharge 20 days out of 31 days.

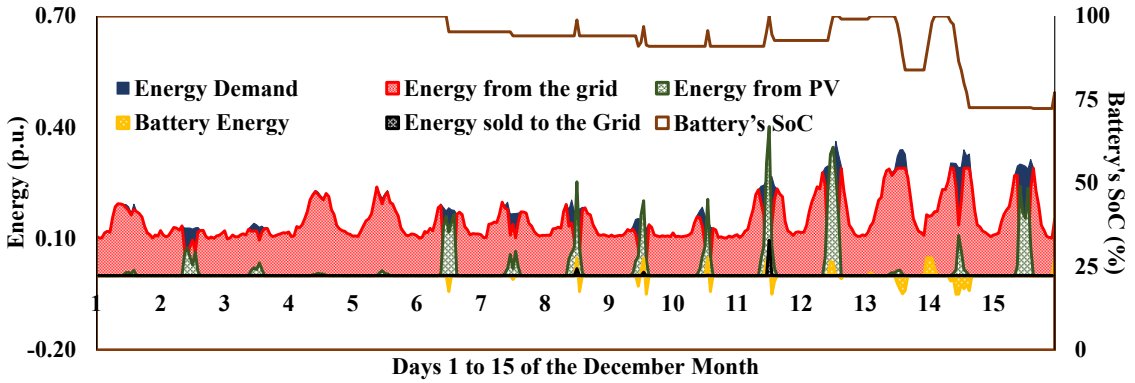

Fig. 4.14 Energy Contribution from 1-15 Days of December (Case 4.b)

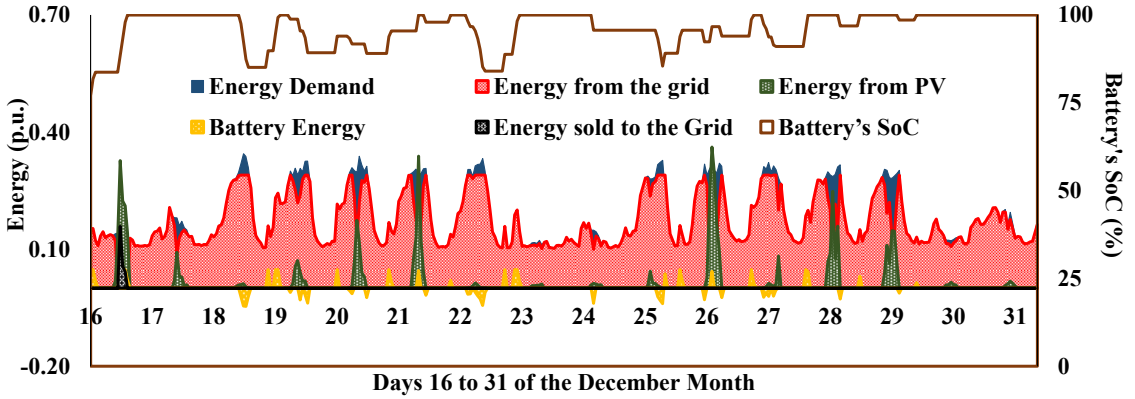

Fig. 4.15 Energy Contribution from 16-31 Days of December (Case 4.b)

It has been analyzed that integration of PV and battery energy storage in the Skagerak Arena with energy management strategy has improved the overall system performance and reduce the annual grid contribution by 38%. The role of battery energy storage becomes very important during summer season as PV generation is more than demand. In this situation, extra PV generation energy is fed into the grid as well as stored in the battery and system is effectively used for reducing the peak load demand from grid.

4.5.5 Energy Contribution for a Typical Day

Energy contribution from different sources for a typical day of the July month has shown in the Fig. 4.16. It has been noted that total load demand of the typical day in July month is 5.38 MWh. In the Case 4.a (i.e. without PV and battery), load demand of the typical day is fulfilled by the grid however, in the Case 4.b (i.e. with PV and battery integration) energy supply from the grid is reduced to 64%. Battery energy contribution and energy supply to the grid are noted 0.24 p.u. and 0.19 p.u. respectively of the base value as described in the Section 4.3. It has been observed from the Fig. 4.16 that battery is discharging during morning time (i.e. 06:00 hours to 10:00 hours) and evening time (i.e. 16:00

hours to 20:00 hours) and it is effectively contributing for reducing grid supply. Energy sold to the grid is represented during the peak sunshine hours. In this next section, detail analysis for operational analysis of battery energy storage is presented.

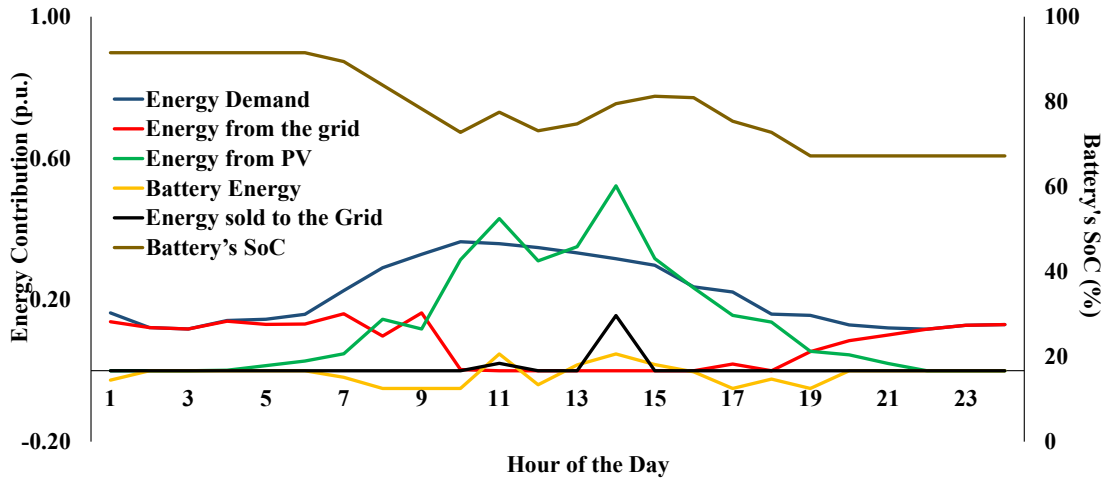

Fig. 4.16 A Typical Day Profile of the July (Case 4.b)

4.5.6 Battery Performance Analysis

The role of BES becomes very important when it relates to distributed energy sources (i.e. PV) for fulfilling the local demand, contributing for demand side management, and improving economic performance of the system. In this section, performance of battery is analyzed through battery energy throughput and its comparison is done with saving through electricity sell to the grid as well as saving through reduction in the grid demand. The performance of the battery is evaluated based on the hourly variation of energy content in the battery, and it's monthly & annual energy throughput. A monthly variation of the battery energy throughput has illustrated in Fig. 4.17.

In this analysis, the six months from 'April to September' have been considered to represent as 'summer' and the remaining six months 'October to March' as winter. It has been observed that average battery energy throughput of the summer season (i.e. April-Sept) is 154% more as compare to the winter season (i.e. Oct-Mar). This indicates that battery is used more during the summer season compare to the winter season as battery is primarily charged by PV. The battery energy throughput is always more than 30% throughout the year except for January, October, November, and December months. However, average annual throughout of the battery is 38% and there are four months (i.e. May, June, July

and August) represent more than 55% of energy throughput. The variation in the battery' SoC for each month of the year has illustrated in the Fig. 4.9. Although, few instances are observed in the months of May, August and September when battery's SoC reached to below 40% but it always above minimum SoC level of battery.

It has been observed from Fig. 4.17 that battery energy throughput follows the same pattern as for 'saving through reduction in grid demand', whereas 'saving through electricity sell to the grid' is following the PV generation pattern.

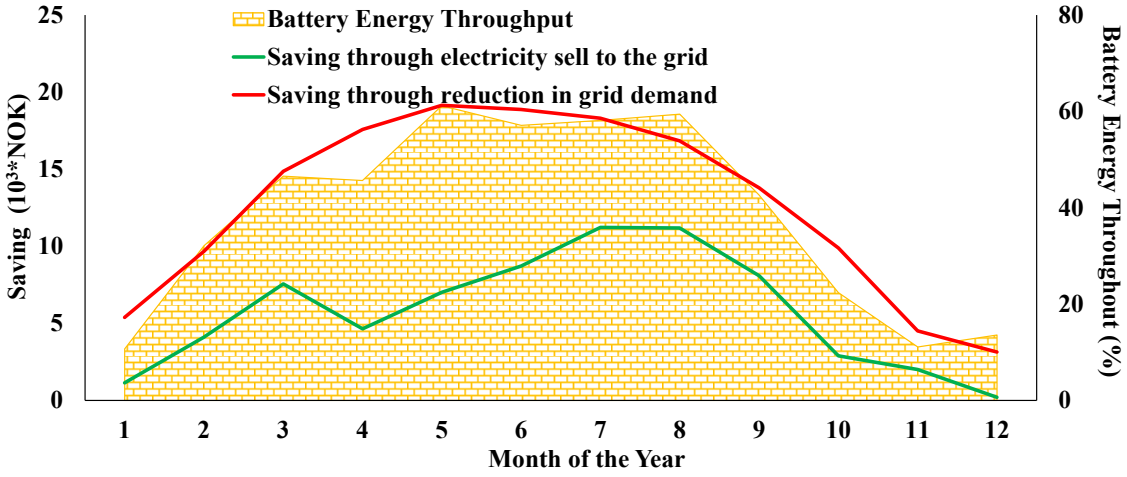

Fig. 4.17 Battery Energy Throughput and Saving (Case 4.b)

The saving through electricity sell to the grid and reduction from the grid supply represent 31% and 69% respectively of total saving. In indicates that reduction in the grid supply makes major contribution in the saving components. The saving in the summer season (i.e. April to September) and in the winter (i.e. October to March) season are recorded 70% and 30% of the total saving of the year.

4.6 Economic Analysis and Comparison of Cases 4.a & 4.b

In the presented micro-grid system, the capital cost components consist of PV, battery, micro-grid controller and installation and commissioning cost. The component costs are mainly categorized into four types: capital, operating, replacement and salvage cost. In this section, economic performance of the micro-grid for Cases 4.a and 4.b, have been analyzed. In this study, the project lifetime, discount rate and inflation rate are considered as 25 years, 5.5% and 1.9% respectively [4.19]. The PV, BES and their operational parameters are taken from the ref [4.16]. The electrical energy pricing for calculation is taken from the

NordPool market [4.15]. The net present cost (NPC) summary of different components is shown in the Fig. 4.18.

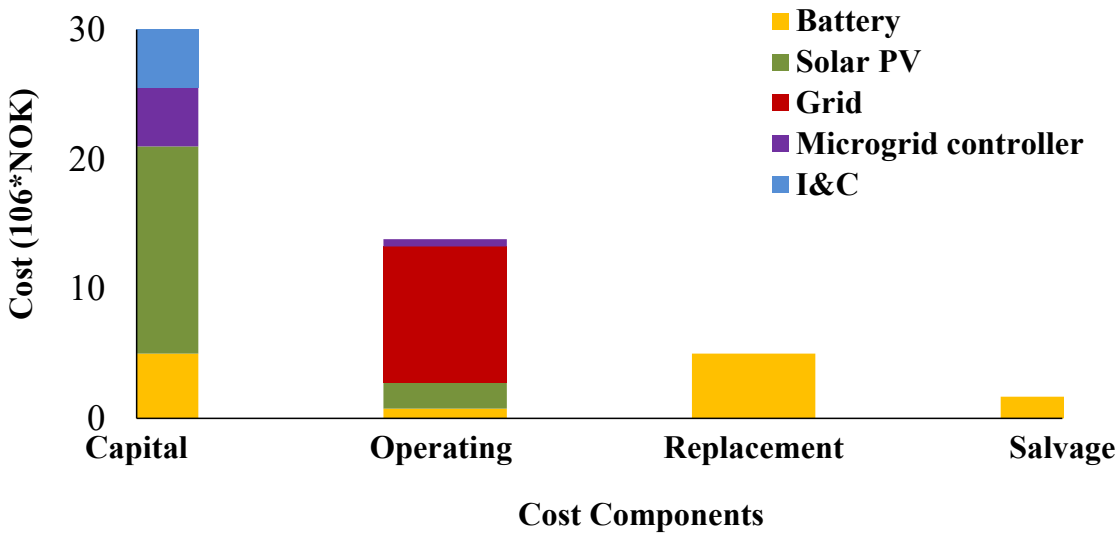

Fig. 4.18 Cost Comparison of Micro-grid's Components

Out of total capital cost, PV system represents the maximum cost share, and it is 53% followed by 27% battery energy storage, 15% micro-grid controller and 15% installation and commissioning. The initial capital cost of grid is zero as it is considered that grid infrastructure is already available however, operating cost of grid if maximum (i.e. 79% of total operating cost) as compare to the other components. The operating cost of PV and battery are 15% and 6% respectively.

It has been observed from the Table 4.2 that levelized cost of energy (CoE) and NPC are increased by and 28% and 39% respectively compare to the Case 4.a scenario. Also, annual grid contribution is reduced by 38%. It has also been observed that out of total energy generation, 9% energy is sold to the grid, and annual battery energy throughput is 37%. The annual electricity bill is reduced by 21% as compare to the base case (i.e. Case 4.a). The results obtained after integrating PV and BES with grid for micro-grid system (i.e. Case 4.b) are shown in the Table 4.2.

Table 4.2 Economic Results Comparison of Case 4.b with Case 4.a

Parameters	Value in Case 4.b	Changes as compare to the Case 4.a (%)
CoE (NOK/kWh)	1.23	28 (↑)
Net present cost (m NOK)	38.5	39 (↑)
Annual grid contribution to the total generation ratio (%)	62	38 (↓)
Annual PV contribution to the total generation ratio (%)	38	-
Annual battery energy throughput (%)	38	-
Annual energy sold to grid compare to total generation ratio (%)	9	-
Annual electricity bill (10^3*NOK)	1521	21 (↓)

The signs downward (↓) and upward (↑) indicate, percentage reduction and increment in the parameter's value.

The cashflow summary of different components over the project lifetime of 25 years has given in the Fig. 4.19. Although, PV has the highest capital cost share (i.e. 53% of the total capital cost). But over the 25 years project lifetime, PV system cost is only 35% of the total project cost followed by the battery 25%, grid 21%, controller 10% and I&C cost 9%.

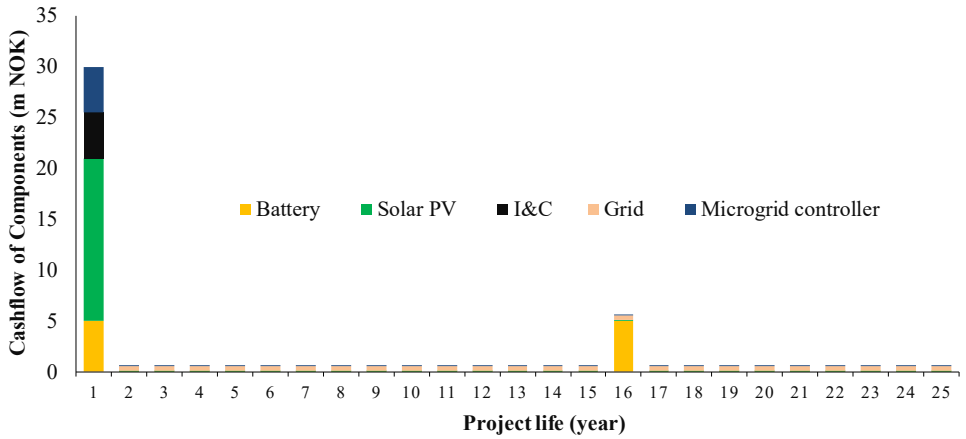

Fig. 4.19 Net Cashflow Summary of Different Components

In this Chapter operational performance of the micro-grid system at Skagerak Arena has analyzed for Norway whereas in the Chapter 2 (Fig. 2.6) the operational performance of the institutional micro-grid system in India is analyzed. In the next section a comparative analysis of the operational performance of the micro-grid system has analyzed for India and Norway climatic conditions.

4.7 Comparative Analysis of Performance of the Micro-Grid System in India and Norway Geographical Locations

The micro-grid system presented in the Chapter 2 (Fig. 2.6), consists of 50 kWp PV, 120 kWh lead acid battery bank, grid supply and 30 kVA DG to meet the institutional load. The considered micro-grid in Norway (Fig. 4.5) consists of 800 kW_p PV, 1 MWh lithium-ion battery bank and grid supply to meet the load demand of Skagerak Arena. In the subsequent sections, different operational parameters are compared and analyzed for India and Norway such as specific energy of PV output, contribution from different energy sources, battery performance, etc.

4.7.1 Specific PV Output

To compare the performance of PV system in Indian and Norwegian climatic zones, a parameter i.e. 'specific energy (SE)' per month and per day have been used. The specific energy profiles of PV for each month of the year for Indian and Norwegian climatic conditions are illustrated in the Fig. 4.20. It has been observed that annual specific energy of the PV in the India is 36% more compare to the selected Norwegian geographical locations. The specific energy generation in India is more than 100 kWh/kWp for each month of the year except December, whereas for Norwegian location only six months (i.e. Mar-Sept), specific energy is more than 85 kWh/kWp.

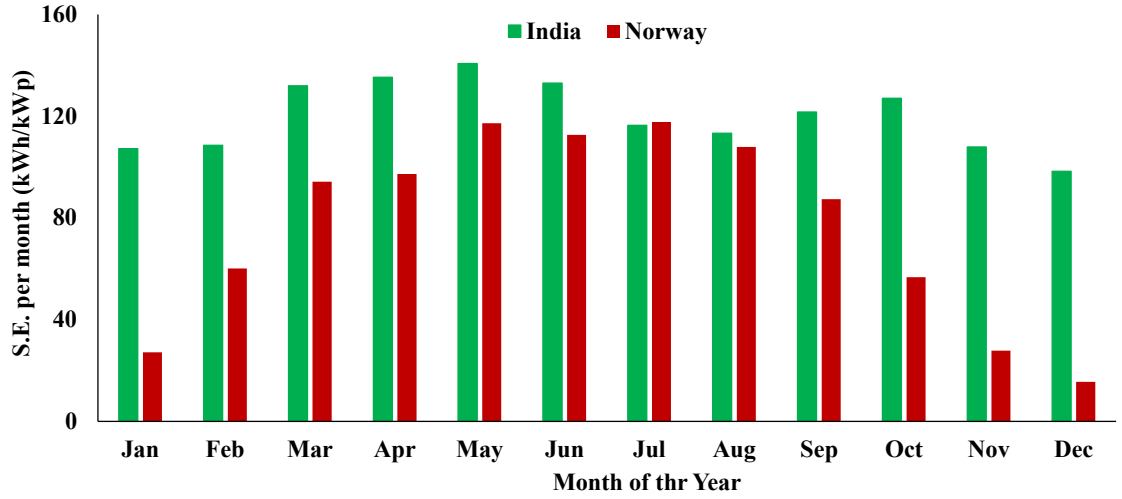

Fig. 4.20 Specific Energy of PV at Selected Locations of India & Norway

The specific energy per day of PV modules in India and Norway are shown in the Figs. 4.21 and 4.21 respectively. In case of India, PV generation in the

summer and winter seasons are 53% and 47% respectively of the total PV generation of the year and it has been observed that PV generation only 6% more in the summer season as compare to the winter season. However, for Norway, PV generation in the summer and winter seasons are 69% and 31% respectively of the total PV generation of the year and it has been observed that PV generation is more than two times in the summer season as compare to the winter season and it is worst in the winter season months (e.g. November, December and January) as PV generation varies 2-3% of the total annual generation.

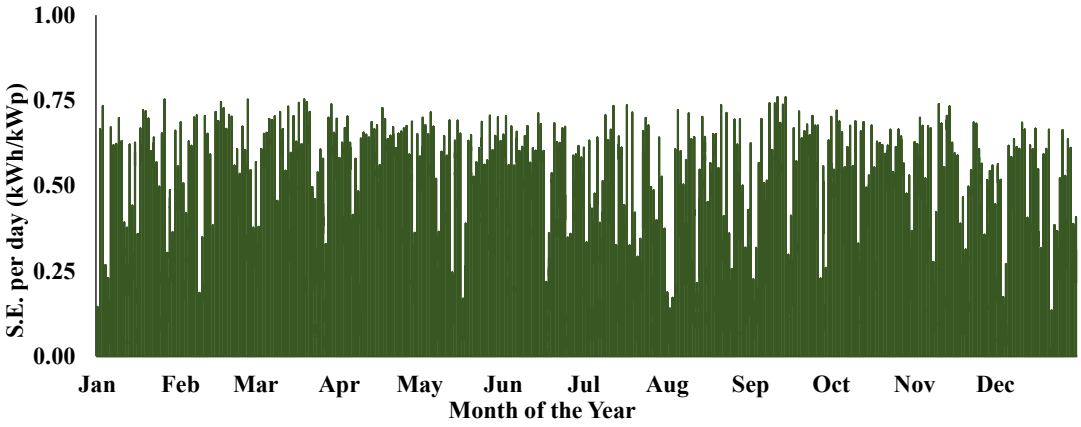

Fig. 4.21 Specific Energy Per Day of PV in India

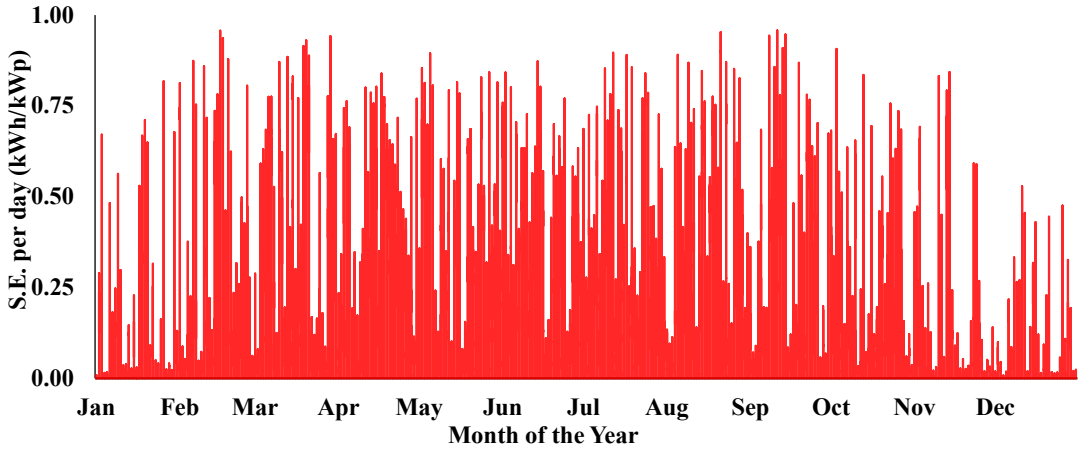

Fig. 4.22 Specific Energy Per Day of PV in Norway

4.7.2 Energy Contribution without and with Micro-grid System in India and Norway

In India, grid outage problem is quite often and therefore DG as a back-up power supply is always kept for meeting at least essential load demand during grid outage conditions. In this work, two hours per day of 'grid-outage' is considered and it is randomly distributed throughout the year. However, grid supply is quite

reliable in Norway and therefore no need to integrate DG as a power-backup. In this section, energy contribution from different energy sources with and without micro-grid system (i.e. integration of PV and battery energy storage) for Indian and Norwegian climatic conditions are analyzed and illustrated in the Figs. 4.23 and 4.24 respectively. For Indian scenario, integration of PV and battery energy storage help to reduce DG and grid contribution in the overall supply. It has been observed that DG contribution has reduced from 12.7% to only 1 % and grid contribution from 83.7% to 51% and battery energy throughput is recorded 33%. The schematics of institutional system without and with PV and battery energy storage are described for India, in the Chapter 2 (Figs. 2.1 and 2.6 respectively).

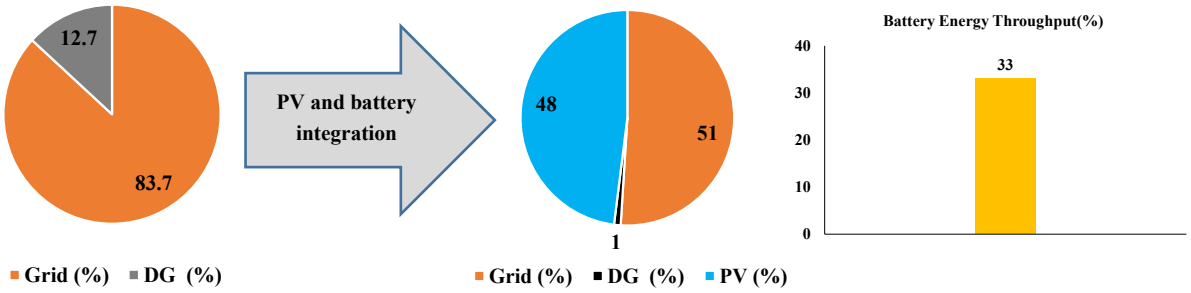

Fig. 4.23 Energy Contribution without and with Micro-grid System in India

For Norwegian scenario, integration of PV and battery energy storage can help to reduce grid contribution in the overall supply. It has been observed that grid contribution is reduced by 38% and it is replaced by PV and battery energy throughput is recorded 38%. The schematics of institutional system without and with PV and battery energy storage are described in the Chapter 4 (Figs. 4.1 and 4.5 respectively).

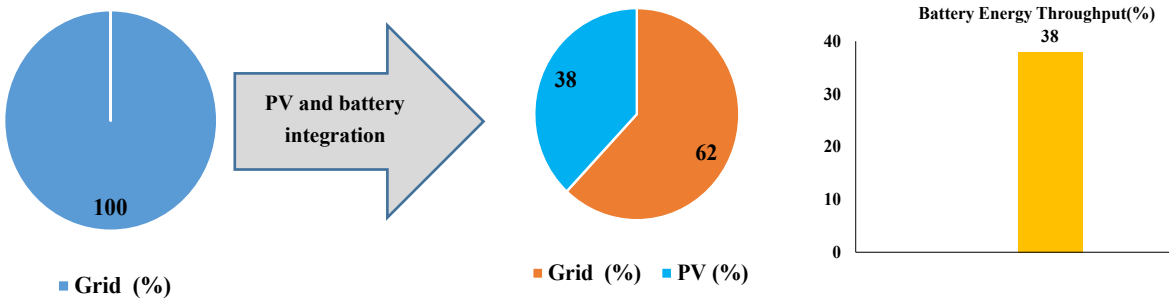

Fig. 4.24 Energy Contribution without and with Micro-grid System in Norway

4.7.3 Comparative Battery Performance Analysis for India and Norway

It has been observed that for both the scenarios (Fig. 4.25), variation in the average annual battery energy throughput is only 5%, but operational performance of the battery is quite different throughout the year and it is illustrated in the Figs. 4.26 and 4.27. It has been observed for India that the average battery energy throughput of the winter season (i.e. October-March) is 5% more as compare to the summer season (i.e. April-September). However, in case of Norway, average battery energy throughput of the summer season (i.e. April-Sept) is 154% more as compare to the winter season (i.e. April-September). The performance assessments of all presented cases in this Chapter have been tested with the 'Homer Pro' tool. The average battery energy throughput for India and Norway varies 21-43% and 11-61% respectively. The large variation of battery energy throughput for Norwegian climatic scenario is observed due to the solar PV generation profile.

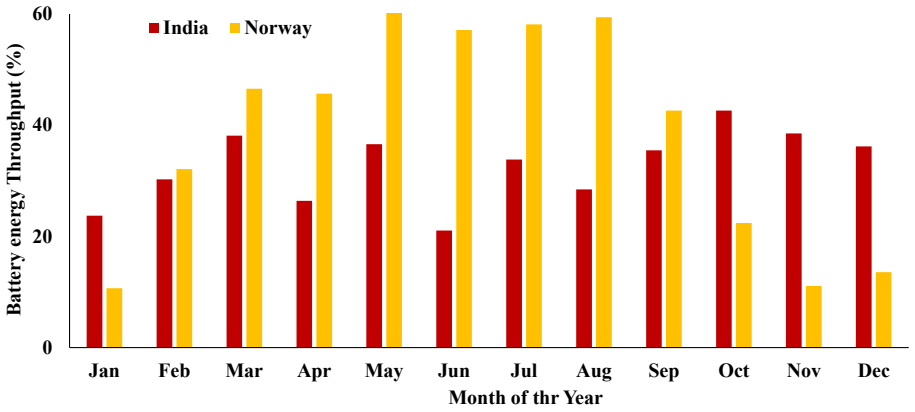

Fig. 4.25 Monthly Battery Energy Throughput in India and Norway

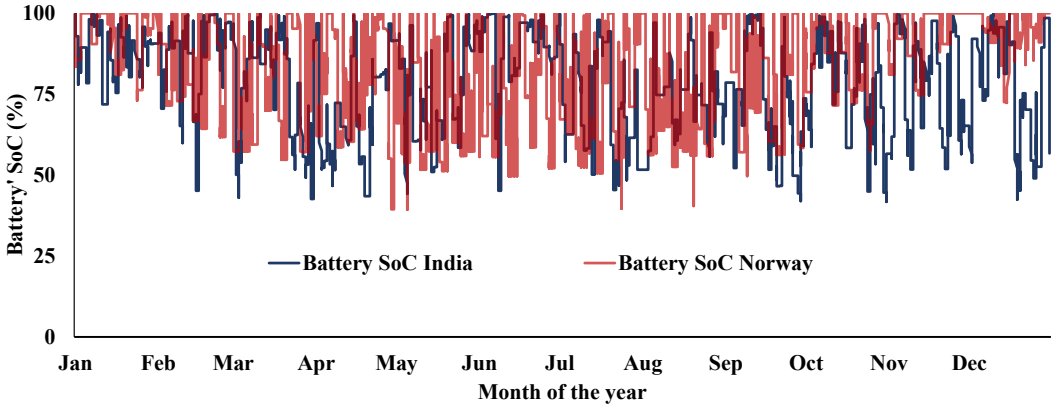

Fig. 4.26 Variation of Battery' SoC

The variation in the battery' SoC for India and Norway has illustrated in the Fig. 4.26. In Case of India, few instances are observed in the months of March, April, May, September, October, and November, when battery's SoC reached to

below 45% but due to availability of DG, the blackout situation has never been happened and battery SoC remains above 40%. However, in Case of Norway, few instances are observed in the months of May, August, and September when battery's SoC reached to below 40% but it always above minimum SoC level (i.e. 20%) of battery. For both the locations battery SoC's always above the minimum SoC levels.

4.8 Conclusions

In this chapter, techno-economic performance has been presented for installed PV and battery based micro-grid system at Skagerak Arena, Norway. It has been noticed that in the July month (i.e. best month), energy contribution from the PV and grid, are 58% are 42% respectively whereas, battery energy throughput is 59%. In the December month (i.e. worst month), energy contribution from PV and grid, are 9% are 91% respectively, and battery energy throughput is 7%. In the economic analysis, the initial capital cost of PV system has contribution of 53%, but over the considered project lifetime of 25 years, total PV system net present cost share is 35% of the total project NPC followed by the battery 25% and grid contribution 21%, controller 10% and I&C cost 9%. In this work, the techno-economic analysis results of micro-grid system are further compared for Indian and Norwegian climatic conditions. For Norwegian scenario, integration of PV and battery energy storage, reduced grid contribution by 38% whereas, for Indian scenario, integration of PV and battery energy storage help to reduce DG contribution from 12.7% to only 1 % and grid contribution from 83.7% to 51%. The average battery energy throughput for India and Norway varies 21 to 43% and 11 to 61% respectively.

PV based micro-grid system integrated with battery energy storage can be a solution to reduce the grid demand for institutional or commercial buildings. However, the impact of electricity tariffs dynamics on the operational performance of such micro-grid system is needed further investigation. In the Chapter 5, the impacts of the electricity energy tariffs on the Norwegian micro-grid system has been analyzed.

Chapter 5

5. Impact of Energy Pricing Dynamics with Geographical Locations on Techno-Economic Performance of PV based Micro-Grid System[4]

5.1 Summary

In this Chapter, PV based micro-grid system, located in the selected geographical locations (e.g. India and Norwegian), has used for evaluating the techno-economic operational performance under market energy pricing dynamics. The energy management strategy has presented for minimization of annual generation cost with maximization of battery energy throughput with grid constraints as demand limits. Operational energy management strategies for micro-grid have evaluated for managing peak demand under market energy pricing dynamics. The impact of local grid buying and selling tariffs on geographically located micro-grid's techno-economic operational performance have presented.

5.2 Introduction

The integration of PV system with battery has vast potential to function as a microgrid and fulfill the local load demand during islanding mode and as well as grid-connected mode. The operational performance of a PV-battery based microgrid can be enhanced with suitable energy management strategies, and it can also contribute to demand-side management considering grid constraints. In the past few years, several research studies [5.1-5.4] have been conducted, and these studies are mainly focused on technical sizing and performance evaluation of grid connected rooftop PV system, off-grid system, and hybrid energy systems for different geographical regions. The study presented in ref [5.1], analysed an ideal combination of a micro-hydro, photovoltaic, battery, and diesel generator to fulfill the electricity demand of rural village of Chamba District Himachal Pradesh in India however, this work has not included the sensitivity analysis of hybrid system with future energy tariffs. An optimization approach is used in ref [5.2], for

[4] This chapter is based on peer reviewed journal paper, Sharma, *et.al.* 'Economic Performance Assessment of Building Integrated Photovoltaic System with Battery Energy Storage under Grid Constraints', *Renewable Energy* (Elsevier), vol. 145, pp. 1901-1909, 2020.
doi: 10.1016/j.renene.2019.07.099.

developing PV, wind and battery-based system for Kuala Terengganu, Malaysia whereas role of energy management strategy during grid outage conditions have not addressed. The cost-benefits analysis of grid-connected PV system has carried out in ref [5.3] considering the local climates, energy generation cost, emissions of the system, and return on investment. The study [5.3] has covered the impacts of PV system design the economics and environment however impacts of electricity energy tariffs on the techno-economic evaluation of the system has not covered. A techno-economic study of grid-connected PV system for residential and commercial consumers in Germany, Switzerland and Austria has presented in ref [5.4]. The paper [5.4] analysed the potential of rooftop PV for different consumers considering technological, economical, and geographical factors but dynamics of electricity pricing has not sufficiently covered. In the most of reviewed literatures [5.1-5.4], impact of electrical energy pricing dynamics on techno-economic performance of microgrid system and role of energy management techniques for peak demand saving have not sufficiently covered.

Within Europe, interest of PV and battery system are also growing in the Nordic countries, due to economics & environmental concerns. In the Nordic countries, industry, commercial and households' consumers are seeking to reduce their electricity bills by integrating rooftop PV modules with batteries and it shows a vast prospective for peak load saving through PV based micro-grid integration [15]. Within the Nordic countries, Norway is using mainly hydroelectricity (i.e. 96%), but in the recent years PV market has grown up as the installed cumulative PV capacity in Norway has reached 119.8 MWp at the end of 2019, and it was only 15.3 MWp at the end of 2015 [5.5]. It indicates that the PV market has increased eightfold in the last five years. It is mainly due to National policy such as Plusskundeordningen, subsidy payouts for small solar PV installations [5.6]. The increasing PV penetration as well as energy market dynamics of the Norwegian system can contribute for local energy management for institutional systems to operate as microgrid. Some studies [5.7-5.10], have reported operation of PV based system in the Nordic climatic conditions. The performance evaluation of a grid-connected building integrated photovoltaic (BIPV) system in Norway has described with real functioning results in ref. [5.7]. In the study [5.7], integration of an appropriate battery storage with grid constraints, has been highlighted for improving the operational performance of the grid connected BIPV system however, impact of electricity energy tariffs on the operational energy management strategies has not been discussed. In the ref. [5.8], the economic

performance of BIPV system integrated with battery storage has assessed under electricity energy pricing and grid constraints for a residential household, but it has not sufficiently included the energy management strategies during dynamics of energy pricing. The study [5.9], has focused on grid tariffs rates for domestic customers with rooftop PV system of Norway and presented how different grid tariffs can influence the cost-benefits. The results of study presented in ref [5.9], have shown that grid power tariff can provide more economic benefits to the prosumer compare to the grid energy tariff. The performance assessment results of a 45 kWp grid-connected PV system in Norway has reported in ref [5.10]. The paper [5.10] highlights the growing interest in BIPV systems for residential homes as well as for larger industrial buildings, and also creates knowledge and valuable asset for planners in the building sector and grid operators. In the reviewed literatures [5.7-5.10], technical and economic performance assessment of the PV-battery based microgrid under electricity energy pricing dynamics have not significantly analyzed for their role of energy management strategy in peak demand reduction with grid constraints.

In Norway, electricity energy tariffs have mainly two components; electricity price and grid rent. Based on the type of customers, electricity energy tariffs are divided into three types of contracts [5.11]: (i) Fixed price contracts: In this type of contract, grid tariff is fixed, or associated with a fixed price route, are considered as fixed price contracts. (ii) Contracts tied to spot price: It includes contracts directly linked to the spot price in addition to the overhead charge or price ceiling. It has drawn from the elspot price [5.11]. (iii) Variable price contracts: In this category, price fluctuates during the year (e.g. quarterly), based on energy market demand. The electricity supplier is free to change any price but inform to the end user at least 14 days in advance. These price contracts have applied to domestic, industries, and commercial buildings. It has observed that the average price of electricity from the year 2015 to 2018 had risen from 0.18 NOK per kWh to 0.41 NOK per kWh, and it is 135% greater relate to the 2015 [5.12]. The annual variation of the electricity tariffs has shown in the Fig. 5.1.

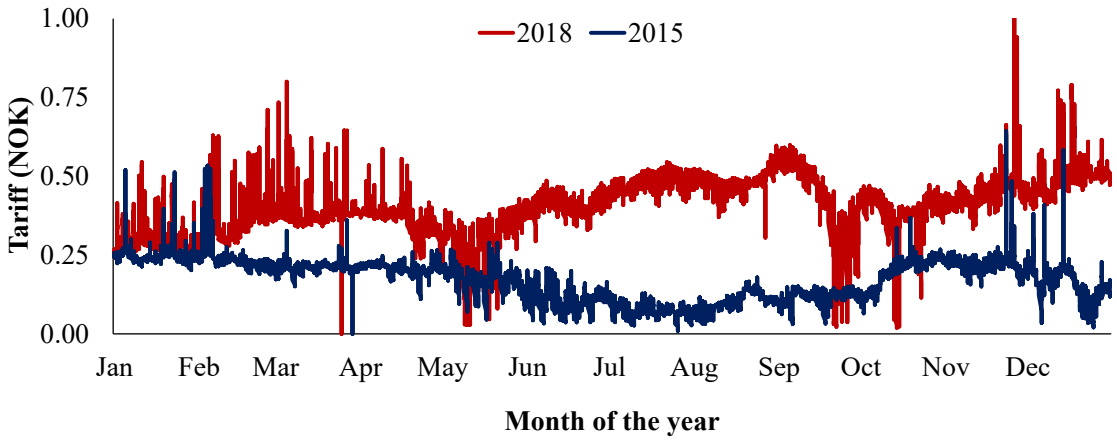

Fig. 5.1 Hourly Variation of the Electricity Energy Prices for Years 2015 and 2018

The average energy price of summer and winter seasons of 2015 have increased by 211% and 88% respectively in the year 2018. Generally, average energy price of the summer period is lower compare to the winter period, but in the year 2018 the average energy of the summer season was 4.22% more compare to the winter season. The main reason to increase of energy price in the summer 2018 was the lack of rainfall in the year 2018 and therefore Norwegian hydropower generation was lower [5.13]. In addition to the load demand and electricity price's pattern in Norway, there are challenges with the distribution of the solar irradiance over the year, as very good amount of solar irradiance has presented during the summer period, but very limited quantity has presented in the winter season [5.14]. There are several industries, institutional and commercial buildings which have lot of potential to integrate PV & battery storage and have their specific demand patterns. Such consumers need to take immediate action on how they can reduce their load demand or use any other source of energy based on the electricity energy pricings. Therefore, technical, and economic performance analysis of PV-battery based micro-grid system is essential for analyzing the effective usage of distributed energy sources and developing decentralized demand-side management techniques with grid constraints under dynamics of electrical energy pricing.

In this Chapter, the Skagerak Arena institutional energy system (as depicted in the Fig. 4.5), integrated with PV and battery storage, has been used for evaluating the techno-economic performance under market energy pricing dynamics. The key objective of this work is to maximize the usage of local energy resources through battery energy throughput considering peak demand, and to evaluate the techno-economic performance under dynamics of energy tariffs. In

this work, the impact of grid buying and selling tariffs on techno-economic performance of micro-grid have analyzed conspiring the energy management strategies. To analyze the impact of energy tariffs on the operation of the Soccer Club Skagerak Arena micro-grid system, different tariffs scenarios are considered. Since the average cost of electricity supply during the period 2015 to 2018 had increased from 0.18 NOK/kWh to 0.41 NOK/ kWh (i.e. 135% high compare to the 2015) and annual variation of the electricity tariffs are shown in the Fig. 5.1. Therefore, it has assumed that the energy tariffs may vary from 100% to 200% and these variations are considered with 25% intervals (i.e. 'Tariff 100%', 'Tariff 125%', 'Tariff 150%', 'Tariff 175%' and 'Tariff 200%' as shown in the Fig. 5.2).

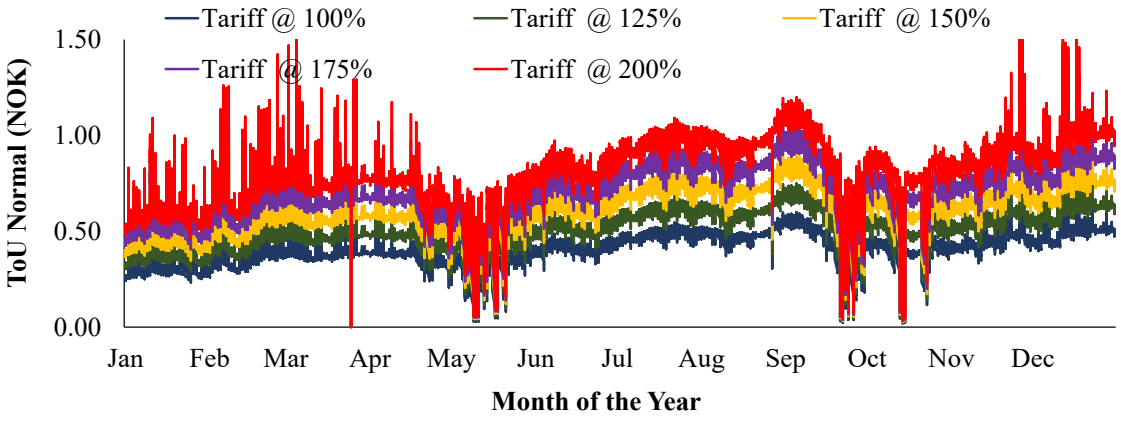

Fig. 5.2 Variation of Different Energy Tariff

The chapter has divided into the mainly seven sections; the first section (i.e. Section 5.2) begins with introduction and considered electricity price for analysis. In the Section 5.3, performance evaluation of the micro-grid system has analyzed with operational energy management strategy under the different energy tariffs, institutional micro-grid at Skagerak Arena. The impacts of different cost components on the CoE, NPC and battery energy throughput, has presented in Section 5.4. Economic performance analysis of micro-grid system in the selected geographical location (i.e. India and Norway) has presented in the Section 5.5. Impacts on CoE of the micro-grid with different grid buying and selling prices for India and Norway has analyzed in the section 5.6. The key economic benefits with future opportunities for operating an institutional energy system as a micro-grid have concluded in the Section 5.7.

5.3 Energy Management Strategy for Micro-grid Operation

The energy management strategy is very important for improving economic performance and operation of micro-grid system. In this work, the main aim to formulate the energy management strategy is to reduce peak load demand from the grid and increase PV energy contribution through optimal battery energy usage. A minimization approach [5.16-5.17] has applied for minimizing the overall energy generation cost (i.e. f(cost)), and it has been explained through the Eq. (5.1). The cost function includes energy cost from grid, reduction in peak demand cost and battery energy cost. In the Eq. (4.1), if $P_{Grid}(t)$-$P_{PV}(t)$ is positive (+ve) then $E_{Grid}(t)$ is considered and $E_{Sell}(t)$ will be zero whereas in case $P_{Grid}(t)$-$P_{PV}(t)$ is negative (-ve) then $E_{Sell}(t)$ is considered and $E_{Grid}(t)$ will be zero.

$$\min f_{(cost)} = \sum_{t=1}^{T} \begin{bmatrix} [((P_{Grid}(t) - (P_{PV}(t)) * d(\Delta t)) * (E_{Grid}(t)] \\ +[((P_{PV}(t) - P_{Grid}(t)) * d(\Delta t)) * E_{Sell}(t)] \\ +[D_n(t) * (D_{Grid}(t)] \\ +[(P_{Bat}(t) * d(\Delta t)) * (E_{Bat})\,] \end{bmatrix} \quad \text{Eq. (5.1)}$$

where:

$P_{Grid}(t)$: Power bought from the grid at time t

$D_n(t)$: Grid electricity demand at time t

$D_{Grid}(t)$: Grid electricity demand price at time t

$E_{Grid}(t)$: Grid electricity buying price at time t

$E_{Sell}(t)$: Grid electricity buying price at time t

$d(\Delta t)$: Time duration

$P_{Bat}(t)$: Power from the battery at time t

E_{Bat}: Battery energy cost

T: Total cumulative time interval in a year

The upgraded system at Skagerak Arena is considered to operate in the grid-connected mode as well as in the islanding mode and therefore, PV, battery and the grid are operated with the constraints using the operational limits. The details of considered constraints are explained in the following sub-sections.

Power Balance Through DERs

The power from all DERs along with the grid at time (t) is expressed in the Eq. (5.2).

$$P_{Grid}(t) + P_{PV}(t) + P_{Dis}(t) = P_{Load}(t) + P_{Chg}(t) + P_{Sell}(t) + P_{Loss}(t) \quad \text{Eq. (5.2)}$$

In this work due to configuration of the micro-grid, energy generated from PV is directly fed into the grid without battery interface (i.e Chapter 4 Fig. 4.5). Institutional load is supplied through the grid with battery interface. For economic calculation, the energy system is considered as a unit and the net energy provided to the grid is taken as $P_{PV}(t)$-$P_{Load}(t)$. It should be noted that battery discharging has taken as positive, whereas battery charging as negative. P_{Load} (t) and P_{Loss} (t) represent the total system's load and power loss at time t.

Power from PV Array

The PV power output (P_{out}) has been calculated using solar radiation data from the US National Renewable Energy Laboratory (NREL) [5.18]. The PV power output ($P_{PV}(t)$) limits are given in Eq. (5.3).

$$0 \leq P_{PV}(t) \leq Max.\, P_{PV}(t) \quad \text{Eq. (5.3)}$$

The detail description of the annualized energy cost calculation of the PV array has presented in Appendix I.

Battery Energy Storage

The minimum SoC of the battery is taken as 20% and initial SoC to be 100%. The battery energy content has been calculated using Eq. (5.2) and it is expressed as battery energy throughput considering after charging and before discharging losses [5.15]. The battery energy content limits are given in Eq. (5.4), and it has been described through Eqs. (5.5) and (5.6) for charging and discharging respectfully. The charging and discharging efficiency of the battery are η_{Chg} & η_{Dis} .

$$SoC_{min} \leq SoC(t) \leq SoC_{max} \quad \text{Eq. (5.4)}$$

$$SoC(t + \Delta t) = SoC(t) + \eta_{Chg}.\, P_{Chg}(t).\, \Delta t \quad \text{Eq. (5.5)}$$

$$SoC(t + \Delta t) = SoC(t) - \frac{P_{Dis}(t).\Delta t}{\eta_{Dis}} \qquad \text{Eq. (5. 6)}$$

The key input battery parameters are 'battery capacity', 'battery voltage', 'depth of discharge', and 'lifetime throughput' have been explained in the Section 4.5 [5.19]. The detail description of the annualized energy cost calculation of the battery has been described in the Appendix I.

Energy Management Strategy

The modified energy management strategy (as shown in the Fig. 5.3) is used and implemented for evaluating performance of the energy system at Soccer Club's Skagerak Arena. The main aim of the energy management strategy is to minimize the annual generation cost and maximize the battery energy throughput as well as to reduce the peak load demand from the grid.

As illustrated in the Fig. 5.3, the program starts at t=0 and it checked if grid maximum power limit is more than the load demand, the extra energy will be used to charge the battery (if $SoC(t) < SoC_{max}(t)$). However, if the maximum grid power limit is less comparing the load demand, then extra energy to meet the institutional load demand will be delivered by the battery (if, $SoC_{min}(t) < SoC(t)$).

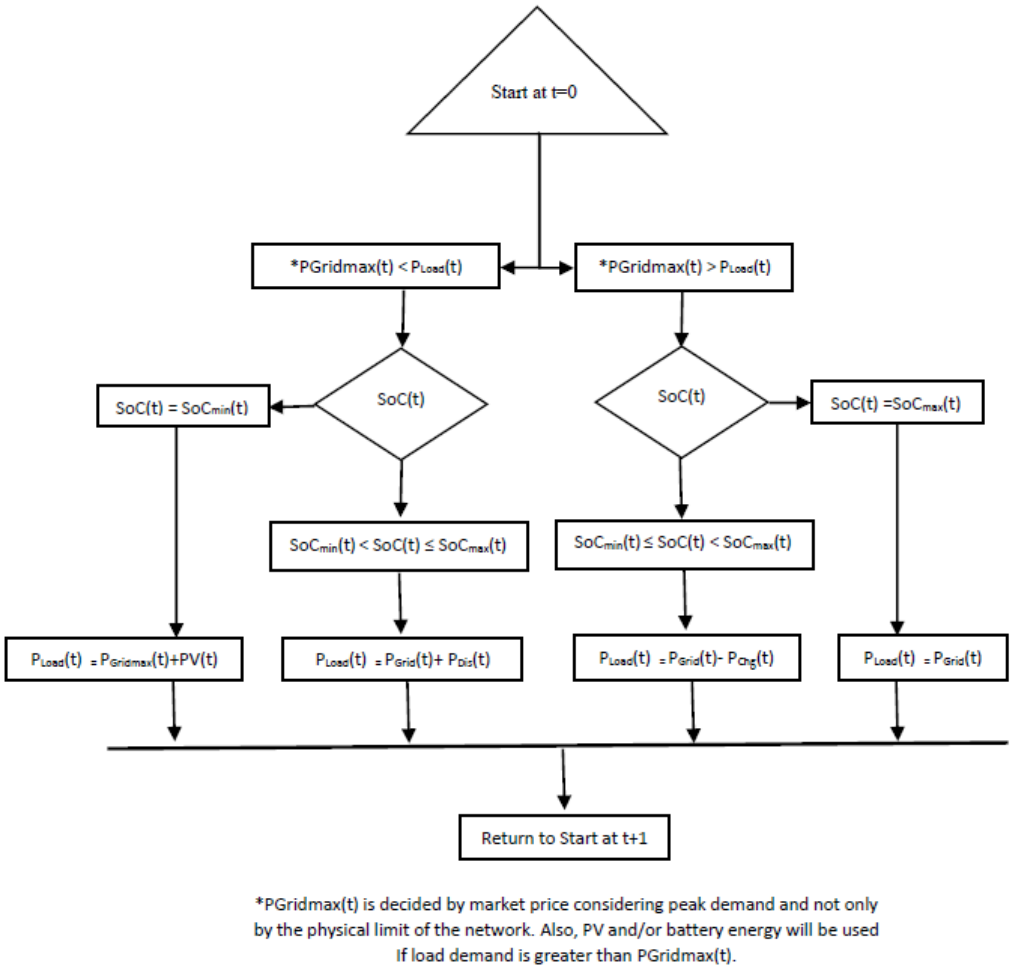

Fig. 5.3 Energy Management Strategy for Micro-grid Operation

In this work, energy supply selection from the DERs is based on the maximum peak demand limit for maximizing the local PV utilization and battery energy throughput, as well as minimizing the total energy generation cost of the system.

5.3.1 Results & Analysis of Micro-Grid with Increasing Tariffs

In this Section (i.e. Cases 5.a to 5.e), the impact of increasing electricity energy tariffs on the operational and performance of the micro-grid system, has evaluated. The considered electricity energy tariffs are increased with a rate 25% of the real time tariff of the year 2018. The Case 5.a, Case 5.b, Case 5.c, Case 5.d and Case 5.e represent the tariff scenarios of 'Tariff @100%', 'Tariff @ 125%', 'Tariff @ 150%', 'Tariff @ 175%' and 'Tariff @ 200%' respectively and they have shown in the Fig. 5.2. In this analysis, the grid tariff is assumed to be fixed for each case during the project lifetime period and it has considered in the market inflation rate. During the period of high energy tariff, the role of battery energy

storage and role of energy management strategies become very critical. To get the maximum economic benefits from the micro-grid system, battery is considered to charge during non-peak hours. Therefore, it is necessary to use the battery power in the best manner, during peak demand hours, or grid electricity prices are high.

To analyze the role of battery energy storage during the different energy tariffs, a comparison of two scenarios is analyzed with Tariff @100% and Tariff @200%. In both scenarios, energy management strategy has been used for peak demand saving as well as for market energy tariffs. The energy contribution from PV, battery and grid at Tariff @100% and Tariff @ 200% are shown in the Figs. 5.4 and 5.5 respectively. It has been observed that in both Cases (i.e. 5.a & 5.e) PV and grid energy contribution didn't change however, battery energy throughput increased in the Case 5.e.

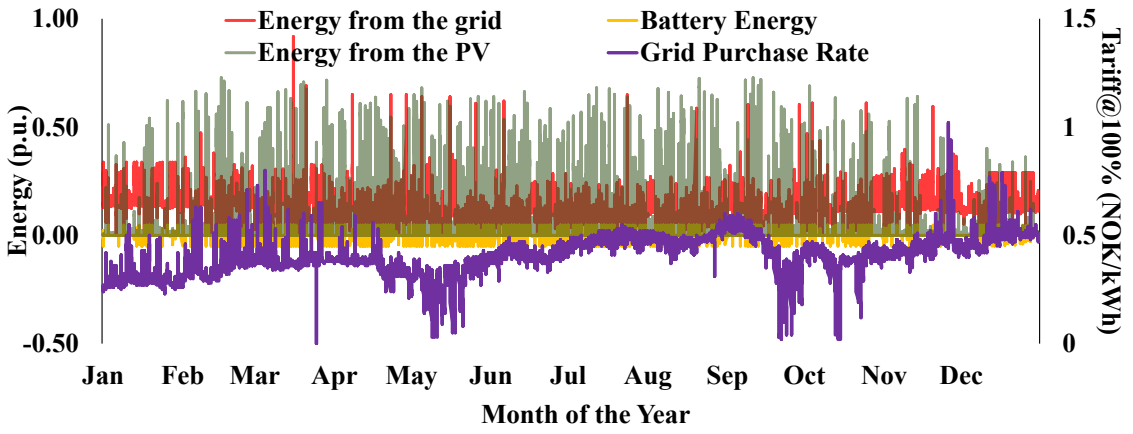

Fig. 5.4 Energy from PV, Grid and Battery @100% Tariff (Case 5.a)

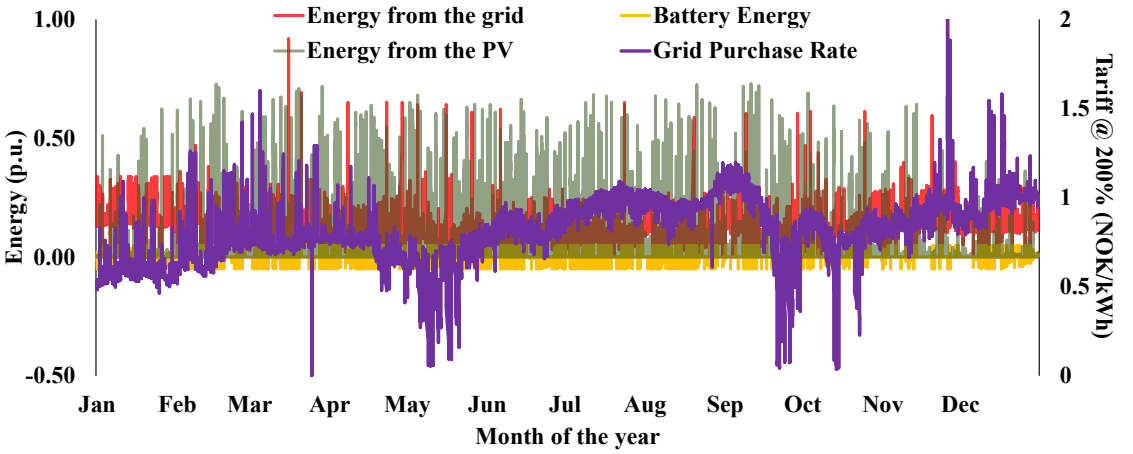

Fig. 5.5 Energy from PV, Grid and Battery @200% Tariff (Case 5.e)

It has been observed that with increase in the electricity energy tariffs, NPC and CoE of the micro-grid system have increased. The values of NPC and CoE

have increased by 14% when electricity energy tariff varies from 100% to 200%. It has been observed that incrasing the grid tarffs, no changes have been appeared in the grid energy purchase and energy sold to the grid. It is assumed that if PV generation is more than load demnad then additional energy will be used to charge the battery through grid and then reamining PV energy is considered to feed to the grid. It has been observed from Table 5.1 that battery energy throughput has increased by 3% with increase in grid tariff from 100% to 200% and there is no change in the battery energy throughput when tariff changes from 100% to 125%. The increase in the annual electricy bill has recorded by 116% with tariff changes from 100% to 200%. A variation of selected economic parameters with increase in the electricity tariffs have shown in the Table 5.1.

Table 5.1 Performance Results of Micro-grid with Different Grid Tariffs

	Different Grid Tariff Rates				
Performance parameters		Changes in percentage as compare to the tariff @100% (Case 5.a)			
	@100% (Case 5.a)	@125% (Case 5.b)	@150% (Case 5.c)	@175% (Case 5.d)	@200% (Case 5.e)
Net present cost (10^6 NOK)	56.6	4 (↑)	7 (↑)	11 (↑)	14 (↑)
CoE (NOK)	1.80	4 (↑)	7 (↑)	11 (↑)	14 (↑)
Total grid energy purchased (MWh)	1188	0	0	0	0
Total energy sold to the grid (MWh)	162	0	0	0	0
Total battery energy throughput (MWh)	54	0	1 (↑)	2 (↑)	3 (↑)
Annual bill (10^3 NOK)	420	29 (↑)	58 (↑)	87 (↑)	116 (↑)

The signs downward (↓) and upward (↑) indicate, percentage reduction and increment in the parameter's value.

The changes in the battery energy throughput and CoE with different energy tariffs have shown in the Fig 5.6. It has been observed that when tariff is increased by 100% to 200% then battery energy throughput increased only 3% whereas CoE increased by 14%.

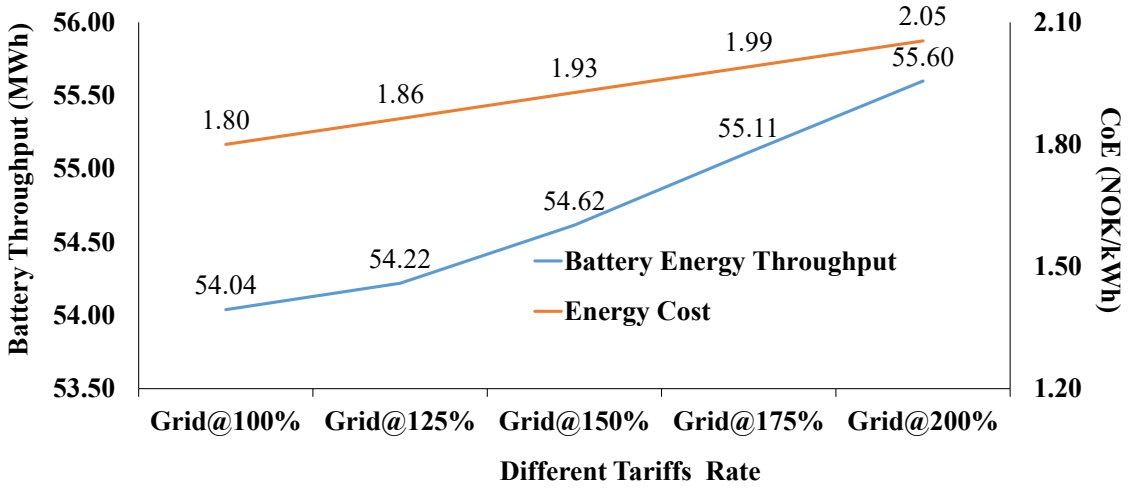

Fig. 5.6 Variation of CoE and Battery Energy Throughput with Different Tariffs

The monthly variation of electricity bill with different energy tariffs have shown in the Fig 5.7. In this work, the electricity bill is calculated based net energy buy from the grid. It has been observed that electricity bill in the winter season is 54% of the total electricity bill of the year and it is because as the PV generation is very low during winter season and therefore more grid energy is used for fulfilling the load demand. In the summer season PV generates 65% of the total annaul energy generation and during this period if PV generation is more than load demand then extra enegy is considered to feed into the grid.

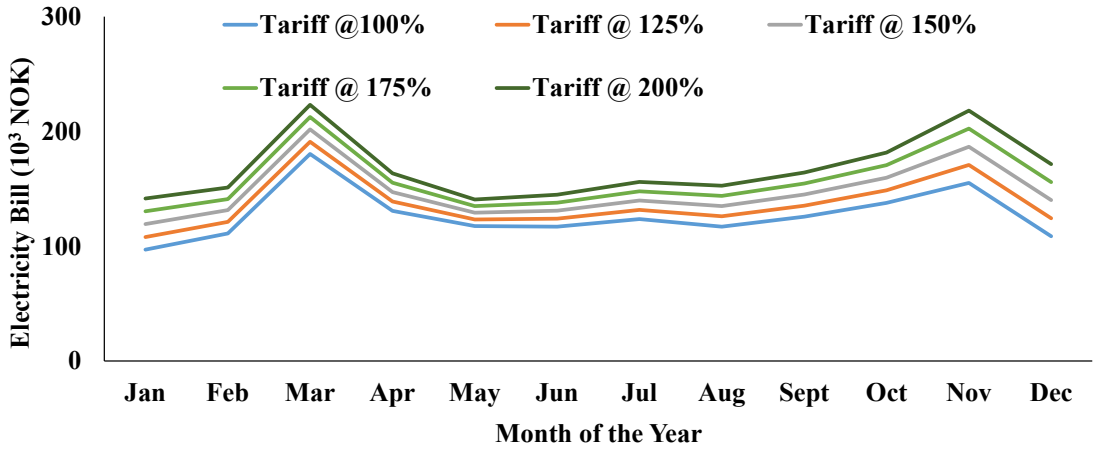

Fig. 5.7 Monthly Electricity Bill with Different Energy Tariffs

A monthly variation of energy sold to the grid with different tariffs has shown in the Fig. 5.8. It has been observed that during summer season more energy is sold to the grid and it is 73% of the total annual energy sold to the grid. However, with increase in electricity tariffs doesn't reflect any impacts on the electricity sold to the grid and it is observed that no change in the shape of the graph for electricity sold to the grid when tariff increased from 100% to 200%.

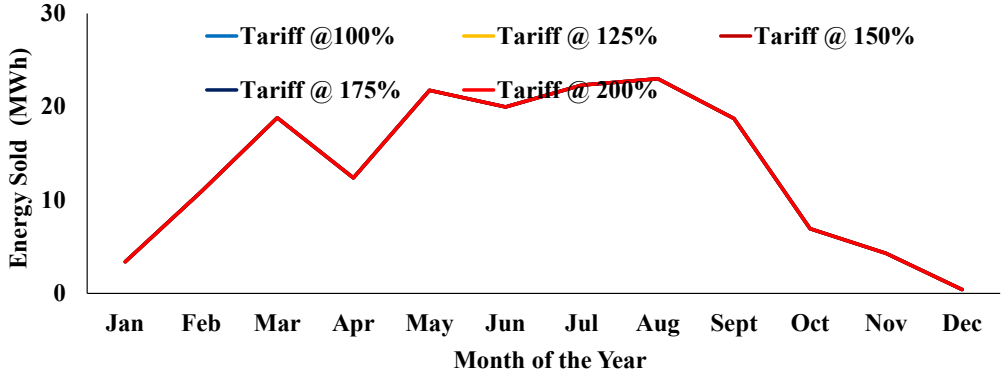

Fig. 5.8 Variation of Energy Sold to the Grid with Different Energy Tariffs

It has been observed that energy management strategy plays very crucial role to optimize battery operation during the different tariff scenarios. The optimal use of battery not only enhance the technical performance of the institutional micro-grid, but also improve the economic benefits. In future, the grid power supply may become more expensive as energy tariffs and demand charges are increasing specially for non-domestic consumers. Therefore this study will be useful for analyzing the battery's techno-economic operational performance considering different electricity energy tariff scenarios. In the next section, impacts of the electricity selling price to the grid has been analysed and described in details.

5.3.2 Results & Analysis of Micro-grid with Different Selling Prices to Grid

In this study (i.e. Cases 5.f to 5.j), the impact of increasing electricity selling prices on the operation and performance of the micro-grid system, has evaluated. The considered electricity selling prices are increased with a rate 25% of the real time tariff of the year 2018. The Case 5.f, Case 5.g, Case 5.h, Case 5.i and Case 5.j represent the tariff scenarios of 'Selling @100%', 'Selling @ 125%', 'Selling @ 150%', 'Selling @ 175%' and 'Selling @ 200%' respectively and shown in the Fig. 5.2). During the period of high selling price, the role of battery energy storage and role of energy management strategies become very critical. To get the maximum economic benefits from the micro-grid system, battery is considered to

charge during non-peak hours. Therefore, it is necessary to use the battery power in the best manner, during peak demand hours, or grid electricity prices are high.

To analyze the role of battery energy storage during the different energy tariffs, a comparison of two scenarios is analyzed with Selling @100% and Selling @200%. In both scenarios, energy management strategy has been used for peak load saving as well as for market energy tariffs. The energy contribution from PV, battery, and grid @ Selling 100% and Selling @ 200% are shown in the Figs. 5.9 and 5.10 respectively. It has been observed that in both Cases (i.e. 5.f & 5.j) PV and grid energy and battery contribution did not change.

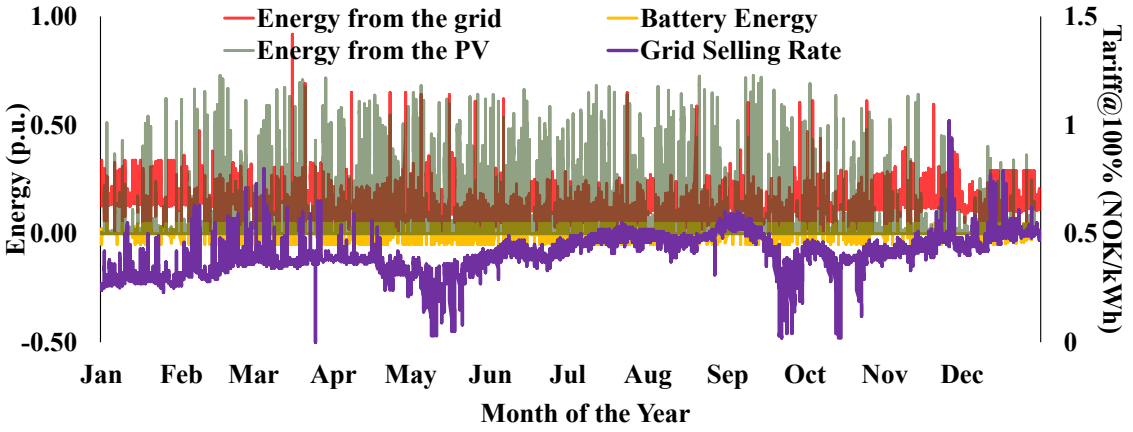

Fig. 5.9 Energy from PV, Grid & Battery, Grid Selling Price @100% (Case 5.f)

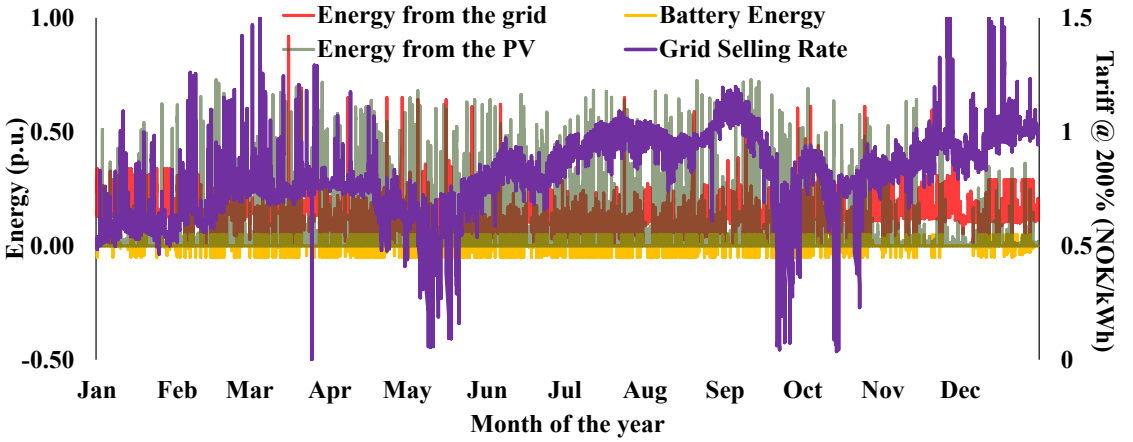

Fig. 5.10 Energy from PV, Grid & Battery, Grid Selling Price @200% (Case 5.j)

It has been observed that with increase in the electricity energy tariffs, NPC and CoE of the micro-grid system have decreased. The value of NPC and CoE is decreased by 2% when grid selling price varies from 100% to 200%. It has been observed that energy purchased from the grid has increased by only 1% with electricity selling price to grid varies from 100% to 200% because energy sold to

the grid is increased. It has been observed from Table 5.2 that there is not significant change in the battery energy throughput when selling price is increased from 100% to 200%. The reduction in the annual electricity bill is observed by 17% with tariff changes from 100% to 200%. A variation of selected economic parameters with increase in the grid selling price have shown in the Table 5.2.

Table 5.2 Economic Performance of Micro-grid with Different Selling Prices

Performance parameters	Different selling prices to grid				
		Changes in percentage as compare to grid selling price @100%			
	@100% (Case 5.f)	@125% (Case 5.g)	@150% (Case 5.h)	@175% (Case 5.i)	@200% (Case 5.j)
Net present cost (10^6 NOK)	4.28	0	1 (↓)	2 (↓)	2 (↓)
CoE (NOK)	1.35	0	1 (↓)	2 (↓)	2 (↓)
Total grid energy purchased (MWh)	1197	0	0	0	1(↑)
Total energy sold to the grid (MWh)	174	0	0	0	4 (↑)
Total battery energy throughput (MWh)	42414	0	0	0	1 (↓)
Annual bill (10^3 NOK)	420	4 (↓)	8 (↓)	12 (↓)	17 (↓)

The signs downward (↓) and upward (↑) indicate, percentage reduction and increment in the parameter's value.

The changes in the battery energy throughput and CoE with different energy tariffs have shown in the Fig 5.11. It has been observed that when grid selling price is increased by 100% to 125%, CoE does not change whereas CoE decreased by only 2% when grid selling has change to 200%. The analysis also reveals that in the near future if grid energy price further increased (i.e. 200%) then micro-grid configuration need to be modified so that attractive financial returns could be achieved.

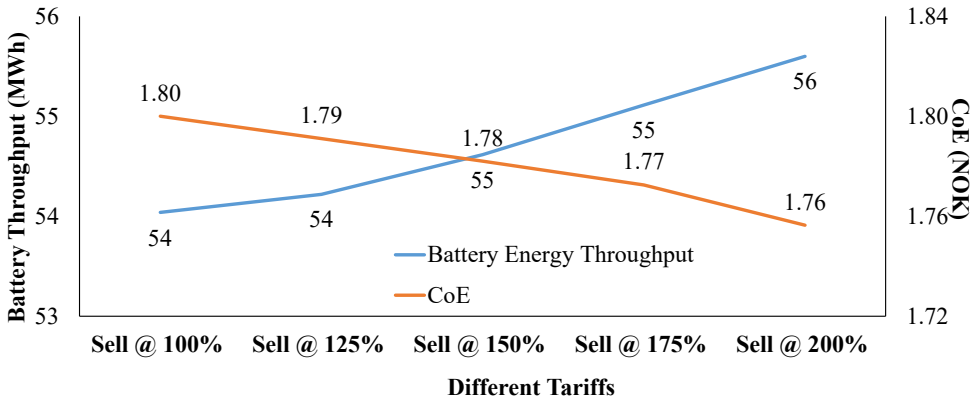

Fig. 5.11 CoE and Battery Energy Throughput with Different Grid Selling Prices

The monthly variation of electricity bill with different grid selling price have shown in the Fig 5.12. In this work, the eletricity bill is calculated based on net energy buy from the grid. It has been observed when grid selling price is @200% then electricity bill in the winter season 79% of the total electricity bill of the year and it is because as the PV generation is very low during winter season and therefore more grid energy is used for fulfilling the load demand. In the summer season PV generates 65% of the total annual energy generation and during this period more PV generation has fed into the grid as grid selling price is high.

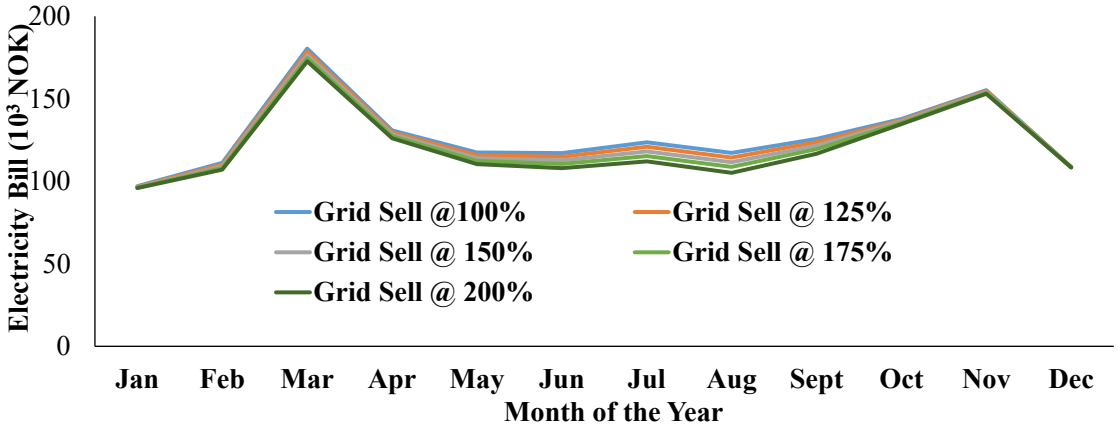

Fig. 5.12 Monthly Electricity Bill with Different Grid Selling Prices

A monthly variation of energy sold to the grid with different grid selling price is shown in the Fig. 5.13. It has been observed that during summer season more energy is sold to the grid and it is 72% of the total annual energy sold to the grid. It has been observed that increased in the grid selling price from 100% to 200%, increase the total energy sold to the grid by 4%.

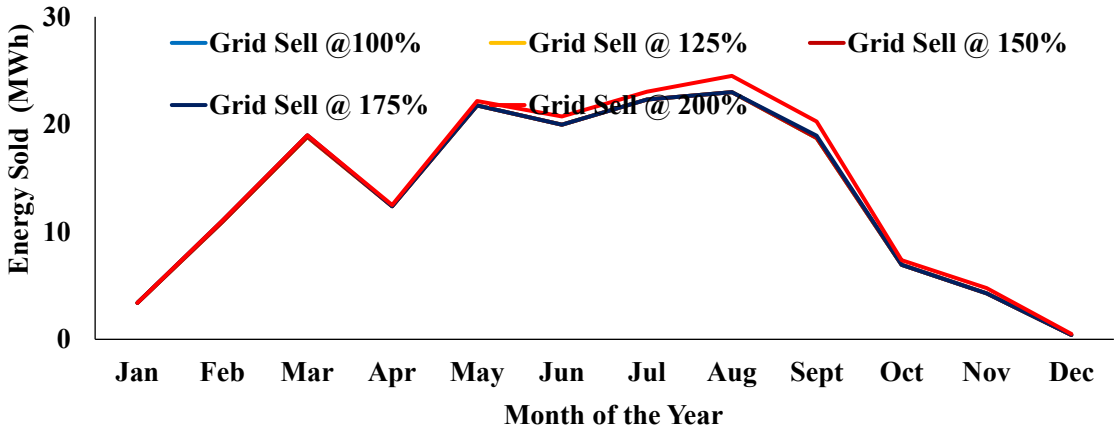

Fig. 5. 13 Energy Sold to the Grid with Diferent Grid Selling Prices

It has been observed that increased in the grid selling price, maximum generated PV energy has feed into the grid as selling electricity to the grid provides more economic values.

5.4 Impact of PV, Battery, and Energy Tariff on the CoE

The economic performance of the micro-grid very much depends on the different cost components e.g. PV, battery, power conditioning devices and energy tariffs etc. However, the cost of PV, battery and grid tariff represent significant share of the net present cost therefore impacts of PV, battery cost and grid energy tariffs on CoE are analyzed with multiplier factors of 0.5, 1, 1.5 and 2. Here, the multiplier factor '1' represents the base case scenario having component cost as described in Case 5.a therefore change in the CoE with multiplier factor '1' is zero. The multiplier factor '0.5', '1.5' and '2' represents that the components costs are '0.5', '1.5' and '2' times respectively compare to the Case 5.a. In the Fig 5.14, 'BBx0.5', 'BBx1', 'BBx1.5' and 'BBx2' are representing battery cost with multiplier factors of '0.5', '1', '1.5' and '2' respectively. In this analysis 100% of battery capacity is used for peak load saving.

It has been analyzed from the Fig. 5.14 that multiplier factor 0.5 for PV (PVx0.5), battery (BBx0.5) and unit factor for energy tariff (Tariffx1) reduce the CoE by 42% whereas with multiplier factor '2' for PV (PVx2), battery (BBx2) and energy tariff (Tariffx2) increased the CoE by 105%. To analyze the impact of energy tariff on the CoE, multiplier factor is kept '1' for PV (PVx1) and battery (BBx1) whereas the multiplier factor of energy tariff is changed from 1(Tariffx1) to 2 (Tariffx2). It has been observed that changing tariff multiplier factor from 1 (Tariffx1) to 2 (Tariffx2), CoE is increased by 27%. Similarly, to analyze the impact of battery cost on the CoE, multiplier factor is kept '1' for PV (PVx1) and energy tariff (Tariffx1) whereas the multiplier factor of battery cost is changed from 1 (BBx1) to 2 (BBx2) and 0.5 (BBx0.5). It has been observed that changing multiplier factor of battery cost from 1 (BBx1) to 2 (BBx2) and 0.5 (BBx0.5), CoE is increased by 53% and decreased by 27% respectively. In the same way, the impact of PV cost on the CoE has been analyzed and therefore multiplier factor is kept '1' for battery (BBx1) and energy tariff (Tariffx1) whereas the multiplier factor of PV cost is changed from 1 (PVx1) to 2 (PVx2) and 0.5 (PVx0.5). It has been observed that changing multiplier factor of PV cost from 1 (PVx1) to 2 (PVx2) and 0.5 (PVx0.5), CoE is increased by 31% and decreased by 15%

respectively. It indicates that battery cost has more impact on the CoE as compare to the PV and energy tariff.

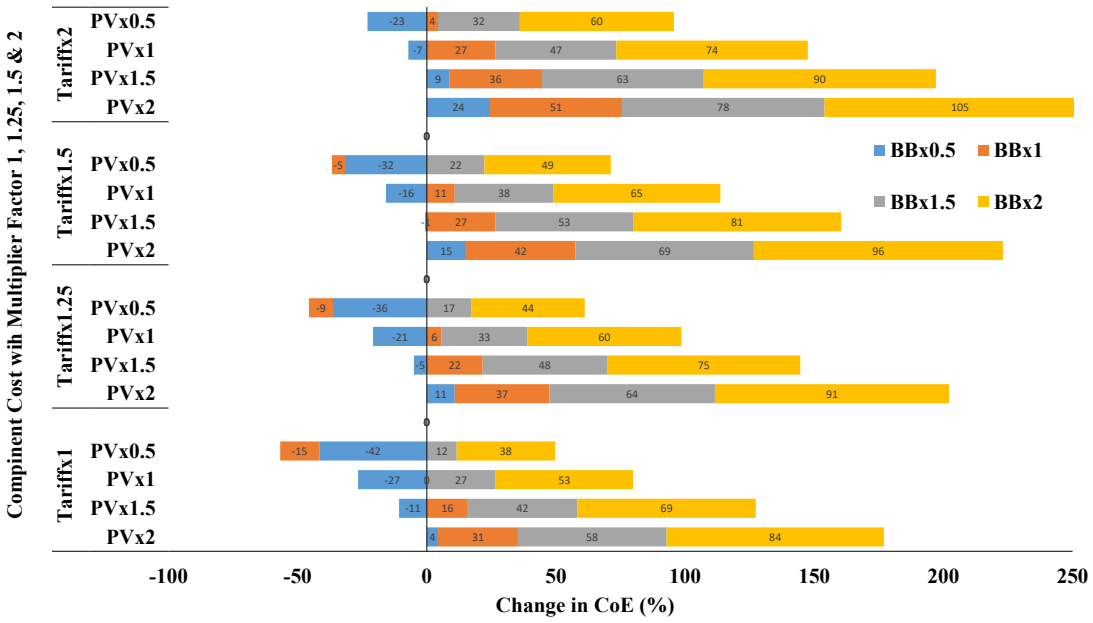

Fig. 5.14 Variation of CoE with PV, Battery and Grid Traiffs

5.5 Economic Performance Analysis for Micro-grid System in India and Norway at Selected Geographic Locations

The economic performance analysis of the institutional system without and with PV and battery integration (i.e. operating as micro-grid) has already described in the Chapter 2 (i.e. Section 2.5) and Chapter 4 (i.e. Section 4.5). In this Section a comparison of Cases 2.b and 4.b for India and Norway respectively are presented in the Table 5.3. In Case of India, integration of solar PV and battery energy storage in the institutional energy system and operating it as a micro-grid, reveals improvement in all economic parameters. It has been observed that CoE, NPC, peak demand, grid contribution and DG contribution are reduced by 48%, 48%, 10%, 45% and 93% respectively and 45% saving in the annual electricity bill is achieved. However, in Case of Norway, peak demand and grid contribution are reduced by 8% and 38% respectively and 21% saving on the electricity bill is achieved. It has been observed that CoE and NPC are increased by 62% and 78% respectively for Norway. Due to grid outage situation in India, there is significant DG contribution initially (i.e. 12.7% in Case 2.a) which has reduced to 1% (Case 2.b whereas in Norway grid is quite stable and reliable and integration of PV and battery energy storage, reduces that grid contribution and electricity bill but cost

of PV and battery energy storage contribute major role in increasing the CoE and NPC. In both scenarios (India and Norway), it has been observed that a PV based micro-grid system can help in reduction in peak energy demand from the grid and significant saving in the energy bill.

Table 5.3 Economic Performance of the Case 2.b and Case 4.b

S. No.	Parameters	India		Norway	
		Value in Case 2.b	Changes compare to Case 2.a (%)	Value in Case 4.b	Changes compare to Case 4.a (%)
1.	CoE (*€/kWh)	0.076	48 (↓)	0.123	62 (↑)
2.	Net present cost (10^6€)	0.26	47 (↓)	3.85	78 (↑)
3.	Peak demand(kW)	45	10 (↓)	965	8 (↓)
4.	Annual grid to total generation ratio (%)	48	45 (↓)	62	38 (↓)
5.	Annual PV to total generation ratio (%)	51	No PV in Case 2.a	38	No PV in Case 4.a
6.	Annual DG to total generation ratio (%)	1	93	NA	NA
7.	Annual battery energy throughput to total generation (%)	33	No battery in Case 2.a	38	No battery in Case 4.a
8.	Annual energy sold to the total generation ratio (%)	4	No grid sell in Case 2.a	9	No grid sell in Case 4.a
9	Annual DG fuel consumption (Litre)	407	93 (↓)	NA	NA
10	Annual electricity bill (10^3 €)	7.62	45(↓)	152	21(↓)

*1 Euro (€) = 86.04 INR and 1 Euro (€) = 10 NOK

The signs downward (↓) and upward (↑) indicate, percentage reduction and increment in the parameter's value.

5.6 Impacts on CoE of the Micro-grid System with Different Grid Buying and Selling Prices in India and Norway Geographical Locations

The impacts on the CoE with different buying and selling price to grid has been analyzed in the Chapter 3 (Section 3.4 and 3.5) and Chapter 5 (Section 5.3.1 and 5.3.2). In this section, percentage changes in the CoE with grid buying and selling tariffs for India and Norway climatic zones has been analyzed in the Figs. 5.15 and 5.16 respectively. It has been observed that while increasing the grid buying price from 100% to 200%, increase in the CoE for India and Norway are 172% and 114% respectively. The impact on the CoE is much higher in case of India as compare to the Norway climatic zones. This is because of the fact that in

India, grid has major contribution (72%) of the total net present value of the micro-grid system followed by the battery (11%), solar PV (10%), DG (4%) and system converter (3%) (Chapter 2, Table 2.5).

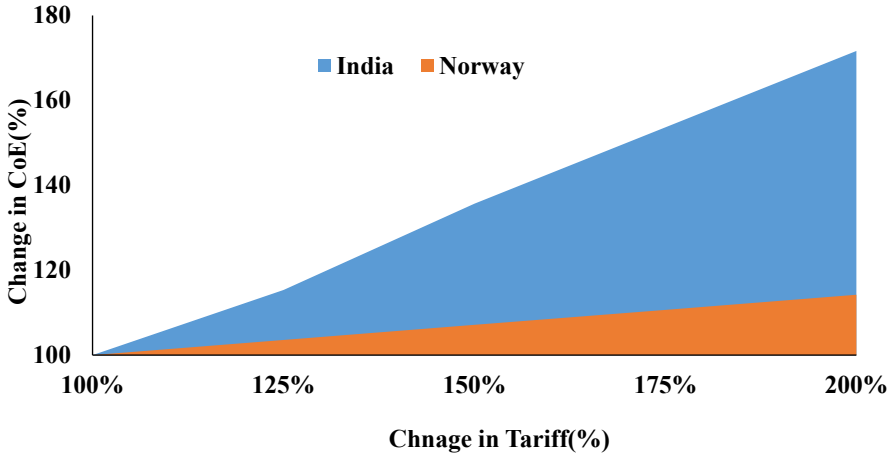

Fig. 5.15 Changes on CoE with Different Grid Buying Prices

It has been observed that while increasing the grid selling price from 100% to 200%, decrease in the CoE for India and Norway are 108% and 102% respectively. The impact of the grid selling price on the CoE is quite small as compare to the grid buying price but its impacts on CoE is still higher in India. In Case of Norway, over the 25 years project lifetime, PV system cost is only 35% of the total project cost followed by the battery 25%, grid 21%, controller 10% and I&C cost 9% (Chapter 4, Section 4.6).

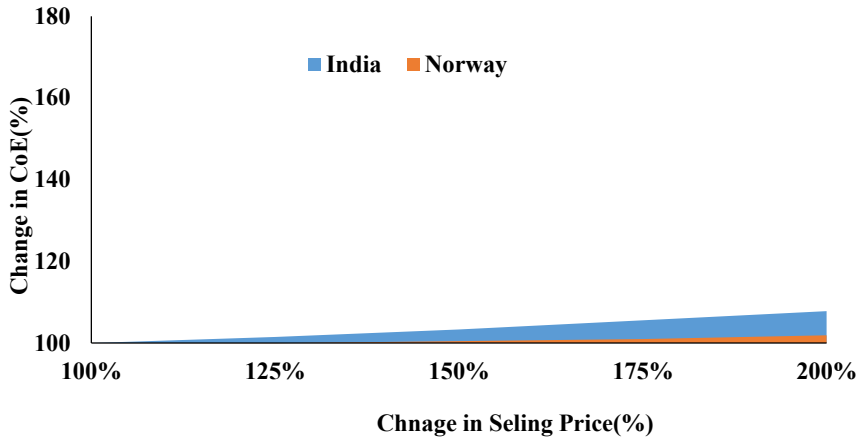

Fig. 5.16 Changes on CoE with Different Selling Price to Grid

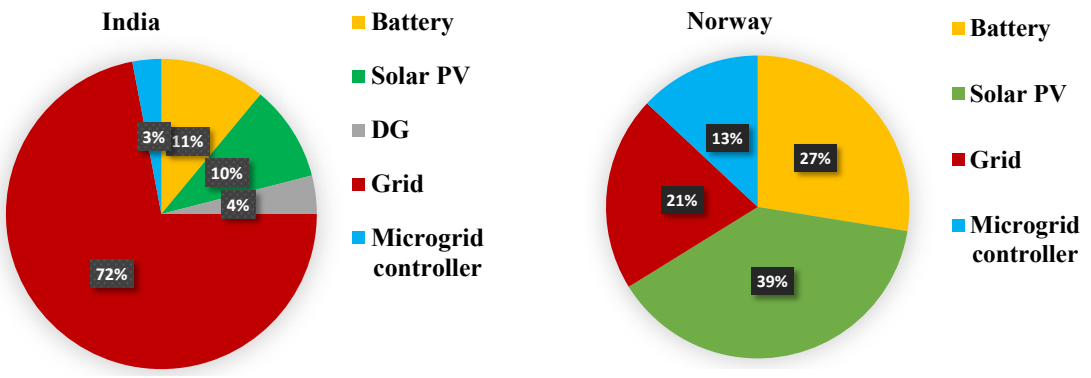

Fig. 5.17 Micro-grid Component's Cost for India (left) and Norway (right)

A comparison of micro-grid system components cost for India and Norway have shown in the Fig. 5.17. It has been observed that over the project lift time of 25 years, percentage cost contribution of different components in the micro-grid system varies significantly. The share of solar PV system cost for India and Norway's are 10% and 39% of total net present cost of the micro-grid system whereas share of battery cost for India and Norway are 11% and 27% of the total net present cost of the system. In this work, the installation and commission cost has been distributed into the different components (i.e. PV, battery, controller), for comparing the different components' cost. The performance assessments of all cases presented in this chapter have been tested with the 'Homer Pro' tool. In case of India, DG cost contribution is 4% of the total net present cost of the micro-grid system however DG cost is not applicable for Norway. The share of grid cost for India and Norway are recorded 72% and 21% respectively of the total cost of the micro-grid system.

5.7 Conclusions

In this work, an operational energy management strategy for micro-grid has been presented and evaluated for maximizing the local energy resources utilization with contemplation of peak demand under energy pricing dynamics. It has been observed that with increase in the electricity energy tariffs, NPC and CoE of the micro-grid system have increased. The value of NPC and CoE is increased by 14% when electricity energy tariff varies from 100% to 200%. It has been observed (i.e. Table 5.1) that battery energy throughput is increased by 3% with increase in tariff from 100% to 200% and there is no change in the battery energy throughput observed when tariff changes from 100% to 125%. The increase in the annual electricity bill is observed by 116% with tariff changes from 100% to 200%.

It has been observed that with increase in the electricity selling price to grid, NPC and CoE of the micro-grid system have decreased. The value of NPC and CoE is decreased by 2% when grid selling price varies from 100% to 200%. It has been observed that energy purchased from the grid is increased by only 1% when electricity selling price to grid varies from 100% to 200% because energy sold to the grid is increased. It has been observed from Table 5.2 that there is not significant change in the battery energy throughput when selling price from 100% to 200%. The reduction in the annual electricity bill is observed by 17% with grid selling tariff changes from 100% to 200%.

While comparing the economic results of India and Norway, It has been observed that CoE, NPC, peak demand, grid contribution and DG contribution are reduced by 48%, 48%, 10%, 45% and 93% respectively, and 45% saving in the annual electricity bill is achieved However, PV based micro-grid system in Norwegian case, peak demand and grid contribution are reduced by 8% and 38% respectively and 21% saving on the electricity bill. It has been observed that CoE and NPC are increased by 62% and 78% respectively for Norway. Also, it has been observed that the impact on the CoE is much higher in case of India as compare to the Norway climatic zones as grid cost contribution of the total net present value of the micro-grid system for India and Norway are 72% and 21% respectively.

Chapter 6

6. PV based Micro-Grid Hosting Capacity and Voltage Quality Analysis within a Distributed Network

6.1 Summary

In this chapter, solar photovoltaic hosting capacity within the electrical distribution network is estimated, by considering different operational constraints within the acceptable limits. Some of the network operational parameters (e.g. voltage, and voltage with loading) are analyzed and their acceptable limits are used as constraints, while determining the hosting capacity at different network buses. It is observed that with the increasing photovoltaic penetration, some of the network buses can be reached up to maximum hosting capacity, and impacting the network operation (e.g. bus voltages, line loading). To maintain the network buses' voltage within acceptable limits, reactive power-voltage based droop control is implemented in the photovoltaic conditioning devices to test the dynamics of network operation. The results are verified using experimental setup of digital real-time simulator and power hardware-in-loop. The results show that implementation of droop control reduced the maximum voltage rise from 9% to 4% in the considered case. Also, this study is analyzed operational performance of a mesh and radial type electrical distribution network with photovoltaic penetration. It is observed that the cumulative effect of mesh type network along with droop control strategy can further improve the voltage profile with increasing photovoltaic penetration. The results from this work are going to be useful for finding the photovoltaic hosting capacity within a distribution network, and implementation of droop control strategy in the power conditioning devices for keeping the network operational parameters within the specified limits.

6.2 Introduction

Over the last 15 years, the production volume of photovoltaic system (PV) has expanded with a compound annual growth rate of over 40 %, and it makes the PV industry one of the fastest growing in the world. [6.1]. Most of the PV generation units are distributed in nature and connected within low or medium voltage distribution networks. Due to limitations of the electrical energy distribution network, an appropriate PV capacity can be incorporated at different

buses for keeping the operational parameters within the acceptable limits without making any significant modifications in the existing distribution network [6.2]. The PV capacity at nodes of electrical distribution network is going to impact on operational parameters (e.g. bus voltages, line loadings, reverse current flow, short circuit current, etc.).

The PV hosting capacity (HC) can be analyzed in two categories: (i) based on network performance and load characteristics and (ii) based on network operational parameters for future planning and expansion of electrical network. The network operational parameters (e.g. bus overvoltage, line overloading, power quality etc.,) need to be critically evaluated for estimating PV HC at different nodes of distribution network. In ref [6.2], the PV hosting capacity within electrical distribution network has analyzed at different buses considering only the rated PV capacity, but PV output and simultaneous load profile at a particular bus has not considered. An approach to improve PV HC based on reactive power control strategy has presented in ref [6.3], but it has not included load flow analysis with simultaneous penetration of PV capacity at different nodes. Probabilistic approach-based method for PV HC has presented in ref [6.4] considering worst-case scenario (i.e. maximum PV and low load), but network operational parameters have not analyzed. The placement of distributed generation within the network has evaluated through power quality (harmonic distortion) in the ref [6.5], but the HC at individual buses with loading impacts have not analyzed. The PV HC within the electrical distribution network have evaluated using Monte Carlo probabilistic technique in ref [6.6] with random PV placements, but it has not provided analysis on individual buses. The distribution network operational parameters (e.g. bus overvoltage, line overloading, power quality, etc.) are going to impact the PV HC [6.7-6.8]. Therefore, it is very essential to analyze PV HC within the distribution network at different nodes with simultaneous PV and load profiles.

The operational parameters can be managed within the prescribed limits through appropriate embedded control strategies in the PV power conditioning devices. In ref [6.9], phasor measurement analysis has reported for PV system, but potential mitigation techniques have not elaborated. A PV penetration study has conducted by the Department of Energy ‘s SunShot Program [6.10] and reported the voltage at the PV plant has surpassed at maximum PV generation and has presented a mitigation technique.

Another, PV impacts study, for urban LV network in Sri Lanka, has presented in ref [6.11]. The results of the study [6.11], endorsed that the maximum rise in

feeder voltage observed in the daytime when energy demand is low and maximum solar radiation is available, but mitigation technique have not sufficiently tested in real time conditions by using digital real-time simulator (DRTS) and power hardware-in-loop (PHIL) method. In ref [6.12], the major impacts of PV integration have been presented for power quality issues, protection relays etc. but daily load and generation profiles have not considered. An optimal centralized coordinated voltage control algorithm in PV inverter has tested and validated using PHIL configuration method for a low voltage distribution network [6.13]. The operational performance of standard droop control techniques of PV inverters has investigated during the transition to islanded operation from grid connected mode [6.14] and the results showed that PHIL simulation of local control on the benchmark system substantiate the suitability of the proposed real-time simulation approach. To address the voltage quality problems some countries have implemented technical solutions at the device level (i.e. PV inverter). For example, in Germany, to overcome over-voltage events, from January 2012, a fixed limitation of the active power (i.e. 70% of the nominal peak-output power of the PV system) feed-in by each PV system has become mandatory [6.15]. Similarly, some other alternative solutions to curtailment of active power by domestic load shifting, to increase local consumption, and energy storage are discussed in ref [6.16]. To improve the power factor of three phase inverter PV inverter, a reactive power control technique has proposed in ref [6.17-6.18]. Different techniques e.g. active power curtailment, reactive power compensation and energy storage, for addressing voltage quality challenges due to high PV penetration have presented in the ref [6.19].

However, penetration of PV has also been increasing through PV based microgrid and it has not been sufficiently addressed in the reviewed literatures [6.20-6.22]. Based on the above-mentioned key issues / challenges, three main objectives are formulated in this chapter. The first objective is to estimate the HC at different buses of the distribution network with voltage and loading as constraints, by considering average daily solar generation and load profiles. The second objective is to analyze the impact of high PV penetration on the selected buses of the distribution network, using DRTS and power hardware in-loop PHIL method. And the third objective of this paper is focused on testing possible mitigation techniques (i.e. reactive vs. voltage droop control) to mitigate the voltage quality problems during high PV penetration. To analyze the test results, various parameters have been recorded e.g. voltage at bus terminals, line loading,

transformer loading, active and reactive power of the inverter and power flow at each bus terminal. The experimental work has been carried out at the *'Smart grids Research Unit of the Electrical and Computer Engineering School (Smart RUE) of the National Technical University of Athens'.*

Performance analysis of distributed network without PV integration and HC analysis of the distributed network have been evaluated using DIgSILENT, in the Sections 6.3 and 6.4, respectively. In the Section 6.5, impact of high PV penetration into the distribution network have been tested and analyzed using DRTS and PHIL testing method. A reactive power versus voltage (Q-V) droop control technique have been implemented in PV inverter. The DRTS and PHIL testing setup are described in the Section 6.6. In the Section 6.7, mesh network has been used, and a cumulative impacts of droop control techniques in a mesh network has studied. Results are concluded in the Section 6.8.

6.3 Distributed Network Without PV Integration (i.e. Case 6.a)

6.3.1 System Description

In this work, a typical medium voltage (MV) distribution network (i.e. CIGRE electrical network) [6.23] has been considered, and its schematic is shown in the Figure 6.1. The technical details of transformers, cable's line length, voltage current rating, resistance, inductance, load type and power factor are taken from ref [6.23]. The considered distribution network consists of two feeders (i.e. 1 and 2) and they are connected separately with transformers (i.e. T_1 and T_2 each with rated capacity 25 MVA at 110kV/20kV). The network consists of 14 buses (i.e. B_1 to B_{14}), in which buses B_1 to B_{11} are connected to feeder 1, and buses B_{12} to B_{14} with the feeder 2. To compare and analyze the results of distribution network, all 14 buses are categorized into the three Groups e.g. A, B and C. *Group A* represents buses B_1 to B_6, *Group B* buses include B_7 to B_{11}, whereas *Group C* represents buses B_{12} to B_{14}.

There are total 12 lines (i.e. $L_{1\text{-}2}$, $L_{2\text{-}3}$, $L_{3\text{-}4}$, $L_{4\text{-}5}$, $L_{5\text{-}6}$, $L_{7\text{-}8}$, $L_{8\text{-}9}$, $L_{9\text{-}10}$, $L_{10\text{-}11}$, $L_{3\text{-}8}$, $L_{12\text{-}13}$ and $L_{13\text{-}14}$) and these lines are also categorized in Group A, B and C e.g. lines $L_{1\text{-}2}$, $L_{2\text{-}3}$, $L_{3\text{-}4}$, $L_{4\text{-}5}$ and $L_{5\text{-}6}$ are in *Group A*, lines $L_{7\text{-}8}$, $L_{8\text{-}9}$, $L_{9\text{-}10}$, $L_{10\text{-}11}$ and $L_{3\text{-}8}$ are in *Group B*, and lines $L_{12\text{-}13}$, $L_{13\text{-}14}$ in the *Group C*. There are three switches (i.e. S_1, S_2 and S_3) which can be used to create a mesh type electrical network.

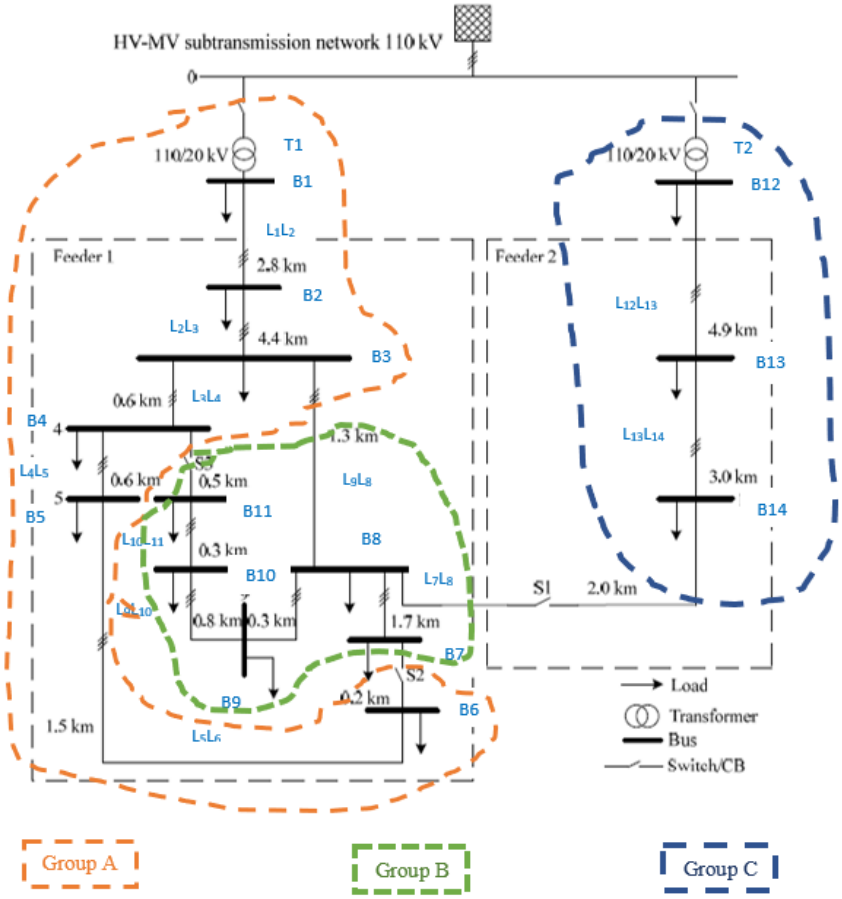

Fig. 6.1 Line Diagram of MV CIGRE Electrical Network

A typical load profile of a day is used to evaluate the performance of distribution network, and its illustration has shown in the Fig. 6.2. The daily load profile for all the buses has considered same however, maximum load demands are varied for different buses and values of the maximum load have taken from ref [6.23]. The apparent power for buses B_1-: 12.71MVA (12.44 + j 2.53), B_2-:(0), B_3-: 0.30 MVA (0.27 + j 0.12), B_4-: 0.22 MVA (0.22 + j0.05), B_5-:0.37 MVA (0.36 + j 0.09), B_6-:0.28 MVA (0.27 + j 0.07), B_7-: 0.08 MVA (0.07 + j 0.04), B_8-: 0.48 MVA (0.47 + j 0.12), B_9-: 0.61 MVA (0.59 + j 0.15), B_{10}-: 0.46 MVA (0.44 + j 0.13), B_{11}-: 0.27 MVA (0.26 + j 0.07), B_{12}-: 11.99 MVA (3.17+j 11.56), B_{13}-: 0.04 MVA (0.03 + j 0.02), and B_{14}-: 6.71 MVA (6.48+j 1.73).

In the selected distribution network, the nominal bus voltage (i.e. 20 kV line to line (1 p.u.)), maximum active load (i.e. 12.44 MW) and maximum reactive load (i.e. 2.53 MVAr), have considered as 1 p.u. (i.e. 12.70 MVA). The load profile has been considered to cover two scenarios; the first includes minimum load and

maximum PV generation and in the second scenario, maximum load, and minimum PV generation. It has been observed from a typical daily load profile that the minimum load demand is 0.10 p.u. and it is appeared during the night-time (i.e. 00:00 hours to 01:00 hours), however, the maximum load demand of 0.90 p.u. has been observed in the morning (i.e. 08:00 hours to 09:00 hours) as well as during the evening (i.e. from 19:00 hours 20:00 hours).

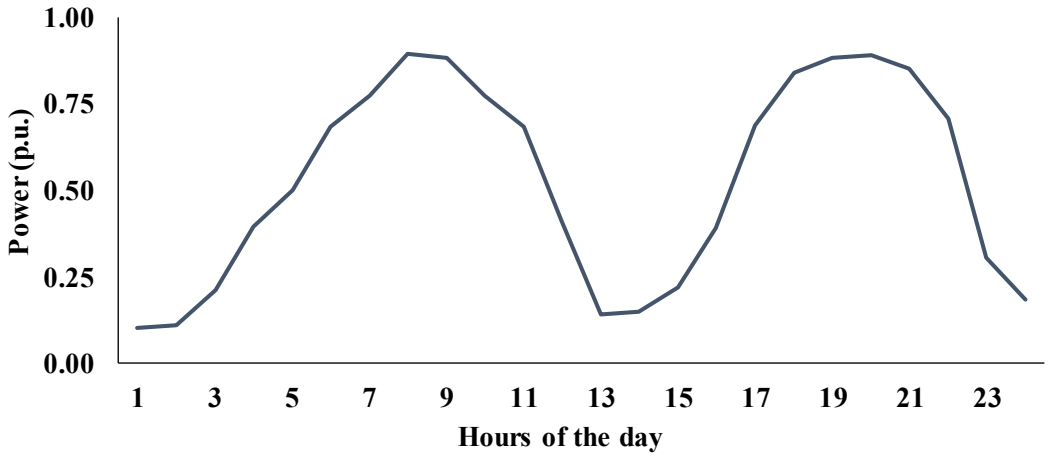

Fig. 6.2 A Typical Load Profile

6.3.2 Results & Analysis for Case 6.a

The *Case 6.a* represents, when PV is not integrated into the distribution network, and the switches S_1, S_2 and S_3 are in the open conditions. The distribution network has studied using the DIgSILENT Power Factory [6.24]. In the *Group A*, voltage of the six buses (i.e. V_1 to V_6) and % loading (of the rated capacity of the power line) on the of five lines (i.e. $L_{1\text{-}2}$, $L_{2\text{-}3}$, $L_{3\text{-}4}$, $L_{4\text{-}5}$ and $L_{5\text{-}6}$) are shown in the Figs. 6.3 & 6.4 respectively. In the considered distribution network, bus B_1 represents as slack bus and its voltage is stable as compare to all other buses within the network. It has been observed from the Fig. 6.3 that the bus voltage of all six buses (i.e. V_1 to V_6) never goes below than 0.98 p.u., however maximum voltage of buses has reached to the 1 p.u. The lowest voltage has been appeared during the peak demand's hours (i.e. 08:00 hours to 09:00 hours and 19:00 hours to 21:00 hours). It has noticed that the buses voltages do not violate the defined voltage regulation criteria (i.e. $0.90 \leq V_i \leq 1.10$).

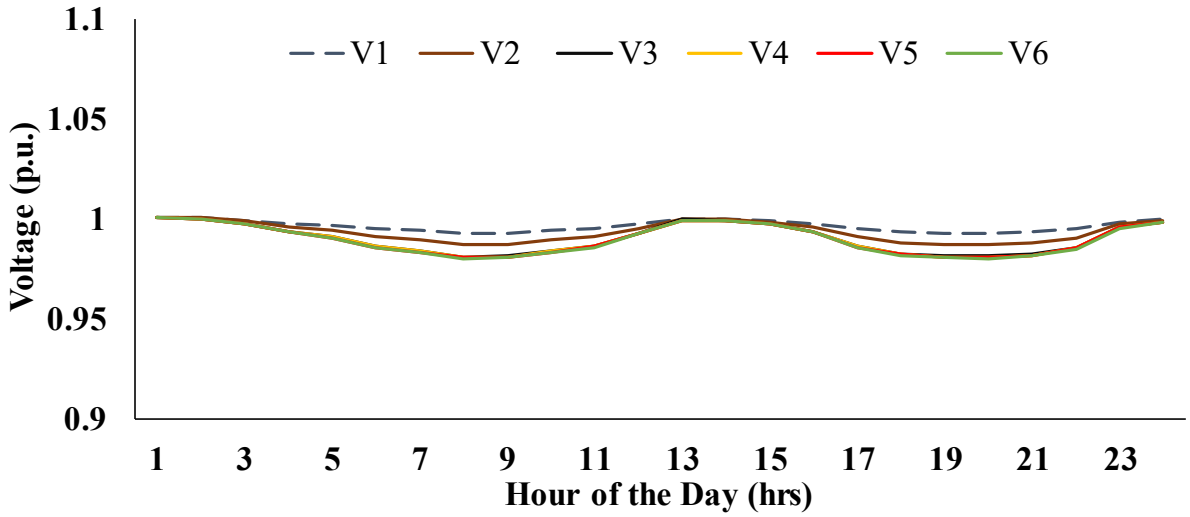

Fig. 6.3 Variation of Bus Voltages in Group A of Case 6.a

In the *Group A*, the maximum line loading has recorded 9%, for the lines $L_{1\text{-}2}$ and $L_{2\text{-}3}$, whereas loadings of the remaining lines (e.g. $L_{3\text{-}4}$, $L_{4\text{-}5}$ and $L_{5\text{-}6}$) have been below 4% throughout the day. It has been clearly observed that the line loading graph follows the same characteristics as the load demand curve shown in the Fig. 6.2.

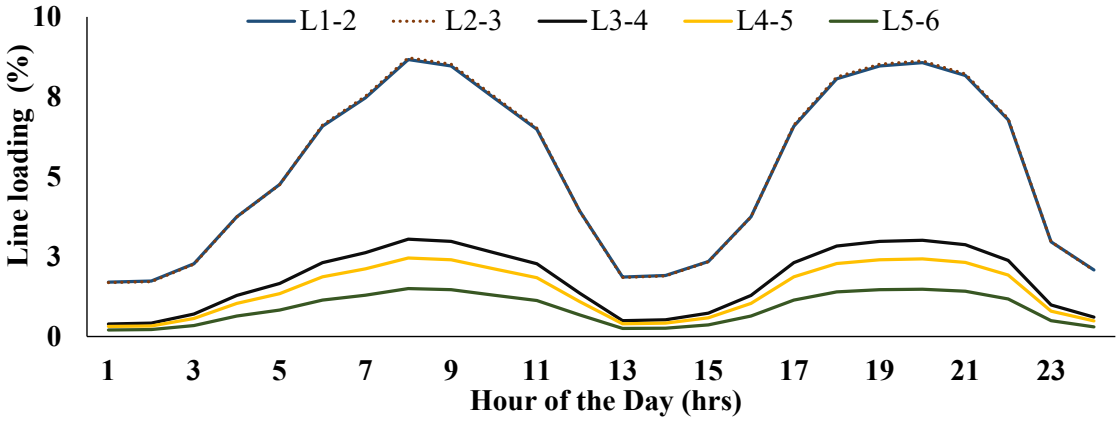

Fig. 6.4 Variation of Line Loading of Group A of Case 6.a

In the *Group B*, voltages of the five buses (i.e. V_7 to V_{11}), and loading of the five lines (i.e. $L_{7\text{-}8}$, $L_{8\text{-}9}$, $L_{9\text{-}10}$, $L_{10\text{-}11}$ and $L_{3\text{-}8}$) are shown in the Figs. 6.5 & 6.6 respectively. It has been observed that the voltage of buses (i.e. V_7 to V_{11}) never goes lower than 0.97 p.u. The lowest bus voltages are appeared during the peak demand's hours (i.e. 08:00 hours to 09:00 hours and 19:00 hours to 21:00 hours), and the maximum voltage has been recorded 1 p.u. All the buses don't violate the defined voltage regulation criteria (i.e. $0.90 \leq V_i \leq 1.10$).

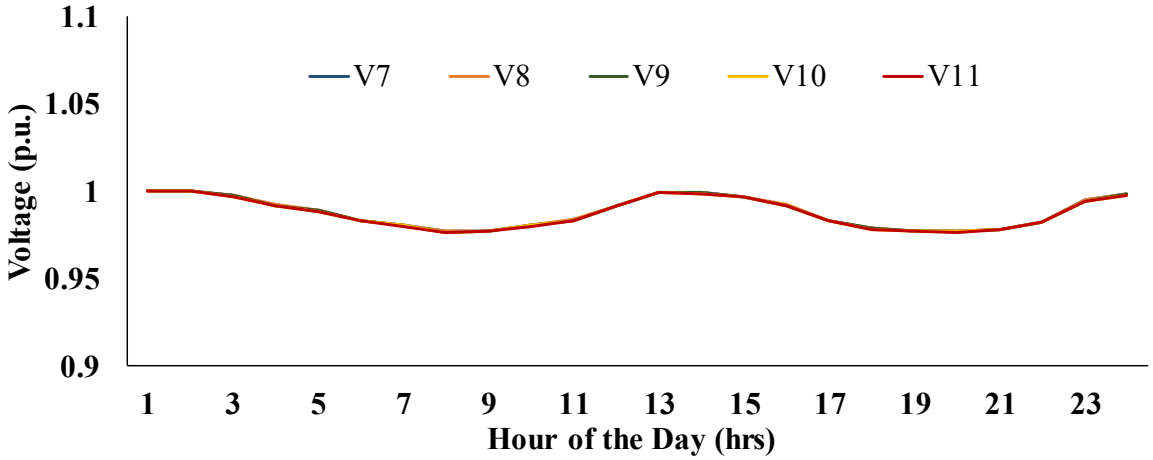

Fig. 6.5 Variation of Bus Voltages of Group B of Case 6.a

In the *Group B*, the maximum line loadings are recorded 4% and 5% for the lines $L_{8\text{-}9}$ and $L_{3\text{-}8}$ respectively whereas, loadings of the remaining lines (e.g. $L_{7\text{-}8}$, $L_{9\text{-}10}$ and $L_{10\text{-}11}$) are remained below 3% throughout the day. The loading of line $L_{3\text{-}8}$ is influenced by the load connected at the buses 7, 8, 9, 10 and 11, and therefore loading of line $L_{3\text{-}8}$ is higher as compare to the other lines loading. It has been observed from the Fig. 6.6 that the line loadings are under the defined limit (i.e. 100%).

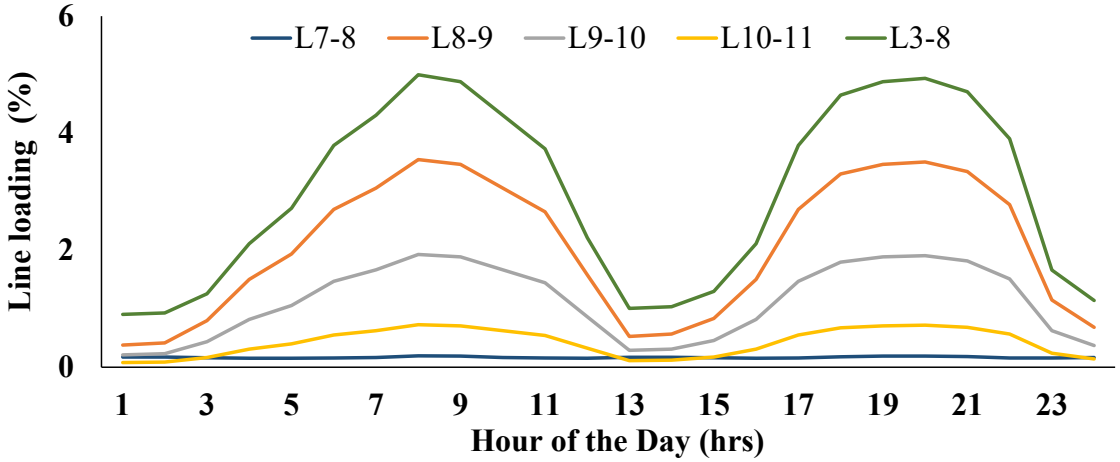

Fig. 6.6 Variation of Line Loadings of Group B of Case 6.a

In the *Group C*, voltage of three buses (i.e. V_{12}, V_{13} and V_{14}) and loading of two lines (i.e. $L_{12\text{-}13}$ and $L_{13\text{-}14}$) are shown in the Figs. 6.7 & 6.8 respectively. It has been observed from the Fig. 6.7 that the bus V_{12} represents as slack bus of the feeder 2 and its bus voltage is quite stable (i.e. $0.98 < V_{12} < 1.0$). However, voltages at buses V_{13} and V_{14} varies between 0.97 to 0.99 p.u. The lowest voltage 0.97 p.u. is recorded for bus V_{14} during the peak demand hours (i.e. 08:00 hours to 09:00 hours and 19:00 hours to 21:00 hours).

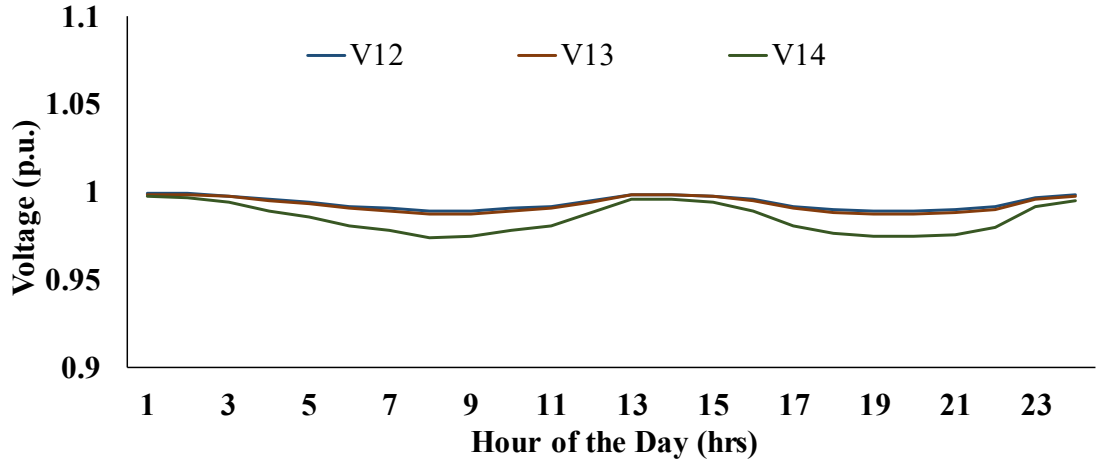

Fig. 6.7 Variation of Bus Voltages of Group C of Case 6.a

In the *Group C*, the maximum line loading is recorded 18% for the lines $L_{12\text{-}13}$ and $L_{13\text{-}14}$. The loads connected at both feeders 1 and 2 are the almost same however, in case of feeder 1, the total load is placed at 11 buses (i.e. B_1 to B_{11}), and in feeder 2, load has been connected at the three buses (i.e.B_{12}, B_{13} and B_{14}) therefore maximum line loading of feeder 2 is twice (i.e. 18%) as compare to the feeder 1 (i.e. 9%).

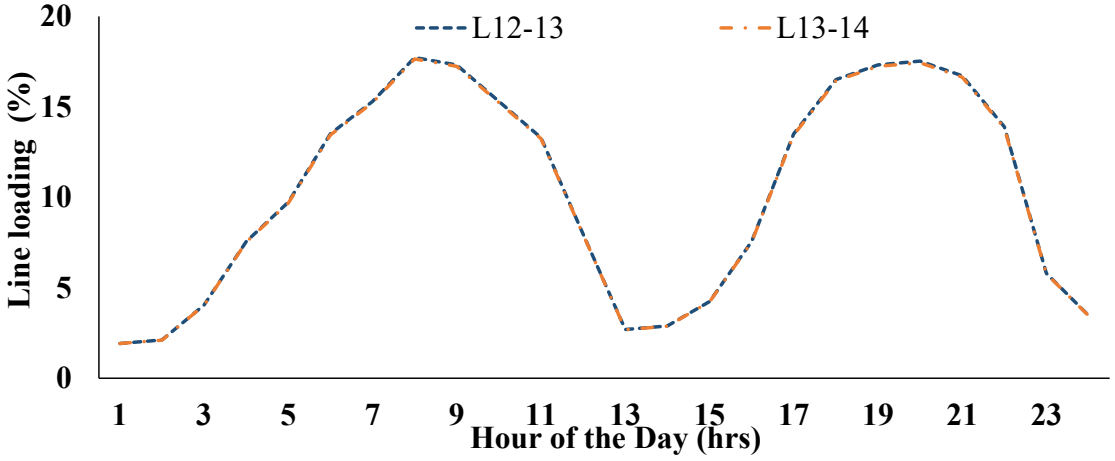

Fig. 6.8 Variation of Line loadings of Group C of Case 6.a

The variation of transformer loadings (i.e.T_1 and T_2) of typical day are shown in the Fig. 6.9. The maximum loading of transformer T_1 and T_2 (i.e. power loading) are recorded 29% and 34% respectively however, minimum loading for both transformers are in between 3-4% during the night-time (i.e. 00:00 hours to 01:00 hours). The average daily energy loading of transformer T_1 and T_2 have been noted 17% and 20% respectively.

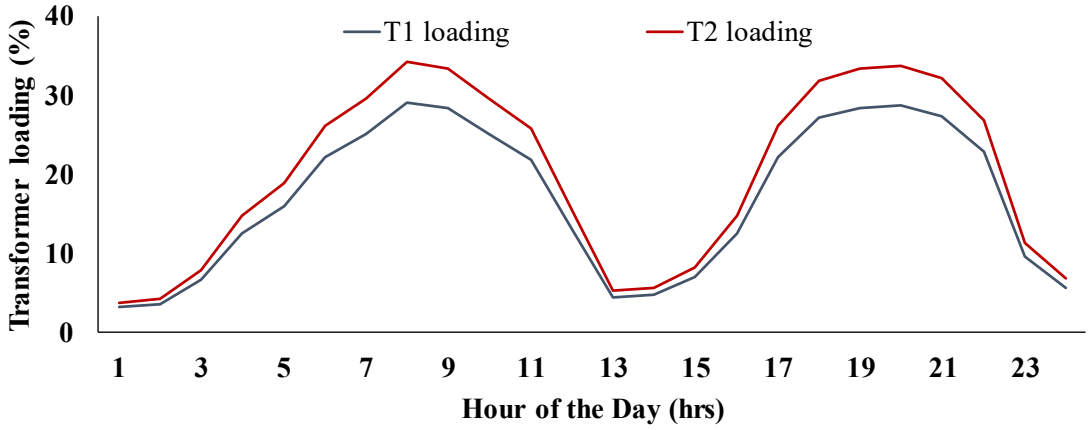

Fig. 6.9 Variation of Transformers Loading of the Typical Day of Case 6.a

The results of Case 6.a show that for the considered load profile, distributed network does not violate any voltage and overloading conditions. It indicates that distributed network has capacity to integrate solar PV based micro-grid, but how much PV can be connected to the distribution network depends on HC of the network.

In this chapter, the HC of the distributed network has been assessed using the DIgSILENT Power factory [6.24], and then impacts of the PV integration within the distribution network has analysed using DRTS and PHIL simulation method. The HC of the individual bus in the distribution network has been estimated so that appropriate capacity of PV could be connected to the distribution network without violating the network operational constraints.

6.4 Hosting Capacity Analysis within a Distributed Network

In this work, HC has been estimated for two scenarios, in the first scenario (i.e. HC_1) only voltage parameter is considered as constraint, however in the second scenario (i.e. HC_2) voltage and as well loading (i.e. line and transformer loading) are taken as constraints. The methodology for estimating the hosting capacity is given in the subsequent section.

6.4.1 Methodology for Estimating PV Hosting Capacity

This work has investigated HC of a distribution network considering a typical daily load profile and as well as PV generation profile. The selected constrains and objective function are described in Eqs. (6.1) to (6.6) for estimating the maximum HC at any of the 14 buses within distributed network. The considered main variables are PV capacities, voltage at bus terminals, line current, active and reactive line power flow, active and reactive power exchange with the

upstream grid. As the HC depends on the load, therefore different peak load demands are considered at different buses within the distribution network. An optimization technique [6.24] is used to calculate the maximum HC. In a 'n' bus network system, the maximum hosting capacity of a bus within the network is given by Eq. (6.1).

$$PV_{max}(X_n) = \text{Max } PV(X_n, t) \quad \text{Eq. (6.1)}$$

$$0.90 \leq V_n(t) \leq 1.0 \quad \text{Eq. (6.2)}$$

$$0 \leq T_{R1}(t) \leq 0.80 \qquad 0 \leq T_{R2}(t) \leq 0.80 \quad \text{Eq. (6.3)}$$

$$I_{jk}^{min} \leq I_{jk}(t) \leq I_{jk}^{max} \quad \text{Eq. (6.4)}$$

$$P_n^{L,min} \leq P_n^L(t) \leq P_n^{L,max} \quad \text{Eq. (6.5)}$$

$$Q_n^{L,min} \leq Q_n^L(t) \leq Q_n^{L,max} \quad \text{Eq. (6.6)}$$

where:

$DG_{Max}(X_n, t)$: Maximum hosting capacity of bus 'n' at time t

$V_n(t)$: Voltage of bus terminal 'n' at time t

$I_{jk}(t)$: Loading of line jk at time t

$T_1(t)$ & $T_2(t)$: Transformers loadings at time 't'

$P_n^L(t)$: Active load connected to the bus 'n' at time t

$Q_n^L(t)$: Reactive load connected to the bus 'n' at time t

The flow chart of proposed methodology for estimating HC at a bus within the distribution network has shown in the Fig. 6.10. To estimate the HC at bus within the network, initial conditions are set up e.g. maximum load connected to the different buses, load profile, voltage limits, lines current carrying capacity, transformer loadings. Initially, minimum PV capacity (i.e. 1% of transformer capacity) is allocated at a bus 'n' and it is increased in steps, until it does not violate the defined conditions as given in the Eqs. (6.2-6.6). In this study, the network behavior is analyzed for entire day (i.e. 24 hours) and it mainly covers two circumstances; (i) voltage rise problem due to low load demand and high PV generation (ii) loading problem due to high demand and high generation. The proposed methodology estimated the HC of individual bus for a typical daily load profile, is illustrated in the Fig. 6.10.

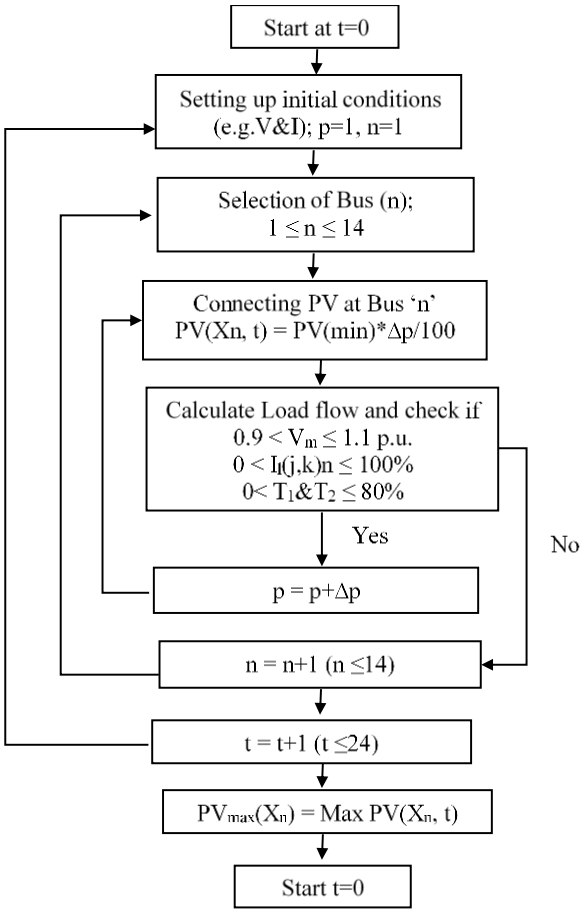

Fig. 6.10 Flow Diagram for Estimating HC of the Network

6.4.2 PV Hosting Capacity Estimation

In this work, HC has been estimated for two different scenarios, in the first scenario (i.e. HC_1) only voltage parameter is considered constraint however, in the second scenario (i.e. HC_2) voltage as well loading of lines are taken as constraints. In the Table 6.1, hosting capacities (i.e. HC_1 and HC_2) of the individual bus with most impacted line and bus are given. The parameter 'most impacted bus / line due to voltage or loading constraints' reveals that the HC of a bus is limited by that component within the distribution network. In case of HC_1, bus voltage is the limiting component for all 14 buses as only 'voltage' parameter is constraint in this scenario. It has been observed that the B_{10} is the most impacted bus for estimating the HC of B_1, and B_{10}, however, B_{14} is most impacted bus when HC is estimated for bus B_{12} & B_{14}. In other words, we can say that increasing PV at buses B_1 and B_{10}, highly influence the voltage of bus B_{10}, and similarly increasing PV at bus B_{12} & B_{14} showed maximum impact bus voltage of B_{14}. The values of HC examined in the both the cases and shown in the Table 6.1.

Table 6.1 Hosting Capacity of Each Bus in a Distribution Network

Bus No.	With only voltage as constraint		With voltage and loading as constraints		Changes in HC2 as compare to HC_1(%)
	HC_1 (MW)	Most impacted bus due to voltage constraint	HC_2(MW)	Most impacted bus / line due to voltage and loading constraints	
1	80.66	B_{10}	32.46	T_1	60↓
2	46.42	B_2	19.81	L_{1-2}	57↓
3	14.93	B_3	14.93	B_3	0
4	13.60	B_4	13.60	B_4	0
5	12.54	B_5	12.54	B_5	0
6	10.17	B_6	10.17	B_6	0
7	6.59	B_7	6.59	B_7	0
8	7.97	B_8	7.97	B_8	0
9	7.69	B_9	7.69	B_9	0
10	7.06	B_{10}	7.06	B_{10}	0
11	6.81	B_{11}	6.81	B_{11}	0
12	80.82	B_{14}	33.54	T_2	59↓
13	84.66	B_{12}	20.52	L_{12-13}	76↓
14	39.82	B_{14}	21.46	L_{13-14}	46↓

The signs downward (↓) and upward (↑) indicate, percentage reduction and increment in the parameter's value.

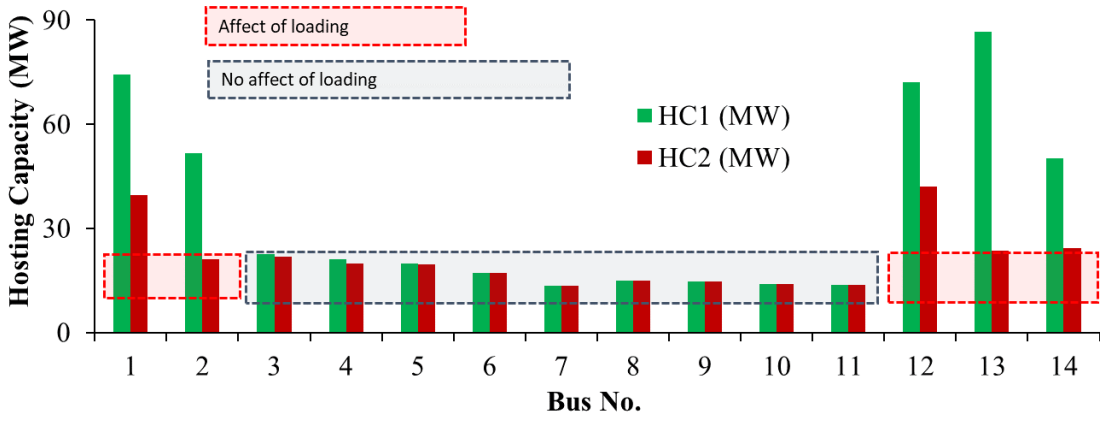

Fig. 6.11 Hosting Capacity without and with Loading

The illustration of HC_1 and HC_2 are shown in the Fig.6.11. In the Feeder 1, HC_2 of buses B_1 and B_2 have decreased by 60% and 57% respectively as compare to HC_1 however, there is no change in the hosting capacities of remaining buses.

In the Feeder 1, it has been observed that the hosting capacity (i.e. HC_1) of only bus B_1 highly impacted by voltage of bus B_{10} whereas as hosting capacity (i.e. HC_1) of remaining buses B_2 and B_{11} have been regulated by their own bus voltages. In the Feeder 2, hosting capacity (i.e. HC_2) of buses B_{12} and B_{13} and B_{14} have decreased by 59%, 76% and 46% respectively as compare to HC_1. It has been observed that the HC of buses B_{12}, B_{13} and B_{14} have been highly impacted by the loading of transformer T_2, line $L_{12\text{-}13}$ and line $L_{13\text{-}14}$ respectively. It shows that loading has significant impact on finding the hosting capacity at a bus within a distribution network.

The maximum value of HC_2 has been estimated 32.46 MW at Bus B_1 in feeder 1 however, in the feeder 2 maximum HC_2 is 33.54 MW at bus B_{12}. In this work, only feeder 1 is considered for further analysis purpose, and the impact of PV penetration has been analyzed. In the next section, performance of distribution network is evaluated with PV integration at buses B_7, B_8, B_9, and B_{10} and bus voltage, line loadings and transformer loadings are analyzed using DRTS and PHIL method.

6.5 Impact of PV Penetration into the Distribution Network (i.e. Case 6.b)

In the Section 6.4, the maximum hosting capacity (only a bus at a time) is estimated for 14 buses (i.e. Fig. 6.11). In this analysis, selected buses (i.e. B_7, B_8, B_9, and B_{10}) of *Group* B are considered for integrating PV because the hosting capacity of these buses falls in the lowest range (i.e. 6.6 to 7.9 MW) as compare to other groups (Group A and Group C). In addition, HC of these buses (i.e. B_7, B_8, B_9, and B_{10}) of *Group* B don't change for both the cases (i.e. HC_1 and HC_2). Also, limitation of testing setup for carrying out PHIL experiments, HC of selected buses (i.e. B_7, B_8, B_9, and B_{10}) of *Group* B represents suitable range and therefore the individual hosting capacity of buses B_7, B_8, B_9, and B_{10} has exploited for distributing the PV capacity among these buses.

In this study, 7 MW capacity of solar PV system is distributed into the feeder 1 (i.e. B_7, B_8, B_9, and B_{10}). At B_7, B_9, and $B_{10,}$ 2 MW of PV system is connected on each bus using RTDS. Due to physical limitations of the testing setup, 1 MW of PV system is connected at B_8 through PHIL testing setup. It has been represented in the Fig. 6.12 and explained in the next Section.

6.5.1 Testing Setup

To analyze the impact of high PV penetration into the distribution network, PHIL testing setup is used as shown in the Fig. 6.12. A PV simulator is used to generate characteristics e.g. irradiance, maximum power point, temperature etc. The output of PV simulator is connected to the DC side of the 3 kW PV inverter. The output of the 3 kW PV inverter (AC side) has been further connected through a linear four-quadrant power amplifier which was upscaled inside DRTS to 1 MW of PV power output at B_8. The communication between the DRTS and the PV inverter is performed via a communication interface which consists of analogue and digital input/output modules and a real-time target (RTT) computer [6.25]. The I/O modules communicate through EtherCat protocol with the RTT, which in turn interfaces these signals directly connected with the MATLAB Workspace.

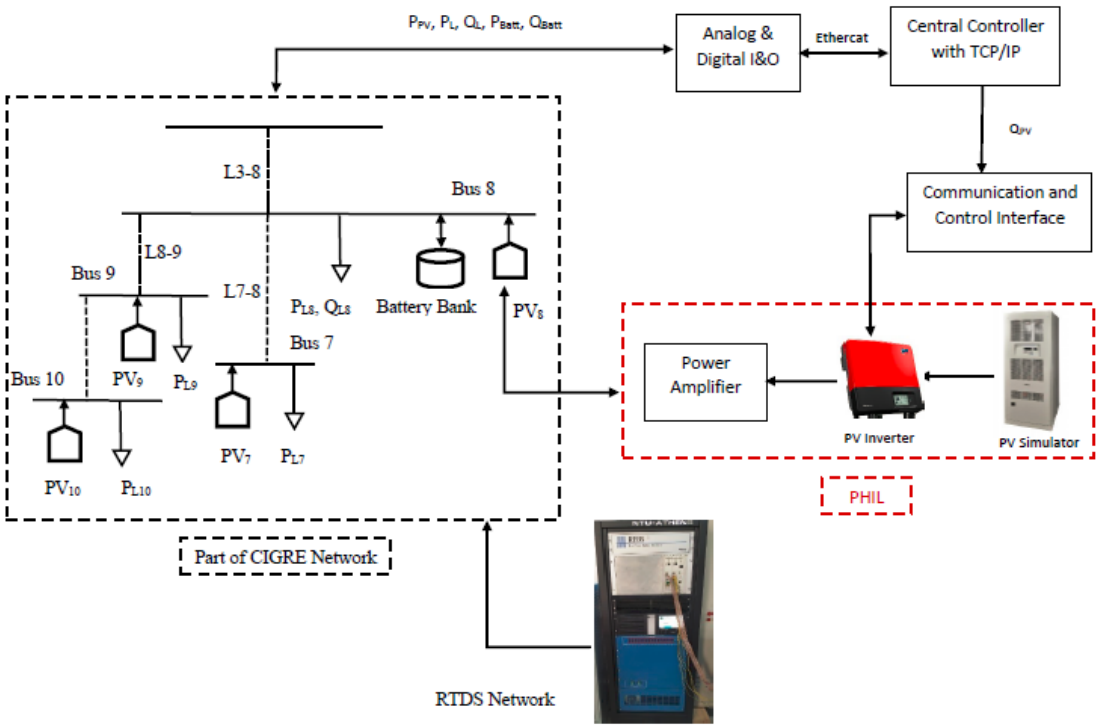

Fig. 6.12 Laboratory Testing Setup of and PHIL

A battery energy storage of 1 MWh (using DRTS) has been integrated with the B_8. The power output of the battery has been controlled through a pre-defined profile of PV+ Battery (in DRTS) as shown in the Fig. 6.13. In the study, battery charging, and discharging have been taken negative (-) and positive (+) signs, respectively.

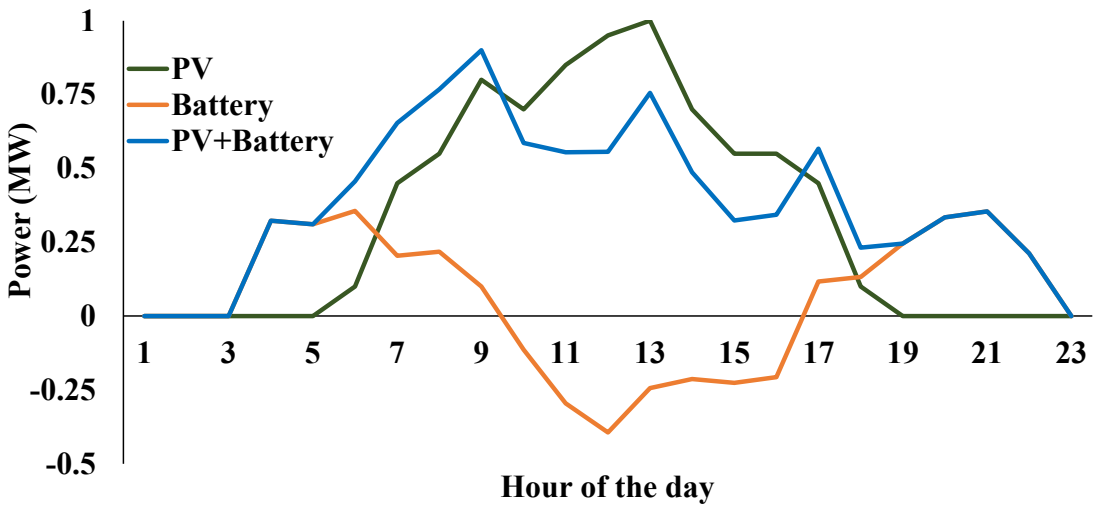

Fig. 6.13 PV, Battery and PV+ Battery Profiles

6.5.2 Results and Analysis of Case 6.b

The PV simulator generates its own voltage and current characteristics based on the given input profile. The output of physical PV inverter is controlled using the PV simulator during the experiment, whereas the other PV system and loads obtained their respective curves from the MATLAB and simulated using DRTS. The PV simulator is synchronized with MATLAB, so that all the PV inverters (i.e. one PHIL and other three simulated in DRTS) follow the same irradiance profile. The results of the PHIL testing are compared with the base case scenario (Case 6.a) and presented in the subsequent section.

In the *Group A*, voltage of six buses (i.e. V_1 to V_6) and loading of five lines (i.e. $L_{1\text{-}2}$, $L_{2\text{-}3}$, $L_{3\text{-}4}$, $L_{4\text{-}5}$ and $L_{5\text{-}6}$) are shown in the Figs. 6.14 & 6.15 respectively. It has been observed from the Fig. 6.14. that the bus voltages (i.e. V_1 to V_6) never goes below 0.98 p.u. however, the maximum voltage reached to the 1.05 p.u. The lowest voltage has appeared during the peak demand's hours in the nighttime (i.e. 20:00 hours to 21:00 hours). It has been observed that integration of PV at buses B_7, B_8, B_9, and B_{10}, improves the voltage profile during the morning peak hours (i.e. 08:00 hours to 09:00 hours). The minimum voltage during the daytime has been increased from 0.98 p.u. (i.e. Case 6.a) to 0.99 p.u. (Case 6.b). However, during the peak sunshine hours the maximum voltage is raised by 5%, as compare to the Case 6.a. It has been observed that in the different circumstance's buses' voltages do not violate the defined voltage regulation criteria (i.e. $0.90 \leq V_i \leq 1.10$).

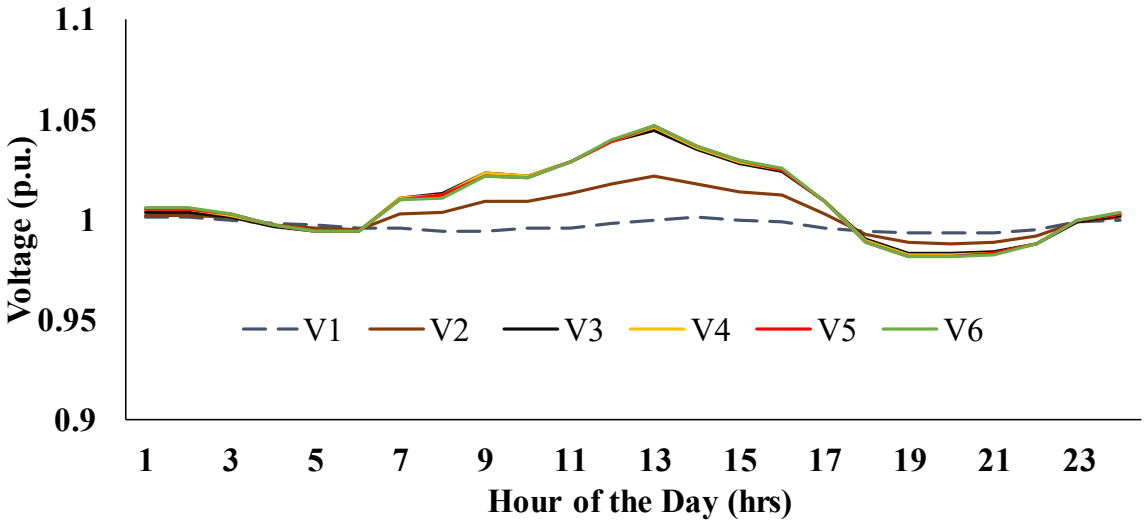

Fig. 6.14 Variation of Bus Voltages of Group A of Case 6.b

The line loading of *Group A* has been presented in Fig. 6.15. It has been observed that the maximum line loading is recorded 34% (i.e. 25% higher as compare to Case 6.a) for the lines $L_{1\text{-}2}$ and $L_{2\text{-}3}$. And loadings of the remaining lines (e.g. $L_{3\text{-}4}$, $L_{4\text{-}5}$ and $L_{5\text{-}6}$) are below 2% throughout the day. It indicates that PV system, connected to the buses B_7, B_8, B_9, and B_{10} doesn't affect the line loading of $L_{3\text{-}4}$, $L_{4\text{-}5}$ and $L_{5\text{-}6}$ as these lines are connected with a separate string to the bus B_3 and therefore line loadings are remained within the defined limit.

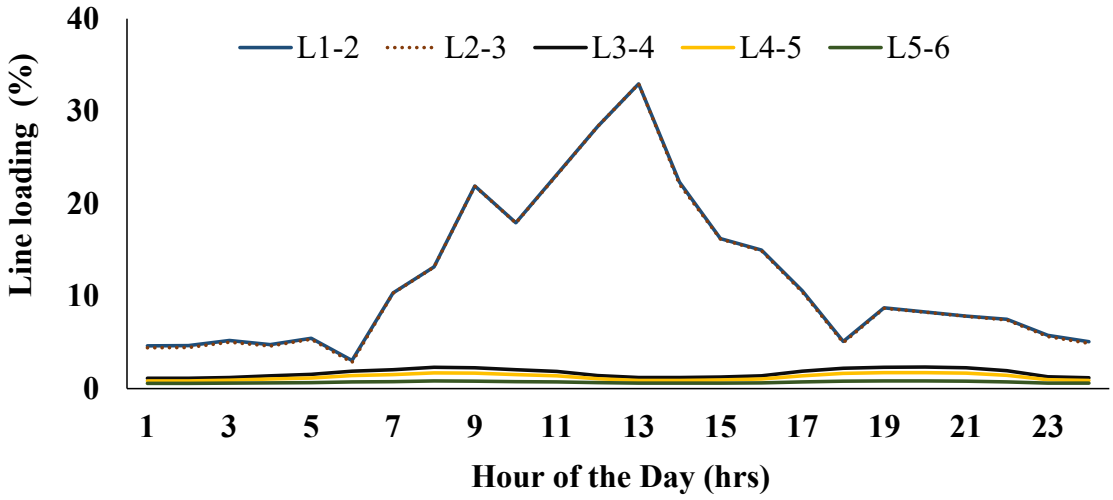

Fig. 6.15 Variation of Line Loading of Group A of Case 6.b

In the *Group B*, voltage of five buses (i.e. V_7 to V_{11}) and loading of five lines (i.e. $L_{7\text{-}8}$, $L_{8\text{-}9}$, $L_{9\text{-}10}$, $L_{10\text{-}11}$ and $L_{3\text{-}8}$) are shown in the Figs. 6.16 & 6.17 respectively. The maximum bus voltages (i.e. V_7 to V_{11}) are recorded and it is 9% more (i.e. 1.09 p.u.) as compare to the Case 6.a. However, minimum bus voltage is noted 0.98 p.u. during night-time (i.e. 19:00 hours to 21:00 hours). It has been observed that although, the voltage of five buses (i.e. V_7 to V_{11}), are within the

defined voltage regulation criteria (i.e. (i.e. $0.90 \leq V_i \leq 1.10$), but due to further increase of the PV capacity, it may violate the voltage regulation.

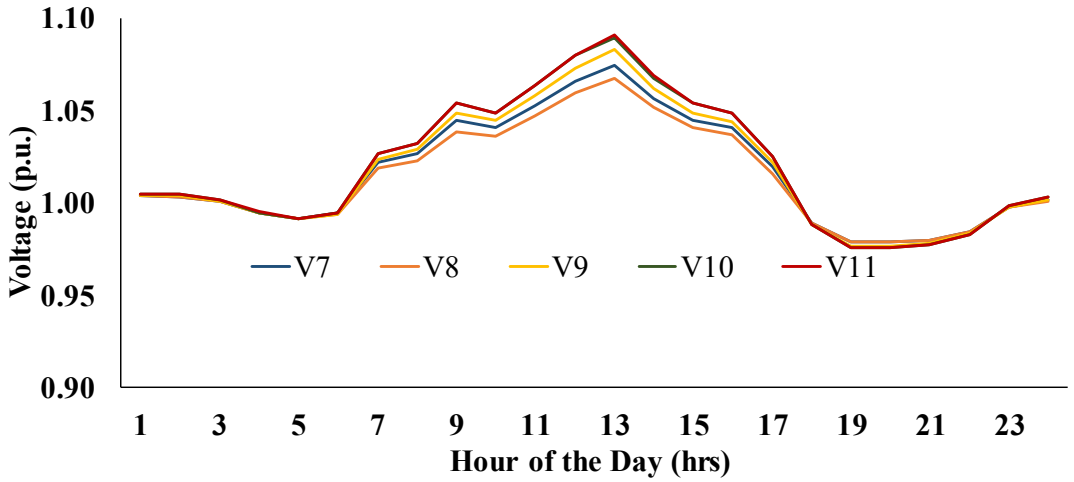

Fig. 6.16 Variation of Bus Voltages of Group B of Case 6.b

In the *Group B*, the maximum line loading of lines $L_{3\text{-}8}$ and $L_{8\text{-}9}$ has been recorded 33% (i.e. 28% higher as compare to the Case 6.a) and 21% (i.e. 17 % higher as compare to Case 6.a) respectively. However, loadings of the remaining lines (e.g. $L_{7\text{-}8}$, $L_{9\text{-}10}$ and $L_{10\text{-}11}$) are below 11% throughout the day. The loading of line $L_{3\text{-}8}$ is influenced by the load connected to the buses (i.e. B_7, B_8, B_9, B_{10} and B_{11} and therefore, loading of line $L_{3\text{-}8}$ is high as compare to the other line loading (i.e. $L_{7\text{-}8}$, $L_{9\text{-}10}$ and $L_{10\text{-}11}$). It has been observed from the Fig. 6.17 that the all lines (except $L_{10\text{-}11}$) follow the PV generation curve, but as no PV is connected to the bus B_{11} so loading curve of line $L_{10\text{-}11}$ does not influence by PV. It has also been observed that the line loadings are within the defined limit (i.e. ≤100%).

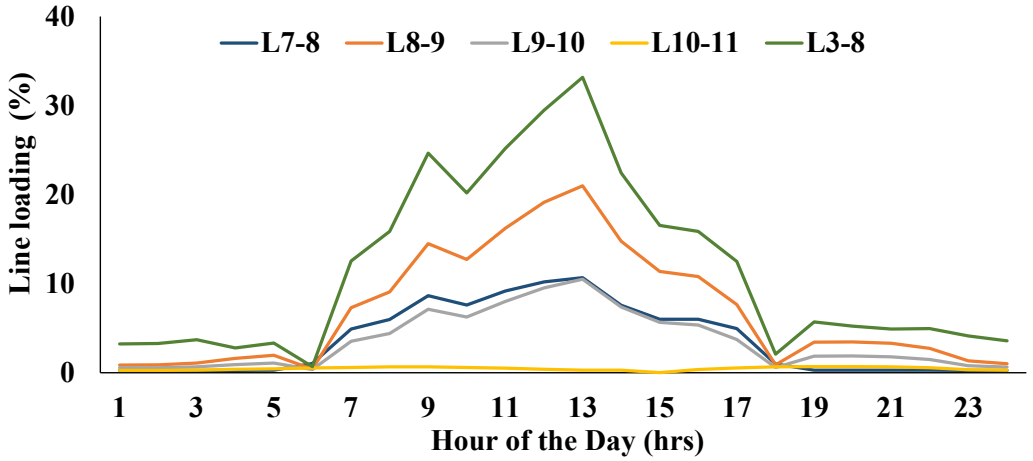

Fig. 6.17 Variation of Line Loadings of Group B of Case 6.b

In the *Group C*, three buses (i.e. B_{12}, B_{13} and B_{14}) and two lines (i.e. $L_{12\text{-}13}$ and $L_{13\text{-}14}$) are connected to feeder 2, but no PV is integrated with this feeder. Therefore, bus voltages (i.e. V_{12}, V_{13} and V_{14}) and line loadings (i.e. $L_{12\text{-}13}$ and $L_{13\text{-}14}$) are not affected in this case. The bus voltages (i.e. V_{12}, V_{13} and V_{14}) and line loadings (i.e. $L_{12\text{-}13}$ and $L_{13\text{-}14}$) follow the same characteristics as shown in the Figs 6.7 & 6.8 respectively.

The variation of transformer loadings (i.e.T_1 and T_2) of a typical day, has shown in the Fig. 6.18. Loading of transformer T_1 during the daytime (i.e. 09:00 hours and 18:00 hours) has been reduced from 29% (i.e. Case 6.a) to 19%, whereas maximum loading during the night-time (i.e. 19:00 hours to 21:00 hours) is the same as the base case scenario (i.e. Case 6.a). It has been observed that integrating PV system into the feeder 1, the transformer loading T_1 is reduced as generated PV power is injected into the grid as well as to meet the local load demand. The average energy loading of transformer T_1 has also reduced from 17% (i.e. Case 6.a) to 14%. The loading of transformer T_2 does not change as PV is not connected with feeder 2 and it represents the same characteristics as shown in the Fig. 6.9 (i.e. Case 6.a).

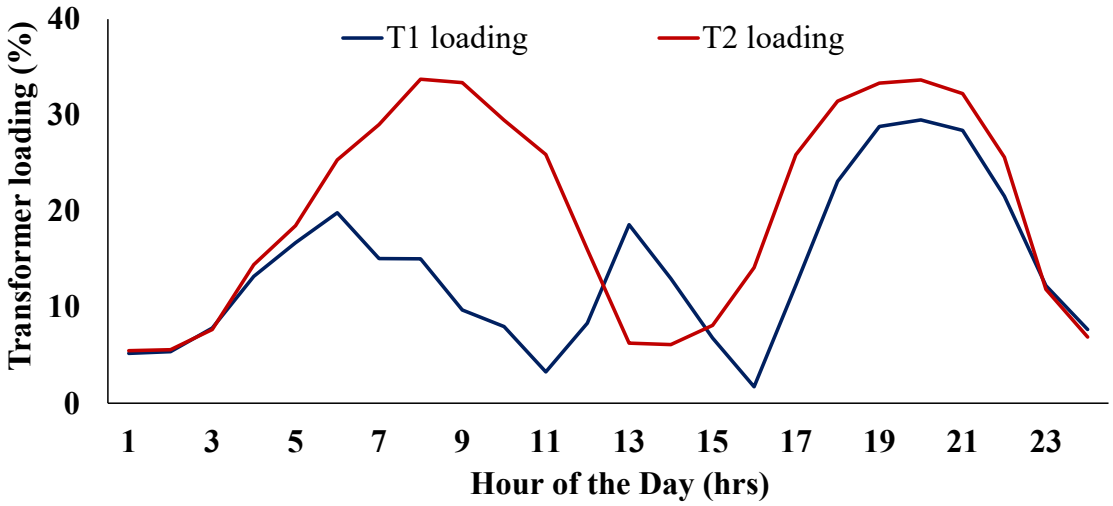

Fig. 6.18 Variation of Transformers Loading of Case 6.b

In this section, PV system is integrated at the buses B_7, B_8, B_9 and B_{10} and its impact into the other buses, lines and transformer's loading are analyzed. The major impacts of PV integration are observed into the bus voltages and line loadings. It has been observed that the bus voltages (i.e. V_7 to V_{11}) in the feeder 1 has increased by 9% and maximum loading of line $L_{3\text{-}8}$ is increased by 28% as compare to the Case 6.a. The average loading of transformer T_1 has been reduced

by 3% and there is no change in the loading of transformer T_2. It has been clearly observed that integrating more PV at the buses (i.e. B_7, B_8, B_9 and B_{10},), there may be further increase in the bus voltages and violate the defied voltage regulation criteria. Therefore, it is essential to implement appropriate mitigation techniques to address the voltage rise problem within the distribution network.

In the next section, Q-V droop control strategy has been implemented into the PV inverter using power hardware in-loop the test bed. A comparative analysis has carried out without and with droop strategies in the Section 6.6.

6.6 Impact of Q-V Droop Control Strategy using DRTS and PHIL Methods (i.e. Case 6.c)

In this section, the application of the droop control concept has been explored to improve the voltage profiles so that more PV could be connected to the distribution network. In this work, Q-V droop control strategy has been implemented into the PV inverter, and as well as into the battery's control system. The Q-V droop control corrects voltage errors in the network by injecting or absorbing reactive power as a result of changes to the nominal voltage. The extent of the inverter's response is based on the configured parameters of the droop controller, i.e. the voltage dead-bands, Q_{min} and Q_{max} as shown in Fig. 6.19. The fixed voltage change Q-V droop characteristic has been considered in this work and droop control strategy has been used into the hardware PV inverter to test the dynamics of the system in real time conditions based on a PHIL setup as shown in the Fig. 6.12. The QV droop control strategy has also been used into the other PV systems (PV_7, PV_9 and PV_{10}), connected into the buses B_7, B_9 and B_{10} and it has same characteristics as considered for PV_8.

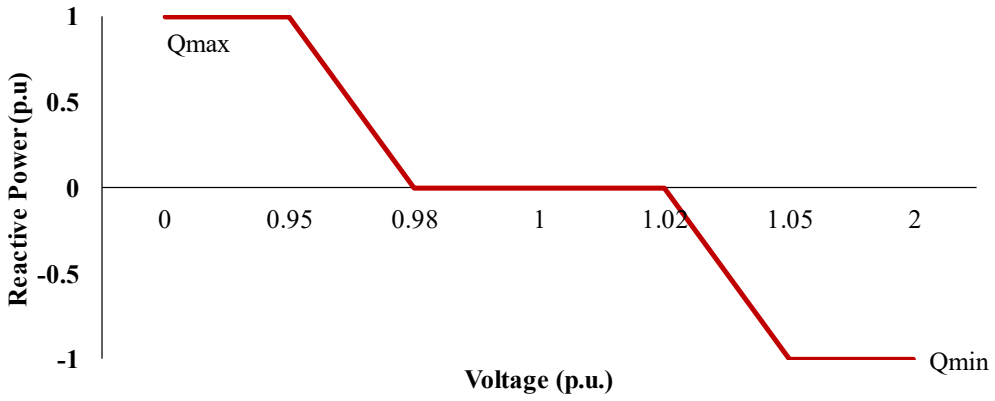

Fig. 6.19 The Q-V Droop Characteristics

After implementing the Q-V droop control strategy, reactive power contribution from the PV systems (i.e. PV_7, PV_8, PV_9 and PV_{10}) and battery at bus B_8, have been recorded and their values are shown in the Fig. 6.20. It has been observed that reactive power support has been provided during the daytime when voltage rise problem has been appeared within the network. The reactive power absorption from the PV_{10} is maximum, however, PV_7 and PV_8 have the lowest reactive power absorption. Since the PV_8 has absorbed enough reactive support to improve the voltage rise issues therefore the reactive power contribution from the battery energy storage is almost zero. The improvement in the voltage profiles compared with results obtained from the Section 6.5 (i.e. Case 6.b) and the groupwise results and analysis are presented in the subsequent section.

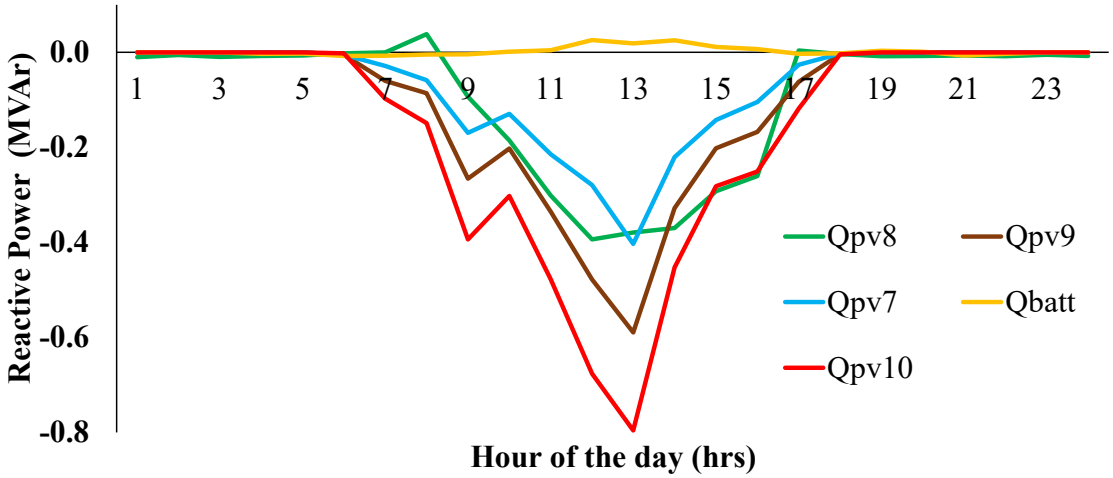

Fig. 6.20 Reactive Power from PV Connected at B_7, B_8, B_9 and B_{10}

6.6.1 Results and Analysis of Case 6.c

In the Case 6.c, PV has been integrated at buses B_7, B_8, B_9 and B_{10} network and Q-V droop control strategy has been implemented. The output of the PV inverter has been controlled using the PV simulator, whereas the simulated PVs and loads obtained their respective curve values from MATLAB. The PV simulator was synchronized with MATLAB, so that all PV inverters (i.e. PV_7, PV_8, PV_9 and PV_{10}) follow the same irradiance profile. The results obtained from Case 6.c are analyzed in the subsequent section.

In the *Group A*, voltage of six buses (i.e. V_1 to V_6) and loading of five lines (i.e. $L_{1\text{-}2}$, $L_{2\text{-}3}$, $L_{3\text{-}4}$, $L_{4\text{-}5}$ and $L_{5\text{-}6}$) are shown in the Figs. 6.21 & 6.22 respectively. It has been observed from the Fig. 6.21. that the maximum bus voltage is reduced from 1.05 p.u. (i.e. Case 6.b) to 1.02 p.u. and voltages of all six buses (i.e. V_1 to

V_6) never goes below than 0.99 p.u. The lowest voltage of 0.99 p.u. has been appeared during the peak demand's hours (i.e. 19:00 hours to 21:00 hours). It indicates that voltage profile has been improved by implementing the droop control strategy with the PV inverter.

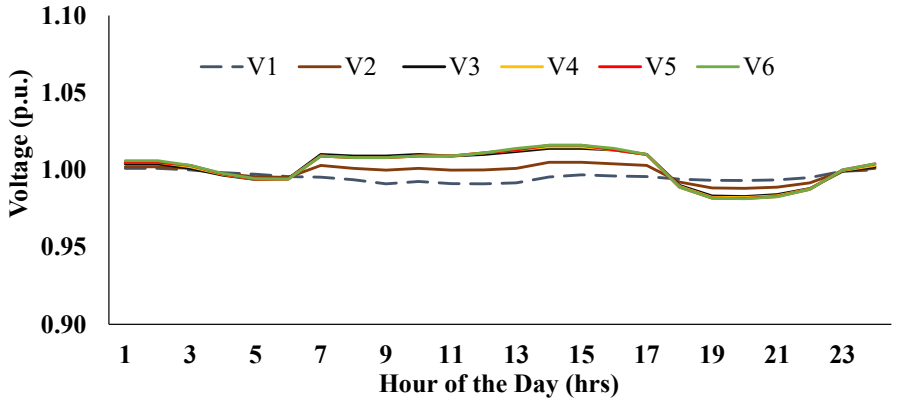

Fig. 6.21 Variation of Bus Voltages of Group A of Case 6.c

It has been observed from the Fig. 6.22 that the loading curve follow the same characteristics as shown in the Fig. 6.15 (Case 6.b). The maximum line loading is observed 35% (i.e. 1% higher than of Case 6.b) for the lines L_{1-2} and L_{2-3}, whereas, maximum loadings of the remaining lines (e.g. L_{3-4}, L_{4-5} and L_{5-6}) are almost same as of Case 6.b and it remains below 2% throughout the day.

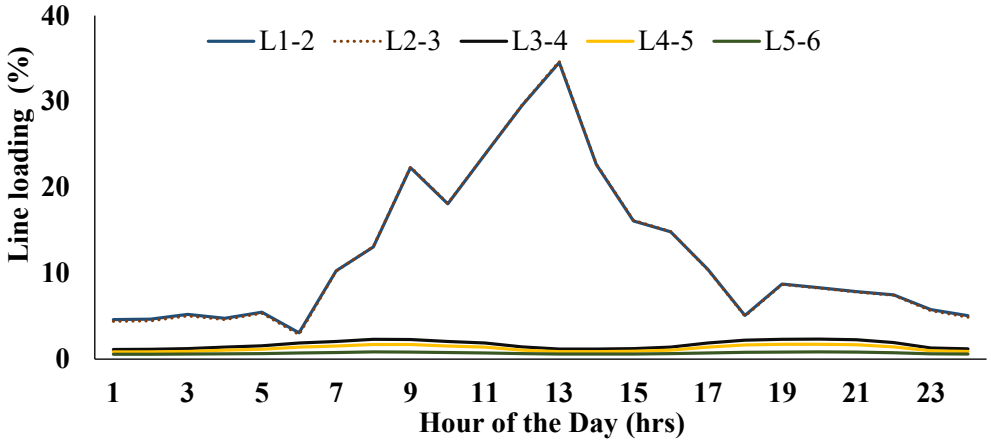

Fig. 6.22 Variation of Line Loading of Case A of Case 6.c

In the *Group B*, voltage (p. u.) of five buses (i.e. V_7 to V_{11}) and loading of five lines (i.e. L_{7-8}, L_{8-9}, L_{9-10}, L_{10-11} and L_{3-8}) are shown in the Figs. 6.23 & 6.24. In Case of 6.b, the maximum voltage rise issues are observed in the buses (B_7, B_8, B_9, and B_{10}) but after implementing Q-V droop control strategy the maximum voltage is reduced from 1.09 p.u. to 1.04 p.u. The droop control strategy

implemented through RTDS and PHIL method at B_8 test bed has been verified. And on the remaining buses (i.e. B_7, B_9, B_{10}), the Q-V characteristics are implemented through RTDS. It has been observed that the Q-V droop control strategy can help in improving the voltage profile during high PV penetration scenario.

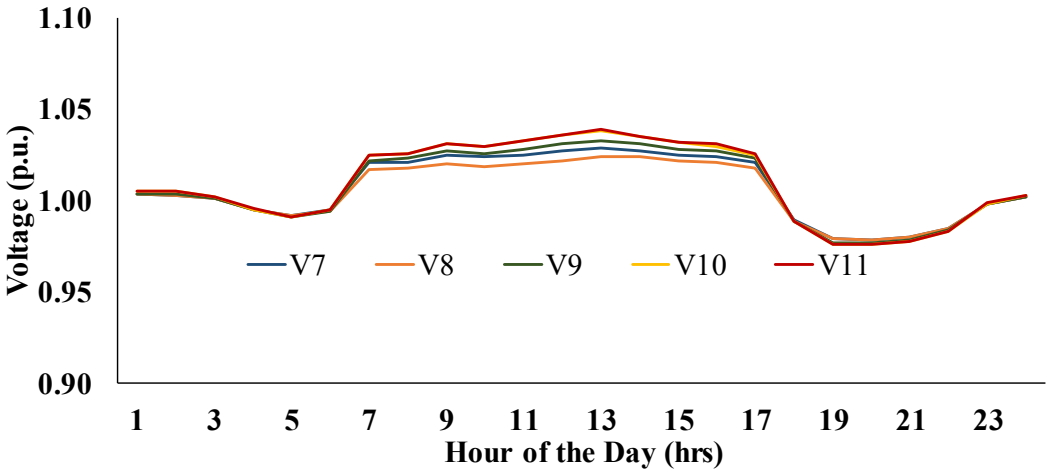

Fig. 6.23 Variation of Bus Voltages of Group B of Case 6.c

In the *Group B*, it has been observed from the Fig. 6.24 that the loading curve follow the same characteristics as for Case 6.b (i.e. Fig. 6.17). The maximum loading of lines $L_{3\text{-}8}$ and $L_{8\text{-}9}$ for Case 6.c are recorded 35% and 22% respectively, and these line loadings are only 1% higher than compare to Case 6.b (without Q-V droop control). And there is no significant change observed for loadings of the remaining lines (e.g. $L_{7\text{-}8}$, $L_{9\text{-}10}$ and $L_{10\text{-}11}$), and it remains below 12% throughout the day. A small increase in the line loading have been appeared due reactive power support provided by the PV inverters.

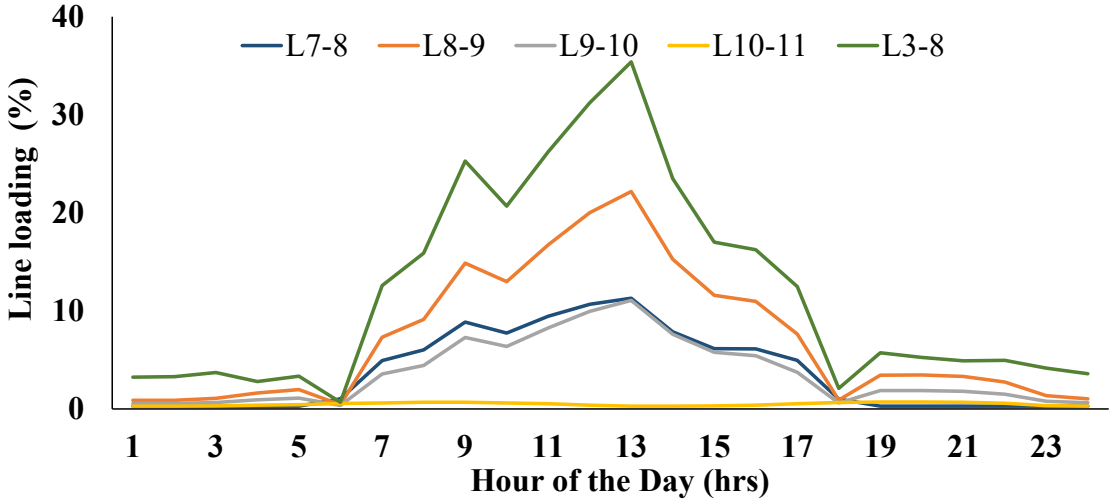

Fig. 6.24 Variation of Line Loadings of Group B of Case 6.c

In the *Group C*, three buses (i.e. B_{12}, B_{13} and B_{14}) and two lines (i.e. $L_{12\text{-}13}$ and $L_{13\text{-}14}$) are connected with feeder 2 and no PV has integrated with this feeder, therefore the bus voltages (i.e. V_{12}, V_{13} and V_{14}) and line loadings (i.e. $L_{12\text{-}13}$ and $L_{13\text{-}14}$) have not affected in this case. The bus voltages (i.e. V_{12}, V_{13} and V_{14}) and line loadings (i.e. $L_{12\text{-}13}$ and $L_{13\text{-}14}$) follow the same characteristics as shown in the Figs 6.7 & 6.8 respectively.

The variation of transformer loadings (i.e.T_1 and T_2) of a typical day, is shown in the Fig. 6.25. The loading characteristics of transformer T_2, do not change as PV has not connected with feeder 2 and it represents the same characteristics as shown in the Fig. 6.9 (i.e. Case 6.a). However, maximum loading of transformer T_1 during the morning peak load hours (i.e. 08:00 hours and 09:00 hours) is increased by 1% compare to the Case 6.b (without Q-V droop control strategy), whereas maximum loading during the night peak hours (i.e. 19:00 hours to 21:00 hours) is same as of Case 6.b. The average daily energy loading of transformer T_1 has increased from 14% (Case 6.b) to 15%.

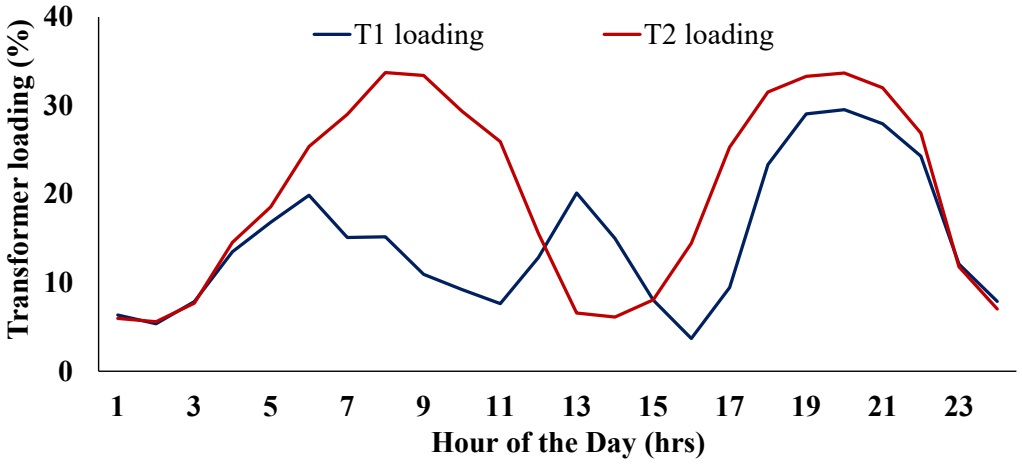

Fig. 6.25 Variation of Transformers Loading of Case 6.c

In this section, PV system is integrated to the buses B_7, B_8, B_9 and B_{10} and Q-V droop control strategy has been implemented in all inverters at all buses for improving the voltage profiles. It has been observed that by implementing the Q-V droop control strategy, maximum bus voltage has been reduced from 1.09 p.u. to 1.04 p.u. The average loading of lines and transformers have increased by only 1% with Q-V droop control strategy. It has been clearly observed that by implementing the Q-V droop control strategy more PV can be integrated at the buses (i.e. B_7, B_8, B_9 and B_{10},) and PV can be used to meet the local load demand.

In this section the voltage rise problem has been addressed by using the Q-V droop control strategy. However, the CIGRE distribution network also has a

potential to operate as mesh network by connecting both the feeders through switch S_1. This study is further extended to analyze the impacts high PV penetration on the mesh type distribution network and its results are compared with the radial network (Case 6.c PV integration with QV droop) and presented in the next section.

6.7 Impact of PV Penetration within Mesh Network (Cases 6.d & 6.e)

The switch S_1 is important as it is connected between both the feeders, therefore a mesh network could be created by closing switch S_1. In this section a mesh network has been formed and two experiments (i.e. Cases 6.d and 6.e) are carried out. In the Case 6.d, the distribution network configuration is same as the Case 6.b but switch S_1 is closed. Whereas in the Case 6.e the distribution network configuration is the same as Case 6.c and switch S_1 closed. It means that the Case 6.d has analyzed the impacts of only radial network formation (S_1 closed) during high PV penetration however in the Case 6.e, cumulative impacts of Q-V droop control strategy as well as formation of radial network (S_1 closed) has analyzed. In order to conduct the experiment, same methodology has used as explained in the Sections 6.4. The groupwise results are analyzed and discussed in the subsequent section.

6.7.1 Comparison of Cases 6.d and 6.e with 6.b

In the *Group A*, the voltage of six buses (i.e. V_1 to V_6) for Cases 6.d. and 6.e, are shown in the Figs. 6.26 and 6.27 respectively. In the Case 6.b, the maximum voltage rise of *Group A* in the feeder 1 is noted 1.05 p.u. (refer Fig. 6.14) and it reduced to 1.04 p.u. when distribution network is converted to a radial network (Case 6.d) as shown in the Fig. 6.26. However, in the Case 6.e, the cumulative effect of radial network as well as Q-V droop control strategy reduced maximum voltage from 1.05 p.u. (Case 6.b) to 1.02 p.u. It shows that Q-V droop control strategy and mesh network formation, together effectively improve the voltage profiles of the distribution network.

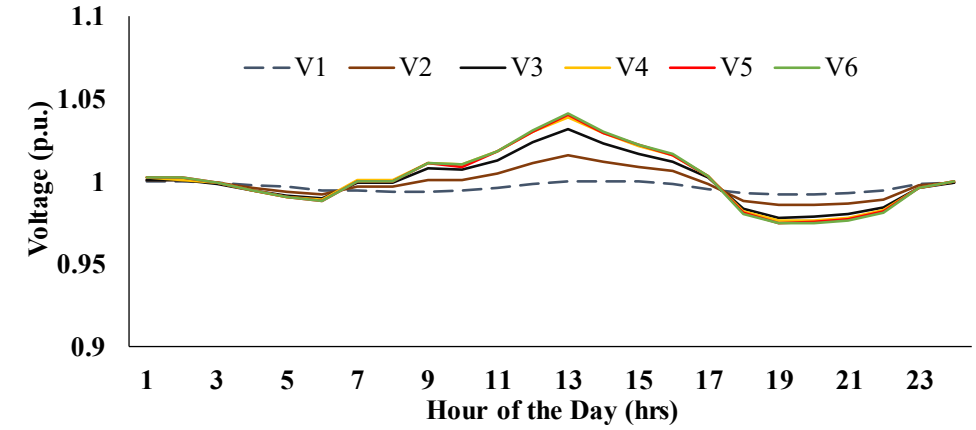

Fig. 6.26 Bus Voltages of Group A in Case 6.d

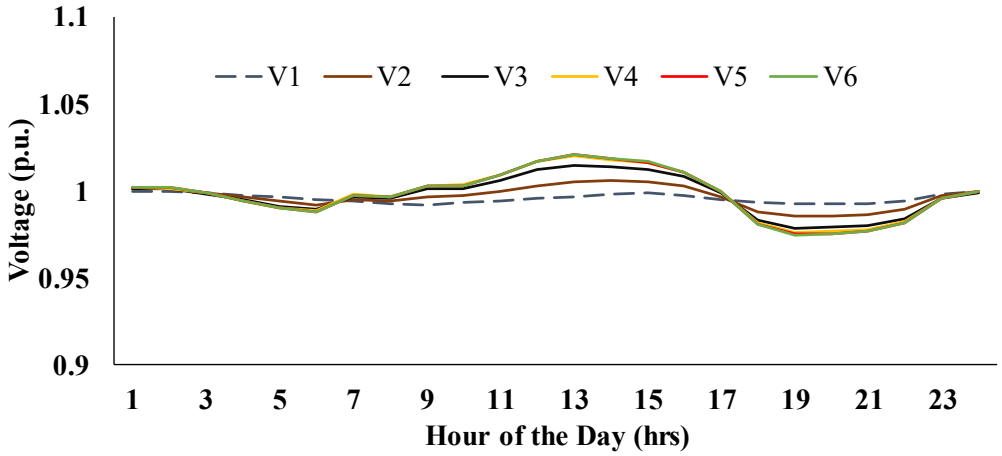

Fig. 6.27 Bus Voltages of Group A in Case 6.e

The maximum change in the loading of lines $L_{1\text{-}2}$ and $L_{2\text{-}3}$ are observed in the *Group A* therefore a comparison of only line loading $L_{2\text{-}3}$ for the Case 6.b, Case 6.d and Case 6.e are considered for analysis purpose, and it is shown in the Fig. 6.28. It has been observed from the Fig. 6.28 that the line loading of line $L_{2\text{-}3}$ follows the same characteristics for all three cases (i.e. Case 6.b, 6.d and 6.e) however, maximum loading of line $L_{2\text{-}3}$ for Case 6.d and Case 6.e are reduced from 33% (i.e. Case 6.b) to 15% and 16% respectively. It indicates that creating mesh network also reduce the overall line loading of feeder 1.

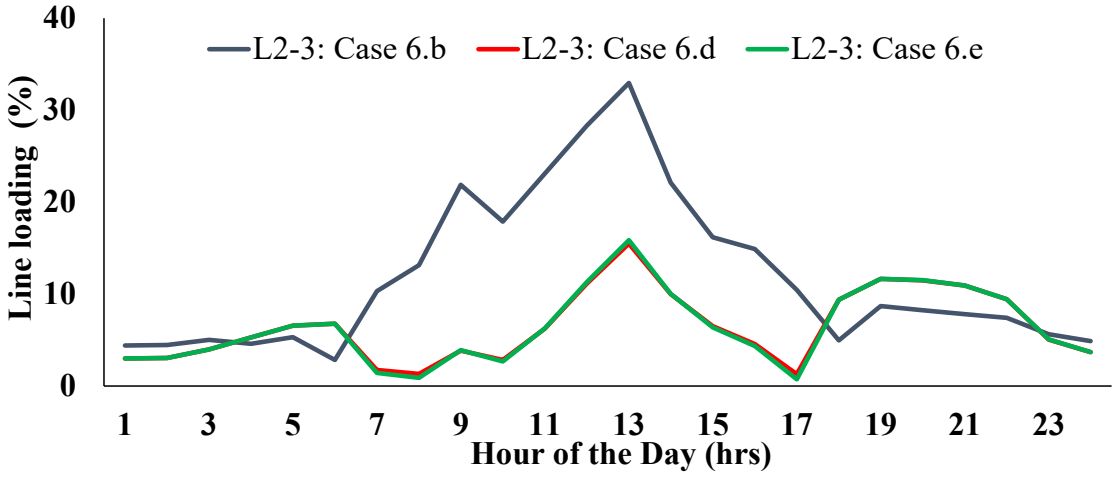

Fig. 6.28 Line Loading of $L_{2\text{-}3}$ for Cases 6.b, 6.d and 6.e

In the *Group B*, the bus voltages (i.e. V_7 to V_{11}) for both cases 6.d. and 6.e, are shown in the Figs. 6.29 and 6.30 respectively. In the Case 6.b, the maximum voltage rise in the feeder 1 is noted 1.09 p.u. (refer Fig. 6.16) and it has reduced to 1.05 p.u., when distribution network is converted to a radial network (Case 6.d) as shown in the Fig. 6.29. However, in the Case 6.e, the cumulative effect of radial network as well as Q-V droop control strategy reduced maximum voltage from 1.09 p.u. (Case 6.b) to 1.03 p.u. It shows that Q-V droop control strategy and mesh network formation, together effectively improves the voltage profiles of the distribution network.

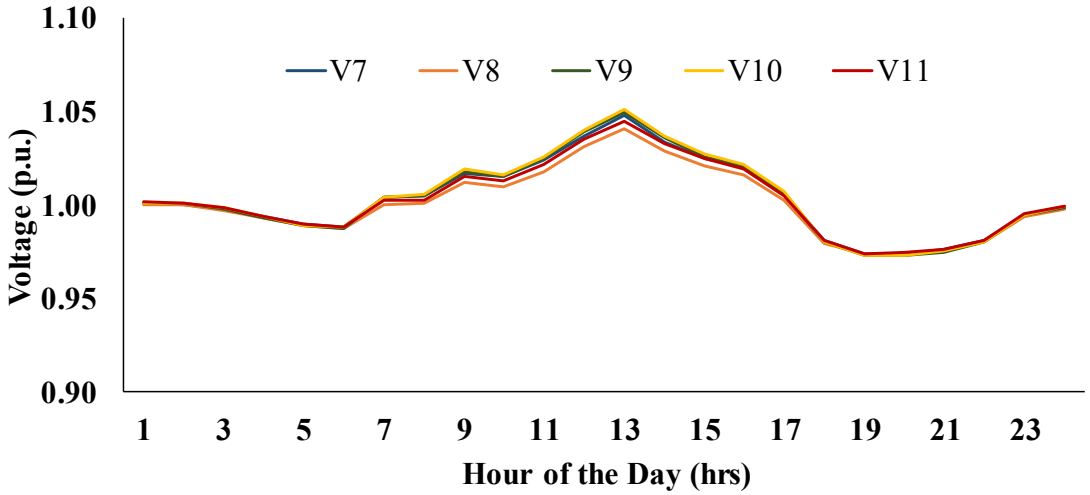

Fig. 6.29 Bus Voltages of Group B in Case 6.d

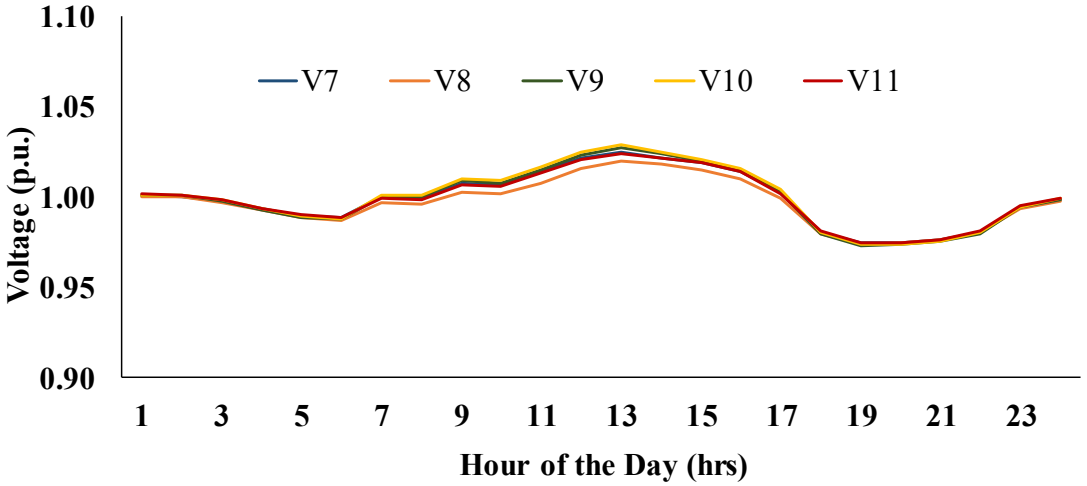

Fig. 6.30 Bus Voltages of Group B in Case 6.e

The maximum changes in the loading of line $L_{3\text{-}8}$ has been observed in the *Group B* therefore a comparison of only line loading $L_{3\text{-}8}$ for the Cases 6.b, Case 6.d and Case 6.e are considered for analysis purpose and shown in the Fig. 6.31. It has been observed from the Fig. 6.31 that the loading of line $L_{3\text{-}8}$ follows the same characteristics for all three cases (i.e. Cases 6.b, 6.d and 6.c) however, maximum loading of line $L_{3\text{-}8}$ for Case 6.d and Case 6.e has reduced from 33% (i.e. Case 6.b) to 6.7% and 7% respectively. It indicates that creating mesh network, reduce the overall line loading of feeder 1.

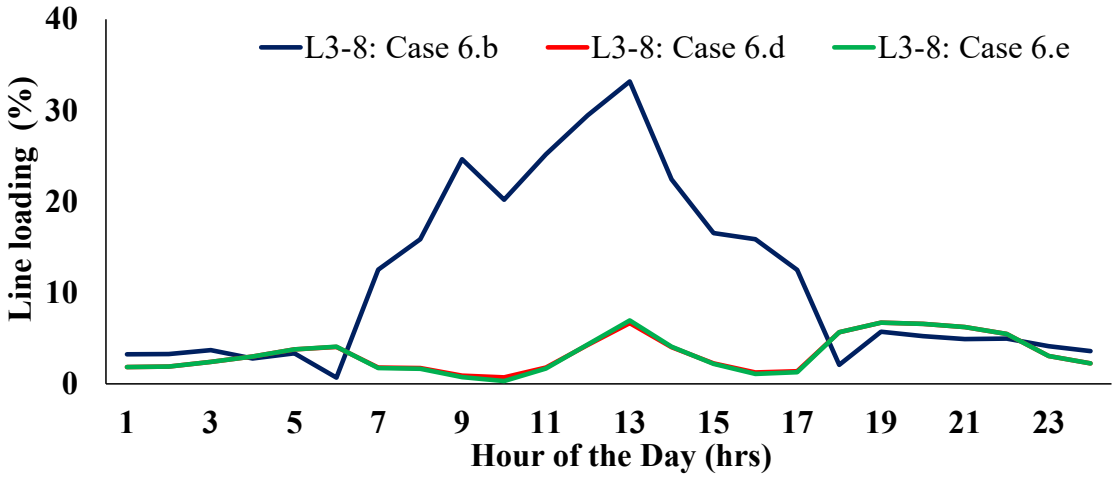

Fig. 6.31 Line Loading of Line $L_{3\text{-}8}$ for Cases 6.b, 6.d and 6.e

In the *Group C*, bus voltages (i.e. V_{12}, V_{13} and V_{14}), for both cases 6.d. and 6.e, are shown in the Figs. 6.32 and 6.33 respectively. In the Case 6.b, the maximum voltage rise of the B_{14} in the feeder 2 is noted 0.99 p.u. (refer Fig. 6.7) and it is increased to 1.01 when radial distribution network is converted to a mesh

network (Case 6.d) as shown in the Fig. 6.32. The cumulative effect into the bus voltage B_{14}, due to mesh network as well as Q-V droop control strategy (Case 6.e) don't make significant change on the bus voltage V_{14} (Fig. 6.33).

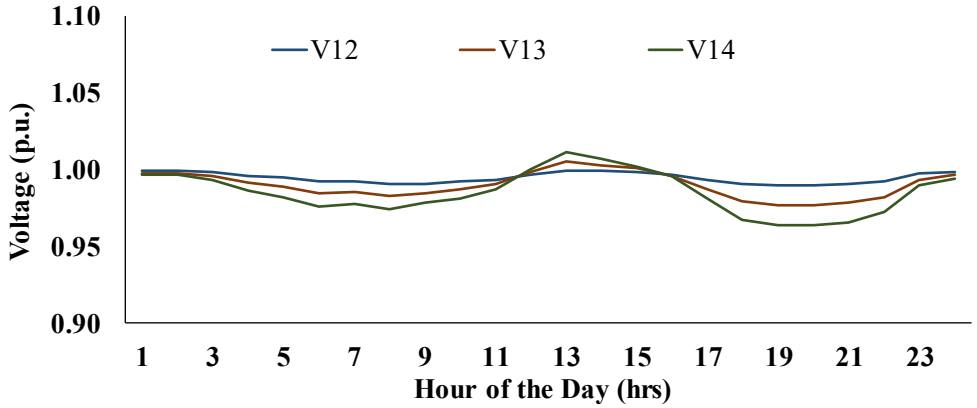

Fig. 6.32 Bus Voltages of Group C for Case 6.d

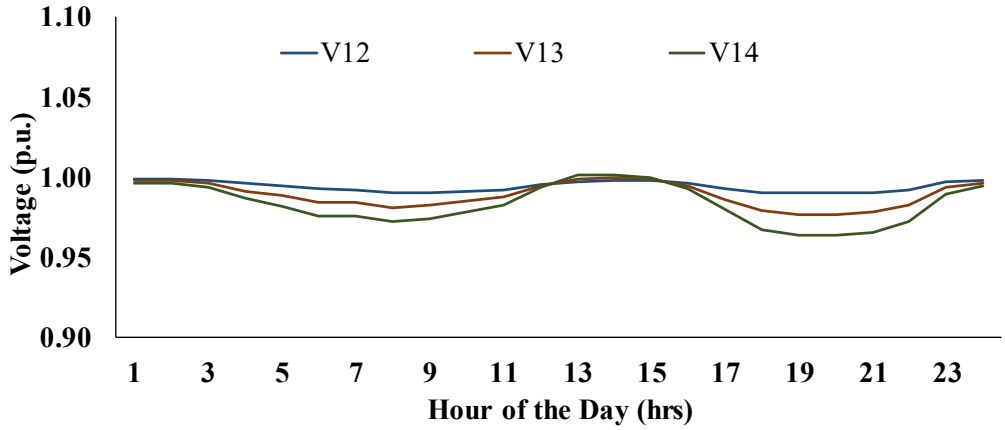

Fig. 6.33 Bus Voltages of Group C for Case 6.e

The loading of the lines $L_{12\text{-}13}$ and $L_{13\text{-}14}$ in the *Group C* are almost same therefore a comparison of only line loading $L_{13\text{-}14}$ for the Case 6.b, Case 6.d and Case 6.e are considered for analysis purpose and shown in the Fig. 6.34. It has been observed from the Fig. 6.34 that the loading of line $L_{13\text{-}14}$ follows the characteristics as for the Cases 6.d and 6.e but it different for Case 6.b. The maximum line loading for the Case 6.b is observed during the morning peak hours (i.e. 08:00 hours to 09:00) and evening peak hours (20:00 hours to 21:00 hours) and it is 18%. In the Case 6.d and 6.e, the maximum line loading is shifted to the peak sunshine hours (i.e.13:00 hours) and its value for Cases 6.d and 6.e are 16% and 17% respectively. The average line loading for the Cases 6.d and 6.e are reduced from 11% (Case 6.b) to 7% and 8% respectively.

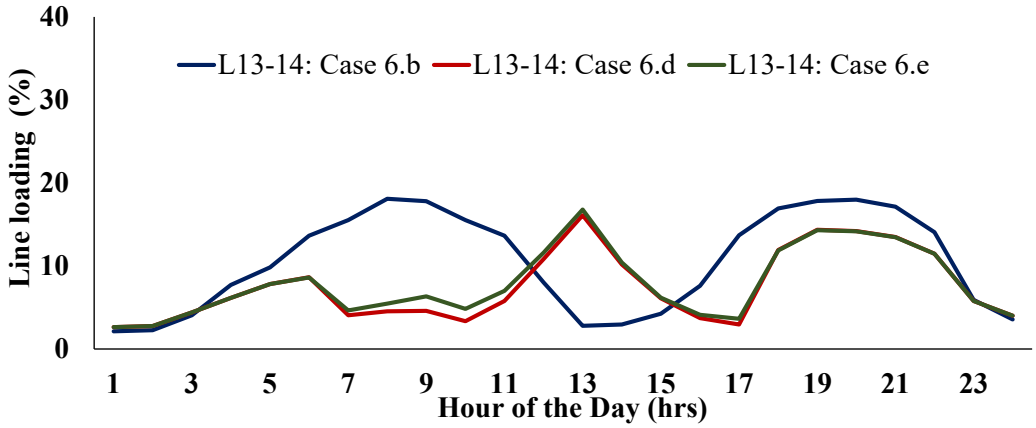

Fig. 6.34 Line Loading of $L_{13\text{-}14}$ for Cases 6.b, 6.d and 6.e

The loading of transformer T_1 for the Cases 6.b, 6.d and 6.e, are in the Fig. 6.35. By connected both feeders together through switch S_1, transformer loading T_1 is also changed for the Case 6.d and Case 6.e as compare to the Case 6.b. The maximum transformer loading of T_1, during morning peak hours (i.e. 08:00 hours to 09:00 hours) increased from 15% (Case 6.b) to 20% and 20% for Cases 6.d and Case 6.e respectively. However, maximum transformer loading of T_1 of Case 6.b, during the night peak hours (20:00 hours to 21:00 hours) only decreased by 1% for Cases 6.d and Case 6.e. The transformer loading T_1, during the peak sunshine hours (i.e. 13:00 hours) is decreased from 19% (Case 6.b) to 11% and 10% for Case 6.d and Case 6.e respectively. The average daily energy loading of transformer T_1 for the Cases 6.b, 6.d and 6.e is same and it is 14 %.

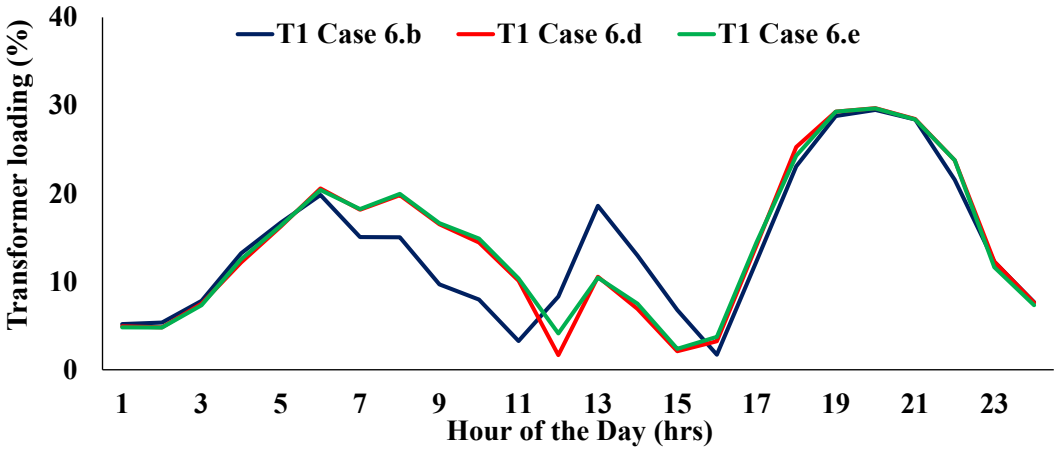

Fig. 6.35 Loading of Transformer T_1 for Cases 6.b, 6.d and 6.e

The loading of transformer T_2 for the Cases 6.b, 6.d and 6.e, are shown in the Fig. 6.36. The maximum transformer loading of T_2 of Case 6.b, during the morning peak hours (i.e. 08:00 hours to 09:00 hours) is decreased from 34% to 27% for Cases 6.d and 6.e however maximum transformer loading of T_2 of Case 6.b, during the night peak hours (19:00 hours to 21:00 hours), decreased by only 1% for Cases 6.d and 6.e. The transformer loading T_2, during the peak sunshine hours (i.e. 13:00 hours) is decreased from 6% (Case 6.b) to 2% and 4% for Case 6.d and Case 6.e respectively. The average transformer loading of T_2 for the Cases 6.b is 20% and for the Cases 6.d and 6.e, is 17% for each. It indicates, by connecting feeder through Switch S_1, transformer loading T_2 reduced by 3%.

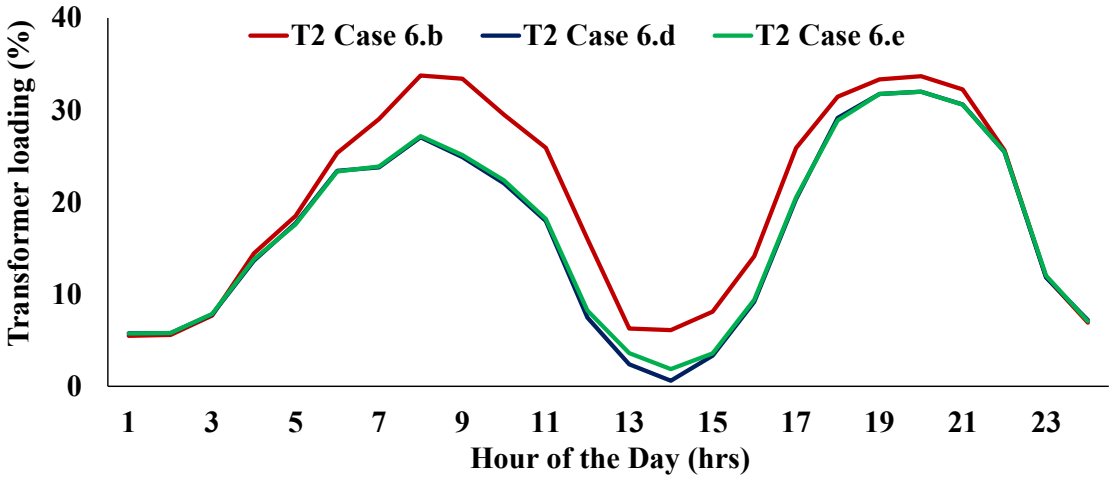

Fig. 6.36 Loading of Transformer T2 for Cases 6.b, 6.d and 6.e

6.8 Conclusions

In this chapter, PV hosting capacity within a distribution network has been estimated considering network operational parameters (i.e. voltage, power line loading). The load variations and simultaneous PV outputs at different buses have been considered for a typical selected CIGRE network. The PV hosting capacity has been varied on selected buses of the network to maintain the network operational parameters within the prescribed limits. In case 1 (i.e. HC_1), voltage constraint has been used for a typical daily load and PV profiles to analyze the PV hosting capacity on the selected buses. Also, the case 2 (i.e. HC_2) has considered voltage and power line loading variations to evaluate the impact of PV hosting capacity on the selected buses. It has been observed that by considering voltage and loading as constraints, the PV hosting capacity (i.e. HC_2), at buses B_1, B_2, B_{12}, B_{13} and B_{14} of the selected network has reduced by more than 50% compared to

the case when only voltage has taken as constraint (i.e. HC_1). It has been observed that the network operational constraints have significant impact on the PV hosting capacity within the network.

This work has examined the impacts of PV system integration at selected buses of feeder 1 using the digital real time simulator and power hardware in loop testing method. The results show that the maximum bus voltages (i.e.V_7 to V_{11}) in the feeder 1 has increased by 9% during the peak sunshine hours (i.e. 13:00 hours), when 2 MW of PV has connected to each buses B_7, B_9 and B_{10} and 1 MW of PV at bus B_8. Moreover, the maximum line loading (i.e. $L_{1\text{-}2}$ and $L_{2\text{-}3}$) has increased by 24% as compare to the base case scenario (i.e. Case a, no PV integrated). The integration of PV at feeder 1 also affect loading curve of transformer T_1. It has been observed that the average loading of transformer T_1 has reduced from 17% (i.e. Case 6.a, no PV integrated) to 14% (i.e. Case 6.b, with PV integration) however, loading of transformer T_2 has not changed as no PV connected to the feeder 2.

The voltage rise problem due to integration of PV has addressed by using the Q-V droop control strategy into the PV inverter. It has been observed that by using the QV droop control strategy (i.e. Case 6.c) into the PV inverter the maximum bus voltages (i.e. V_7 to V_{11}) in the feeder 1 has reduced to 1.05 p.u. from 1.09 p.u. (Case 6.b, without QV droop control); however, no significant changes have observed in the line loading and as well transformer loadings. In this work, operational performance of the mesh type network has compared with the with the radial network specially during high PV penetration scenario. It has been observed that the cumulative effect of mesh type network along with QV droop control strategy can further improve the voltage profile during high PV penetration scenario.

The presented results are going to be useful for electricity distribution companies, industries, and policy makers for analyzing impacts of high PV penetration into the distribution network for future grid operation or grid reinforcement planning. This work is going to contribute on analyzing operational risk scenarios with high PV penetration and to implement mitigation technique (e.g. QV droop functionality) with further investigation on power quality.

Chapter 7

7. Conclusions

The operational performance of the grid connected micro-grid system is influenced by many factors e.g. techno-economic sizing, appropriate energy management strategy, geographical locations, grid constrains and electricity energy pricing dynamics. To make renewable energy based micro-grid system more reliable, efficient, and economically viable, it is imperative to consider a holistic approach and look into all these factors for design and operation of the micro-grid system. The identified challenges in the state-of-art section and the key research objectives have been addressed appropriately in the thesis. The obtained results are concluded as:

- The techno-economic sizing of renewable energy based distributed generators for operating as a micro-grid is necessary. It is important to analyze techno-economic performance for a grid connected renewable energy (e.g. PV) based micro-grid reliability. In this work, a typical case of Indian institutional energy system (i.e. Sections 2.3 & 2.4), is considered for analyzing techno-economic sizing of PV based micro-grid components. It has been observed that the operation of techno-economic sized PV based micro-grid can reduce the local energy cost by 48% and the grid supply reduction by 45%.
- Appropriate energy management strategies for operation of renewable energy based micro-grid can improve the techno-economic performance of micro-grid system even during the non-expected grid outage conditions. In this work, PV based energy system is integrated with techno-economic sizing of distributed generator(s) and battery energy storage for operating micro-grid during the grid outage period. In the considered typical case (i.e. Section 2.4), the integration of PV and battery energy storage with distributed generator in the institutional energy system can reduce the distributed generator energy contribution from 12.7% to only 1% of the institutional energy demand. In this work, typical energy management operational scenario(s) (i.e. Sections 2.3 and 2.4), with minimization of energy cost, have been evaluated, and it has been found that the annual electricity bill can be reduced by 45% with renewable energy fraction of 49% considering typical daily grid outage period.

- The techno-economic performance of micro-grid can be significantly controlled through the appropriate energy management strategy for maximizing the use of local energy resources through battery energy throughput. In the considered typical case (i.e. Section 3.2), an energy management strategy (Section 3.3) has presented and it has contributed in increase of annual battery energy throughput by 9.5% for maximizing use of local energy resources, and reduction in the local energy generation cost by 8%.
- The electricity energy pricing dynamics has significant influence on economic performance of the grid-connected micro-grid system. In the considered typical case(s) (i.e. Sections 3.4. and 3.5); if the grid tariff is doubled and grid selling tariff is at normal value; then the local energy generation cost can be increased by 71.6%. And; if the grid selling tariff is doubled, but grid tariff is at normal value; then the local micro-grid energy generation cost can be reduced by 8%.
- Geographical locations and local grid conditions have significant influence on techno-economic performance of renewable energy (e.g. PV) based micro-grid. In this study, two typical geographical locations, from tropical and Nordic climates, are compared (i.e. Sections 4.7) for PV based micro-grid system operation with local electrical energy tariff changes. The annual specific energy output from PV system has been 36% more at selected Indian location compare to the Norwegian location.
- The regional energy pricing market has considerable impact on energy economic performance of PV based micro-grid. The considered typical cases of two geographical regions (Section 5.6) are evaluated for some grid tariff scenarios, and it has observed that if the grid tariff is doubled, but the grid selling tariff is at normal value, then the micro-grid energy generation cost can be increased by 71.6% and 14% for Indian and Norwegian cases respectively.
- The distributed power network analysis is studied for finding the maximum penetration of PV based micro-grid (i.e. hosting capacity study). PV hosting capacity within the distribution network is affected by the technical constraints (e.g. voltage or/and loading of the power lines, etc.). In this study, a typical CIGRE network has used for PV hosting capacity analysis and typical case(s) of only voltage constraint and voltage-loading constraint

conditions are compared. The PV hosting capacity of buses B_1, B_2, B_{12}, B_{13} and B_{14} (i.e. Section 6.4.2) are reduced by 60%, 57%, 59%, 76% and 46% respectively, with voltage-loading constraint conditions compared to only voltage constraint. It is concluded that voltage-loading constrains should be used, while estimating the hosting capacity of PV based micro-grid within the distribution network.

- The increasing penetration of PV based micro-grid system can influence the voltage quality within the distribution network, and the voltage variations are related to the incident solar radiation. In the considered scenario (i.e. Section 6.5), the voltage variation (i.e. V_7 to V_{11}) in the Feeder 1 has increased up to 9%, and the maximum line loading (i.e. $L_{1\text{-}2}$ and $L_{2\text{-}3}$) increased up to 24%, compare to the base scenario (i.e. Section 6.3).
- Use of reactive power vs. voltage (Q-V) droop control technique in the PV inverter can be quite effective for improving the voltage profile within the distributed network. In the considered scenario (i.e. Section 6.6), Q-V droop control technique has incorporated in the PV inverters using power hardware-in-loop method of the real-time digital simulator (RTDS). The maximum voltage changes have been observed on some of the buses (i.e. V_7 to V_{11}). The bus voltages have been reduced from 1.09 p.u. to 1.04 p.u. after implementing the Q-V droop control technique in the PV inverters.

The presented results conclude that appropriate techno-economic sizing of the grid connected renewable energy-based micro-grid system is required to improve the technical and economic performance. The role of energy management strategy becomes very important to enhance the local energy participation through battery energy throughput for making the micro-grid system more reliable and efficient, even during the grid outage conditions. The geographical locations and regional electrical energy pricings have significant influence on techno-economic functioning of renewable energy based micro-grid system. Moreover, to enhance the penetration of PV based micro-grid within the distributed network, a holistic approach should be considered for estimating the PV hosting capacity of the network to ensure the safe and reliable operation of the distributed network. Also, the reactive power vs. voltage (Q-V) droop control technique is quite effective for improving the voltage profile within the distributed network.

7.1 Future Scope of Work

Based on presented results, the following topics have identified as future scope of work

- Grid integration of photovoltaic based micro-grid can contribute further in improving the distributed network dynamics for stability and control in addition to facilitating demand side management.
- Integration of PV with hybrid energy storage can be further investigated through innovative control strategies for operating as an active generator within the micro-grid. The load management strategies can be used for managing the micro-grid local power demand considering the main grid constraints.
- The economic incentive of PV based micro-grid investments should be further investigated under various market dynamics through sensitivity analysis. Such studies will be beneficial for identifying the appropriate energy policy measures, energy tariff structure for buying and selling of electricity to the main grid for promoting PV based micro-grid solutions.
- The renewable energy based micro-grid system is going to be operated as Cyber-Physical System. The IoT based control and operation techniques need to be further studied on analyzing as well as mitigating the impacts of potential cyber-attacks for safe and reliable operation of micro-grid.
- Further investigation is required for developing business models for promotion and operation (built-operate-lease-transfer) of renewable energy based micro-grids and improving local supply and balancing energy portfolio.

Appendix I

I.1.1 Energy generation cost of PV system

In this section energy generation cost of PV, battery and DG have been calculated based on the methodology given in the ref [2.25-2.26]. The energy management strategy explained in the chapter 2, 3, 4 and 5 indicates that energy system load demand is met by energy source(s), having minimum energy generation cost. In this work, cost annuity method has been used to convert all the net cash-flow (NCF) with an investment project into a series of annual payment of equal amounts. While calculating the energy generation cost for PV, it has been assumed that PV modules and inverter are the part of PV system and battery is an independent energy source. Energy generated from the PV system has used to charge the battery, fulfil the load demand and, also feed into the grid (if $P_{PV} > P_{Load}$). The energy generation cost from the PV system is given by Eq. (A.1).

$$E_{\mathrm{pv}} = \frac{\mathrm{C}_{NCF,PV} * CRF}{\sum_{m=1}^{12} \mathrm{N}_d * \mathrm{L}_m} \qquad \text{Eq. (A. 1)}$$

where N_d is the number of days per month, L_m is monthly energy supplied by the PV system and CRF is the capital recovery factor. The CRF is given by Eq. (A.2).

$$CRF = \left(\frac{d}{1-(1+d)^{-N}}\right) \qquad \text{Eq. (A. 2)}$$

The net cash flow ($C_{NCF, PV}$) of a solar PV system consist of the total capital investment ($C_{PV, SYS}$), the present value of operation and maintenance cost (OM_{PV}) and the present value of system replacement cost (R_{PV}). The Eq. (A.3), describes the net cash flow ($C_{NCF, PV}$) and its associated components.

$$\mathrm{C}_{NCF,PV} = \mathrm{C}_{PV,\ SYS} + \mathrm{OM}_{PV} + R_{INV} \qquad \text{Eq. (A. 3)}$$

The total capital investment ($C_{PV, SYS}$) is the sum of the investments of each component of the PV system i.e. PV array cost (C_{PV}), inverter cost (C_{INV}) and installation & commissioning cost ($C_{I\&C}$) and given in the Eq. (A.4).

$$C_{PV,\ SYS} = C_{PV} + C_{INV} + C_{I\&C} \qquad \text{Eq. (A. 4)}$$

I.1.2 Operation and maintenance costs of PV system

Operation and maintenance costs (OM_{PV}) includes taxes, insurance, maintenance, recurring costs, etc. It is generally specified as a percentage (say m) of the initial capital cost. All operating costs are escalated at a rate e_0 and discounted at rate d. The life-cycle maintenance cost for a lifetime of N years is given by Eq. (A.5):

$$OM_{PV} = OM_0 \left(\frac{1+e_0}{d-e_0}\right) * \left[1 - \left(\frac{1+e_0}{d-e_0}\right)^N\right] \quad if\ d \neq e_0 \qquad \text{Eq. (A. 5)}$$

$$OM_{PV} = OM_0 * N \quad if\ d = e_0 \qquad \text{Eq. (A. 6)}$$

Where, $OM_0 = m(C_{PV, SYS})$

I.1.3 Replacement cost of PV system components

The inverter replacement cost (R_{INV}) is mainly a function of the number of inverter replacements (v) over the system lifetime, without taking the salvage value of replaced inverter. It is given by Eq. (A.7).

$$R_{INV} = \sum_{j=1}^{v} C_{INV} * \left(\frac{1+e_0}{1+d}\right)^{\frac{Nj}{v+1}} \qquad \text{Eq. (A. 7)}$$

In the Eq. (A.7), v is the total number of replacements for inverter over a life period of N years (i.e. 25 year). In case of inverter, replacement period is considered 15 years and efficiency is 95%.

I.2.1 Energy generation cost of diesel system

The net cash flow ($C_{NCF, DG}$) of a diesel engine consists of the total capital investment ($C_{Cost, DG}$), the present value of fuel cost ($C_{Total, Fuel}$), the present value of operation and maintenance cost (OM_{DG}) and the present value of system replacement cost (R_{DG}). The Energy generation cost of diesel system is given by Eq. (A.8).

$$E_{DG} = \frac{C_{NCF,DG} * CRF}{\sum_{m=1}^{12} N_d * L_{DG}} \qquad \text{Eq. (A. 8)}$$

where N_d is the number of days per month, L_{DG} is monthly energy supplied by the DG system and capital recovery factor (CRF) is given by

$$CRF = \left(\frac{d}{1-(1+d)^{-N}}\right)$$

Eq A.9, describes the net cash flow of DG ($C_{NCF,\ DG}$) and its associated components.

$$C_{NCF,DG} = C_{Cost,DG} + Fuel_{Total,\ Fuel} + OM_{DG} + R_{DG} \qquad \text{Eq. (A. 9)}$$

The rated power capacity vs. fuel consumption curve of a DG set at different load factor is shown in the Fig.A.1 [2.25]

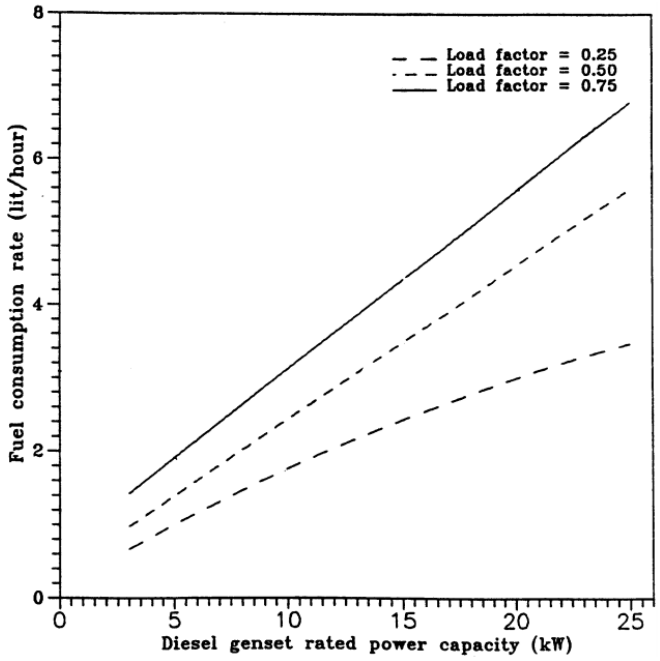

Fig. A.1 Rated Power vs. Fuel Consumption Curve of a Diesel Generator

I.2.2 Operation and maintenance costs of DG

In case of diesel engine two main recurring cost components are fuel cost and maintenance cost. The mathematical expression for these costs has been given in Eq. (A.10) and (A.11).

$$Fuel_{Total,Fuel} = C_{Annual,Fuel} * \left(\frac{1+E}{d-FE}\right) * \left[1-\left(\frac{1+FE}{d-\mathrm{FE}}\right)^{N}\right] \ if\ d \neq FE \qquad \text{Eq. (A. 10)}$$

$$\mathrm{OM}_{DG} = \mathrm{OM}_{DG0} * \left(\frac{1+e_0}{d-e_0}\right) * \left[1 - \left(\frac{1+e_0}{1+d}\right)^N\right] \quad if\ d \neq e_0 \qquad \text{Eq. (A. 11)}$$

$$\mathrm{OM}_{DG} = \mathrm{OM}_{DG0} * N \qquad if\ d = e_0 \qquad \text{Eq. (A. 12)}$$

Where OM_{DG0} represents the annual maintenance cost and it is the annual non-fuel expenditure and e0 represents general escalation and FE represents fuel escalation.

$$\mathrm{OM}_{\mathrm{DG0}} = \mathrm{m}(\mathrm{C}_{\mathrm{Cost,\ DG}})$$

I.2.3 Replacement costs of DG

In case of DG, the replacement cost is presented by the component engines/generator and it is given by Eq. (A.13)

$$R_{DG} = C_{Cost,\ DG} \sum_{j=1}^{w} \left(\frac{1+e_0}{1+d}\right)^{\frac{Nj}{w+1}} \qquad \text{Eq. (A. 13)}$$

In the Eq. (A.13), w is the total number of replacements over a life period of K years.

I.3.1 Energy generation cost of battery storage

In this work, battery storage has assumed as an independent energy source to meet the load demand during grid outage conditions. The battery energy storage system has mainly two components e.g. battery bank and power conditioning device (PDC e.g. charge controller and inverter). Similar to DG, the net cash flow ($C_{NCF, Bat}$) of a battery energy storage system consists of the total capital investment ($C_{Cost, Bat}$), the present value of input energy cost ($C_{Total, Energy}$), the present value of operation and maintenance cost ($OM_{Batt\ Sys}$) and the present value of system replacement cost (R_{Batt} and R_{PDC}).

$$\mathrm{C}_{NCF,Batt} = \mathrm{C}_{Cost,\ SYS} + R_{Bat,Sys} + \mathrm{OM}_{Bat,SYS} + \mathrm{C}_{Total,SYS} \qquad \text{Eq. (A. 14)}$$

The total capital investment of battery storage system ($C_{Cost, SYS}$) is the sum of the investments of battery bank cost (C_{Bat}), PDC cost (C_{PDC}) and installation & commissioning cost of battery ($C_{Bat, I\&C}$) and given by Eq. (A.15).

$$C_{Cost,\ SYS} = C_{Bat} + C_{PCD} + C_{Bat,\ I\&C} \qquad \text{Eq. (A. 15)}$$

As described in the previous section that the battery is mainly charged by the PV module therefore energy generation cost of PV is considered the input energy cost for battery energy storage and it is given by Eq. (A.16).

$$E_{Bat} = \frac{C_{NCF,bat} * CRF}{\sum_{m=1}^{12} N_d * L_{Bat}} \qquad \text{Eq. (A. 16)}$$

where N_d is the number of days per month, L_{Bat} is monthly energy supplied by the battery energy storage system and CRF is given by Eq. (A.17).

$$CRF = \left(\frac{d}{1-(1+d)^{-N}}\right) \qquad \text{Eq. (A. 17)}$$

I.3.2 Operation and maintenance costs of battery storage system

Operation and maintenance costs ($OM_{Bat, SYS}$) includes taxes, insurance, maintenance, recurring costs, etc. It is generally specified as a percentage (say m) of the initial capital cost. All operating costs are escalated at a rate e_0 and discounted at rate d. The life-cycle maintenance for a lifetime of N years is given by Eq. (A.18) and (A.19).

$$OM_{Bat,SYS} = OM_0 \left(\frac{1+e_0}{d-e_0}\right) * \left[1 - \left(\frac{1+e_0}{d-e_0}\right)^N\right] \quad if\ d \neq e_0 \qquad \text{Eq. (A. 18)}$$

$$OM_{Bat,\ SYS} = OM_0 * N \quad if\ d = e_0 \qquad \text{Eq. (A. 19)}$$

Where, $OM_0 = m(C_{Bat, SYS})$

I.3.3 Replacement costs of battery system components

The replacement cost of the battery energy storage system ($R_{Bat, SYS}$) is mainly a function of the number of battery and power conditioning devices replacements over the system lifetime, without taking the salvage value of replaced batteries. It is given by Eq. (A.20), (A.21) and (A.22).

$$\mathrm{R}_{Bat,\ SYS} = \mathrm{R}_{Bat} + R_{PCD} \qquad \text{Eq. A. (20)}$$

$$R_{Bat} = C_{Bat} \sum_{j=1}^{x} \left(\frac{1+e_0}{1+d}\right)^{\frac{Nj}{x+1}} \qquad \text{Eq. (A. 21)}$$

$$R_{PCD} = C_{PCD} \sum_{j=1}^{y} \left(\frac{1+e_0}{1+d}\right)^{\frac{Nj}{y+1}} \qquad \text{Eq. (A. 22)}$$

In the Eq. (A.21) & (A.22), x and y are the total number of replacements for battery and power conditioning device respectively over a life period of N years (i.e. 25 year). In case of battery, number of replacement (i.e. x) depends on the depth of discharge, battery lifetime throughput, charging discharging rate etc. In this work, battery energy throughput is used to calculate battery lifetime by considering fixed amount of energy cycles through the storage, regardless of the depth of the individual charge-discharge cycles.

References of Chapter 1

[1.1] A.N. Azmi, ‘Grid Interaction Performance Evaluation of BIPV and Analysis with Energy Storage on Distributed Network Power Management’, Ph.D. Thesis, Supervised by M. Kolhe, University of Agder, Norway, ISBN: 978-82-7117-848-2, March 2017.

[1.2] A. Sharma, M. Kolhe, U. Nils, A. Mudgal, K. Muddineni and S. Garud, "Comparative Analysis of Different Types of Micro-grid Architectures and Controls," International Conference on Advances in Computing, Communication Control and Networking (ICACCCN), IEEE, pp. 1200-1208, 2018. doi: 10.1109/ICACCCN.2018.8748491.

[1.3] A. Sharma, M. Kolhe, K. M. S. Y. Konara, K. Muddineni, A. Mudgal, S. Garud and N. Ulltveit-Moe, “Operational Analysis of Institutional Energy System for Developing a Micro-grid”, 5th International Symposium on Hydrogen Energy, Renewable Energy and Materials, IOP Conference series- Materials Science and Engineering, vol. 605, paper no. 012008, pp. 1-8, 2019. doi:10.1088/1757-899X/605/1/012008.

[1.4] S. Twaha, M. A.M. Ramli, “A Review of Optimization Approaches for Hybrid Distributed Energy Generation Systems: Off-Grid and Grid-Connected Systems”, Sustainable Cities and Society, vol. 41, pp. 320-331, 2018. doi: 10.1016/j.scs.2018.05.027.

[1.5] A. Sharma, M. Kolhe, U. Nils, K. Muddineni, A. Mudgal and S. Garud, "Voltage Rise Issues and Mitigation Techniques Due to High PV Penetration into the Distribution Network," International Conference on Automation and Computational Engineering (ICACE), IEEE, pp. 72-78, 2018. doi: 10.1109/ICACE.2018.8687041.

[1.6] A. N. Azmi, I. N. Dahlberg, M. L. Kolhe, A. G. Imenes, "Impact of Increasing Penetration of Photovoltaic (PV) Systems on Distribution Feeders,” International Conference on Smart Grid and Clean Energy Technologies (ICSGCE), IEEE, pp. 70-74, 2015. doi: 10.1109/ICSGCE.2015.7454271.

[1.7] M. Lee, D. Soto, and V. Modi, "Cost Versus Reliability Sizing Strategy for Isolated Photovoltaic Micro-Grids in the Developing World," Renewable Energy, vol. 69, pp. 16-24, 2014. doi: 10.1016/j.renene.2014.03.019.

[1.8] M. Kolhe, K.M.I.U. Ranaweera, and A. G. B. S. Gunawardana, "Techno-Economic Sizing of Off-Grid Hybrid Renewable Energy System For Rural Electrification in Sri Lanka," Sustainable Energy Technologies and Assessments, vol. 11, pp. 53-64, 2015. doi: 10.1016/j.seta.2015.03.008

[1.9] L. He, S. Zhang, Y. Chen, L. Ren, J. Li, “Techno-Economic Potential of a Renewable Energy-Based Microgrid System For a Sustainable Large-Scale Residential Community in Beijing, China,” Renewable and Sustainable Energy Reviews, vol. 93, pp. 631-641, 2018. doi: 10.1016/j.rser.2018.05.053

[1.10] A. Rouhani, H. Kord, M. Mehrabi, “A Comprehensive Method for Optimum Sizing of Hybrid Energy Systems Using Intelligence Evolutionary Algorithms” Indian Journal of Science and Technology, vol. 6, pp. 4702-4712, 2013. doi: 10.1016/j.enconman.2010.09.028

[1.11] I. B. Askari, L. B. Askari, M.M. Kaykhah, H. B. Askari, “Optimization and Techno-Economic Feasibility Analysis of Hybrid (Photovoltaic/Wind/Fuel Cell) Energy Systems in Kerman, Iran; Considering The Effects of Electrical Load and Energy Storage Technology” International Journal of Sustainable Energy, vol. 33, no.3, pp. 635-649, doi: 10.1080/14786451.2013.769991.

[1.12] S. Aissou, D. Rekioua, N. Mezzai, T. Rekioua, S. Bacha, “Modeling and Control of Hybrid Photovoltaic Wind Power System with Battery Storage”, Energy Conversion and Management, vol. 89, pp. 615-625, 2015. doi: 10.1016/j.enconman.2014.10.034.

[1.13] L. Ling, Y. Hongyong, and C. Xia, "Model Differences Between IEC 61970/61968 and IEC 61850," Third International Conference on Intelligent System Design and Engineering Applications, IEEE, pp. 938-941, 2013. doi: 10.1109/ISDEA.2012.224.

[1.14] I. Ranaweera and O.-M. Midtgård, "Optimization of Operational Cost for a Grid-Supporting PV System with Battery Storage," Renewable Energy, vol. 88, pp. 262-272, 2016. doi: 10.1016/j.renene.2015.11.044.

[1.15] M. Kolhe, et al, “Algorithms for Demand Response and Load Control”, D5.1, EU FP7 Scalable Energy Management Infrastructure for Aggregation of Households, project no. 619560, STREP-FP7-ICT-2013-11, 2015.

[1.16] S.H.C. Cherukuri, B. Saravanan, “A Novel Energy Management Algorithm for Reduction of Main Grid Dependence in Future Smart Grids Using Electric Springs,” Sustainable Energy Technologies and Assessments, vol. 21, pp. 1-12, 2017. doi: 10.1016/j.seta.2017.03.001.

[1.17] M.N. Ambia, A. Al-Durra, C. Caruana, S. M. Muyeen, “Power Management of Hybrid Micro-Grid System by a Generic Centralized Supervisory Control Scheme,” Sustainable Energy Technologies and Assessments, vol. 8, pp. 57-65, 2014. doi: 10.1016/j.seta.2014.07.003.

[1.18] S. Wang, Z. Li, L. Wu, M. Shahidehpour and Z. Li, "New Metrics for Assessing the Reliability and Economics of Microgrids in Distribution System," IEEE Transactions on Power Systems, vol. 28, no. 3, pp. 2852-2861, 2013. doi: 10.1109/TPWRS.2013.2249539.

[1.19] H. Anand, R. Ramasubbu, "A Real Time Pricing Strategy for Remote Micro-Grid with Economic Emission Dispatch and Stochastic Renewable Energy Sources", Renewable Energy, vol. 127, pp. 779-789, 2018. doi: 10.1016/j.renene.2018.05.016.

[1.20] H. Chen, H. Leng, H. Tang, J. Zhu, H. Gong, and H. Zhong, "Research on Model Management Method for Micro-Grid," IEEE 2nd Information Technology, Networking, Electronic and Automation Control Conference (ITNEC), pp. 163-166, 2017. doi:10.1109/ITNEC.2017.8284930.

[1.21] Z. Abdmouleh, A. Gastli, L. Ben-Brahim, M. Haouari, N. A. Al-Emadi, "Review of Optimization Techniques Applied for the Integration of Distributed Generation From Renewable Energy Sources," Renewable Energy, vol. 113, pp. 266-280, 2017. doi: 10.1016/j.renene.2017.05.087.

[1.22] H.R. Baghaee, M. Mirsalim, G.B. Gharehpetian, H.A. Talebi, "Reliability/Cost-Based Multi-Objective Pareto Optimal Design of Stand-Alone Wind/PV/FC Generation Microgrid System, Energy, vol. 115, no. 1, pp. 1022-1041, 2016. doi: 10.1016/j.energy.2016.09.007.

[1.23] Partnership to Advance Clean Energy - Deployment (PACE-D), 2014. A report on Smart Grids: An Approach to Dynamic Pricing in India. https://www.climatelinks.org/resources/smart-grids-approach-dynamic-pricing-india (Accessed in March 2020).

[1.24] The International Renewable Energy Agency (IRENA), 2019. A report on Time-of-Use Tariffs, Innovation Landscape Brief. https://www.irena.org/ (Accessed in March 2020).

[1.25] S. Nadel, "Demand Response Programs for Reducing Utilities Peak Demand," American Council for an Energy Efficient Economy (ACEEE). https://www.aceee.org/ (Accessed in March 2020).

[1.26] P. Sharma, M. Kolhe, A. Sharma, "Economic Performance Assessment of Building Integrated Photovoltaic System with Battery Energy Storage Under Grid Constraints," Renewable Energy, vol. 145, pp.1901-1909, 2020. doi: 10.1016/j.renene.2019.07.099.

[1.27] J. C. Oviedo, J. E. Solano, C. Duarte, D. L. St-Pierre and L. Boulon, "Day Ahead Tariff Setting for Islanded Microgrids Considering Customers Response," IEEE

Conference Utility Exhibition on Green Energy for Sustainable Development (ICUE), pp. 1-7, 2018. doi: 10.23919/ICUE-GESD.2018.8635716.

[1.28] S. L. Blond, R. Li, F. Li and Z. Wang, "Cost And Emission Savings from the Deployment of Variable Electricity Tariffs And Advanced Domestic Energy Hub Storage Management," IEEE PES General Meeting Conference & Exposition, pp. 1-5, 2014. doi: 10.1109/PESGM.2014.6939329.

[1.29] A. Sharma, F. Zhao, J. W. Sutherland, "Econological Scheduling of Manufacturing Enterprise Operating Under a Time-of-Use Electricity Tariff," Journal of Cleaner Production, vol. 108, part A, pp. 256-270, 2015. doi: 10.1016/j.jclepro.2015.06.002.

[1.30] L. Li, Y. Yao, R. Yang, K. Zhou, "Is It More Effective to Bring Time-of-Use Pricing into Increasing Block Tariffs? Evidence from Evaluation of Residential Electricity Price Policy in Anhui Province," Journal of Cleaner Production, vol. 181, pp. 703-716, 2018. doi: 10.1016/j.jclepro.2018.01.209.

[1.31] Y. Yang, M. Wang, Y. Liu, L. Zhang, "Peak-off-Peak Load Shifting: Are Public Willing To Accept the Peak And Off-Peak Time-of-Use Electricity Price?," Journal of Cleaner Production, vol. 199, pp. 1066-1071, 2018. doi: 10.1016/j.jclepro.2018.06.181.

[1.32] S. Annala, J. Lukkarinen, E. Primmer, S. Honkapuro, K. Ollikka, K. Sunila, T. Ahonen, "Regulation As An Enabler of Demand Response in Electricity Markets and Power Systems," Journal of Cleaner Production, vol. 195, pp. 1139-1148, 2018. doi: 10.1016/j.jclepro.2018.05.276.

[1.33] J. B. Abikarram, K. McConky, R. Proano, "Energy Cost Minimization for Unrelated Parallel Machine Scheduling Under Real Time and Demand Charge Pricing," Journal of Cleaner Production, vol. 208, pp. 232-242, 2019. doi: 10.1016/j.jclepro.2018.10.048.

[1.34] M. S. Dale, "Assessment of the Norwegian Solar PV Market in 2019' Technical Report of Multiconsult, (Accessed on May 2020).

[1.35] T. A. Brekke, 'Nordic Irradiance Conditions and the Effects on Solar Module Efficiency' Master Thesis, Norwegian University of Life Sciences, 2016.

[1.36] M.A.M. Yassin, M. Kolhe, A. Sharma, S. Garud, "Battery Capacity Estimation for Building Integrated Photovoltaic System: Design Study for Different Geographical Location(s)," Energy Procedia, vol. 142, pp. 3433-3439, 2017. doi: 10.1016/j.egypro.2017.12.226.7.

[1.37] F. Verrilli, G. Gambino, S. Srinivasan, G. Palmieri, C. D. Vecchio, L. Glielmo, “Demand Side Management for Heating Controls in Microgrids,” IFAC-Papers On-Line, vol. 49, no. 1, pp. 611-616, 2016. doi: 10.1016/j.ifacol.2016.03.123.

[1.38] B.B. Navarro, M. M. Navarro, "A Comprehensive Solar PV Hosting Capacity in MV and LV Radial Distribution Networks," IEEE PES Innovative Smart Grid Technologies Conference Europe (ISGT-Europe), pp. 1-6, 2017. doi: 10.1109/ISGTEurope.2017.8260210.

[1.39] W.Y. Atmaja, Sarjiya, M. P. Lesnanto and E. Y. Pramono, "Hosting Capacity Improvement Using Reactive Power Control Strategy of Rooftop PV Inverters," IEEE 7th International Conference on Smart Energy Grid Engineering (SEGE), pp. 213-217, 2019. doi: 10.1109/SEGE.2019.8859888.

[1.40] W. Niederhuemer, R. Schwalbe, "Increasing PV Hosting Capacity in LV Grids with a Probabilistic Planning Approach," International Symposium on Smart Electric Distribution Systems and Technologies (EDST), pp. 537-540, 2015. doi: 10.1109/SEDST.2015.7315266.

[1.41] A.Y. Saber, T. Khandelwal and A.K. Srivastava, "Fast Feeder PV Hosting Capacity Using Swarm Based Intelligent Distribution Node Selection," IEEE Power & Energy Society General Meeting (PESGM), pp. 1-5, 2019. doi: 10.1109/PESGM40551.2019.8973389.

[1.42] M. Al-Saffar, S. Zhang, A. Nassif, P. Musilek, "Assessment of Photovoltaic Hosting Capacity of Existing Distribution Circuits," IEEE Canadian Conference of Electrical and Computer Engineering (CCECE), pp. 1-4, 2019. doi: 10.1109/CCECE.2019.8861957.

[1.43] H. Samet, “Evaluation of Digital Metering Methods Used in Protection and Reactive Power Compensation of Micro-Grids,” Renewable and Sustainable Energy Reviews, vol. 62, pp. 260-279, 2016. doi: 10.1016/j.rser.2016.04.032.

[1.44] L.B.G. Campanhol, S.A. O. Silva, A. A. Oliveira, V.D. Bacon, “Single-Stage Three-Phase Grid-Tied PV System With Universal Filtering Capability Applied to DG Systems and AC Microgrids”, IEEE Transactions on Power Electronics, vol. 32, no. 12, pp. 9131 – 9142, 2017. doi: 10.1109/TPEL.2017.2659381.

[1.45] F. Katiraei, B. Mather, A. Momeni, Y. Li, and G. Sanchez, "Field Verification and Data Analysis of High PV Penetration Impacts on Distribution Systems," IEEE 42nd Photovoltaic Specialist Conference (PVSC), pp. 1-5, 2015. doi: 10.1109/PVSC.2015.7356255.

[1.46] SunShot initiative of the U.S. Department of the Energy (DoE). http://www1.eere.energy.gov/solar/sunshot/index.html (Accessed in May 2020).

[1.47] D. Chathurangi, U. Jayatunga, M. Rathnayake, A. Wickramasinghe, A. Agalgaonkar, S. Perera, "Potential Power Quality Impacts on LV Distribution Networks With High Penetration Levels of Solar PV," 18th International Conference on Harmonics and Quality of Power (ICHQP), pp. 1-6, 2018. doi: 10.1109/ICHQP.2018.8378890.

[1.48] P.K.C. Wong, A. Kalam, R. Barr, "Modelling And Analysis of Practical Options to Improve the Hosting Capacity of Low Voltage Networks for Embedded Photovoltaic Generation," IET Renewable Power Generation, vol. 11, no. 5, pp. 625 – 632, 2017. doi: 10.1049/iet-rpg.2016.0770.

[1.49] S. Amelang, "The reform of the Renewable Energy Act: Germany's Energy Transition Revamp Stirs Controversy Over Speed, Participation,". Clean Energy Wire (CLEW), Berlin, Germany, 2016. https://www.cleanenergywire.org (Accessed May 2020).

[1.50] M. Katsanevakis, R.A. Stewart, J. Lu, "Energy Storage System Utilization to Increase Photovoltaic Penetration in Low Voltage Distribution Feeders," Journal of Energy Storage, pp. 1-19, 2017. doi: 10.1016/j.est.2017.07.022.

References of Chapter 2

[2.1] A.N. Azmi, 'Grid Interaction Performance Evaluation of BIPV and Analysis with Energy Storage on Distributed Network Power Management', Ph.D. Thesis, Supervised by M. Kolhe, University of Agder, Norway, ISBN: 978-82-7117-848-2, March 2017.

[2.2] A. Sharma, M. Kolhe, U. Nils, A. Mudgal, K. Muddineni and S. Garud, "Comparative Analysis of Different Types of Micro-grid Architectures and Controls," International Conference on Advances in Computing, Communication Control and Networking (ICACCCN), IEEE, pp. 1200-1208, 2018. doi: 10.1109/ICACCCN.2018.8748491.

[2.3] A. Sharma, M. Kolhe, K. M. S. Y. Konara, K. Muddineni, A. Mudgal, S. Garud and N. Ulltveit-Moe, "Operational Analysis of Institutional Energy System for Developing a Micro-grid", 5th International Symposium on Hydrogen Energy, Renewable Energy and Materials, IOP Conference series- Materials Science and Engineering, vol. 605, paper no. 012008, pp. 1-8, 2019. doi:10.1088/1757-899X/605/1/012008.

[2.4] M. Lee, D. Soto, V. Modi, "Cost Versus Reliability Sizing Strategy for Isolated Photovoltaic Micro-Grids in the Developing World", Renewable Energy, vol. 69, pp. 16-24, 2014. doi: 10.1016/j.renene.2014.03.019.

[2.5] A. Sharma, M. Kolhe, U. Nils, K. Muddineni, A. Mudgal and S. Garud, "Voltage Rise Issues and Mitigation Techniques Due to High PV Penetration into the Distribution Network," International Conference on Automation and Computational Engineering (ICACE), IEEE, pp. 72-78, 2018. doi: 10.1109/ICACE.2018.8687041.

[2.6] A. N. Azmi, I. N. Dahlberg, M. L. Kolhe, A. G. Imenes, "Impact of Increasing Penetration of Photovoltaic (PV) Systems on Distribution Feeders," International Conference on Smart Grid and Clean Energy Technologies (ICSGCE), IEEE, pp. 70-74, 2015. doi: 10.1109/ICSGCE.2015.7454271.

[2.7] M. Kolhe, K. M. I. U. Ranaweera, and A. G. B. S. Gunawardana, "Techno-Economic Sizing of Off-Grid Hybrid Renewable Energy System For Rural Electrification in Sri Lanka," Sustainable Energy Technologies and Assessments, vol. 11, pp. 53-64, 2015. doi: 10.1016/j.seta.2015.03.008.

[2.8] S. Twaha, M.A.M. Ramli, "A review of optimization approaches for hybrid distributed energy generation systems: Off-grid and grid-connected systems," Sustainable Cities and Society, vol. 41, pp. 320-331, 2018. doi: 10.1016/j.scs.2018.05.027.

[2.9] L. Ling, Y. Hongyong, and C. Xi, "Model Differences Between IEC 61970/61968 and IEC 61850," Third International Conference on Intelligent System Design and Engineering Applications, IEEE, pp. 938-941, 2013. doi: 10.1109/ISDEA.2012.224.

[2.10] I. Ranaweera and O.-M. Midtgård, "Optimization of Operational Cost For a Grid-Supporting PV System with Battery Storage," Renewable Energy, vol. 88, pp. 262-272, 2016. doi: 10.1016/j.renene.2015.11.044.

[2.11] S.H.C. Cherukuri, B. Saravanan, "A Novel Energy Management Algorithm for Reduction of Main Grid Dependence in Future Smart Grids Using Electric Springs," Sustainable Energy Technologies and Assessments, vol. 21, pp. 1-12, 2017. doi: 10.1016/j.seta.2017.03.001.

[2.12] M. Kolhe, et al, "Algorithms for Demand Response and Load Control", D5.1, EU FP7 Scalable Energy Management Infrastructure for Aggregation of Households, project no. 619560, STREP-FP7-ICT-2013-11, 2015.

[2.13] M.N. Ambia, A. Al-Durra, C. Caruana, S. M. Muyeen, "Power Management of Hybrid Micro-Grid System by a Generic Centralized Supervisory Control Scheme," Sustainable Energy Technologies and Assessments, vol. 8, pp. 57-65, 2014. doi: 10.1016/j.seta.2014.07.003.

[2.14] S. Wang, Z. Li, L. Wu, M. Shahidehpour and Z. Li, "New Metrics for Assessing the Reliability and Economics of Microgrids in Distribution System," IEEE Transactions on Power Systems, vol. 28, no. 3, pp. 2852-2861, 2013. doi: 10.1109/TPWRS.2013.2249539.

[2.15] H. Anand, R. Ramasubbu, "A Real Time Pricing Strategy for Remote Micro-Grid with Economic Emission Dispatch and Stochastic Renewable Energy Sources", Renewable Energy, vol. 127, pp. 779-789, 2018. doi: 10.1016/j.renene.2018.05.016.

[2.16] H. Chen, H. Leng, H. Tang, J. Zhu, H. Gong, and H. Zhong, "Research on Model Management Method for Micro-Grid," IEEE 2nd Information Technology, Networking, Electronic and Automation Control Conference (ITNEC), pp. 163-166, 2017. doi:10.1109/ITNEC.2017.8284930.

[2.17] T. Häring, A. Rosin, H. Biechl, "Using Common Household Thermal Storages To Support the PV and Battery System in Nearly Zero Energy Buildings in Off-Grid Mode," Sustainable Energy Technologies and Assessments, vol. 35, pp. 12-24, 2019. doi: 10.1016/j.seta.2019.05.014.

[2.18] L.P. Amaral, A. Araújo, E. Mendes, N. Martins, "Economic and Environmental Assessment of Renewable Energy Micro-Systems in a Developing Country," Sustainable

Energy Technologies and Assessments, vol. 7, pp. 101-110, 2014. doi: 10.1016/j.seta.2014.04.002.

[2.19] Z. Abdmouleh, A. Gastli, L. Ben-Brahim, M. Haouari, N. A. Al-Emadi, "Review of Optimization Techniques Applied for the Integration of Distributed Generation From Renewable Energy Sources," Renewable Energy, vol. 113, pp. 266-280, 2017. doi: 10.1016/j.renene.2017.05.087.

[2.20] H.R. Baghaee, M. Mirsalim, G.B. Gharehpetian, H.A. Talebi, "Reliability/Cost-Based Multi-Objective Pareto Optimal Design of Stand-Alone Wind/PV/FC Generation Microgrid System, Energy, vol. 115, no. 1, pp. 1022-1041, 2016. doi: 10.1016/j.energy.2016.09.007.

[2.21] B. Chen, X. Zhang, B. Zhang, L. Wang, W. Li, S.Wang, "Multi-Microgrids System Reliability Assessment Algorithm Considering Energy Dispatch Strategy Among Microgrids," Energy Procedia, vol. 145, pp. 15-19, 2018. doi: 10.1016/j.egypro.2018.04.004.

[2.22] V. Natarajan, S. Amit 'Statistical Analysis of Cost of Energy Due to Electricity Outages in Developing Countries' 4th International Conference on Future Computational Technologies and Applications (IARIA), pp. 1-6, 2012.

[2.23] M. Kolhe, S. Kolhe, J. C. Joshi, "Economic Viability of Stand-Alone Solar Photovoltaic System in Comparison with Diesel-Powered System for India," Energy Economics, vol. 24, no. 2, pp. 155-165, 2002. doi.org/10.1016/S0140-9883(01)00095-0.

[2.24] A. Ali, N. Liu and L. He, "Multi-Party Energy Management and Economics of Integrated Energy Microgrid with PV/T and Combined Heat and Power System," IET Renewable Power Generation, vol. 13, no. 3, pp. 451-461, 2019. doi: 10.1049/iet-rpg.2018.5071.

[2.25] Distribution and Retail Electricity Supply Tariffs of the Dakshin Haryana Bijli Vitran Nigam, Circular Number D-29/2017. www. dhbvn.org.in (Accessed on May 2020).

[2.26] A. Sharma, M. Kolhe, K.M.S.Y. Konara, N. Ulltveit-Moe, K. Muddineni, A. Mudgal, S. Garud, "Performance Assessment of Institutional Photovoltaic Based Energy System for Operating as a Micro-grid, Sustainable Energy Technologies and Assessments (Elsevier), vol.37, pp. 1-13, 2020. doi: 10.1016/j.seta.2019.100563.

[2.27] Ministry of New and Renewable Energy (MNRE), Government of India, 2019. India Solar Radiation Data. https://mnre.gov.in/(Accessed in March 2020).

[2.28] HOMER Pro Ver. 3.13, 2020. Technical User Manual. https://users.homerenergy.com. (Accessed in March 2020).

References of Chapter 3

[3.1] Y. Wang, Y. Huang, Y. Wang, M. Zeng, F. Li, Y. Wang, Y. Zhang, "Energy Management of Smart Micro-Grid with Response Loads and Distributed Generation Considering Demand Response," Journal of Cleaner Production. vol. 197, pp. 1069-1083, 2018. doi: 10.1016/j.jclepro.2018.06.

[3.2] L. M. Halabi, S. Mekhilef, "Flexible Hybrid Renewable Energy System Design for a Typical Remote Village Located in Tropical Climate", Journal of Cleaner Production, vol. 177, pp. 908-924, 2018. doi: 10.1016/j.jclepro.2017.12.248.

[3.3] A. Sharma, M. Kolhe, K. M. S. Y. Konara, , K. Muddineni, A. Mudgal, S. Garud, N. Ulltveit-Moe, "Performance Assessment of Building Integrated Photovoltaic and Battery Energy System: A Case Study of TERI-Retreat Faculty in India,". 4th International Conference on Smart and Sustainable Technologies (SpliTech), IEEE, pp. 1-5, 2019. doi: 10.23919/SpliTech.2019.8783046.

[3.4] A. Sharma, M. Kolhe, K.M.S.Y. Konara, N. Ulltveit-Moe, K. Muddineni, A. Mudgal, S. Garud, "Performance Assessment of Institutional Photovoltaic Based Energy System for Operating as a Micro-grid, Sustainable Energy Technologies and Assessments (Elsevier), vol.37, pp. 1-13, 2020. doi: 10.1016/j.seta.2019.100563.

[3.5] Partnership to Advance Clean Energy - Deployment (PACE-D), 2014. A report on Smart Grids: An Approach to Dynamic Pricing in India. https://www.climatelinks.org (Accessed in March 2020).

[3.6] The International Renewable Energy Agency (IRENA), 2019. A report on Time-of-Use Tariffs, Innovation Landscape Brief. https://www.irena.org/ (Accessed in March 2020).

[3.7] S. Nadel, "Demand Response Programs for Reducing Utilities Peak Demand," American Council for an Energy Efficient Economy. https://www.aceee.org/ (Accessed in March 2020).

[3.8] P. Sharma, M. Kolhe, A. Sharma, "Economic Performance Assessment of Building Integrated Photovoltaic System with Battery Energy Storage Under Grid Constraints," Renewable Energy, vol. 145, pp.1901-1909, 2020. doi: 10.1016/j.renene.2019.07.099.

[3.9] J.C. Oviedo, J. E. Solano, C. Duarte, D. L. St-Pierre and L. Boulon, "Day Ahead Tariff Setting for Islanded Microgrids Considering Customers Response," IEEE Conference Utility Exhibition on Green Energy for Sustainable Development (ICUE), pp. 1-7, 2018. doi: 10.23919/ICUE-GESD.2018.8635716.

[3.10] S.L. Blond, R. Li, F. Li and Z. Wang, "Cost And Emission Savings from the Deployment of Variable Electricity Tariffs And Advanced Domestic Energy Hub Storage Management," IEEE PES General Meeting Conference & Exposition, pp. 1-5, 2014. doi: 10.1109/PESGM.2014.6939329.

[3.11] A. Sharma, F. Zhao, J. W. Sutherland, “Econological Scheduling of Manufacturing Enterprise Operating Under a Time-of-Use Electricity Tariff,” Journal of Cleaner Production, vol. 108, part A, pp. 256-270, 2015. doi: 10.1016/j.jclepro.2015.06.002.

[3.12] L. Li, Y. Yao, R. Yang, K. Zhou, “Is It More Effective To Bring Time-of-Use Pricing into Increasing Block Tariffs? Evidence from Evaluation of Residential Electricity Price Policy in Anhui Province,” Journal of Cleaner Production, vol. 181, pp. 703-716, 2018. doi: 10.1016/j.jclepro.2018.01.209.

[3.13] Y. Yang, M. Wang, Y. Liu, L. Zhang, “Peak-off-Peak Load Shifting: Are Public Willing To Accept the Peak And Off-Peak Time-of-Use Electricity Price?,” Journal of Cleaner Production, vol. 199, pp. 1066-1071, 2018. doi: 10.1016/j.jclepro.2018.06.181.

[3.14] S. Annala, J. Lukkarinen, E. Primmer, S. Honkapuro, K. Ollikka, K. Sunila, T. Ahonen, “Regulation As An Enabler of Demand Response in Electricity Markets and Power Systems,” Journal of Cleaner Production, vol. 195, pp. 1139-1148, 2018. doi: 10.1016/j.jclepro.2018.05.276.

[3.15] J.B. Abikarram, K. McConky, R. Proano, “Energy Cost Minimization for Unrelated Parallel Machine Scheduling Under Real Time And Demand Charge Pricing,” Journal of Cleaner Production, vol. 208, pp. 232-242, 2019. doi: 10.1016/j.jclepro.2018.10.048.

[3.16] Dakshin Haryana Bijli Vitran Nigam (DHBVN), 2019. Retail Supply Tariff from DHBVN Haryana ‘Circular Number D-32/2019’, 2019. http://dhbvn.org.in/(Accessed in March 2020).

[3.17] U.R. Prasad, “Article on Analyzing Tariffs Key trends in retail electricity prices Centre Electricity Regulatory Commission (CERC),” 2019. https://powerline.net.in/ (Accessed in March 2020)

References of Chapter 4

[4.1] A. Sharma, M. Kolhe, K.M.S.Y. Konara, K. Muddineni, A. Mudgal, S. Garud and U. Nils, "Performance Assessment of Building Integrated Photovoltaic and Battery Energy System: A Case Study of TERI-Retreat Faculty in India," 4th International Conference on Smart and Sustainable Technologies (SpliTech), IEEE, pp. 1-5, 2019. doi: 10.23919/SpliTech.2019.8783046

[4.2] A. Ghasemi, M. Enayatzare, "Optimal Energy Management of a Renewable-Based Isolated Microgrid with Pumped-Storage Unit and Demand Response," Renewable Energy, vol. 123, pp. 460-474, 2018. doi: 10.1016/j.renene.2018.02.072.

[4.3] T. Weitzel, M. Schneider, C. H. Glock, F. Löber, S. Rinderknecht, "Operating a Storage-Augmented Hybrid Microgrid Considering Battery Aging Costs," Journal of Cleaner Production, vol. 188, pp. 638-654, 2018. doi.org/10.1016/j.jclepro.2018.03.296.

[4.5] A. Sharma, M. Kolhe, U. Nils, A. Mudgal, K. Muddineni and S. Garud, "Comparative Analysis of Different Types of Micro-grid Architectures and Controls," International Conference on Advances in Computing, Communication Control and Networking (ICACCCN), IEEE, pp. 1200-1208. 2018. doi: 10.1109/ICACCCN.2018.8748491.

[4.6] A. Purvins, H. Wilkening, G. Fulli, E. Tzimas, G. Celli, S. Mocci, F. Pilo, S. Tedde, "A European supergrid for renewable energy: local impacts and far-reaching challenges," Journal of Cleaner Production, vol. 19, no. 17, pp. 1909-1916, 2011. doi: 10.1016/j.jclepro.2011.07.003.

[4.7] A. Sharma, M. Kolhe, U. Nils, K. Muddineni, A. Mudgal and S. Garud, "Voltage Rise Issues and Mitigation Techniques Due to High PV Penetration into the Distribution Network," International Conference on Automation and Computational Engineering (ICACE), IEEE, pp. 72-78, 2018. doi: 10.1109/ICACE.2018.8687041.

[4.8] A. Sharma, M. Kolhe, K.M.S.Y. Konara, K. Muddineni, A. Mudgal, S. Garud and U. Nils, 'Operational Analysis of Institutional Energy System for Developing a Micro-grid', IOP Conference Series- Materials Science and Engineering, vol. 605, no. 012008, pages 1-8, 2019, https://doi:10.1088/1757-899X/605/1/012008.

[4.9] A. Sharma, M. Kolhe, "Techno-Economic Evaluation of PV Based Institutional Smart Micro-Grid Under Energy Pricing Dynamics," Journal of Cleaner Production, vol. 264, pp. 1-14, 2020. doi: 10.1016/j.jclepro.2020.121486.

[4.10] M. Kolhe, K. M. I. U. Ranaweera, and A. G. B. S. Gunawardana, "Techno-Economic Sizing of Off-Grid Hybrid Renewable Energy System For Rural Electrification

in Sri Lanka," Sustainable Energy Technologies and Assessments, vol. 11, pp. 53-64, 2015. doi: 10.1016/j.seta.2015.03.008.

[4.11] M. S. Dale, “Assessment of the Norwegian Solar PV Market in 2019’ Technical Report of Multiconsult, (Accessed in May 2020).

[4.12] A.N. Azmi, ‘Grid Interaction Performance Evaluation of BIPV and Analysis with Energy Storage on Distributed Network Power Management’, Ph.D. Thesis, Supervised by M. Kolhe, University of Agder, Norway, ISBN: 978-82-7117-848-2, March 2017.

[4.13] M. Kolhe, et al, “Algorithms for Demand Response and Load Control”, D5.1, EU FP7 Scalable Energy Management Infrastructure for Aggregation of Households, project no. 619560, STREP-FP7-ICT-2013-11, 2015.

[4.14] P. Sharma, M. Kolhe, A. Sharma, “Economic Performance Assessment of Building Integrated Photovoltaic System with Battery Energy Storage Under Grid Constraints,” Renewable Energy, vol. 145, pp.1901-1909, 2020. doi: 10.1016/j.renene.2019.07.099.

[4.15] Hourly Electricity Price in Norway, 2018. https://www.nordpoolgroup.com, (Accessed in August 2020).

[4.16] A. Sharma, M. Kolhe, K.M.S.Y. Konara, N. Ulltveit-Moe, K. Muddineni, A. Mudgal, S. Garud, "Performance assessment of institutional photovoltaic based energy system for operating as a micro-grid, Sustainable Energy Technologies and Assessments (Elsevier), vol. 37, pp. 1-13, 2020. doi: 10.1016/j.seta.2019.100563.

[4.17] National Solar Radiation Data Base, 1961- 1990: Typical Meteorological Year 2 (TMY2)- https://rredc.nrel.gov (Accessed in April 2020)

[4.18] National Solar Radiation Data Base, 1991- 2005 Update: Typical Meteorological Year 3 (TMY3)- https://rredc.nrel.gov (Accessed in April 2020)

[4.19] HOMER Pro Ver. 3.13, 2020, Technical User Manual (2020), https://users.homerenergy.com, (Accessed in August 2020).

References of Chapter 5

[5.1] S. Kumar, T. Kaur, M.K. Arora & S. Upadhyay, 'Resource estimation and sizing optimization of PV/micro hydro-based hybrid energy system in rural area of Western Himalayan Himachal Pradesh in India', Energy Sources, Part A: Recovery, Utilization, and Environmental Effects, vol. 41, no. 22, pp. 2795-2807, doi: 10.1080/15567036.2019.1576075.

[5.2] T. Khatib, A. Mohamed, K. Sopian & M. Mahmoud, 'Optimal Sizing of Hybrid PV/Wind Systems for Malaysia Using Loss of Load Probability', Energy Sources, Part A: Recovery, Utilization, and Environmental Effects, vo. 37, no.7, pp. 687-695, doi: 10.1080/15567036.2011.592920.

[5.3] G. Liu, M.G. Rasul, M.T.O. Amanullah, M.M.K. Khan, "Techno-Economic Simulation and Optimization of Residential Grid-Connected PV System for the Queensland Climate," Renewable Energy, vol. 45, pp. 146-155, 2012. doi: 10.1016/j.renene.2012.02.029.

[5.4] T. Lang, D. Ammann, B. Girod, "Profitability in Absence of Subsidies: A Techno-Economic Analysis of Rooftop Photovoltaic Self-Consumption in Residential and Commercial Buildings," Renewable Energy, vol. 87, no. 1, pp. 77-87, 2016. doi: 10.1016/j.renene.2015.09.059.

[5.5] M.S. Dale, 'Assessment of the Norwegian Solar PV Market in 2019' Technical Report of Multiconsult', (Accessed in November 2020).

[5.6] National Policy "Plusskundeordningen", www.nve.no(Accessed in November 2020).

[5.7] A.N. Azmi, "Grid Interaction Performance Evaluation of BIPV and Analysis with Energy Storage on Distributed Network Power Management," Ph.D. Thesis, Supervised by M. Kolhe, University of Agder, Norway, ISBN: 978-82-7117-848-2, March 2017.

[5.8] P. Sharma, M. Kolhe, A. Sharma, "Economic Performance Assessment of Building Integrated Photovoltaic System with Battery Energy Storage Under Grid Constraints," Renewable Energy, vol. 145, pp.1901-1909, 2020. doi: 10.1016/j.renene.2019.07.099.

[5.9] H. Sæle, B. A. Bremdal, "Economic evaluation of the grid tariff for households with solar power installed," CIRED - Open Access Proceedings Journal, vol. 10, pp. 2707-2710, 2017. doi: 10.1049/oap-cired.2017.0556.

[5.10] A.G. Imenes, H. G. Beyer, K. Boysen, J. O. Odden, R. E. Grundt, 'Performance of Grid-Connected PV System in Southern Norway', IEEE 42nd Photovoltaic Specialist Conference (PVSC), pp. 1-6, 2015. doi: 10.1109/PVSC.2015.7355823.

[5.11] Definitions of the Main Concepts and Variables for Electrical Energy Tariffs in Norway, https://www.ssb.no (Accessed in November 2020).

[5.12] Hourly Electricity Price 2018. https://www.nordpoolgroup.com (Accessed in November 2020).

[5.13] L. Karagiannopoulos, "Article on Norway's Electricity Market," https://www.reuters.com, (Accessed in May 2020).

[5.14] C.S. Good, G. Lobaccaro, S. Hårklau, "Optimization of Solar Energy Potential for Buildings in Urban Areas – A Norwegian Case Study, Energy Procedia", vol. 58, pp. 166-171, 2014. doi: 10.1016/j.egypro.2014.10.424

[5.15] A. Sharma, M. Kolhe, S. Oluf Kristiansen, S. Simonsen, H. Landsverk, S. Marie Oland, "Techno-Economic Case Study of Micro-Grid System at Soccer Club of Skagerak Arena Norway," 5th International Conference on Smart and Sustainable Technologies (SpliTech), IEEE, pp. 1-5, 2020. doi: 10.23919/SpliTech49282.2020.9243789.

[5.16] A. Sharma et al., "Performance Assessment of Building Integrated Photovoltaic and Battery Energy System: A Case Study of TERI-Retreat Facilty in India," 4th International Conference on Smart and Sustainable Technologies, Croatia, pp. 1-5, 2019. doi: 10.23919/SpliTech.2019.8783046.

[5.17] M. Kolhe, K. M. Iromi Udumbara Ranaweera and A. G. B. Sisara Gunawardana, "Techno-economic optimum sizing of hybrid renewable energy system," IECON 2013 - 39th Annual Conference of the IEEE Industrial Electronics Society, pp. 1898-1903, 2013. doi: 10.1109/IECON.2013.6699421.

[5.18] Radiation Data of Solar: "https://rredc.nrel.gov" (Accessed in April 2020)

[5.19] HOMER Pro Ver. 3.13, 2020. Technical User Manual. https://users.homerenergy.com. (Accessed in March 2020). [5.2] C.S. Good, G. Lobaccaro, S. Hårklau, "Optimization of Solar Energy Potential for Buildings in Urban Areas – A Norwegian Case Study, Energy Procedia", vol. 58, pp. 166-171, 2014. doi: 10.1016/j.egypro.2014.10.424

References of Chapter 6

[6.1] Jäger-Waldau, A., “PV Status Report 2019”, EUR 29938 EN, Publications Office of the European Union, ISBN 978-92-76-12608-9, 2019. doi:10.2760/326629, JRC118058.

[6.2] B.B. Navarro, M. M. Navarro, "A Comprehensive Solar PV Hosting Capacity in MV and LV Radial Distribution Networks," IEEE PES Innovative Smart Grid Technologies Conference Europe (ISGT-Europe), pp. 1-6, 2017. doi: 10.1109/ISGTEurope.2017.8260210.

[6.3] W.Y. Atmaja, Sarjiya, M. P. Lesnanto and E. Y. Pramono, "Hosting Capacity Improvement Using Reactive Power Control Strategy of Rooftop PV Inverters," IEEE 7th International Conference on Smart Energy Grid Engineering (SEGE), pp. 213-217, 2019. doi: 10.1109/SEGE.2019.8859888.

[6.4] W. Niederhuemer, R. Schwalbe, "Increasing PV Hosting Capacity in LV Grids with a Probabilistic Planning Approach," International Symposium on Smart Electric Distribution Systems and Technologies (EDST), pp. 537-540, 2015. doi: 10.1109/SEDST.2015.7315266.

[6.5] A.Y. Saber, T. Khandelwal and A. K. Srivastava, "Fast Feeder PV Hosting Capacity Using Swarm Based Intelligent Distribution Node Selection," IEEE Power & Energy Society General Meeting (PESGM), pp. 1-5, 2019. doi: 10.1109/PESGM40551.2019.8973389.

[6.6] M. Al-Saffar, S. Zhang, A. Nassif, P. Musilek, "Assessment of Photovoltaic Hosting Capacity of Existing Distribution Circuits," IEEE Canadian Conference of Electrical and Computer Engineering (CCECE), pp. 1-4, 2019. doi: 10.1109/CCECE.2019.8861957.

[6.7] H. Samet, “Evaluation of Digital Metering Methods Used in Protection and Reactive Power Compensation of Micro-Grids,” Renewable and Sustainable Energy Reviews, vol. 62, pp. 260-279, 2016. doi: 10.1016/j.rser.2016.04.032.

[6.8] L.B.G. Campanhol, S.A. O. Silva, A. A. Oliveira, V.D. Bacon, “Single-Stage Three-Phase Grid-Tied PV System With Universal Filtering Capability Applied to DG Systems and AC Microgrids”, IEEE Transactions on Power Electronics, vol. 32, no. 12, pp. 9131 – 9142, 2017. doi: 10.1109/TPEL.2017.2659381.

[6.9] F. Katiraei, B. Mather, A. Momeni, Y. Li, and G. Sanchez, "Field Verification and Data Analysis of High PV Penetration Impacts on Distribution Systems," IEEE 42nd Photovoltaic Specialist Conference (PVSC), pp. 1-5, 2015. doi: 10.1109/PVSC.2015.7356255.

[6.10] SunShot initiative of the U.S. Department of the Energy (DoE). http://www1.eere.energy.gov/solar/sunshot/index.html (Accessed in October 2020).

[6.11] D. Chathurangi, U. Jayatunga, M. Rathnayake, A. Wickramasinghe, A. Agalgaonkar, S. Perera, "Potential Power Quality Impacts on LV Distribution Networks With High Penetration Levels of Solar PV," 18th International Conference on Harmonics and Quality of Power (ICHQP), pp. 1-6, 2018. doi: 10.1109/ICHQP.2018.8378890.

[6.12] P.K.C. Wong, A. Kalam, R. Barr, "Modelling And Analysis of Practical Options to Improve the Hosting Capacity of Low Voltage Networks for Embedded Photovoltaic Generation," IET Renewable Power Generation, vol. 11, no. 5, pp. 625 – 632, 2017. doi: 10.1049/iet-rpg.2016.0770.

[6.13] M. Maniatopoulos, D. Lagos, P. Kotsampopoulos, N. Hatziargyriou, "Combined control and power hardware in-the-loop simulation for testing smart grid control algorithms," IET Generation, Transmission & Distribution, vol. 11, no. 12, pp. 3009-3018, 2017. doi: 10.1049/iet-gtd.2016.1341.

[6.14] P. Kotsampopoulos, D. Lagos, N. Hatziargyriou, M.O. Faruque, G. Lauss, O. Nzimako, P. Forsyth, M. Steurer, F. Ponci, A. Monti, V. Dinavahi, K. Strunz, "A Benchmark System for Hardware-in-the-Loop Testing of Distributed Energy Resources", IEEE Power and Energy Technology Systems Journal, vol. 5, no. 3, Sept. 2018. doi: 10.1109/JPETS.2018.2861559.

[6.15] S. Amelang, "The reform of the Renewable Energy Act: Germany's Energy Transition Revamp Stirs Controversy Over Speed, Participation,". Clean Energy Wire (CLEW), Berlin, Germany, 2016. https://www.cleanenergywire.org (Accessed in May 2020).

[6.16] M. Katsanevakis, R.A. Stewart, J. Lu, "Energy Storage System Utilization To Increase Photovoltaic Penetration in Low Voltage Distribution Feeders," Journal of Energy Storage, pp. 1-19, 2017. doi: 10.1016/j.est.2017.07.022.

[6.17] M. Kolhe, M.J.M.A. Rasul, "3-Phase grid-connected building integrated photovoltaic system with reactive power control capability", Renewable Energy, Vol. 154, pp. 1065-1075, 2020. DoI: 10.1016/j.renene.2020.03.075.

[6.18] M.J.M.A. Rasul1, M. Kolhe, "Reactive Power Control of a 3-phase Grid-Connected Building Integrated Photovoltaic System", IOP Conference Series: Materials Science and Engineering, Vol. 605, pp. 1-17, 5th International Symposium on Hydrogen Energy, Renewable Energy and Materials, June 2019, DoI: 10.1088/1757-899X/605/1/012012

[6.19] A. Sharma, M. Kolhe, U. Nils, K. Muddineni, A. Mudgal and S. Garud, "Voltage Rise Issues and Mitigation Techniques Due to High PV Penetration into the Distribution Network," IEEE International Conference on Automation and Computational Engineering, pp. 72-78, 2018. DoI: 10.1109/ICACE.2018.8687041.

[6.20] P. Kotsampopoulos, N. Hatziargyriou, B. Bletterie, G. Lauss, "Review, analysis and recommendations on recent guidelines for the provision of ancillary services by Distributed Generation", IEEE International Workshop on Intelligent Energy Systems (IWIES), Vienna, November 2013

[6.21] He, W., Yu, M. & Yu, J. Distributed finite-time active power sharing control with generation costs considered. SN Appl. Sci. 1, vol. 1692, pp. 10, 2019. doi:10.1007/s42452-019-1745-0.

[6.22] M. B. Saïd-Romdhane, S. Skander-Mustapha & I. Slama-Belkhodja, "Analysis of performance criteria for an optimal PV system configuration". SN Appl. Sci. 2, vol. 1349. Pp. 8, 2020. doi: 10.1007/s42452-020-3106-4

[6.23] Benchmark Systems for Network Integration of Renewable and Distributed Energy Resources: 2014, ISBN: 978-285-873-270-8.

[6.24] Technical Manual, "DIgSILENT Power System Solutions", May 2020.

[6.25] M. Maniatopoulos, D. Lagos, P. Kotsampopoulos, N. Hatziargyriou, "Combined control and power hardware in-the-loop simulation for testing smart grid control algorithms," IET Generation, Transmission & Distribution, vol. 11, no. 12, pp. 3009-3018, 2017. doi: 10.1049/iet-gtd.2016.1341.